e-ISSN:2651-4060

October 2024
Volume 7
Issue 3

SABİAD

SAĞLIK BİLİMLERİNDE İLERİ ARAŞTIRMALAR DERGİSİ

JOURNAL OF ADVANCED RESEARCH IN HEALTH SCIENCES

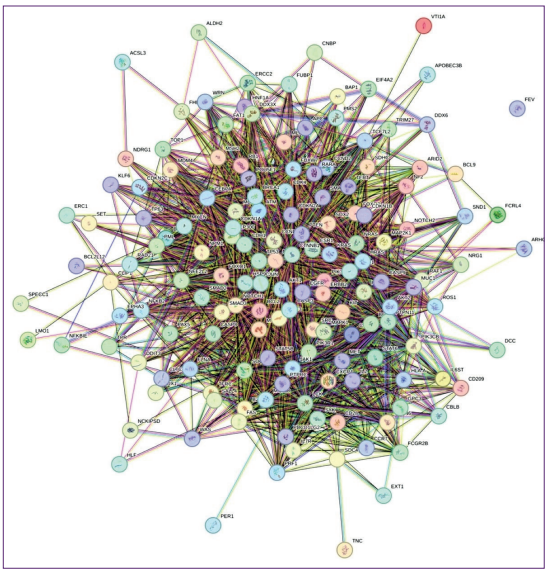

RESEARCH ARTICLES

İSTANBUL UNIVERSITY PRESS

Indexing and Abstracting

ULAKBİM TR Dizin

CAB Abstracts

CABI Global Health

CABI Nutrition and Food Sciences

EBSCO CINAHL Ultimate

EBSCO Central & Eastern European Academic Source

ASOS Index

DOAJ

SABİAD
SAĞLIK BİLİMLERİNDE İLERİ ARAŞTIRMALAR DERGİSİ
JOURNAL OF ADVANCED RESEARCH IN HEALTH SCIENCES
October 2024, Volume 7, Issue 3 e-ISSN:2651-4060

Owner
Prof. Dr. Murat COŞKUN
Istanbul University, Institute of Graduate Studies in Health Sciences, Istanbul, Turkiye

Responsible Manager
Prof. Dr. Murat COŞKUN
Istanbul University, Institute of Graduate Studies in Health Sciences, Istanbul, Turkiye

Correspondence Address
İstanbul Üniversitesi, Sağlık Bilimleri Enstitüsü,
Bozdoğan Kemeri Cad. No: 4 Vezneciler Hamamı Sk.
Vezneciler, Fatih 34126 İstanbul, Türkiye
Telefon / Phone: +90 (212) 440 00 00 (14131)
Faks / Fax: +90 (212) 414 30 16
E-mail: sabiad@istanbul.edu.tr
https://dergipark.org.tr/sabiad
http://iupress.istanbul.edu.tr/tr/journal/jarhs/home

Publisher
Istanbul University Press
İstanbul Üniversitesi Merkez Kampüsü, 34452 Beyazıt,
Fatih / İstanbul, Türkiye
Telefon / Phone: +90 (212) 440 00 00

Cover photo
Öğr.Gör.Dr. Gözde ÖZTAN

The publication language of the journal is English.

This is a scholarly, international, peer-reviewed and open-access journal published triannually in February, June and October.

Publication Type: Periodical

SABİAD
SAĞLIK BİLİMLERİNDE İLERİ ARAŞTIRMALAR DERGİSİ
JOURNAL OF ADVANCED RESEARCH IN HEALTH SCIENCES
October 2024, Volume 7, Issue 3 e-ISSN:2651-4060

EDITORIAL MANAGEMENT BOARD

SABİAD
SAĞLIK BİLİMLERİNDE İLERİ ARAŞTIRMALAR DERGİSİ
JOURNAL OF ADVANCED RESEARCH IN HEALTH SCIENCES
October 2024, Volume 7, Issue 3 e-ISSN:2651-4060

SABİAD
SAĞLIK BİLİMLERİNDE İLERİ ARAŞTIRMALAR DERGİSİ
JOURNAL OF ADVANCED RESEARCH IN HEALTH SCIENCES
October 2024, Volume 7, Issue 2 e-ISSN:2651-4060

CONTENTS

CONTENTS

İSTANBUL UNIVERSITY PRESS

RESEARCH ARTICLE / ARAŞTIRMA MAKALESİ
Journal of Advanced Research in Health Sciences /
Sağlık Bilimlerinde İleri Araştırmalar Dergisi 2024
DOI: 10.26650/JARHS2024-1489999

RETROSPECTIVE EVALUATION OF ASA CLASSIFICATION'S PREDICTIVE ABILITY OF POSTOPERATIVE COMPLICATIONS IN PATIENTS ADMITTED TO INTENSIVE CARE UNIT AFTER MAJOR ABDOMINOPELVIC SURGERY*

MAJOR ABDOMİNOPELVİK CERRAHİ SONRASI YOĞUN BAKIM ÜNİTESİNE KABUL EDİLEN HASTALARIN ASA SINIFLAMASI VE POSTOPERATİF KOMPLİKASYONLAR AÇISINDAN RETROSPEKTİF DEĞERLENDİRİLMESİ

*Congresses: This paper was presented as poster presentation in 54th Turkish Society of Anaesthesiology and Reanimation Congress (on-line, 28th-30th of October 2020).

Emre Sertaç BİNGÜL[1,2], Ayşe HIZAL[2], Başar ERDİVANLI[2], Hızır KAZDAL[2]

[1]İstanbul University, İstanbul Faculty of Medicine, Department of Anaesthesiology, İstanbul, Türkiye
[2]Recep Tayyip Erdoğan University, Training and Research Hospital, Department of Anaesthesiology, Rize, Türkiye

ORCID ID: E.S.B. 0000-0002-8662-5380; A.H. 0000-0002-8046-757X; B.E. 0000-0002-3955-8242; H.K. 0000-0002-0759-4716

Citation/Atıf: Bingül ES, Hızal A, Erdivanlı B, Kazdal H. Retrospective evaluation of ASA classification's predictive ability of postoperative complications in patients admitted to intensive care unit after major abdominopelvic surgery. Journal of Advanced Research in Health Sciences 2024;7(3):143-149. https://doi.org/10.26650/JARHS2024-1489999

ABSTRACT

Objective: The American Society of Anaesthesiologists Physical Status Score (ASA) is a useful tool for indicating the need for intensive care unit (ICU) monitoring in postoperative patients. However, physician misclassification can lead to unnecessary bed occupancy and increased costs. This study examined the relationship between preoperative ASA scores and complications following major abdominopelvic surgery.

Materials and Methods: Patients who underwent postoperative monitoring in a tertiary ICU between November 2016 and February 2019 for semi-urgent and urgent major abdominopelvic surgery were evaluated. Data related to morbidity and mortality were analysed, including acute postoperative complications (hypotension, bleeding, desaturation, prolonged intubation, failed weaning, acute kidney injury, cardiac arrest, exitus), length of ICU stay, recurrent ICU admissions, overall mortality incidence, and 30-day mortality incidence.

Results: A total of 122 patients who underwent gastrointestinal, gynaecological, and urological surgeries were retrospectively analysed. Patients were grouped as ASA II (N=59), ASA III (N=45), and ASA IV (n=18). Overall complication rates among the groups did not differ. The exitus rate was significantly higher in ASA IV (p=0.022). Similarly, the duration of ICU stay, recurrent ICU admissions, and 30-day mortality were significantly higher in ASA IV (p<0.05). When patients were grouped as semi-urgent (n=87) and urgent (n=35), respiratory complications such as prolonged intubation, desaturation, and failed weaning, as well as ICU stay and 30-day mortality rates were higher in urgent cases (p<0.001). No exitus was observed in the semi-urgent oncological surgeries in the ICU.

Conclusion: No difference in respiratory complications was observed in the postoperative ICU follow-up of ASA IV major abdominal surgery patients compared with other ASA groups. However, both respiratory complications and mortality rates were significantly higher in the urgent cases. The low rate of complications in semi-urgent oncological surgeries can be explained by the optimal preoperative surgical preparation.

Keywords: Intensive care, major abdominal surgery, major pelvic surgery, oncologic surgery, postoperative complications, mortality

ÖZ

Amaç: Amerikan Anesteziyoloji Derneği Fiziksel Durum Skoru (ASA) postoperatif hastalarda yoğun bakım ünitesi (YBÜ) takibi endikasyonu koymada yararlı bir araçtır. Öte yandan hekimlerin yanlış skorlamaları yatakların gereksiz meşguliyetine ve artan hastane masraflarına yol açabilir. Bu çalışmada major abdominopelvik cerrahi sonrası komplikasyonların preoperatif ASA skorları ile ilişkisi incelendi.

Gereç ve Yöntem: Kasım 2016 ve Şubat 2019 tarihleri arasında üçüncü düzey YBÜ'de postoperatif takibi gerçekleştirilen semi-acil ve acil major abdominopelvik cerrahi hastaları değerlendirildi. Morbidite ve mortalite ile ilişkili veriler; akut postoperatif komplikasyonlar (hipotansiyon, kanama, desaturasyon, uzamış entübasyon, başarısız "weaning", akut böbrek hasarı, kardiyak arrest, eksitus), YBÜ takip süresi, tekrarlayan YBÜ yatışları, genel mortalite insidansı ve 30-gün mortalite insidansı şeklinde analiz edildi.

Bulgular: 122 gastrointestinal, jinekolojik ve ürolojik cerrahi hastası retrospektif olarak analiz edildi. Hastalar; ASA II (n=59), ASA III (N=45) ve ASA IV (n=18) olarak gruplandırıldı. Genel komplikasyon oranlarında gruplar arasında anlamlı farklılık yoktu. Eksitus oranı ASA IV grubunda anlamlı yüksekti (p=0,022). Aynı şekilde YBÜ yatış süresi, YBÜ'ne tekrarlayan yatış ve 30-gün mortalite yine ASA IV grubunda anlamlı yüksekti (p<0,05). Hasta gruplandırması semi-acil (n=87) ve acil (n=35) olarak yapıldığında uzamış entübasyon, desaturasyon ve başarısız "weaning" gibi solunumsal komplikasyonlar, ayrıca YBÜ yatış süresi ve 30-gün mortalite oranı acil vakalarda daha fazlaydı (p<0,001). Yarı-acil onkolojik cerrahilerde YBÜ'de eksitus gözlenmedi.

Sonuç: ASA IV major abdominopelvik cerrahi hastalarının postoperatif YBÜ takibinde solunumsal komplikasyonlar açısından diğer gruplar ile fark gözlenmedi. Buna karşın acil vakalarda hem solunumsal komplikasyon hem de mortalite oranları anlamlı yüksekti. Yarı-acil onkolojik cerrahilerde komplikasyonların az olması preoperatif optimum cerrahi hazırlık sağlanması ile açıklanabilir.

Anahtar Kelimeler: Yoğun bakım, major abdominal cerrahi, major pelvik cerrahi, onkolojik cerrahi, postoperatif komplikasyonlar, mortalite

Corresponding Author/Sorumlu Yazar: Emre Sertaç BİNGÜL **E-mail:** dremrebingul@gmail.com

Submitted/Başvuru: 25.05.2024 • **Revision Requested/Revizyon Talebi:** 05.09.2024 • **Last Revision Received/Son Revizyon:** 05.09.2024 • **Accepted/Kabul:** 17.10.2024 • **Published Online/Online Yayın:** 25.10.2024

INTRODUCTION

Major abdominopelvic surgery can cause major bleeding, hemodynamic instability, capillary leak, and postoperative respiratory complications. With the increased median life span and improved surgical techniques, more comorbid patients receive such surgical treatments. Intensive care units (ICU) play an essential role in the postoperative care of these patients. However, the ICU is a scarce resource, which obviates the need for a pragmatic, reliable, and easy-to-use tool to predict the outcome of major abdominopelvic surgery.

The American Society of Anaesthesiologists Physical Status (ASA) has been used to define patients' preoperative health status since 1941 (1). Due to its simplicity, ASA is frequently and successfully used to predict patient outcomes such as mortality, complications, and ICU admissions. This ability was criticised due to the interrater variability of ASA and was constantly challenged with several other scoring systems such as NSQIP and POSSUM (2).

Several studies have reported that ASA has a low predictive power (3, 4), despite continuing efforts for optimisation (5). Recent clinical studies attempted to improve the statistical results by dichotomising ASA scores to I and II vs III and IV (6). Even though such techniques provide more significant p values, the descriptive ability of ASA is still arguable.

In the current study, it is aimed to investigate the adequacy of sole ASA scoring for postoperative morbidity prediction, and adding the urgency perspective into this evaluation was also explored. Our hypothesis was that ASA IV patients would represent the highest rate of mortality. However, postoperative complications were also investigated both from the perspective of ASA classification and operative urgency.

MATERIALS AND METHOD

Data inclusion and regulatory aspects

After obtaining the approval of the Recep Tayyip Erdoğan University Ethics Committee (Date: 11.11.2019, No: 2019/44), ICU patient records spanning from November 2016 to February 2019 were screened. Patients who were admitted to the ICU for postoperative care following major abdominal surgery were included. Patients who had undergone surgery while they were in the ICU and "elective" major abdominal surgeries such as bariatric surgery patients were excluded.

Outcome measures

Patient characteristics (such as age, gender, surgical indication, operative urgency, ASA), time to extubation, length of ICU stay, length of hospital stay, readmission to ICU, occurrence and timing of postoperative complications and death (both in ICU and after ICU follow-up) were retrieved from the records. Operative urgency was classified as elective, semi-urgent, and urgent. The postoperative period of 24 h was examined for the occurrence of the following complications:

1. Hypotension: mean arterial blood pressure less than 25% of baseline or <65 mmHg, requiring any treatment with intravenous hydration, vasopressors, or blood products.

2. Bleeding: Any bleeding causing a 2 g/dl drop in serum haemoglobin value or required transfusion of blood products.

3. Desaturation: PaO2 value below 60 mm Hg or a SpO_2 value below 92%.

4. Prolonged intubation: inability to extubate the patient within 4 h of the admission to the ICU.

5. Failure to wean: Failure to pass a spontaneous breathing trial or the need for reintubation within 48 h following extubation.

6. Acute kidney injury: Increase in serum creatinine by ≥0.3 mg/dl within 48 h, or increase in serum creatinine by ≥1.5 times of baseline, or urine volume <0.5 ml/kg/hour for 6 h.

7. Cardiac arrest.

The primary outcome was the comparison of mortality rates in the ASA groups. Secondary outcomes included the effects of operative urgency and surgical indications (oncological and non-oncological) on patient outcomes, including postoperative complications and length of stay, both in the ICU and in the hospital.

Statistical analysis

Data were analysed with R version 3.5.1 (R Foundation, Vienna, Austria). The distribution of data was analysed with Kolmogorov–Smirnov test for normality. Patient characteristics were summarised with descriptive statistics.

The incidence of death within 24 h of surgery was cross-tabulated by ASA separately for each category of operative urgency. Elective cases did not take part in the final analyses, yet were demonstrated as a part of the classification tree of the major determinants for mortality.

Two comparative analyses were performed by first grouping the patients according to ASA (II, III and IV), operative urgency (semi-urgent and urgent), and then according to specific surgical indications (gastrointestinal, gynaecological, urological). In all three cases, data other than patient characteristics were analysed with Kruskal–Wallis Test due to nonhomogenous distribution. In case of a significant difference, the Mann–Whitney U test was used for between-groups analysis by adjusting the p value to 0.017.

A two-sided binomial test was used to compare the mortality rates in the semi-urgent and urgent groups. The Cochran-Armitage trend test was used to evaluate the association between increasing ASA and mortality (DescTools package, version 0.99.32). A binary classification tree was formed with the inputs of patient characteristics, ASA, urgency of operation, and surgical indications (rpart package, version 4.1-15).

Sample size

The required sample size was analysed according to Wolters et al.'s study in which the mortality ratio was defined as under 3.5% for ASA II and III patients and 18.3% for ASA IV patients

(7). When the alpha error was 0.05 and with the power of 80%, a total of 120 patients were calculated for statistical significance for the current study.

RESULTS

Flow diagram of the study and patient characteristics are given in Figure 1 and Table 1, respectively. Gender was distributed homogenously between the groups, and ASA IV patients were significantly older. The majority of patients had gastrointestinal surgery. Also, the majority of patients had undergone planned surgeries for malignancy and were defined as semi-urgent. Approximately one-fourth of the patients had urgent surgery due to such indications such as gastrointestinal bleeding, ileus, or bowel perforation.

Comparison of patient characteristics and outcomes according to ASA scoring are given in Table 2. Postoperative complications did not differ between the ASA groups; however, exitus during ICU follow-up or during the postoperative 30 days was significantly higher in ASA IV.

Comparison of patient characteristics and outcomes according to the urgency of operation are given in Table 3. A classification tree was also represented in Figure 2, in which the most important factors determining the mortality are depicted.

Readmission to the ICU, in ICU exitus ratio and length of stay were significantly higher in the ASA IV group, despite the lowest ratio of oncologic cases ($p<0.05$). Consequently, the 30-day mortality ratio was also highest in the ASA IV group ($p=0.024$). When evaluated according to the urgency of the surgery, the number of semi-urgent cases was more in the ASA II group, and on the contrary, the number of urgent cases was statistically more in the ASA IV group ($p<0.05$). 97% of the urgent cases

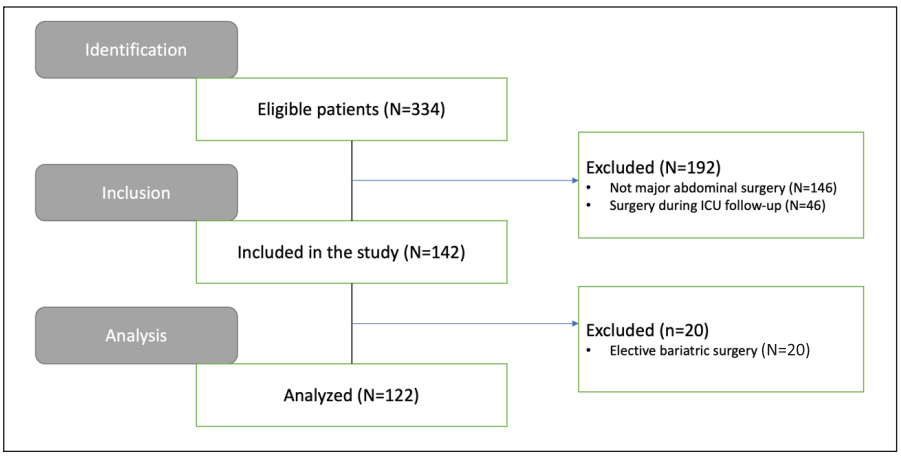

Figure 1. Study flow diagram

ICU: Intensive care unit

Table 1: Patient characteristics (n=122)

Parameter	
Age, years	68±14
Female gender, n (%)	61 (50%)
The type of surgery, n (%)	
Gastrointestinal	95 (78%)
Gynaecological	18 (15%)
Urological	9 (7%)
ASA, n (%)	
II	59 (48%)
III	45 (37%)
IV	18 (15%)
Urgency of operation, n (%)	
Semi-urgent	87 (71%)
Urgent	35 (29%)
Patients with postoperative complications, n (%)	44 (36%)
Readmission to Intensive Care Unit, n (%)	6 (5%)
30-day mortality, n (%)	13 (11%)

ASA: American Society of Anaesthesiologists Physical Status

Table 2: Patient characteristics and outcomes according to the ASA. Categoric data were evaluated with the chi-square test. Nominal data were assessed with Kruskal–Wallis Test

Parameter	ASA 2 (n=59)	ASA 3 (n=45)	ASA 4 (n=18)	p
Age, years	64.2±12.8	69.7±11.7	76.4±16.3	0.001**
Female gender, n (%)	29 (49%)	22 (49%)	10 (56%)	0.877
Urgency, n (%) **Semi-urgent** **Urgent**	 49 (83%) 10 (17%)	 31 (69%) 14 (31%)	 7 (39%) 11 (61%)	 0.002*
The type of surgery, n (%) **Gastrointestinal** **Gynaecological** **Urological**	 45 (76%) 9 (15%) 5 (89%)	 33 (73%) 8 (17%) 4 (9%)	 17 (94%) 1 (6%) -	 0.454
Oncologic cases, n (%)	49 (83%)	37 (82%)	8 (44%)	0.002*
Patients extubated in 24 h, n (%)	5 (9%)	7 (16%)	4 (22%)	0.278
Time to extubation in 24 hours, hours	3 (2 - 5 [1 - 20])	3 (3 - 5 [1 - 20])	3.5 (2 - 7 [2 - 20])	0.676
Time to extubation after 24 hours, days	10 (2 - 16 [1 - 24])	2 (2 - 5 [1 - 27])	3 (3 - 6 [3 - 16])	0.787
Complications in the ICU, n (%) **Hypotension** **Bleeding** **Desaturation** **Prolonged intubation** **Failure to wean** **Acute kidney injury** **Cardiac arrest**	17 (29%) 5 (9%) 1 (2%) 2 (3%) - 2 (3%) 3 (5%) -	17 (38%) 4 (9%) 1 (2%) 2 (4%) 2 (4%) 4 (9%) 1 (2%) -	10 (56%) - - 5 (28%) 3 (17%) - 1 (6%) 1 (6%)	0.115 0.672 0.911 0.395 0.672
In the ICU Exitus	2 (3%)	4 (9%)	4 (22%)	0.022*
ICU stay, days	1 (1 - 2 [1 - 29])	1 (1 - 2 [1 - 29])	3 (1 - 6 [2 - 16])	0.003**
Readmission to the ICU, n (%)	1 (2%)	2 (4%)	3 (17%)	0.036*
Ward stay, days	3 (2 - 6 [1 - 17])	4 (2 - 5 [1 - 29])	2 (1 - 5 [1 - 11])	0.503
30-day mortality, n (%)	3 (5%)	5 (11%)	5 (28%)	0.024*

ASA: American Society of Anaesthesiologists Physical Status, ICU: Intensive care unit. *: Chi-square test, **: Kruskal Wallis Test

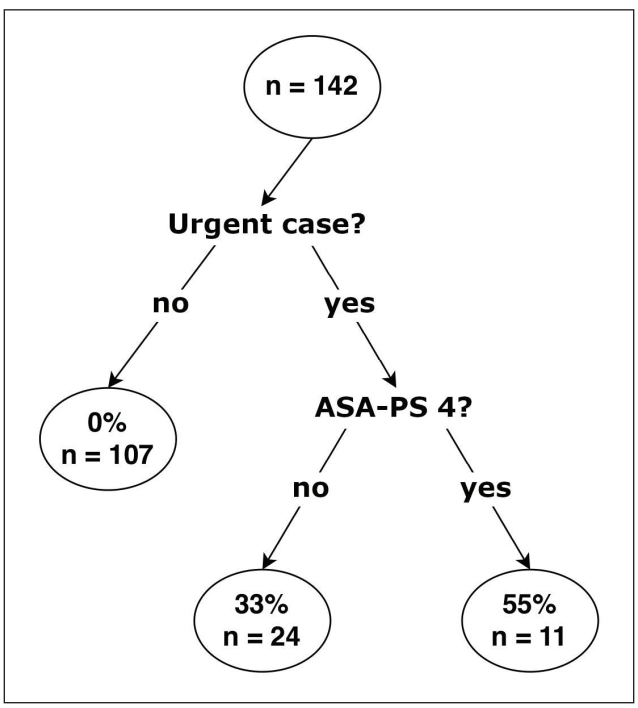

Figure 2: Classification tree showing the important determinants of mortality. Percentages exhibiting the death ratio in the related group

Table 3: Characteristics and outcomes according to the urgency of operation. Categoric data were assessed with the chi-square test. Mann Whitney-U Test was used for between-group nominal data assessment

Parameter	Semi-urgent (n=87)	Urgent (n=35)	p
Age, years	67.2±13	70.2±15	0.207
Female gender, n (%)	41 (47%)	20 (57%)	0.317
ASA, n (%)			
II	49 (56%)	10 (29%)	
III	31 (36%)	14 (40%)	0.001*
IV	7 (8%)	11 (31%)	
The type of surgery, n (%)			
Gastrointestinal	61 (70%)	34 (97%)	
Gynaecological	17 (20%)	1 (3%)	0.005*
Urological	9 (10%)	-	
Oncologic cases, n (%)	79 (91%)	15 (43%)	<0.001*
Patients extubated in 24 h, n (%)	84 (97%)	22 (63%)	<0.001*
Time to extubation in 24 hours, hours	3 (2 - 4 [1 - 20])	7 (3 - 16 [2 - 20])	<0.001**
Time to extubation after 24 hours, hours	24 (24 - 35 [24 - 45])	85 (70 - 380 [45 - 640])	0.009**
Complications in the ICU, n (%)			
Hypotension	22 (25%)	22 (63%)	<0.001*
Bleeding	5 (6%)	4 (11%)	1
Desaturation	1 (1%)	1 (3%)	1
Prolonged intubation	5 (6%)	4 (11%)	<0.001*
Failure to wean	-	5 (14%)	<0.001*
Acute kidney injury	-	6 (17%)	<0.001*
Cardiac arrest	4 (5%)	1 (3%)	0.342
	-	1 (3%)	1
In the ICU exitus	-	10 (29%)	<0.001*
ICU stay, days	4 (3 - 4 [2 - 4])	16 (7 - 20 [3 - 29])	<0.001**
Readmission to the ICU, n (%)	1 (1%)	5 (14%)	0.002*
Ward stay, days	3 (2 - 5 [1 - 24])	4 (2 - 5 [1 - 29])	0.306
30-day mortality, n (%)	3 (3%)	13 (37%)	<0.001*

ASA: American Society of Anaesthesiologists Physical Status, ICU: Intensive care unit, *: Chi-square test.**: Mann-Whitney U test.

were gastrointestinal surgeries, and 91% of the semi-urgent cases were oncological operations. The number of patients weaned from mechanical patients within the first 24 h and the time for extubation were higher in the semi-urgent group. Similarly, this tendency continued after the first 24 h, and the time for extubation following the first 24 h was lower in the semi-urgent patient group (p<0.001). None of the semi-urgent group died during the follow-up, and 14% of the urgent group required readmissions to the ICU, and 29% of the urgent group died during the first ICU followup (p<0.001). As expected, the 30-day mortality was higher in the urgent patient group (p<0.001).

DISCUSSION

Our results revealed a higher mortality but similar postoperative complication rates with ASA IV when compared with the other ASA groups. As ASA is an ordered scoring system, we expected a gradual increase not just in mortality but also in morbidity, which was not observed within our findings. Consequently, ASA appears to be strong at predicting mortality rather than morbidity. However, once the urgency of the case is involved, "morbidity prediction" becomes more evident, and apparently more than half of ASA IV patients die in the postoperative period if the surgery is urgent. None of the semi-urgent cases encountered death after surgery.

ASA is widely used compared to other scoring systems such as NSQIP, POSSUM, and the Charlson comorbidity index (8, 9). These other indexes would represent more benefit in terms of morbidity prediction. As a supporting fact from the current findings, "mortality" would normally be expected to be seen less than postoperative complications, and interestingly, we observed a significant difference in mortality with ASA but "similar" complication rates. The major criticism would be on its extensive definition and subjective nature resulting in misclassifications (4).

Lupei et al. reported that a higher ASA score was related to an increased need for mechanical ventilation (10). However, our findings are in contrast. As it is represented in our results, operative "urgency" would be more determining on postoperative respiratory complications. Urgent surgery patients experience

more prolonged ventilatory support, desaturation or weaning failure. Perhaps, taking "urgency" into consideration would favour more compared to ASA. This proposal seems legited since the ASA class does not focus on the respiratory capacity of the patient, which is exceptionally important to foresee possible respiratory complications in the postoperative period. Yet, in a study with 1332 adults by Hall et al., it was demonstrated that ASA score above II and having chronic bronchitis are independent risk factors for respiratory insufficiency, which was defined as PaO_2 lower than 60 mmHg or prolonged intubation that is more than 24 h (11). Lastly, the renowned ACS NSQIP database-based extensive trials have put an end to the confusion and proved that ASA class is one independent factor for risk "stratification" for "medical" complications that also includes "postoperative pulmonary complications" in abdominal surgeries (12, 13). However, our single centre experience regarding the use of the ASA classification for predicting respiratory complications in patients followed up in the ICU postoperatively did not prove beneficial.

Length of stay in the ICU was considerably longer in patients with ASA IV, yet ward stay was found to be as short as the other groups. This suggests a pattern where comorbid patients with higher ASA are treated in the ICU until they are almost ready to be discharged from the hospital. As we understand, the length of stay in the ICU or ward is surgeon-dependent; therefore, it is a subjective parameter. Although there are some studies implying a prolonged length of stay due to increased postoperative complications in patients with ASA III and above, we can hardly claim that ASA can predict the length of stay in the ICU accurately (14, 15).

ASA was correlated with 30-day mortality in this study. There are studies searching for a better correlation by combining the chronic illness of the patient with their current physical status, and among them, Visnjevac et al. combined ASA with functional status to predict 30-day mortality (16). They reported that every individual's functional capacity was related to postoperative mortality as an independent risk factor and also suggested increasing the ASA score by 1 in functionally limited patients. Most patients in the ICU pose a specific challenge for such examination because they generally require analgesia or sedation, which obscures the actual physical fitness of the patient.

In the current study, the mortality rate in the elective and semi-urgent cases was zero, in contrast to 37% of the mortality in the urgent cases. Although this is an expected finding, it should be interpreted with caution. In this study, significantly more patients with ASA IV underwent urgent surgery, and the literature denotes that mortality rate increases with increasing ASA (12). General understanding regarding delaying urgent surgeries is that it may lead to more complications (17); however, in a study by Sjo et al. the high mortality rates with emergency surgeries and ASA IV were emphasised and some palliative solutions were suggested to avoid immediate surgery in colon cancer (18). These statements are compatible with our findings.

Most oncological interventions are considered to be semi-urgent procedures in medical practise. This retrospective evaluation showed zero in-hospital mortality with semi-urgent cancer surgeries. This is not surprising as patient-centric perioperative care protocols are employed in this institute (19, 20). In other words, patients who had an urgent surgery did not have the chance for preoperative patient optimisation. In our retrospective design, it was impossible to determine if it was possible to optimise patients with ASA IV and whether this optimisation could lead to lower ASA scores such as ASA II or III. No doubt, optimising ASA IV patients would provide utmost benefit, but in our experience, it is questionable whether lowering the ASA from III to II would provide such change. On the other hand, there are other elements such as incision width and duration of the operation that are remarkably important (21). It has been demonstrated that minimally invasive procedures may increase life expectancy or reduce complications in such cases, and this shows that surgical technique is one of the most important determinants (22).

This trial has several limitations. The results from a single-centre obviously are not suitable for generalisation. However, our results are comparable to those of some international trials, which showed a strong correlation between ASA and mortality (12, 23). Considering the statistical techniques, the effect of ASA on the outcomes is further complicated by one final factor; this study included only patients who had a surgery, and patients were not included if they were not operated due to ASA V. However, Horwood et al. demonstrated relatively good recovery ratios in ASA V patients undergoing major surgery (24).

Nevertheless, this work, which was conducted in a regular tertiary hospital, provides a pragmatic explanation for the use of the ASA class for ICU physicians who encounter major abdominopelvic surgery in their everyday practise. Statistically correct explanations by the extensive studies may not be in favour for low patient volume centres since the practise may not fit what is claimed. In summary, the distinctly different results of the ASA IV group suggests that it is a suitable cut-off value for major abdominopelvic surgery, and these patients should be evaluated by including operative urgency. Future studies should include descriptive events to study the possible applicability and effect of enhanced recovery after surgical protocols on urgent surgeries.

Ethics Committee Approval: This study was approved by Recep Tayyip Erdoğan University (Date: 11.11.2019, No: 2019/44).

Informed Consent: All participants received written informed consent after being fully informed about the study.

Peer Review: Externally peer-reviewed.

Author Contributions: Conception/Design of Study- E.S.B., B.E.; Data Acquisition- A.H.; Data Analysis/Interpretation- H.K.; Drafting Manuscript- E.S.B.; Critical Revision of Manuscript- A.H., B.E., H.K.; Final Approval and Accountability- E.S.B., A.H., B.E.,

H.K.; Material and Technical Support- A.H.; Supervision- B.E., H.K.

Conflict of Interest: The authors have no conflict of interest to declare.

Financial Disclosure: The authors declared that this study has received no financial support.

REFERENCES

1. Mayhew D, Mendonca V, Murthy BVS. A review of ASA physical status - historical perspectives and modern developments. Anaesthesia 2019;74(3):373-9.
2. Sankar A, Johnson SR, Beattie WS, Tait G, Wijeysundera DN. Reliability of the American Society of Anesthesiologists physical status scale in clinical practice. Br J Anaesth 2014;113(3):424-32.
3. Lee A, Lum ME, O'Regan WJ, Hillman KM. Early postoperative emergencies requiring an intensive care team intervention. The role of ASA physical status and after-hours surgery. Anaesthesia 1998;53(6):529-35.
4. Helkin A, Jain SV, Gruessner A, Fleming M, Kohman L, Costanza M, et al. Impact of ASA score misclassification on NSQIP predicted mortality: a retrospective analysis. Perioper Med (Lond) 2017;6:23.
5. Hurwitz EE, Simon M, Vinta SR, Zehm CF, Shabot SM, Minhajuddin A, et al. Adding Examples to the ASA-Physical Status Classification Improves Correct Assignment to Patients. Anesthesiology 2017;126(4):614-22.
6. Lima MJM, Cristelo DFM, Mourao JB. Physiological and operative severity score for the enumeration of mortality and morbidity, frailty, and perioperative quality of life in the elderly. Saudi J Anaesth 2019;13(1):3-8.
7. Wolters U, Wolf T, Stutzer H, Schroder T. ASA classification and perioperative variables as predictors of postoperative outcome. Br J Anaesth 1996;77(2):217-22.
8. Al-Homoud S, Purkayastha S, Aziz O, Smith JJ, Thompson MD, Darzi AW, et al. Evaluating operative risk in colorectal cancer surgery: ASA and POSSUM-based predictive models. Surg Oncol 2004;13(2-3):83-92.
9. Sobol JB, Wunsch H. Triage of high-risk surgical patients for intensive care. Crit Care 2011;15(2):217.
10. Lupei MI, Chipman JG, Beilman GJ, Oancea SC, Konia MR. The association between ASA status and other risk stratification models on postoperative intensive care unit outcomes. Anesth Analg 2014;118(5):989-94.
11. Hall JC, Tarala RA, Hall JL. Respiratory insufficiency after abdominal surgery. Respirology 1996;1(2):133-8.
12. Hackett NJ, De Oliveira GS, Jain UK, Kim JY. ASA class is a reliable independent predictor of medical complications and mortality following surgery. Int J Surg 2015;18:184-90.
13. Yang CK, Teng A, Lee DY, Rose K. Pulmonary complications after major abdominal surgery: National Surgical Quality Improvement Program analysis. J Surg Res 2015;198(2):441-9.
14. Badgwell B, Stanley J, Chang GJ, Katz MH, Lin HY, Ning J, et al. Comprehensive geriatric assessment of risk factors associated with adverse outcomes and resource utilization in cancer patients undergoing abdominal surgery. J Surg Oncol 2013;108(3):182-6.
15. Jakobson T, Karjagin J, Vipp L, Padar M, Parik AH, Starkopf L, et al. Postoperative complications and mortality after major gastrointestinal surgery. Medicina (Kaunas) 2014;50(2):111-7.
16. Visnjevac O, Davari-Farid S, Lee J, Pourafkari L, Arora P, Dosluoglu HH, et al. The effect of adding functional classification to ASA status for predicting 30-day mortality. Anesth Analg 2015;121(1):110-6.
17. Ong M, Guang TY, Yang TK. Impact of surgical delay on outcomes in elderly patients undergoing emergency surgery: A single center experience. World J Gastrointest Surg 2015;7(9):208-13.
18. Sjo OH, Larsen S, Lunde OC, Nesbakken A. Short term outcome after emergency and elective surgery for colon cancer. Colorectal Dis 2009;11(7):733-9.
19. Longo WE, Virgo KS, Johnson FE, Oprian CA, Vernava AM, Wade TP, et al. Risk factors for morbidity and mortality after colectomy for colon cancer. Dis Colon Rectum 2000;43(1):83-91.
20. Ahmed J, Lim M, Khan S, McNaught C, Macfie J. Predictors of length of stay in patients having elective colorectal surgery within an enhanced recovery protocol. Int J Surg 2010;8(8):628-32.
21. Zerbib P, Kulick JF, Lebuffe G, Khoury-Helou A, Plenier I, Chambon JP. Emergency major abdominal surgery in patients over 85 years of age. World J Surg 2005;29(7):820-5.
22. Moreira AdL, Kiran RP, Kirat HT, Remzi FH, Geisler DP, Church JM, et al. Laparoscopic versus open colectomy for patients with American Society of Anesthesiology (ASA) classifications 3 and 4: the minimally invasive approach is associated with significantly quicker recovery and reduced costs. Surg Endosc 2010;24(6):1280-6.
23. Pearse RM, Harrison DA, MacDonald N, Gillies MA, Blunt M, Ackland G, et al. Effect of a perioperative, cardiac output-guided hemodynamic therapy algorithm on outcomes following major gastrointestinal surgery: a randomized clinical trial and systematic review. JAMA 2014;311(21):2181-90.
24. Horwood J, Ratnam S, Maw A. Decisions to operate: the ASA grade 5 dilemma. Ann R Coll Surg Engl 2011;93(5):365-9.

RESEARCH ARTICLE / ARAŞTIRMA MAKALESİ
Journal of Advanced Research in Health Sciences /
Sağlık Bilimlerinde İleri Araştırmalar Dergisi 2024
DOI: 10.26650/JARHS2024-1444347

IN SILICO APPROACH TO GENETICS AND EPIGENETIC MECHANISMS IN SYSTEMIC LUPUS ERYTHEMATOSUS: FOCUS ON IMMUNE RESPONSE GENES

IN SİLİKO YAKLAŞIMLA SİSTEMİK LUPUS ERİTEMATOZUS'TA GENETİK VE EPİGENETİK MEKANİZMALAR: BAĞIŞIKLIK YANITI GENLERİNE ODAKLANMA

Feyzanur ÇALDIRAN[1]

[1]Tokat Gaziosmanpasa University, Faculty of Science and Art, Department of Molecular Biology and Genetics, Tokat, Türkiye

ORCID ID: F.Ç. 0000-0001-7778-194X

Citation/Atıf: Çaldıran F. In Silico approach to genetics and epigenetic mechanisms in systemic lupus erythematosus: Focus on immune response genes. Journal of Advanced Research in Health Sciences 2024;7(3):150-159. https://doi.org/10.26650/JARHS2024-1444347

ABSTRACT

Objective: Systemic lupus erythematosus (SLE) is a multifaceted autoimmune condition characterised by irregular immune reactions and genetic susceptibility. The aim of this in silico study was to investigate immune response genes during SLE pathogenesis, focusing on genetic and epigenetic regulation.

Materials and Methods: This study involving 1255 patients with SLE and 453 control subjects aimed to identify genes associated with the immune response and examine their expression and DNA methylation levels in both patients with SLE and controls. The study design utilized the ADEX open-access database.

Results: The study identified 10 differentially expressed immune response-related genes (*FAM117B, ZNF395, PGAP3, PIK3IP1, HLA-DMB, HLA-DPA1, HLA-DRB3, HLA-DQA1, HLA-DPB1,* and *CCL5*) in SLE pathogenesis, with 78 corresponding methylation sites. Upregulation of *HLA-DQA1, HLA-DMB,* and *CCL5* was observed in patients with SLE, whereas the remaining genes exhibited decreased expression. *HLA-DPA1, HLA-DPB1, HLA-DMB, HLA-DQA1, CCL5,* and *ZNF395* were found to be *the most hypermethylated genes in SLE. Methylation of the CpG islands of HLA-DPB1, CCL5, FAM117B, and ZNF395* is correlated with their expression levels in SLE.

Conclusion: Our findings shed light on the genetic and epigenetic mechanisms underlying SLE and underscore the importance of these genes in immune dysregulation and disease progression. Further research on the functional significance of these genes could provide valuable insights into the pathogenesis of SLE and potential therapeutic targets.

Keywords: Systemic lupus erythematosus, Immune response-related genes, HLA-DPB1, epigenetic regulation, FAM117B, ZNF395

ÖZ

Amaç: Sistemik lupus eritematozus (SLE), düzensiz bağışıklık tepkileri ve genetik yatkınlık ile karakterize edilen çok yönlü otoimmün bir durumdur. Bu in siliko çalışmanın amacı, SLE patogenezinde bağışıklık yanıtı genlerini incelemek ve genetik ile epigenetik düzenlemelere odaklanmaktır.

Gereç ve Yöntemler: 1255 SLE hastası ve 453 kontrol grubunu içeren bu çalışma, bağışıklık yanıtı ile ilişkilendirilen genleri belirlemeyi ve hem SLE hastalarında hem de kontrol grubunda bunların ekspresyon ve DNA metilasyon düzeylerini incelemeyi amaçlamaktadır. Çalışmada, açık erişimli bir veri tabanı olan ADEX veritabanını kullanmıştır.

Bulgular: Çalışma, SLE patogenezinde on farklı şekilde ekspresyon gösteren bağışıklık yanıtı ile ilişkilendirilen genleri (*FAM117B, ZNF395, PGAP3, PIK3IP1, HLA-DMB, HLA-DPA1, HLA-DRB3, HLA-DQA1, HLA-DPB1* ve *CCL5*) ve bunlara karşılık gelen 78 metilasyon sitesini belirlemiştir. SLE hastalarında *HLA-DQA1, HLA-DMB* ve *CCL5*'in aşırı ekspresyonu gözlenirken, diğer genlerin ekspresyonunda azalma görülmüştür. *HLA-DPA1, HLA-DPB1, HLA-DMB, HLA-DQA1, CCL5* ve *ZNF395*'in SLE'de en fazla hipermetile edilen genler olduğu bulunmuştur. *HLA-DPB1, CCL5, FAM117B* ve *ZNF395*'in CpG adalarındaki metilasyonları, bunların SLE'deki ekspresyon düzeyleri ile ilişkili bulunmuştur.

Sonuç: Bu bulgular, SLE'nin genetik ve epigenetik mekanizmalarına ışık tutmakta ve bu genlerin bağışıklık düzensizliği ve hastalık ilerlemesi üzerindeki önemini vurgulamaktadır. Bu genlerin fonksiyonel önemine ilişkin daha fazla araştırma, SLE patogenezine ve potansiyel terapötik hedeflere yönelik değerli bilgiler sağlayabilir.

Anahtar Kelimeler: Sistemik lupus eritematozus, İmmün yanıtla ilişkili genler, HLA-DPB1, Epigenetik düzenleme, FAM117B, ZNF395

Corresponding Author/Sorumlu Yazar: Feyzanur ÇALDIRAN **E-mail:** feyzanur.caldiran@gop.edu.tr

Submitted/Başvuru: 28.02.2024 • **Revision Requested/Revizyon Talebi:** 23.03.2024 • **Last Revision Received/Son Revizyon:** 03.06.2024 • **Accepted/Kabul:** 01.07.2024 • **Published Online/Online Yayın:** 22.10.2024

INTRODUCTION

Systemic lupus erythematosus (SLE) is a persistent autoimmune condition that primarily affects women. The global prevalence of SLE varies between 43.7 cases per 100,000 people and is estimated to be 3.41 million people worldwide (1). SLE affects many organs, including the skin, joints, kidneys, heart, and brain. The pathogenesis of SLE involves dysregulated innate and adaptive immune responses regulated by diverse immune cell populations, inflammatory mediators, and cytokines. This dysregulation leads to tissue and organ damage through the formation of autoantibodies and immune complexes (2).

Genetic susceptibility plays a crucial role in this process, with multiple susceptibility loci identified through genome-wide association (GWAS) and the study of candidate genes. Many of these susceptibility loci are located within or near immune response genes; this underlines their importance in SLE susceptibility and disease progression (3, 4). In recent decades, a thorough investigation has revealed many genetic and immunological elements influencing the development of SLE, notably focusing on immune response genes. The interplay between these genes and SLE pathology is intricate and multifaceted, reflecting the delicate equilibrium between host defence mechanisms and autoimmune responses (5, 6). Genes responsible for immune responses encode various proteins vital for immune control, modulation, and regulation of effector functions, thus playing key roles in shaping adaptive immune responses (7). The immune response genes most extensively studied in the context of SLE include those encoding components of the MHC, particularly the human leukocyte antigen (HLA) region. HLA molecules play critical roles in antigen presentation and immune regulation, and some HLA alleles are strongly associated with an increased risk of SLE and altered disease phenotypes (8). Additionally, genes encoding cytokines and chemokine such as tumor necrosis factor (TNF), C-C motif chemokine ligands (CCLs), and interleukins (Ils), have been shown to play a role in SLE susceptibility and disease pathogenesis, influencing immune cell activation and inflammation (9). Although certain HLA alleles are correlated with an increased risk of SLE, the exact mechanisms underlying their contribution to the disease remain unclear.

Furthermore, advances in high-throughput genomic and transcriptomic technologies have facilitated the comprehensive profiling of gene expression patterns and epigenetic modifications in patients with SLE, providing deeper insights into the molecular mechanisms underlying disease pathogenesis. Epigenetic regulation, which encompasses non-coding RNA, histone modifications, and methylation, has emerged as a critical factor affecting the expression and function of immune response genes in SLE (10-12). Dysregulated epigenetic marks contribute to altered gene expression profiles and abnormal immune responses (13). In light of these advances, understanding the complex relationships between immune response genes and SLE disease holds great promise for elucidating the mechanisms driving autoimmunity, identifying new biomarkers for diagnosis and prognosis, and developing targeted therapeutic strategies to restore immune homeostasis and improve the immune system. However, the ongoing investigation of immune response genes in the context of SLE represents a crucial frontier in autoimmune research, with profound implications for improving patient outcomes and advancing personalized medicine approaches for treating this complex and heterogeneous disorder (14).

Given the role of immune dysregulation in SLE pathology, new therapeutic approaches and genetic and epigenetic biomarkers. This study provided valuable evidence that immune response genes involved in the development of SLE are under epigenetic regulation. These findings offer new insights into the regulatory role of epigenetic factors in the immune response implicated in SLE pathogenesis, thereby enhancing our understanding of the molecular mechanisms involved.

MATERIALS AND METHODS

Datasets

Data sets for SLE were obtained from the GEO database. (http://www.ncbi.nlm.nih.gov/), (15). In total, 11 datasets were downloaded, namely GSE45291, GSE65391, GSE110169, GSE108497, GSE72509, GSE61635, GSE38351, GSE10325, GSE110174, GSE50772, and GSE82221. Among these, GSE45291, GSE65391, GSE110169, GSE108497, GSE72509, GSE61635, and GSE110174 involved whole blood (WB) samples, and high-throughput sequencing was employed for the experimental analysis. On the other hand, GSE38351, GSE10325, GSE50772, and GSE82221 utilized peripheral blood mononuclear cells (PBMC), with the experimental type being array-based.

Data analysis and visualization

In this study, the expression and methylation status of CpGs in relation to their known functions in disease progression were examined in SLE. The list of immune response genes with fully hypermethylated or hypomethylated CpGs associated with promoter regions and their expression were examined for enrichment in blood transcription modules (BTMs) using the predefined module DC.M8.83 (16). To ensure the integrity of methylation level assessment in both normal and SLE samples, two distinct peaks were identified, one near 0 and the other near 1. Methylation levels tended to be minimal at approximately 0 and maximal at approximately 1. Subsequently, the beta values are normalized using the ADEX tool to mitigate potential biases. Methylation sites were annotated using the GSE82221 platform file. Subsequently, genes associated with these distinct methylation sites were extracted. Data analysis and visualization were exclusively conducted within the ADEX programming environment (17).

Statistical analysis

The analyses utilized several R/Bioconductor packages, such as limma, to perform differential expression analysis between disease and control samples. The typical visualization approach includes a heatmap that displays the expression levels of the top differentially expressed genes (DEGs), which are arran-

ged based on their adjusted p values using the False Discovery Rate (FDR) method. Gene expression profiles from RNA-Seq platforms were analyzed using the standard pipeline of the DESeq2 package (18). In both cases, the differential expression analysis provided p values, adjusted p values by False Discovery Rate (FDR), and log2 fold change (FC) values. Group mean comparisons were performed using the Wilcoxon test when data did not conform to a normal distribution. To evaluate the normality of the expression data, the Shapiro test function was used in R (19).

RESULTS

Potential link between 10 immune response genes and the development of SLE

With the DC.M8.83 transcriptional module previously designed by Chaussabel et al., 10 potentially relevant genes were identified that were significantly implicated in the progression of SLE disease sites: *FAM117B, ZNF395, PGAP3, PIK3IP1, HLA-DMB, HLA-DPA1, HLA-DRB3, HLA-DQA1, HLA-DPB1,* and *CCL5*. Subsequently, the expression levels of 10 immune response-related genes were examined in a group of 1708 individuals, comprising 1255 patients with SLE and 453 case controls. SLE disease samples were designated cases in each dataset, whereas normal samples served as controls. The specifications of the 11 datasets are summarized in Table 1. The expression changes of these 10 genes were compared in GSE124939 (keratinocytes), GSE13887 (CD3-positive T cells), GSE11907 (blood), GSE30153 (B cells), GSE24706 (PBMC), GSE80183 (Blood), GSE10325 (Blood), and GSE11907 (Blood) as well as in 11 selected SLE datasets (Figure 1).

Heatmap showing the fold change of each relevant immune response gene selected for systemic lupus erythematosus (SLE) shows changes in expression in T cells and myeloid cell lines in the GSE10325 dataset. Upon analysing these genes across various cell and tissue types, it was discerned that *HLA-DRB3, CCL5, HLA-DQA1, FAM117B, HLA-DPA1,* and *HLA-DPB1* exhibited the strongest associations with SLE, contingent upon the specific tissue and cell type under investigation (Figure 1).

Differential expression of immune response genes in patients with SLE

The results demonstrated a notable increase in the expression of *HLA-DQA1* and *HLA-DMB* compared with the control group, as depicted in Figure 2A-2H. Additionally, a decrease in CCL5 expression was observed in all samples, except for those obtained from the GSE61635 dataset (Figure 2I-2L). The expression of the HLA-*DPA1, HLA-DRB3,* and *HLA-DPB1* genes from the HLA family, which are believed to be implicated in the immune response in SLE, were also assessed. A notable decrease in their expression levels was observed compared with the control (Figure 3). The expression of *FAM117B, ZNF395, PGAP3,* and *PIK3IP1*, among other genes potentially linked to the development of SLE, was also investigated. A similar trend was observed in the expression of these genes (Figure 4). These findings highlight the potential significance of these genes in the pathogenesis of SLE and highlight the necessity for further investigation into the roles of these genes in immune dysregulation and disease progression.

Table 1: Sample Characteristics in the SLE Datasets

	GSE45291	GSE65391	GSE110169	GSE108497	GSE72509	GSE61635	GSE38351	GSE10325	GSE110174	GSE50772	GSE82221
Series type	Array	Array	Array	Array	HTS	Array	Array	Array	Array	Array	Array
Case	292	116	82	325	99	79	14	13	144	61	30
Control	20	45	77	187	18	30	12	9	10	20	25
Total	312	161	159	512	117	109	26	22	154	81	55
Platform	GPL13158	GPL10558	GPL13667	GPL10558	GPL16791	GPL570	GPL96 GPL570	GPL96	GPL13158	GPL570	GPL10558 GPL13534
Tissue	WB	WB	WB	WB	WB	PBMC	PBMC	PBMC	WB	PBMC	PBMC
Clinical features	SLE	Pediatric SLE	SLE	Lupus pregnancy	SLE	SLE	SLE	SLE	SLE	SLE	SLE

WB: Whole Blood, HTS: High-throughput sequencing, SLE: Systemic Lupus Erythematosus

The hypermethylated genes most associated with SLE

Epigenetic phenomena have gained significant attention in understanding the molecular mechanisms of SLE. Although aberrant DNA methylation and histone modification have long been recognized as contributing factors to SLE pathogenesis, DNA hydroxymethylation has emerged as a relatively novel focus

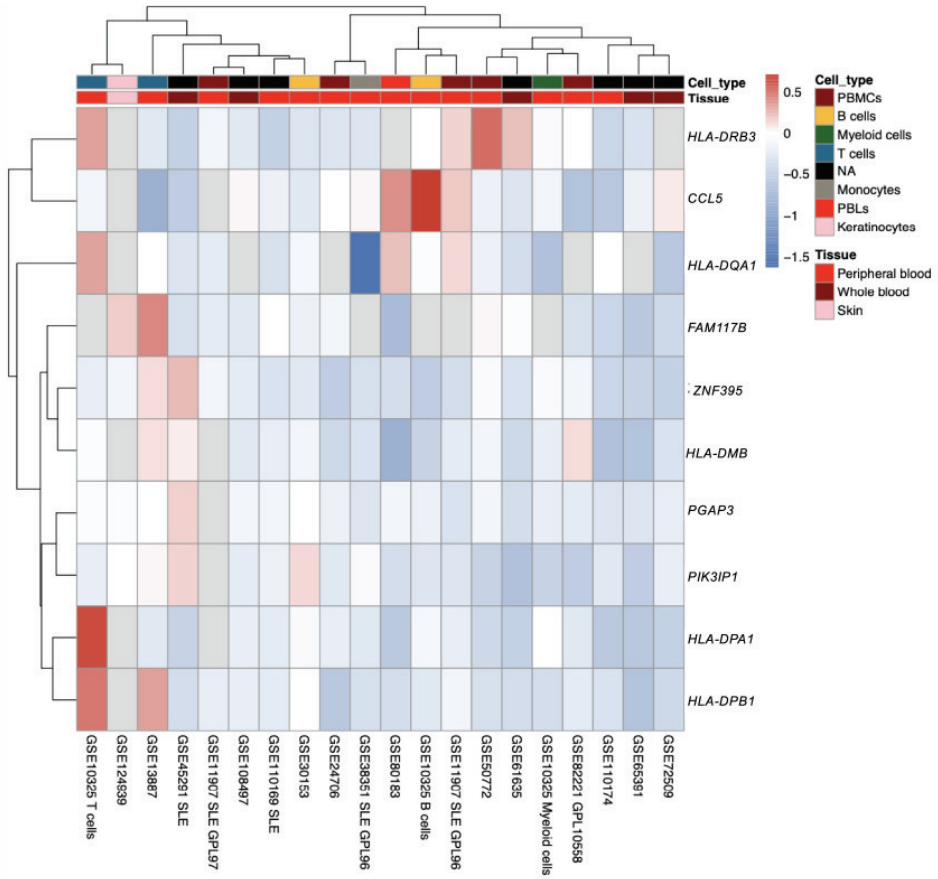

Figure 1: Heatmap with the fold change of each selected related immune response gene in systemic lupus erythematosus (SLE) disease

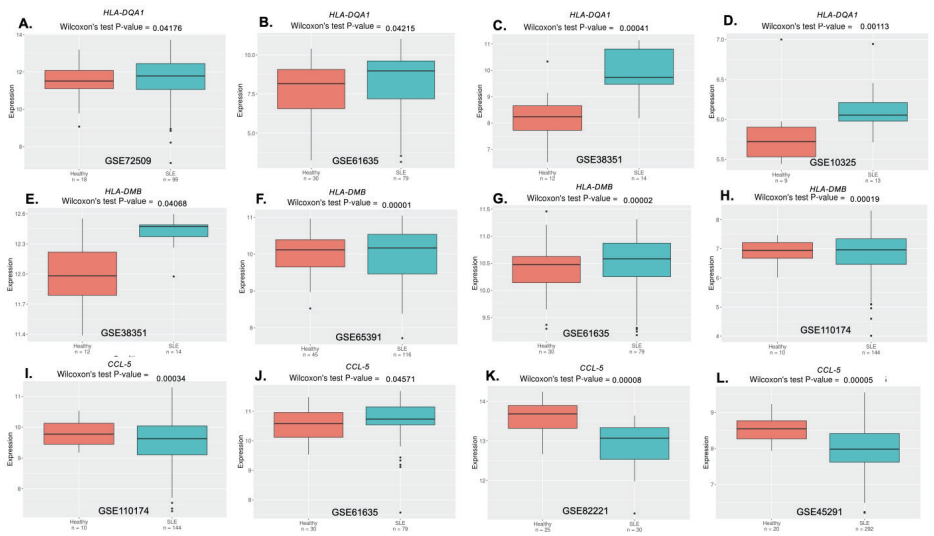

Figure 2: Expression profile of various immune response genes in systemic lupus erythematosus (SLE) disease A. Expression of *HLA-DQA1* in GSE72509 dataset B. Expression of *HLA-DQA1* in GSE61635 dataset C. Expression of *HLA-DQA1* in GSE38351 dataset D. Expression of *HLA-DQA1* in GSE10325 dataset E. Expression of *HLA-DMB* in GSE38351 dataset F. Expression of *HLA-DMB* in GSE65391 dataset G. Expression of *HLA-DMB* in GSE61635 dataset H. Expression of *HLA-DMB* in GSE110174 dataset I. Expression of *CCL5* in GSE110174 dataset J. Expression of *CCL5* in GSE61635 dataset K. Expression of *CCL5* in GSE82221 dataset L. Expression of *CCL5* in GSE45291 dataset

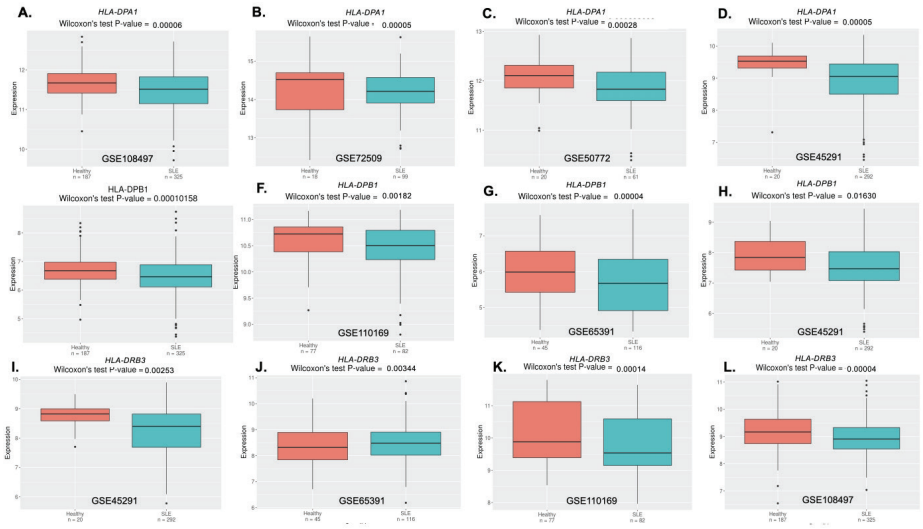

Figure 3: Expression profile of immune response family members in systemic lupus erythematosus (SLE) disease A. Expression of *HLA-DPA1* in GSE108497 dataset B. Expression of *HLA-DPA1* in GSE72509 dataset C. Expression of *HLA-DPA1* in GSE50772 dataset D. Expression of *HLA-DPA1* in GSE45291 dataset E. Expression of *HLA-DPB1* in GSE108497 dataset F. Expression of *HLA-DPB1* in GSE110169 dataset G. Expression of *HLA-DPB1* in GSE65391 dataset H. Expression of *HLA-DPB1* in GSE45291 dataset I. Expression of *HLA-DRB3* in GSE45291 dataset J. Expression of *HLA-DRB3* in GSE65391 dataset K. Expression of *HLA-DRB3* in GSE110169 dataset L. Expression of *HLA-DRB3* in GSE108497 dataset

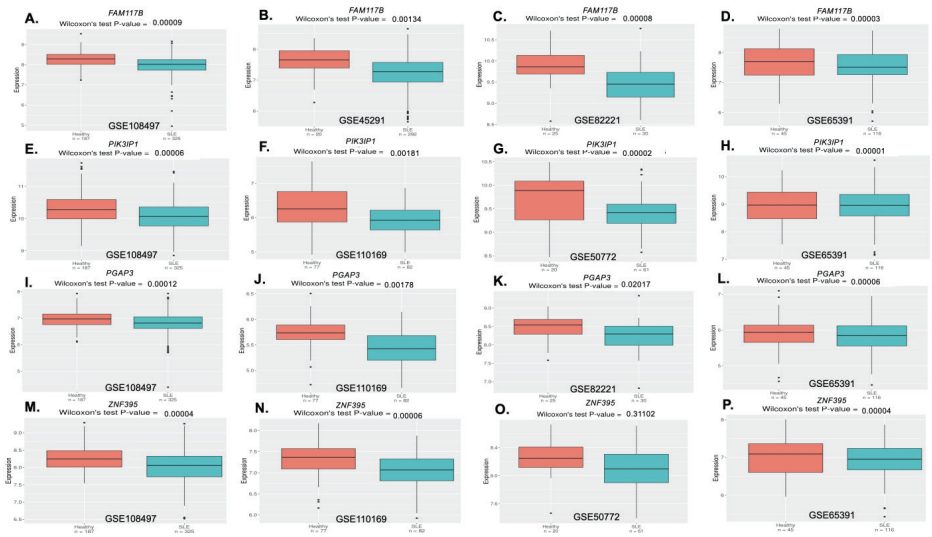

Figure 4: Expression profile of immune response family members in systemic lupus erythematosus (SLE) disease A. Expression of *FAM117B* in GSE108497 dataset B. Expression of *FAM117B* in GSE45291 dataset C. Expression of *FAM117B* in GSE82221 dataset D. Expression of *FAM117B* in GSE65391 dataset E. Expression of *PIK3IP1* in GSE108497 dataset F. Expression of *PIK3IP1* in GSE110169 dataset G. Expression of *PIK3IP1* in GSE50772 dataset H. Expression of *PIK3IP1* in GSE65391 dataset I. Expression of *PGAP3* in GSE108497 dataset J. Expression of *PGAP3* in GSE110169 dataset K. Expression of *PGAP3* in GSE82221 dataset L. Expression of *PGAP3* in GSE65391 dataset M. Expression of *ZNF395* in GSE108497 dataset N. Expression of *ZNF395* in GSE110169 dataset O. Expression of *ZNF395* in GSE50772 dataset P. Expression of *ZNF395* in GSE65391 dataset.

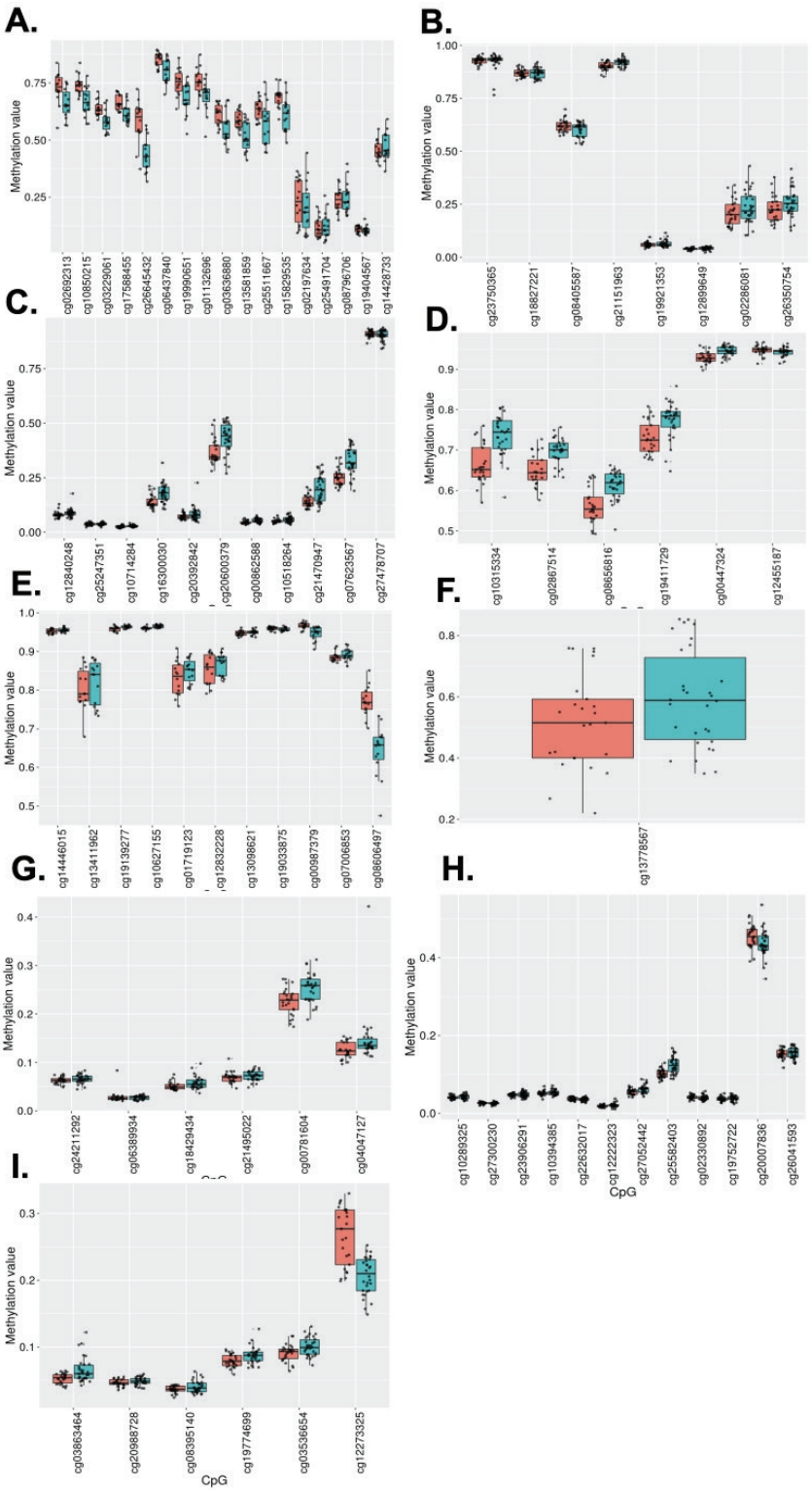

Figure 5: Overview of analyzed methylation sites and genomic organization of related genes. A. *HLA-DPA1* B. *HLA-DPB1* C. *HLA-DMB* D. *CCL5* E. *ZNF395* F. *HLA-DQA1* G. *FAM117B* H. *PGAP3* I. *PIK3IP1*. A boxplot illustrates the distribution of beta-values for individual CpG sites in both case and control samples. Each boxplot represents the beta values observed for a specific CpG site, with the middle line denoting the median value and the box encompassing the interquartile range. Red blots indicate healthy individuals and blue blots indicate systemic lupus erythematosus (SLE) patients

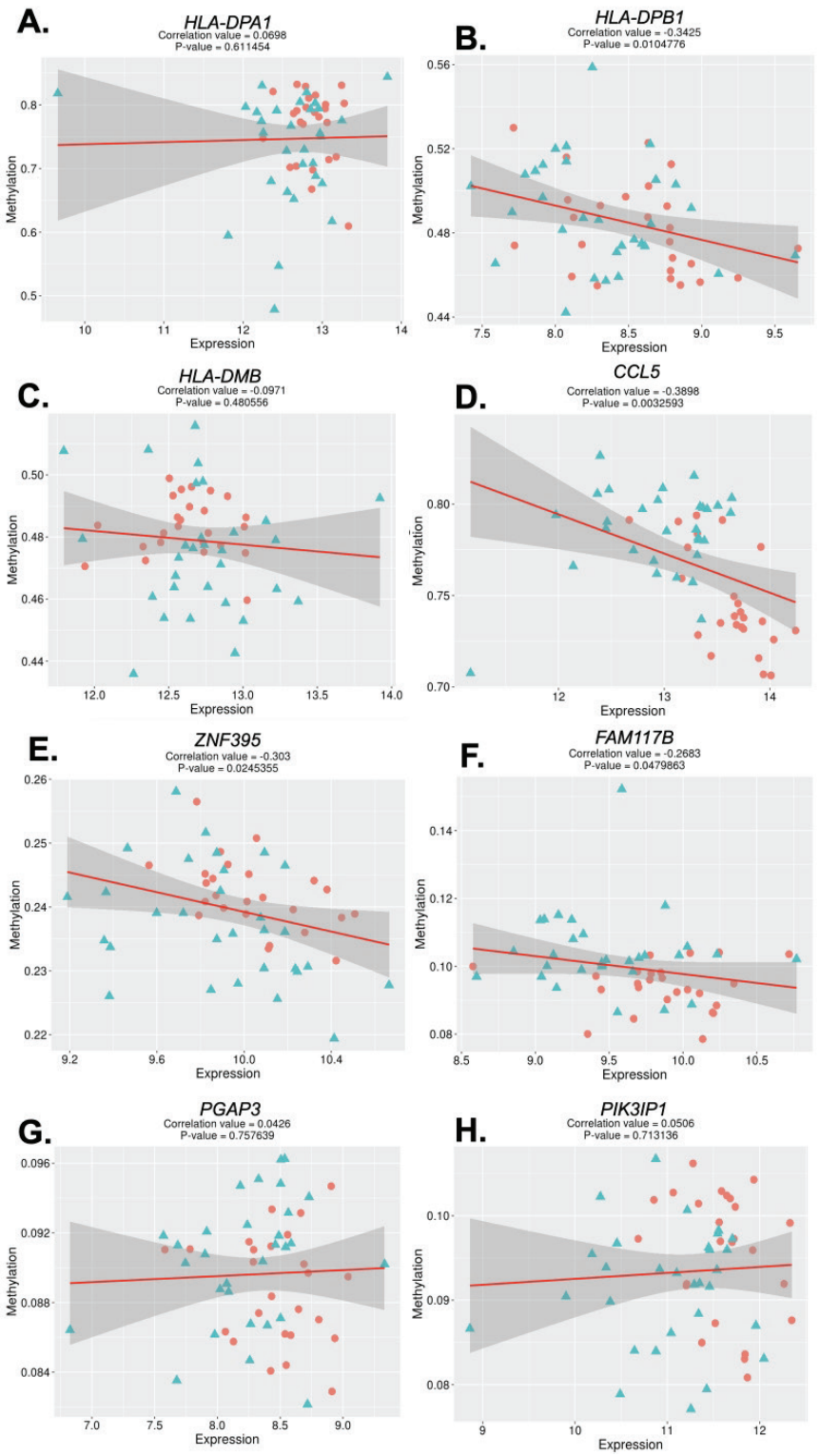

Figure 6: Correlation of methylation and expression of related genes. A. *HLA-DPA1* B. *HLA-DPB1* C. *HLA-DMB* D. *CCL5* E. *ZNF395* F. *FAM117B* G. *PGAP3* H. *PIK3IP1*. A scatter plot depicting the relationship between gene expression levels and mean methylation values of selected CpG sites is displayed. Each data point represents a sample, with the x-axis indicating the expression level of the gene and the y-axis representing the average methylation value across the specified CpG sites. Red blots indicate healthy individuals and blue blots indicate systemic lupus erythematosus (SLE) patients

in epigenetic investigations because of its activating potential. Against this backdrop, an inquiry was undertaken to assess the influence of ten genes implicated in immune response methylation on SLE pathology using data from the GSE82221 dataset.

These findings also revealed that 17 promoter-associated CpG islands were identified for *HLA-DPA1*, 8 for *HLA-DPB1*, 11 for *HLA-DMB*, six for *CCL5*, 11 for *ZNF395*, 1 for *HLA-DQA1*, six for *FAM117B*, 12 for *PGAP3*, and six for *PIK3IP1* in patients with SLE (Figure 5 A, B, C, D, E, F, G, H, I). Inconsistencies were observed among all 10 genes when comparing the methylation levels of genes across GSE82221. Specifically, high methylation levels were detected for *the HLA-DPA1, HLA-DPB1, HLA-DMB, CCL5, ZNF395*, and *HLA-DQA1* genes, whereas low methylation levels were observed for *FAM117B, PGAP3,* and *PIK3IP1*. Furthermore, the CpG islands exhibiting the highest levels of methylation were cg06437840, cg23750365, cg20600379, cg00447324, cg10627155, and cg13778567, respectively. The genes *PIK3IP1, FAM117B,* and *PGAP3* exhibited methylation levels well below 0.5 but did not demonstrate significant hypermethylation. In contrast, a specific subset of six genes, namely *HLA-DPA1, HLA-DPB1, HLA-DMB, CCL5, ZNF395,* and *HLA-DQA1,* maintained consistent methylation levels. The observed stability in methylation levels indicate persistent epigenetic alterations compared with the hypermethylation patterns noted across all samples within this particular subset.

Relationship between methylation status and HLA-DPB1, CCL5, FAM117B, and ZNF395 gene expression in SLE

The interaction between immune response gene expression and methylation status is complex and multifaceted. DNA methylation is typically related to reduced expression or gene silencing, especially in promoter regions. This relationship is influenced by several factors, including the specific genes involved, the methylation patterns of their regulatory regions, and the cellular and environmental contexts in which these genes are active.

This investigation aimed to explore the correlation between immune response gene expression and methylation status in SLE. The study revealed that alterations in the expression of four genes, namely *HLA-DPB1, CCL5, FAM117B*, and *PGAP3*, were linked to hypermethylation in the CpG islands of these genes. In particular, methylation of CpG sites in the promoter regions of these genes inhibited their expression levels (Figure 6). These results indicate that methylation plays a regulatory role in modulating the expression of immune response genes in SLE.

DISCUSSION

SLE is a complex inflammatory condition that affects various organs and has a known genetic component. Epigenetic mechanisms (DNA methylation, histone modification) and mutations (polymorphism) are crucial for the regulation of gene expression (10). Alterations in DNA methylation patterns contribute to the aberrant immune responses characteristic of SLE. Specifically, changes in DNA methylation levels of genes involved in the regulation of T cell function, activation of B cells, and clearance of immune complexes have been implicated in SLE pathogenesis (20). These alterations may disturb the equilibrium of immune response, generating autoantibodies and the inflammatory cascades characteristic of SLE (21). Despite the identification of genes exhibiting altered expression in SLE, the underlying causes of these changes remain unclear. Therefore, this study aimed to elucidate the relationship between gene expression related to immune response and the development of SLE. Additionally, specific CpG methylation sites associated with SLE in patients were identified through the analysis of the analysis of publicly available datasets, integrating clinical, laboratory, and biological factors.

HLA-DQA1 and *HLA-DMB* encode the alpha and beta chains of the HLA-D protein, a major histocompatibility complex (MHC) class II molecule. MHC class II molecules are pivotal in the immune system because they present antigens to T cells, initiating immune responses. Certain variants of these genes may be linked to an elevated risk of developing SLE (22-24). Studies have indicated that specific *HLA-DQ* and *HLA-DM* alleles are more common in individuals with SLE than in the general population (22, 25). In this study, the expression levels of *HLA-DQA1* and *HLA-DMB* were higher in patients with SLE than in controls. These alleles could contribute to the autoimmune response in SLE by presenting self-antigens to T cells, which in turn triggers the production of autoantibodies and inflammation.

HLA alleles can also stimulate an uncontrolled increase in the production of various cytokines, including tumor necrosis factor-alpha (TNF-α), interleukin-6 (IL-6), and interferon-gamma (IFN-γ), which play crucial roles in inflammation and immune responses (26). For instance, certain populations exhibit a heightened risk of SLE with *HLA-DR2, HLA-DR3*, and *HLA-DR4* alleles (23, 25). Shirakawa et al. demonstrated a notable decrease in the number of HLA-DR-positive monocytes and expression of HLA-DR antigens in active patients with SLE. These levels returned to normal in inactive SLE patients (25, 27). The diminished presence of HLA-DR-positive monocytes disrupts the regulation of immune response crucial for SLE development. The observed reduction in HLA-DR3 levels in this study might contribute to an aberrant immune response in patients with SLE, potentially intensifying disease progression (23, 25). Furthermore, Takona et al. noted a marked elevation in HLA-DP+ T-cell counts among patients with SLE compared with healthy individuals. Concurrently, another study indicated that elevated HLA-DP levels in patients with SLE were correlated with increased T cell frequency and insufficient IL-2 expression (28). Moreover, any alteration in carbon metabolism has been shown to downregulate genes involved in the hypermethylation of essential genes like *RFC1* and *MHC2TA* while also affecting other critical genes such as *HLA-DR* by altering promoter CpG island methylation (29). Considering these mutational and epigenetic influences, the decline in *HLA-DPA1, HLA-DPB1,* and *HLA-DRB3* gene expression noted in SLE patients in this investigation could be linked to post-transcriptional elements such as DNA hypermethylation and polymorphism.

CCL5 gene expression was downregulated in all datasets except the GSE61635 dataset. This dataset investigated gene expression in the blood of patients with SLE positive for RNP autoantibodies. The presence of RNP autoantibodies can disrupt the clearance of apoptotic cells, resulting in the release of self-antigens and subsequent activation of the immune system. Ultimately, RNP autoantibodies present in the blood of patients with SLE can disrupt immune responses, sustain inflammation, and play a role in the development of the disease (30). *FAM117B*, or Family with sequence similarity 117 member B, is a protein-coding gene. Its exact role in SLE has yet to be fully understood. This study revealed that *FAM117B* is downregulated in patients with SLE and is implicated in the pathogenesis of this disease. Upon encountering pathogen infection, the interferon (IFN) pathway activation triggers the upregulation of IFN-stimulated genes, including proinflammatory cytokines, essential for robust antiviral immune reactions. Nevertheless, aberrant expression of these genes can pose risks to the host. *ZNF395* has been recognized as a gene that operates independently of IFN but boosts the IFN-mediated expression of chemokine (31). In this study, posttranscriptional modifications influenced the expression of *ZNF395*, and its irregular expression could play a role in the development of SLE. These results emphasize the intricate role of immune dysregulation in SLE and underscore the importance of these genes in driving the disease process.

In the present study, a subset of genes with consistent methylation levels, including *HLA-DPA1, HLA-DPB1, HLA-DMB, CCL5, ZNF395,* and *HLA-DQA1, were* identified. Consistent methylation levels across all samples indicate that these genes were hypermethylated. Unlike methylation levels, gene silencing is often associated with hypermethylation, although this relationship is not always direct and may be influenced by additional regulatory mechanisms (32). Interestingly, the upregulation of hypermethylated genes, such as *CCL5, HLA-DQA1,* and *HLA-DMB*, was observed. The regulation of gene expression is influenced by various mechanisms beyond methylation, such as specific transcription factors and histone modifications, which can override the repressive effects of DNA methylation (33). Although promoter hypermethylation generally results in gene silencing, methylation at different sites may have contrasting effects, including increased gene expression. Despite the observed consistent methylation patterns in our analysis, the presence of technical and biological variability in high-throughput datasets like GSE61635 might influence gene expression differences in individual samples. These findings highlight the intricate nature of epigenetic regulation, indicating that hypermethylation does not always lead to gene silencing. Further experimental investigations are necessary to elucidate the specific mechanisms driving gene expression patterns in patients with SLE (34). The present study also identified *HLA-DPB1, CCL5, FAM117B,* and *ZNF395* as genes potentially regulated by methylation in SLE, with CpG methylation within their promoter regions likely exerting a suppressive effect on their expression levels. Aberrant DNA methylation is implicated as a contributing factor to the dysregulated expression of these genes in SLE, and other mechanisms, such as RNA interference, may also play a role. Further studies are needed to validate these findings and elucidate the precise regulatory mechanisms.

This study highlighted the complex network of immune response genes and their regulatory elements, providing valuable insights into the molecular mechanisms underlying SLE pathogenesis. Second, the potential use of epigenetic modifications, particularly DNA methylation, as biomarkers for disease diagnosis and prognosis of SLE was highlighted. By elucidating the role of specific genes and their epigenetic regulation in the development of SLE, this study provides a growing body of knowledge to better understand and manage this complex autoimmune disorder.

Limitations of the study

This study has several limitations. Despite extensive analyses across various cell and tissue types, further studies using additional cohorts and experimental models are required to confirm the results and determine their broader significance. Moreover, the cross-sectional design of this study precludes the establishment of causal relationships. The findings highlight the importance of longitudinal studies to elucidate the temporal patterns of gene expression and epigenetic regulation during the progression of SLE. Despite these limitations, these findings provide a solid foundation for future research efforts to understand the intricate mechanisms of SLE pathogenesis and identify novel therapeutic targets for this complex autoimmune disease.

CONCLUSION

This study underscores the intricate regulatory mechanisms of systemic lupus erythematosus (SLE), focusing on the roles of genetic and epigenetic factors. The present study revealed that alterations in DNA methylation patterns, particularly those of genes involved in immune response regulation, play a significant role in SLE pathogenesis. Notably, genes such as HLA-DQA1, HLA-DMB, CCL5, ZNF395, and others were found to exhibit consistent methylation levels, indicating that hypermethylation as a regulatory mechanism. The present study also highlighted the potential of specific CpG methylation sites and gene expression profiles as biomarkers for SLE diagnosis and prognosis. The identification of differentially expressed genes, such as HLA-DQA1, HLA-DMB, CCL5, FAM117B, and ZNF395, linked to immune response dysregulation provides valuable insights into the molecular mechanisms driving SLE. These findings emphasize the importance of further experimental investigations to validate the observed methylation patterns and elucidate the regulatory mechanisms.

Informed Consent: Since this study utilizes data from a publicly available database, no direct contact with human subjects was made, and informed consent was not required. The data was accessed by the terms of use provided by the database.

Peer Review: Externally peer-reviewed.

Conflict of Interest: The author have no conflict of interest to declare.

Financial Disclosure: The author declared that this study has received no financial support.

REFERENCES

1. Tian J, Zhang D, Yao X, Huang Y, Lu Q. Global epidemiology of systemic lupus erythematosus: a comprehensive systematic analysis and modelling study. Ann Rheum Dis 2023;82(3):351-6.
2. Ameer MA, Chaudhry H, Mushtaq J, Khan OS, Babar M, Hashim T, et al. An Overview of Systemic Lupus Erythematosus (SLE) Pathogenesis, Classification, and Management. Cureus 2022;14(10):e30330.
3. Ha E, Bae SC, Kim K. Recent advances in understanding the genetic basis of systemic lupus erythematosus. Semin Immunopathol 2022;44(1):29-46.
4. Ashraf Antar E, Sun C, Looger LL, Hirose M, Salama M, Khalil NM, et al. Genome-wide association study for systemic lupus erythematosus in an egyptian population. Front Genet 2022;13:948505.
5. Zharkova O, Celhar T, Cravens PD, Satterthwaite AB, Fairhurst AM, Davis LS. Pathways leading to an immunological disease: systemic lupus erythematosus. Rheumatology 2017;56(suppl_1):i55-66.
6. Davies EJ, Hutchings CJ, Hillarby MC, Donn RP, Cooper RG, Hay EM, et al. HLA-DP does not contribute towards susceptibility to systemic lupus erythematosus. Ann Rheum Dis 1994;53(3):188-90.
7. Pan L, Lu MP, Wang JH, Xu M, Yang SR. Immunological pathogenesis and treatment of systemic lupus erythematosus. World J Pediatr 2019;16(1):19-30.
8. McHugh J. New evidence for the "cusp theory" to explain HLA associations in SLE. Nat Rev Rheumatol 2022;18(10):552.
9. Richter P, Macovei LA, Mihai IR, Cardoneanu A, Burlui MA, Rezus E. Cytokines in Systemic Lupus Erythematosus-Focus on TNF-α and IL-17. Int J Mol Sci 2023;24(19):14413.
10. Farivar S, Shaabanpour AF. Effects of Major Epigenetic Factors on Systemic Lupus Erythematosus. Iran Biomed J 2018;22(5):294-302.
11. Tiffin N, Adeyemo A, Okpechi I. A diverse array of genetic factors contribute to the pathogenesis of Systemic Lupus Erythematosus. Orphanet J Rare Dis 2013;8:2.
12. Hedrich CM. Epigenetics in SLE. Curr Rheumatol Rep 2017;19(9):58.
13. Araki Y, Mimura T. Epigenetic Dysregulation in the Pathogenesis of Systemic Lupus Erythematosus. Int J Mol Sci 2024;25(2):1019.
14. Pan L, Lu MP, Wang JH, Xu M, Yang SR. Immunological pathogenesis and treatment of systemic lupus erythematosus. World J Pediatr 2019;16(1):19-30.
15. Barrett T, Wilhite SE, Ledoux P, Carlos Evangelista, Irene F Kim, Maxim Tomashevsky, et al. NCBI GEO: archive for functional genomics data sets--update. Nucleic Acids Res 2013;41(Database issue):D991-5 .
16. Li S, Rouphael N, Duraisingham S, Romero-Steiner S, Presnell S, Davis C, et al. Molecular signatures of antibody responses derived from a systems biology study of five human vaccines. Nat Immunol 2014;15(2):195-204
17. Martorell-Marugán J, López-Domínguez R, García-Moreno A, Toro-Domínguez D, Villatoro-García JA, Barturen G, et al. A comprehensive database for integrated analysis of omics data in autoimmune diseases. BMC Bioinformatics 2021;22(1):343.
18. Love MI, Huber W, Anders S. Moderated estimation of fold change and dispersion for RNA-seq data with DESeq2. Genome Biol 2014;15:550.
19. R Core Team. R: A Language and Environment for Statistical Computing [Internet]. Vienna, Austria; 2016. Available from: https://www.R-project.org/
20. Hedrich CM, Mäbert K, Rauen T, Tsokos GC. DNA methylation in systemic lupus erythematosus. Epigenomics 2017;9(4):505-25.
21. Oaks Z, Perl A. Metabolic control of the epigenome in systemic Lupus erythematosus. Autoimmunity 2014;47(4):256-64.
22. Yen JH, Chen CJ, Tsai WC, Tsai JJ, Ou TT, Liu HW. HLA-DMA and HLA-DMB genotyping in patients with systemic lupus erythematosus. J Rheumatol 1999;26(9):1930-3.
23. Kwon Y-C, Chun S, Kim K, Mak A. Update on the Genetics of Systemic Lupus Erythematosus: Genome-Wide Association Studies and Beyond. Cells 2019;8(10):1180.
24. Horton R, Wilming L, Rand V, Lovering RC, Bruford EA, Khodiyar VK, et al. Gene map of the extended human MHC. Nat Rev Genet 2004;5(12):889-99.
25. Rasouli SA, Tahamoli RA, Behzad M, Hajilooi M, Solgi G. Clinical Relevance of HLA-DRB1 and -DQB1 Alleles in Iranian Systemic Lupus Erythematosus Patients. Iran J Allergy Asthma Immunol 2021;20(1):67-75.
26. Richter P, Macovei LA, Mihai IR, Cardoneanu A, Burlui MA, Rezus E. Cytokines in Systemic Lupus Erythematosus-Focus on TNF-α and IL-17. Int J Mol Sci 2023;24(19):14413.
27. Shirakawa F, Yamashita U, Suzuki H. Decrease in HLA-DR-positive monocytes in patients with systemic lupus erythematosus (SLE). J Immunol 1985;134(6):3560-2.
28. Tokano Y, Hishikawa T, Hirose T, Sekigawa I, Hashimoto H, Okumura K, et al. HLA-DP-Positive T Cells in Patients with Systemic Lupus Erythematosus. Autoimmunity 1990;5(3):179-83.
29. Rupasree Y, Naushad SM, Rajasekhar L, Kutala VK. Epigenetic modulation of RFC1, MHC2TA and HLA-DR in systemic lupus erythematosus: association with serological markers and six functional polymorphisms of one-carbon metabolic pathway. Gene 2014;536(1):45-52.
30. Liao X, Pirapakaran T, Luo XM. Chemokines and Chemokine Receptors in the Development of Lupus Nephritis. Mediators Inflamm 2016;2016:6012715.
31. Schroeder L, Herwartz C, Jordanovski D, Steger G. ZNF395 Is an Activator of a Subset of IFN-Stimulated Genes. Mediators Inflamm 2017;2017:1248201.
32. Caldiran, FY, Berkel, C, Deveci, K, Cacan, E. In silico analysis of expression and DNA methylation profiles of NLRP13 inflammasome in tumor cells. Human Gene 2022;33:201067.
33. Caldiran F, Deveci K, Cacan E. Epigenetic insights into Familial Mediterranean Fever: Increased RGS10 expression and histone modifications accompanies inflammation in familial Mediterranean fever disease. Gene 2024;906:148222.
34. Hedrich CM, Mäbert K, Rauen T, Tsokos GC. DNA methylation in systemic lupus erythematosus. Epigenomics 2017;9(4):505-25.

RESEARCH ARTICLE / ARAŞTIRMA MAKALESİ
Journal of Advanced Research in Health Sciences /
Sağlık Bilimlerinde İleri Araştırmalar Dergisi 2024
DOI: 10.26650/JARHS2024-1435041

INVESTIGATION OF THE EFFECT OF PLA2R1 POLYMORPHISM IN PATIENTS WITH MEMBRANOUS NEPHROPATHY

MEMBRANÖZ NEFROPATİLİ HASTALARDA PLA2R1 POLİMORFİZMİNİN ETKİSİNİN ARAŞTIRILMASI

Aida ADIKOZALOVA[1], Sebahat USTA AKGÜL[2], Erol DEMİR[3], Hayriye ŞENTÜRK ÇİFTCİ[2], Fatma SAVRAN OĞUZ[2], Halil YAZICI[3], Çiğdem KEKİK ÇINAR[2]

[1]İstanbul University, Institute of Graduate Studies in Health Sciences, İstanbul, Türkiye
[2]İstanbul University, İstanbul Faculty of Medicine, Department of Medical Biology, İstanbul, Türkiye
[3]İstanbul University, İstanbul Faculty of Medicine, Department of Internal Diseases, Division of Nephrology, İstanbul, Türkiye

ORCID ID: A.A. 0000-0003-2897-3624; S.U.A. 0000-0003-0176-3344; E.D. 0000-0003-0128-5645; H.Ş.Ç. 0000-0003-3507-482X; F.S.O. 0000-0002-6018-8936; H.Y. 0000-0003-2526-3483; Ç.K.Ç. 0000-0003-2098-381X

Citation/Atıf: Adikozalova A, Usta Akgül S, Demir E, Şentürk Çiftci H, Savran Oğuz F, Yazıcı H, et al. Investigation of the effect of PLA2R1 polymorphism in patients with membranous nephropathy. Journal of Advanced Research in Health Sciences 2024;7(3):160-164.https://doi.org/10.26650/JARHS2024-1435041

ABSTRACT

Objective: Membranous nephropathy (MN) is the most common cause of nephrotic syndrome in adults. Phospholipase A2 receptor (PLA2R1) is a glycoprotein belonging to the mannose receptor family (~180 kDa). PLA2R1 was found to be associated with idiopathic MN pathogenesis, and the presence of PLA2R1 antibodies was supported by the diseases. In this study, the association of PLA2R1 rs35771982 with membranous nephropathy was investigated.

Material and Methods: The study included 88 patients diagnosed with MN and 101 healthy individuals unrelated to the patients. The PLA2R1 rs35771982 levels of the patient and control groups were examined using the Real Time PCR (Polymerase Chain Reaction) method.

Results: The comparison of the patients with healthy controls in this study showed that the rs35771982 GG genotype was significantly higher in the patients. The genotype of rs35771982 in the Turkish population was found to be common to the CG genotype.

Conclusion: Our findings revealed that the PLA2R1 rs35771982 GG genotype is associated with susceptibility to MN.

Keywords: Membranous nephropathy, PLA2R1, rs35771982, Real-time PCR

ÖZ

Amaç: Membranöz nefropati (MN), erişkinlerde nefrotik sendromun en sık nedenidir. Fosfolipaz A2 reseptörü (PLA2R1), mannoz reseptör ailesine (~180 kDa) ait glikoproteindir. PLA2R1, idiyopatik MN patogenezi ile ilişkili bulunmuş, PLA2R1 antikorlarının varlığının hastalıkla ilişkisi desteklenmiştir. Bu çalışmada PLA2R1 rs35771982'nin Membranöz Nefropati ile ilişkisi araştırıldı.

Gereç ve Yöntemler: Çalışmaya MN tanısı alan 88 hasta ve bu hastalarla ilişkisi olmayan 101 sağlıklı birey dahil edildi. Hasta ve kontrol gruplarının PLA2R1 rs35771982'si Real Time PCR (Polimeraz Zincir Reaksiyonu) yöntemi ile incelendi.

Bulgular: Hastaları sağlıklı kontrollerle karşılaştırdığımızda rs35771982 GG genotipinin hastalarda anlamlı derecede yüksek olduğu görüldü. Türk popülasyonunda rs35771982 CG genotipinin yaygın olduğu bulundu.

Sonuç: PLA2R1 rs35771982 GG genotipinin MN'ye duyarlılıkla ilişkili olduğu bulundu.

Anahtar Kelimeler: Membranöz nefropati, PLA2R1, rs35771982, Gerçek zamanlı PZR

Corresponding Author/Sorumlu Yazar: Aida ADIKOZALOVA **E-mail:** aslanaida8593@gmail.com

Submitted/Başvuru: 29.02.2024 • **Revision Requested/Revizyon Talebi:** 28.04.2024 • **Last Revision Received/Son Revizyon:** 22.09.2024 • **Accepted/Kabul:** 07.10.2024 • **Published Online/Online Yayın:** 24.10.2024

INTRODUCTION

Membranous nephropathy (MN) is a glomerular pathology that is the most common cause of idiopathic nephrotic syndrome in adults (1). Kidney biopsy is used in the definitive diagnosis of the disease. Considering that biopsy protocols differ in many countries, there are regional differences in the incidence of the disease. The disease is seen twice as often in men compared with the level in women. MN is a chronic disease and spontaneous remission occurs in approximately 30% of the patients. Despite spontaneous remission, 30-40% of MN patients progress to end-stage renal disease (ESRD) within 5 to 15 years (2). Approximately 75% of membranous nephropathy cases are idiopathic (Primary MN-IMN). Secondary MN is associated with autoimmune diseases, infection, and malignancies.

Phospholipase receptor (PLA2R1) is a type I transmembrane receptor that is a member of the mannose receptor family and has been identified as a target podocyte antigen involved in membranous nephropathy. Researchers have shown that the circulating antibodies of the IgG4 subtype against the epitope in PLA2R develop in 70-80% of patients with idiopathic MN (3). Some studies have shown that polymorphisms in the PLA2R1 gene may have a direct effect on the function of the gene (4). The rs35771982 variants are the conversion of the Guanine (G) allele to Cytosine (C) in exon 5 of the gene, which causes the replacement of Histidine with Aspartic acid at position 300 of the PLA2R protein. The G allele of rs35771982 in exon 5 results in a residue change (H300D) at the second of the 8 CTLDs in the protein structure. They reported that this change reduces the collagen-binding activity of cells and may alter antigenicity (5). Several studies have shown that this SNP locus is significantly associated with IMN in Korea, Taiwan, European Caucasians, Beijing, North American Caucasians, and the Indian population (6-10). Two different Chinese cohorts confirmed that the variations in PLA2R1 SNPs (rs35771982, rs4664308, rs3749117) were the risk factors for idiopathic membraneous nephropathy (11, 12).

Researchers studying IMN patients suggested that the G allele of SNP rs35771982 was more selectively expressed in patients than in the controls. The rs35771982 CC genotype is protective, and the rs35771982 GG genotype is a high-risk genotype (7).

Based on the conducted studies, we suggest that the rs35771982 genotype in the gene of the transmembrane protein PLA2R1, which causes podocyte damage, may have an effect on protein function. For this purpose, the association of PLA2R1 rs35771982 with membranous nephropathy was investigated.

MATERIAL AND METHOD

Patients and controls

Eighty-eight patients who presented to the Istanbul Faculty of Medicine, Department of Nephrology and were diagnosed with MN under biopsy were included in the study. One tube of blood, 5 cc EDTA (Ethylenediamine tetraacetic acid) was drawn from the patients. The clinicopathological findings of the patients were obtained from the Nephrology Department. The control group included 101 healthy individuals aged over 18 years and younger than 70 years who had no consanguineous relationship with each other and had no diagnosed kidney disease in their family. One tube of blood with 5 cc EDTA was collected from the control groups included in the study. After the ethics committee approval was obtained, the informed consent form was obtained from the volunteers (patients and healthy individuals) included in the study. This study was approved by the Istanbul Medical Faculty Clinical Research Ethics Committee (Date: 28.09.2017, No: 16).

rs35771982 genotyping

Blood samples were centrifuged immediately after being collected. EDTA tubes were used to isolate DNA (EZ1, QİAgen) and stored at 20 °C until the study period. The rs35771982 genotyping was performed with the Real Time Polymerase Chain Reaction (RT-PCR) method using the TaqMan SNP Genotyping (Thermo Scientific, Appliedbiosystems, Carlsbad, CA USA) kit. The probes used in this study were gene- specific FAM labelled MGB (minor Groove binder) probes. TaqMan MGB probes contain an MGB moiety at the 3' end, increasing the probe's melting temperature (Tm) and stabilising probe/target hybrids. TaqMan Universal Master Mix II was used. The results were read using the real-time PCR (Rotor Gene Q) instrument, which can read fluorescence by way of VIC and FAM channels. The sequence used is forward. (CCATCAGACCACTGCCAGCCAGCGT **[C/G]** TTCATCCAGCTGATTGAGGCCCATC)

Statistical analysis

Statistical analysis of the data was performed using the Statistical Package for the Social Sciences version 28.0 (IBM SPSS Corp., Armonk, NY, USA) software programme. Descriptive analysis and descriptive statistical methods were used. In the statistical analysis of the data, continuous data were tested using the Kolmogorov-Smirnov test for normality distribution. The mean ± standard deviations of the data in normal distribution were used. The control and patient groups were in Hardy–Weinberg balance. The chi-square test was used to compare the genotype between the patient and control groups. Chi-square and Fisher's exact tests were used to evaluate the categorical data within the patient group. The chi-square test was used to compare the genotype between the patient and control groups. The chi-square test was used for the odd ratio. One-way ANOVA test was used to measure the P value in table 3. Results were expressed as percentage values. p values<0.05 were considered statistically significant.

RESULTS

The mean age of the patient group was 53.59±13.82 years (age range 25-77y), while the mean age at diagnosis was 46.30±13.53years (age range 19-70y). The patient group consisted of 51 men (58%) and 37 women (42%). In our study, the mean age of 101 healthy individuals was 40.76±12.5 years. 49 men (48.5%) and 52 women (51.5%) were included in the control group. No statistical significance was observed in terms of gender and age in the evaluation of the patient and control groups (Table 1).

Table 1: Demographic and clinical data of the study groups

		Patient group	Control group
		mean±SD	mean±SD
Age		53.59±13.82	40.76±12.5
Age at diagnosis		46.3±13.5	
Gender	Male	51	49
	Female	37	52
BMI (kg/m^2)		78.90±14.7	
Systolic BP (mmHg)		131.42±19.2	
Diastolic BP (mmHg)		81.13±12.5	
Serum albumin (g/dl)		2.80±0.8	
Serum creatinine (mg/dl)		0.9±0.4	
Serum creatinine (mg/dl) follow-up		1.2±1.1	
Haemoglobin (g/dl)		12.93±2.3	
eGFR (ml/min/1.73m^2)		102.21±52.1	
Proteinuria		5677.79±3545.6	
Proteinuria follow-up		2869.82±3003.5	

BMI: Body Mass Index, Systolic BP: Systolic Blood Pressure, Diastolic BP: Diastolic Blood Pressure, eGFR: Glomerular Filtration Rate, *: p<0.05

Table 2: rs35771982 genotype and allele distribution in the patient and control groups

Genotypes	Patient group	Control group	OR	95%CI	p
	n: 88 (%)	n: 101 (%)			
CC	4 (4.5%)	9 (8.9%)	0.644	0.281-1.479	0.265
CG	40 (45.5%)	76 (75.3%)	0.524	0.388-0.708	**0.0001**
GG	44 (50.0%)	16 (15.8%)	2.150	1.618-2.857	**0.0001**
CG + CC vs GG	44 (50%)	85 (84.2%)	0.188	0.095-0.370	**0.0001**
Alleles	n:176 (%)	n:202 (%)			
C	48 (27.3%)	94 (%46.5)	0.623	0.481-0.807	0.828
G	128 (72.7%)	108 (53.5%)			
HWEp	0.171	0.052			

C: Cytosine, G: Guanin, HWEP: Hardy Weinberg, *: p<0.05

Table 3: Correlation of rs35771982 genotypes with clinical parameters

	CC	CG	GG	p
	mean±SD	mean±SD	mean±SD	
Age(years)	54.8±13.3	53.1±14	45.3±18	0.403
GDF-15	6448±5415	5915±3156	9613±6527	0.303
Proteinuria	5186±2735	6279±4362	5180±1996	0.395
Proteinuria tracing	2878±2615	2989±3440	1380±2183	0.678
Creatinine	0.86±0.35	0.95±0.53	0.81±0.45	0.595
Creatinine tracing	1.1±0.92	1.09±0.77	2.85±4.14	***0.01***
eGFR	95.9±35.5	107.1±63.6	122±77.8	0.457

GDF-15: Growth Differentiation Factor-15, eGFR: Glomerular Filtration Rate, C: Cytosin, G: Guanin, *: p<0.05

Distribution of the rs35771982 genotype in the patient and control groups

The variant homozygous GG genotype (p=0.0001) in the patients and the heterozygous CG genotype (p=0.0001) were found to be significantly higher in the control group. Although the wild CC genotype was numerically higher in the control group, there was no significant difference between the patient and control groups (p=0.05) (Table 2).

Relationship of the genotypes with the clinical parameters

Considering all genotypes of rs35771982, no significance was found between serum GDF-15 level, gender, age, serum creatinine, proteinuria, post-follow-up proteinuria,and eGFR. However, in patients with the CC genotype, the creatine value was found to be significantly higher after follow-up (p=0.01) (Table 3).

DISCUSSION

Membranous nephropathy (MN) is characterised with subepithelial immune complex deposition and thickening of the glomerular basement membrane. MN is typically a disease of adult age and is more common among men compared with the level in women. The progression of the disease is more rapid in older men diagnosed with membraneous nephropathy (13). No significant difference was detected in terms of gender between the patients included in this study. In addition, we found no correlation between disease progression and gender and age. The possible reason may be the difference in the progression of the disease and the smaller number of patients in the advanced stage.

Some studies have shown that polymorphisms in the PLA2R1 gene may have direct effects on the function of the gene. Studies with patients with MN have shown that PLA2R1 SNPs may be associated with the aetiology of the disease. In a study conducted in the Caucasus, researchers have shown that the rs35771982 GG genotype has a strong effect on anti-PLA2R1-positive patients compared with the effect on the negative patients. In the same study, PLA2R1 variants were evaluated in African Americans and no association was detected with the disease (5). In another study, the rs35771982 CC genotype was found to be significantly higher in idiopathic MN patients compared with the level in the control group (6). In a study conducted in China, researchers found that the CC genotype was disease-related and correlated with anti-PLA2R1 positivity (14). In another study, researchers found that the combination of the GG genotype at rs35771982 and AA genotype at rs2715928 was the highest risk of IMN (15). In this study, the evaluation of the rs35771982 genotypes showed that the GG genotype in patients was found to be significant compared with the control group, consistent with the literature. The heterozygous CG genotype was found to be statistically significant in the control group.

The rs35771982 G allele was reported to be a risk marker for the disease, and the C allele is protective in Japanese and Chinese populations (16, 17). A study conducted in the Caucasus found that the G allele was associated with the disease, while a study conducted in China found that the C allele was associated with the disease (5, 14). No significance was found in the allele basis comparison of the patient and control groups included in our study.

No relationship was found between the rs35771982 variants and renal survival and clinical parameters. Disease progression of the CG genotype in the Chinese population in Taiwan was correlated with a low remission rate. No significant difference was found in the gender distribution, age, body mass index, systolic/diastolic blood pressure, serum albumin and creatine levels, haematuria and proteinuria of the rs35771982 variants (7). Thiri et al. stated that the relationship of both alleles of rs35771982 with the disease was independent of the clinical symptoms (16). In our study, although 27 of 39 patients with the CG genotype entered remission, no statistical significance was found. No significant difference was found between the rs35771982 genotypes with gender, age, proteinuria, eGFR and creatine level.

In conclusion; the aim of our study was to determine whether the rs35771982 variant could be used as a serum biomarker that would enable us to diagnose patients with MN. More detailed and larger population research is needed to define the rs35771982 GG genotype as a biomarker that can be used in the diagnosis of the disease. Our study will also be able to eliminate the lack of data regarding the frequencies of rs35771982 variants, which have not been previously studied in the Turkish population.

Ethics Committee Approval: Ethics committee approval was received for this study from the ethics committee of Istanbul Medical Faculty Clinical Research Ethics Committee (Date: 28.09.2017, No: 16).

Informed Consent: After the ethics committee approval was obtained, the informed consent form was obtained from the volunteers (patients and healthy individuals) included in the study.

Peer Review: Externally peer-reviewed.

Author Contributions: Conception/Design of Study- A.A., Ç.K.Ç., H.Y., F.S.O.; Data Acquisition- A.A., H.Y., E.D.; Data Analysis/Interpretation- A.A., Ç.K.Ç., S.U.A., H.Ç.Ş.; Drafting Manuscript- A.A., Ç.K.Ç.; Critical Revision of Manuscript- F.S.O., H.Y., Ç.K.Ç.; Final Approval and Accountability- F.S.O., Ç.K.Ç.

Conflict of Interest: The authors have no conflict of interest to declare.

Financial Disclosure: The study was funded with the approval of Istanbul University Scientific Research and Project (BAP) commission with code number TYL-2018-32358.

REFERENCES

1. Stanescu HC, Arcos-Burgos M, Medlar A, Bockenhauer D, Kottgen A, Dragomirescu L, et al. Risk HLA-DQA1 and PLA2R1 alleles in idiopathic membranous nephropathy. N Engl J Med 2011;364(7):616-26.

2. Lai WL, Yeh TH, Chen PM, Chan CK, Chiang WC, Chen YM, et al. Membranous nephropathy: a review on the pathogenesis, diagnosis, and treatment. J Formos Med Assoc 2015;114(2):102-11.
3. Beck LHJr, Bonegio RG, Lambeau G, Beck DM, Powell DW, Cummins TD, et al. M-type phospholipase A2 receptor as target antigen in idiopathic membranous nephropathy. N Engl J Med 2009;361(1):11-21.
4. Ancian P, Lambeau G, Mattéi MG, Lazdunski M. The Human 180-kDa Receptor for Secretory Phospholipases a2 molecular clonıng, ıdentıfıcatıon of a secreted soluble form, expressıon, and chromosomal localızatıon. J Biol Chem 1995;270(15):8963-70.
5. Saeed M, Beggs ML, Walker PD, Larsen CP. PLA2R-associated membranous glomerulopathy is modulated by common variants in PLA2R1 and HLA-DQA1 genes. Genes Immun 2014;15(8):556-61.
6. Kim S, Chin HJ, Na KY, Kim S, Oh J, Chung W, et al. Single nucleotide polymorphisms in the phospholipase A2 receptor gene are associated with genetic susceptibility to idiopathic membranous nephropathy. Nephron Clin Pract 2011;117(3):c253-8.
7. Liu YH, Chen CH, Chen SY, Lin YJ, Liao WL, Tsai CH, et al. Association of phospholipase A2 receptor 1 polymorphism with idiopathic membranous nephropathy in Chinese patients in Taiwan. J Biomed Sci 2010;17(1):81.
8. Coenen MJ, Hofstra JM, Debiec H, Stanescu HC, Medlar AJ, Stengel B, et al. Phospholipase A2 receptor (PLA2R1) sequence variants in idiopathic membranous nephropathy. J Am Soc of Nephrol 2013;24(4):677-83.
9. Lv J, Hou W, Zhou X, Liu G, Zhou F, Zhao N, et al. Interaction between PLA2R1 and HLA-DQA1 variants associates with anti-PLA2R antibodies and membranous nephropathy. J Am Soc Nephrol 2013;24(8):1323-9.
10. Ramachandran R, Kumar V, Kumar A, Yadav AK, Nada R, Kumar H, et al. PLA2R antibodies, glomerular PLA2R deposits and variations in PLA2R1 and HLA-DQA1 genes in primary membranous nephropathy in South Asians. Nephrol Dial Transplant 2016;31(9):1486-93.
11. Wang F, Wang TT, Liang XW, Lu JD, Xie QH, Chen RY, et al. PLA2R1 and HLA-DQA1 gene variations in idiopathic membranous nephropathy in South China. Ann Acad Med Singap 2021;50(1):33-41.
12. Tian CX, Li L, Qiu P, Qiu YR. Association of SNPs in PLA2R1 with idiopathic and secondary membranous nephropathy in two Chinese cohorts. Br J Biomed Sci 2020;77(1):24-8.
13. Zhu H, Han Q, Zhang D, Wang Y, Gao J, Yang X, et al. The clinicopathological features of patients with membranous nephropathy. Int J Nephrol Renovasc Dis 2018;18(11):33-40.
14. Zhou GY, Liu F, Zhang WL. Association of single nucleotide polymorphism in M-type phospholipase A2 receptor gene with membranous nephropathy. Zhonghua Yi Xue Yi Chuan Xue Za Zhi 2013;30(6):706-10.
15. Liu X, Xu W, Yu C, Wang M, Liu R, Xie, R. Associations between m-type phospholipase A2 receptor, human leukocyte antigen gene polymorphisms and idiopathic membranous nephropathy. Bioengineered 2021;12(1):8833-8844.
16. Thiri M, Honda K, Kashiwase K, Mabuchi A, Suzuki H, Watanabe K, et al. High-density association mapping and interaction analysis of PLA2R1 and HLA regions with idiopathic membranous nephropathy in Japanese. Sci Rep 2016;6(1):38189.
17. Kaga H, Komatsuda A, Omokawa A, Okuyama S, Mori K, Wakui H, et al. Analysis of PLA2R1 and HLA-DQA1 sequence variants in Japanese patients with idiopathic and secondary membranous nephropathy. Clin Exp Nephrol 2018;22(2):275-82.

RESEARCH ARTICLE / ARAŞTIRMA MAKALESİ
Journal of Advanced Research in Health Sciences / Sağlık Bilimlerinde İleri Araştırmalar Dergisi 2024
DOI: 10.26650/JARHS2024-1389533

EFFECT OF TWO DIFFERENT CARE PRODUCTS ON PREVENTION OF INCONTINENCE-ASSOCIATED DERMATITIS IN PATIENTS

İNKONTİNANSLA İLİŞKİLİ DERMATİTİN ÖNLENMESİNDE İKİ FARKLI BAKIM ÜRÜNÜNÜN ETKİSİNİN İNCELENMESİ

Gülsün ÖZDEMİR AYDIN[1], Hatice KAYA[2]

[1]İstanbul University Faculty of Nursing, Department of Fundamentals of Nursing, İstanbul, Türkiye
[2]İstanbul University-Cerrahpaşa, Faculty of Florence Nightingale Nursing, İstanbul, Türkiye

ORCID ID: G.Ö.A. 0000-0003-0550-3195; H.K. 0000-0002-8427-0125

Citation/Atıf: Özdemir Aydın G, Kaya H. Effect of two different care products on prevention of incontinence-associated dermatitis in patients. Journal of Advanced Research in Health Sciences 2024;7(3):165-173. https://doi.org/10.26650/JARHS2024-1389533

ABSTRACT

Objectives: Incontinent individuals continue to face a major health concern known as Incontinence-Associated Dermatitis (IAD). After a stroke or other neurological condition, the chance of developing IAD increases. Prevention of IAD is critical for maintaining skin integrity. The aim of this study was to examine the effectiveness of two different care products used in the prevention of IAD.

Material and Methods: An experimental study was conducted. Incontinent patients were randomly assigned to one of two groups: intervention (experimental group received perineal treatment with dimethicone pomade impregnated wipes, n=66) or control (control group received perineal care with soapy water, n=66). The rate of IAD was determined.

Results: During the 10-day follow-up period, 31.8% of the experimental group's patients acquired IAD, whereas 40.9% of the control group's patients got IAD. However, no significant change was observed. IAD was predominantly seen to grow on the curve between the genitals and the thigh in the experimental group (15.2%), whereas labia/scrotum was observed to develop in the control group (27.3%). According to the IAD development, there was a substantial difference in the number of semi-formed and liquid stools.

Conclusion: There was no statistical difference between the two different care products in the prevention of IAD. However, it is important to study the continuation of nursing care. It may be recommended to repeat the study in clinics where incontinence is common, with a longer follow-up.

Keywords: Incontinence, incontinence-associated dermatitis, nursing care, care products

ÖZ

Amaç: İnkontinansla ilişkili dermatit (İİD) inkontinansı olan hastalarda ciddi bir sağlık sorunu olmaya devam etmektedir. İnme veya diğer nörolojik hastalıklardan sonra İİD gelişme riski artmaktadır. İİD'nin önlenmesi, cilt bütünlüğünün kontrolünü sağlama da oldukça önemlidir. Bu araştırmanın amacı, İİD'nin önlenmesinde kullanılan iki farklı bakım ürününün etkinliğini incelemektir.

Gereç ve Yöntem: Deneysel tasarımda planlanan bu çalışmada; inkontinansı olan hastalar deney grubu (dimetikon pomad emdirilmiş mendil ile perineal bakım yapılan grup, n=66) ve kontrol grubuna (rutin olarak uygulanan sabunlu su ile perineal bakım yapılan grup, n=66) rastgele ayrıldı. İİD oranı değerlendirildi. Bu gruplara ait veriler karşılaştırıldı.

Bulgular: Hastalar 10 gün takip edildi. Deney grubundaki hastaların %31,8'inde, kontrol grubundaki hastaların %40,9'unda İİD geliştiği görüldü. Ancak, anlamlı bir fark tespit edilmedi. Deney grubunda en çok genital bölge ile uyluk arasındaki çizgide (%15,2), kontrol grubunda labia/skrotumda (%27,3) İİD geliştiği gözlendi. Sıvı ve yarı şekilli dışkılama sayısı arttıkça İİD gelişiminde istatistiksel olarak anlamlı farklılık saptandı.

Sonuç: İİD'nin önlenmesinde iki farklı bakım ürünü arasında istatistiksel olarak fark saptanmadı. Ancak hemşirelik bakımının sürdürülmesi adına bu çalışma önemlidir. Araştırmanın daha uzun süreli izlenerek inkontinansın sık görüldüğü kliniklerde tekrarlanması önerilebilir.

Anahtar Kelimeler: İnkontinans, inkontinans ile ilişkili dermatit, hemşirelik bakımı, bakım ürünleri

Corresponding Author/Sorumlu Yazar: Gülsün ÖZDEMİR AYDIN **E-mail:** gulsunoz@istanbul.edu.tr

Submitted/Başvuru: 07.12.2023 • **Revision Requested/Revizyon Talebi:** 11.02.2024 • **Last Revision Received/Son Revizyon:** 11.03.2024 • **Accepted/Kabul:** 25.03.2024 • **Published Online/Online Yayın:** 22.10.2024

INTRODUCTION

IAD is a type of incontinence-related dermatitis that causes discomfort, vesiculation, and itching in the perineal area and upper and lower hip skin because of urine or stool contact. It affects approximately 30% of neurological patients with urinary or faecal incontinence. IAD has previously been linked to incontinence in studies (1-5). Diaper change frequency, perineal skin contact time of urine or faeces, high humidity in the perineal area, deterioration of the pH structure of the skin, increased bacterial colonisation in this region, friction, used drugs, individual laboratory values, nutrition, decreased movement, changes in consciousness level, and an increase in BMI are all linked to more severe IAD (BMI). IAD skin damage is common in neurology patients (6-10). When compared with other types of skin damage, IAD is associated with a higher death rate, a worse quality of life, and greater health-care expenses, which makes IAD more urgent. IAD levels were shown to be higher in neurology patients in previous investigations (11-14). On the other hand, IAD may be avoided with good nursing care and the correct care items (7, 15-19). Perineal skin care is commonly conducted in our nation with a non-rinse wash cloth in many hospitals' perineal care protocols. The patient, patient family, and nurses, in addition to the washcloth ratio, utilise ready-to-use perineal wipes. Although numerous treatments are used to clean the perineal area, no research has been conducted to determine whether one prevents dermatitis in neurological patients who have a high rate of dermatitis (20, 21). It is clear that research conducted in other countries is aimed at evaluating the link between prevalence and incidence, as well as the variables that may play a role in the development of IAD; nevertheless, IAD is a relatively recent problem in Turkey (2, 20, 22). Although dermatitis is noticed in neurology clinics, it is clear that preventive measures are rarely used to their full potential (10, 12, 13, 21, 22). The purpose of this study was to determine whether perineal care products were more helpful in preventing incontinence-related dermatitis in patients who visited these clinics. Considering these findings, new care procedures were developed.

MATERIALS AND METHODS

Design

This experimental study was designed as an experimental study. Participants were assigned to the intervention and control groups.

Participants

The goal of the research was to determine how two different types of care items (disposable non-rinse wash cloths and dimethicone pomade cleaning wipes) affected the prevention of incontinence-related dermatitis and to inform nursing practises. The research was planned as an experimental study to determine whether perineal care with 3% dimethicone impregnated wipes may help patients with incontinence-related dermatitis who were hospitalised to neurology and neurosurgery units. Between January 2015 and March 2018, 132 individuals were asked to participate in the study. Individuals who did not match the inclusion criteria (n=564) were excluded from the study; these patients did not have incontinence, had a urinary catheter, and were able to use the restroom. The study included 132 patients who satisfied the study's inclusion criteria and were willing to participate (66 patients in the intervention group and 66 patients in the control group).

The following were the inclusion criteria: patient age 18, urine or faecal incontinence, and double incontinence, no IAD in the perineal area, no allergies in the patients, changing diapers at least four times a day, and examination within the first 24 h of arrival.

The exclusion criteria were as follows: IAD or pressure ulcer in the perineal area.

Researchers gathered data for the study between January 2015 and March 2018. Patients who were eligible for the study were informed after being admitted to the clinic, and those who agreed to participate in the study gave written authorisation, and intervention and control groups were established.

Patient Information Form: The Patient Information Form developed by the researcher in accordance with the literature data consisted of individual characteristics like the individual's income, working status, education, marital status, gender, age, place of living, and health insurance, and the variables that may affect the formation of incontinence-associated dermatitis, such as presence of chronic diseases, medical diagnosis, drugs used continuously, type of incontinence, level of mobility, and the form of nutrition (2, 3, 22).

Incontinence-Associated Dermatitis and Its Severity Instrument Scoring (IADES): The Incontinence-Associated Dermatitis Rating Scale was developed by Borchert et al. (2010), and its content validity was ensured by evaluation by seven specialist nurses. This scale is commonly used worldwide for evaluating IAD. This measurement instrument was tested with interobserver compliance, and the content validity was scored by two wound and ostomy specialist nurses. The nurse divides the perineal region into 13 regions and scores them in terms of redness, skin loss, and rash into the skin. No redness: 0 points, pink colour: 1 point, red colour: 2 points, rash: 3 points, and skin loss: 4 points. The total score to be obtained from the scale ranges from 0 to 52 (3, 7). A high score obtained from the scale indicates an increased risk and severity of dermatitis (3). The reliability and validity scales used in the study were developed by Aydın and Kaya (23).

Patient Monitoring Form: This form was created by the researcher using literature data in order to analyse the patient on a daily basis in terms of vital signs, medications used, oxygen treatment, quantity of stools, and consistency of stools (formed, semi formed, liquid, etc.).

Randomisation

For easy randomisation, the lottery approach was employed: one (for the intervention group) and two (for the control gro-

up) were inscribed on 66 cards. The cards were placed in a bag and properly mixed. The cards were chosen by lot, and the patients were divided into two groups: intervention and control. The patients, nurses, and researcher performed the intervention and measurements, and the patients identified their own groups when perineal treatment was administered to them. Blinding was not possible because of the nature of the technique. Non-rinse washcloths were used on patients who were randomly allocated to the intervention group. The control group received standard medical treatment (ie, disposable non-rinse wash cloth).

The study conducted in two phases

Phase I: Training nurses to prevent IAD

The training programme's material was created by researchers and is based on a review of the literature. The developed training content was presented to wound, ostomy, and incontinence experts and was subsequently offered to nurses in the form of face-to-face training in small groups at each clinic. An hour was given to nurses in the neurology and neurosurgery wards. Skin structure, description of IAD, aetiology and associated aspects of IAD, how to avoid IAD, and how to provide perineal care were all covered in the training programme. Nurses in these units continued to provide care in their normal routine perineal care in the control group. The patients in the control group underwent perineal treatment using a standard disposable non-rinse wash towel. Changes in this skin region were observed for 10 days using IADES and the Patient Follow-up Form after the patients were seen by the researcher every morning.

Phase II: Implementation of the research in the intervention group

After training the nurses, the second phase of the research was concluded between June 2015 and March 2018. Both groups used the same protocols for patient follow-up. The researcher conducted the first examination of the patient using the Patient Introduction Form. The patients in the intervention group underwent perineal treatment using a disposable non-rinse washcloth (with dimethicone wipes). The care of the perineum Dimethicone wipes, which were utilised in the intervention group, hydrates the skin while also protecting and providing a barrier. Changes in this skin region were observed for 10 days using IADES and the Patient Follow-up Form after the patients were seen by the researcher every morning.

Ethical considerations

The research was conducted at the neurology and neurosurgery units of three university hospitals in Istanbul. The hospital management gave written consent, and the ethics committee gave its clearance (Date: 02.12.2014, No:E-01). The families of the patients provided their informed permission.

Statistical analysis

For statistical analysis, IBM SPSS Statistics 24 software (IBM SPSS, Turkey) was used. The Shapiro-Wilk test was used to determine whether the parameters were normal. The chi-square test was used in order to compare descriptive statistical values (mean, standard deviation), qualitative data, and normally distributed parameters between the groups. The time-causing difference was determined using the Fisher Exact Test. To compare qualitative data, the chi-square test was applied. The significance level was set at $p<0.05$.

RESULTS

Comparison of the intervention and control groups' demographic and disease characteristics

The patients in the control and intervention groups were 62.77±13.45 and 65.82±10.70 years old, respectively, on average. The gender, degree of consciousness, presence and type of chronic illnesses, mobility, diet, BMI, and several laboratory values of patients in the intervention and control groups were similar, with no statistically significant differences ($p>0.05$). In this context, as can be seen in Table 1, both groups are correlated.

Presence, Type, and Duration of Incontinence in Patients

It was observed that 34.8% and 25.8% of the patients in the intervention and control groups, respectively, had no incontinence before admission to the hospital. It was determined that 65.2% urine was observed to be the highest in the intervention group before admission to the hospital and that both types of incontinence was 71.2% during admission to the hospital. Similarly, it was observed in the control group that 70.6% urinary incontinence had the highest priority for admission to the hospital and that each incontinence was 74.2% during admission to the hospital. No statistically significant difference was determined between both groups in terms of the presence, type, and average duration of incontinence ($p>0.05$). The findings are summarised in Table 2.

Comparison of the Development IAD

When IAD development was examined between both groups, it was determined that it developed in 31.8% and 40.9% of the patients in the control and intervention groups, respectively, and that the mean IAD total score was 2.92 in the control group and 2.52 in the intervention group. However, although IAD development and IAD score were higher in the control group, no statistically significant difference was determined ($p>0.05$). The findings showing the IAD development rates are summarised in Table 3.

It was determined that the development regions of IAD were not different in both groups. It was also observed that IAD mostly developed in the genital region (labia/scrotum) and the fold between the genital and femur (18.2%), right front inner femur (11.4%), and left front (10.6%).

Comparison of IAD Development by Individual and Disease Characteristics of Patients

Table 4 shows the elements that contribute to IAD and its progression. Some laboratory values, such as age, gender, BMI, level of consciousness, presence of incontinence before admission to the hospital, presence of chronic disease, movement, nutrition, haemoglobin, haematocrit, and IAD development, were not

Table 1: Comparison of the demographic and disease characteristics of the intervention and control groups

Demographic and disease characteristics		Intervention (N=66)	Control (N=66)	Total (N=132)	Chi-square test	
		N (%)	N (%)	N (%)	X^2	p- value
Gender	Female	50 (75.8)	44 (66.7)	94 (71.2)	1.330	0.168
	Male	16 (24.2)	22 (33.3)	38 (28.8)		
Consciousnes status	Opened	48 (72.7)	44 (66.7)	92 (69.7)	0.624	0.732
	Closed	8 (12.1)	9 (13.6)	17 (12.9)		
	Confused	10 (15.2)	13 (19.7)	23 (17.4)		
Diagnosis	schemic Serebrovascular Disease	23 (34.8)	15 (22.7)	38 (28.8)	10.863	0.145
	Cerebrovascular Disease	32 (48.5)	35 (53.0)	67 (50.8)		
	Multiple Sklerozis	5 (7.6)	4 (6.1)	9 (6.8)		
	ADEM (Acute Demyelinated Ensafloapatia)	1 (1.5)	2 (3.0)	3 (2.3)		
	Spinalcord injury	1 (1.5)	4 (6.1)	5 (3.8)		
	Parkinson Disease	4 (6.1)	1 (1.5)	5 (3.8)		
	Brain Tumour	0 (0)	4 (6.1)	4 (3.0)		
	Julian Barré Disease	0 (0)	1 (1.5)	1 (0.8)		
Chronic Disease	Yes	59 (89.4)	49 (74.2)	108 (81.8)	5.093	0.020
	No	7 (10.6)	17 (25.8)	24 (18.2)		
Chronic disease types	Multiple Sklerozis	4 (6.1)	3 (4.5)	7 (5.3)	0.15	0.500
	Hypertension	50 (75.8)	37 (56.1)	87 (65.9)	5.698	0.014
	Diabetes Mellitus	25 (37.9)	25 (37.9)	50 (37.9)	0.000	0.571
	Coronary Artery Disease	5 (7.6)	3 (4.5)	8 (6.1)	0.532	0.359
	Hypothyroidism	2 (3.0)	7 (10.6)	9 (6.8)	2.981	0.082
	Kidney Disease	1 (1.5)	0 (0.0)	1 (0.8)	1.008	0500
	Heart Failure Disease	17 (25.8)	9 (13.6)	26 (19.7)	3.065	0.062
	Parkinson Disease	2 (3.0)	2 (3.0)	4 (3.0)	0.000	0.690
	Demans Disease	1 (1.5)	3 (4.5)	4 (3.0)	1.031	0.310
Mobility	Completely immobile	3 (4.5)	1 (1.5)	4 (3.0)	1.483	0.476
	Very limited	8 (12.1)	11 (16.7)	19 (14.4)		
	Slightly limited	55 (83.3)	54 (81.8)	109 (82.6)		
Nutrition status	Oral	46 (69.7)	35 (53.0)	81 (61.4)	5.374	0.068
	Enteral	19 (28.8)	31 (47.0)	50 (37.9)		
	Parenterally	1 (1.5)	0 (0.0)	1 (0.8)		
		Intervention (N=66) Mean (SD)	**Control (N=66) Mean (SD)**	**Total (N=132) Mean (SD)**	**Student t-testi**	
					t	**p- value**
Biochemistry tests	Haemoglobin (mg/dl) (Min.-Max.)	12.04 (1.63) (9.30-15.10)	11.87 (1.78) (5.1-16.3)	11.95 (1.70) (5.1-16.3)	0.570	0.570
	Hemotokrit (%) (Min-Max)	35.11 (5.31) (27-45.10)	35.90 (4.99) (24-49.6)	35.50 (5.15) (24.0-49.6)	0.878	0.381
	Albumin (mg/dl) (Min-Max)	3.37±0.56 (2.07-4.40)	3.43±0.46 (2.4-4.5)	3.40 (0.51) (2.1-4.5)	0.655	0.513
Age/Years (Mean±SD)		65.82 (10.70)	62.77 (13.45)	64.30 (12.20)	1.440	0.155
BMI		26.19 (4.26)	26.04 (4.02)	26.11 (4.13)	0.208	0.836

BMI: Body mass index, Min.: Minimum, Max.: Maximum, SD: Standard deviation, p<0.05.

Table 2: Presence, type, and duration of incontinence in patients

		Intervention (n=66)	Control (n=66)	Total (N=132)	Chi-square test	
		N (%)	N (%)	N (%)	X^2	p-value
Before hospital presence of incontinence	Yes	23 (34.8)	17 (25.8)	40 (30.3)	1.291	0.172
	No	43 (65.2)	49 (74.2)	92 (69.7)		
Before hospital types of incontinence	Urine incontinence	15 (65.2)	12 (70.6)	27 (67.5)	0.784	0.676
	Faecal incontinence	1 (4.3)	0 (0.0)	1 (2.5)		
	Double incontinence	7 (30.4)	5 (29.4)	12 (30.0)		
Admission to hospital types of incontinence	Urine incontinence	8 (12.1)	4 (6.1)	12 (9.1)	1.497	0.473
	Faecal incontinence	11 (16.7)	11 (16.7)	22 (16.7)		
	Double incontinence	47 (71.2)	51 (77.3)	98 (74.2)		
Duration of before to hospital Mean (SD/ month)		**Intervention (n=66) Mean (SD)**	**Control (n=66) Mean (SD)**	**Total (N=132) Mean (SD)**	**Student t-testi**	
					t	**p-value**
		22.30 (19.08)	30.00 (27.19)	25.68 (23.01)	1.065	0.294

SD: Standard deviation, p<0.05

Table 3: Comparison of Development IAD

		Intervention group (n=66)	Control group (n=66)	Total (N=132)	Chi-square test	
		N (%)	N (%)	N (%)	X^2	p-value
IAD	Yes	21 (31.8)	27 (40.9)	48 (36.4)	1.179	0.183
	No	45 (68.2)	39 (59.1)	84 (63.6)		
IAD development day	2nd day	5 (23.8)	4 (14.8)	9 (18.8)	3.256	0.776
	3rd day	2 (9.5)	6 (22.2)	8 (16.7)		
	4th day	5 (23.8)	4 (14.8)	9 (18.8)		
	5th day	2 (9.5)	4 (14.8)	6 (12.5)		
	6th day	2 (9.5)	4 (14.8)	6 (12.5)		
	7th day	2 (9.5)	3 (11.1)	5 (10.4)		
	8th day	3 (14.3)	2 (7.4)	5 (10.4)		
		Intervention (N=66) Mean (SD)	**Control (N=66) Mean (SD)**	**Total (N=132) Mean (SD)**	**Student t-testi**	
					t	**p-value**
Total IADES	Mean (SD) (Min.-Max.)	2.524 (2.657) (1-12)	2.926 (2.986) (1-13)	2.75 (2.825) (1-13)	-0.485	0.630

IAD: Incontinence-associated dermatitis; IADES: Incontinence-associated dermatitis evaluation scores; SD: Standard deviation, p<0.05.

significantly different between the groups (p>0.05). The ratio of IAD development was higher in patients with perspiration in the control and intervention groups, and there was a statistically significant difference (p<0.05). While there was no statistically significant difference in IAD development between the two groups in terms of haemoglobin and hemotocrit levels, IAD development was higher in patients with low albumin levels in the control group, and this difference was statistically significant. It was also shown that in the intervention group, patients taking anticoagulant and antidiabetic medication developed IAD at a greater rate, with a statistically significant difference (p0.05). In the control group, individuals receiving antibiotic therapy had a greater rate of IAD development (51.9%) than those who did not, and the difference was statistically significant (p≤0.05).

Comparison of IAD Development According to the number of stool of patients

When IAD development according to the number of stools of patients was examined, the average number of daily stools was 1.46 times/day in patients with IAD development in the intervention group and 1.12 times/day in patients with IAD development in the control group. However, the average number of liquid stools of patients with IAD development was 2.48 times/day in the intervention group and 2.26 times/day in the control group, and the average number of semi-formed stools was 5.57

Table 4: Comparison of IAD development by individual and disease characteristics of patients

Individual and disease characteristics		Intervention				Control			
		IAD No (n=45)	IAD Yes (n=21)	Chi-square test		IAD No (n=39)	IAD Yes (n=27)	Chi-square test	
		N (%)	N (%)	X^2	p-value	N (%)	N (%)	X^2	p-value
Gender	Female	33 (73.3)	17 (81.0)	0.453	0.365	27 (69.2)	17 (63.0)	0.282	0.394
	Male	12 (26.7)	4 (19.0)			12 (30.8)	10 (37.0)		
BMI	Normal weight	22 (48.9)	8 (38.1)	0.911	0.634	15 (38.5)	14 (51.9)	1.562	0.458
	Overweight	16 (35.6)	10 (47.6)			16 (41.0)	10 (37.0)		
	Obesity	7 (15.6)	3 (14.3)			8 (20.5)	3 (11.1)		
Consciousness Status	Opened	35 (77.8)	13 (61.9)	2.139	0.343	29 (74.4)	15 (55.6)	2.545	0.280
	Closed	5 (11.1)	3 (14.3)			4 (10.3)	5 (18.5)		
	Confused	5 (11.1)	5 (23.8)			6 (15.4)	7 (25.9)		
Incontinence before admission	No	28 (62.2)	15 (71.4)	0.535	0.328	31 (79.5)	18 (66.7)	1.371	0.188
	Yes	17 (37.8)	6 (28.6)			8 (20.5)	9 (33.3)		
Chronic Disease Types	Yes	39 (86.7)	20 (95.2)	1.110	0.278	30 (76.9)	19 (70.4)	0.358	0.375
	No	6 (13.3)	1 (4.8)			9 (23.1)	8 (29.6)		
Incontinence admission to the hospital	Urine	6 (13.3)	2 (9.5)	3.165	0.205	3 (7.7)	1 (3.7)	5.691	0.058
	Faecal	5 (11.1)	6 (28.6)			3 (7.7)	8 (29.6)		
	Double	34 (75.6)	13 (61.9)			33 (84.6)	18 (66.7)		
Mobility	Completely immobile	2 (4.4)	1 (4.8)	1.411	0.494	1 (2.6)	0 (0.0)	3.378	0.185
	Very limited	4 (8.9)	4 (19.0)			4 (10.3)	7 (25.9)		
	Slightly limited	39 (86.7)	16 (76.2)			34 (87.2)	20 (74.1)		
Nutritional status	Oral	33 (73.3)	13 (61.9)	2.632	0.268	20 (51.3)	15 (55.6)	0.117	0.464
	Enteral	12 (26.7)	7 (33.3)			19 (48.7)	12 44.4		
	Parenterally	0 (0.0)	1 (4.8)			0 (0.0)	0 (0.0)		
Perspretion	Yes	5 (41.7)	7 (58.3)	4.753	0.036	3 (21.4)	11 (78.6)	10.427	0.002
	No	40 (74.1)	14 (25.9)			36 (69.2)	16 (30.3)		
Anticoagulants medication	Yes	37 (82.2)	21 (100)	4.248	0.038	35 (89.7)	24 (88.9)	0.012	0.608
	No	8 (17.8)	0 (0.00)			4 (10.3)	3 (11.1)		
Antidiabetic medication	Yes	18 (40)	14 (66.7)	4.076	0.039	16 (41.0)	10 (37.0)	0.106	0.474
	No	27 (60.0)	7 (33.3)			23 (59.0)	17 (63.0)		
Antibiotics medication	Yes	18 (40)	9 (42.9)	0.048	0.517	9 (23.1)	14 (51.9)	5.818	0.016
	No	27 (60)	12 (57.1)			30 (76.9)	13 (48.1)		
				Student's t-test				Student's t-test	
				t	p value			t	p value
Age	Mean (SD)	65.76 (11.00)	65.95 (10.28)	0.069	0.945	62.46 (14.04)	63.22 (12.80)	0.224	0.823
	Min.-Max.	36.0- 81.0	31.0- 79.0			36.0 -85.0	36.0 -90.0		
HGB	Mean (SD)	12.12 (1.57)	11.85 (1.78)	0.629	0.532	11.9 (71.57)	11.73 (2.07)	0.539	0.592
	Min.-Max.	9.3-14.7	9.3-15.1			8.4-15.5	5.1-16.3		
HCT	Mean (SD)	35.39 (5.39)	34.50 (5.23)	0.627	0.533	36.32 (4.63)	35.28 (5.49)	0.835	0.407
	Min.-Max.	27.0-44.6	28.0-45.1			28.0-48.7	24.0-49.6		
Albumin	Mean (SD)	3.38 (0.57)	3.36 (0.55)	0.072	0.943	3.54 (0.44)	3.28 (0.45)	2.331	0.023
	Min.-Max.	2.1-4.4	2.1-4.3			2.6-4.5	2.4-3.9		
Duration of Incontinence before admission (month)	Mean (SD)	21.88 (18.56)	23.50 (22.30)	-0.175	0.863	21.56 (19.17)	38.44 (32.29)	-1.349	0.196
	Min..-Max.	1.0-48.0	1.0-60.0			1.0-48.0	2.0-96.0		

IAD: Incontinence-associated dermatitis, HGB: Hemoglabin, HCT: Hemotocrit, Min.: Minumum, Max.: Maximum, SD: Standard deviation, p<0.05.

Table 5: Comparison of IAD development according to the number of stools of patients

	Intervention		Student's t-test		Control		Student's t-test	
	IAD No (n=45)	IAD Yes (n=21)	t	p-value	IAD No (n=39)	IAD Yes (n=27)	t	p-value
	Mean (SD)	Mean (SD)			Mean (SD)	Mean (SD)		
Number of stools	1.19 (0.74)	1.46 (1.04)	-1.208	0.231	1.12 (0.58)	1.22 (0.65)	-0.658	0.513
Liquid stools	1.38 (2.64)	2.48 (3.25)	-1.461	0.149	0.67 (1.72)	2.26 (3.37)	-2.520	0.030
Semi-formed stools	6.47 (2.77)	5.57 (3.01)	1.190	0.238	7.69 (2.40)	6.26 (3.08)	2.122	0.038
Formed stools	0.13 (0.41)	0.14 (0.66)	-0.073	0.942	0.10 (0.31)	0.04 (0.19)	0.981	0.291

SD: Standard deviation, p<0.05.

times/day in the intervention group and 6.26 times/day in the control group. The IAD development status according to the average number of stools is presented in Table 5.

DISCUSSION

IAD prophylaxis is critical for avoiding the development of additional advanced skin issues, such as pressure sores caused by incontinence. The increased variety of products used in perineal skin care nowadays produces uncertainty as to which product the nurse prefers. The major goal of this study was to determine how much dermatitis was averted using incontinence care wipes with non-rinse disposable soapy water and 3% dimethicone.

When disease and individual characteristics of patients in the control and intervention groups were examined, such as the type of incontinence and when it began, it was discovered that there was no difference between the two groups. The similarity of person and disease features guaranteed that these factors that may be effective in the development of IAD were minimised.

IAD may create other major complications in patients if it is not avoided in the near term. The most serious of these issues is pressure sores, which can lead to profound tissue damage (9, 24-27). In nursing, soapy water has been used for the cleaning of the perineal region from the past to the present. Perineal care with soapy water has been shown to be the most known and reliable method used in the removal of microorganisms in the body and the cleaning of harmful pathogens. However, non-rinse wash clothes have emerged and are commonly used to facilitate patient care because the direct use of solid or liquid soaps damages the skin pH. Wet wipes are another product that makes life simpler for people. Ordinary wet wipes, on the other hand, are ineffective in preventing IAD. It has been claimed that wipes containing specific ingredients such as dimethicone prevent the onset of IAD (7). When the rates of IAD development in the literature are examined, they vary between 5% and 52% (7, 28). In the study in which Coyer et al., compared two different perineal skin hygiene protocols, it was observed that perineal dermatitis developed in 15% of the intervention group and 32.8% of the control group (29). In a study conducted with 3406 patients, Boronat-Garrido et al. reported that IAD developed in 5.2% of the incontinence patients with urine, stool or both of them (30). It was determined that IAD developed in 31.8% of the intervention group and 40.9% of the control group. This finding is parallel to a similar study in which a wipe with soapy water and 3% dimethicone with a pH in the range of 6.5-7.5 was compared (IAD developed in 22.3% of the intervention group and 22.8% of the control group). The IADES score indicates the severity of dermatitis. As the IADES score increases, skin damage increases (3). The measurement tools for determining IAD and severity are not standard and the mean scores are different (3, 7, 16). In the studies within this scope, IAD development levels are higher than the IAD score (2, 22, 31). Dermatitis occurs because of skin contact with urine and/or stool. However, there is not enough evidence on how long dermatitis develops (22). In some literature, it is seen to develop on day 4 (2, 22) and on day 13 (32). It usually developed on days 2 and 4 (23.8%) in the intervention group and between days 2 and 6 (14.8% -22.2%) in the control group, according to the findings of this study. These findings were found to be consistent with previous prevalence and incidence studies compared with the literature.

Several variables contribute to the development of IAD. Bliss et al. found that the patient's level of awareness and the frequency of liquid or semi-liquid faeces are two major factors in the development of IAD in prospective research with ICU patients (2). Skin exposure to urine and/or faeces is the most important element in the development of IAD. Many variables such as age, female gender, high BMI, nutritional deficiency, limitation of movement activity, closed or confused consciousness, liquid stools, faecal incontinence, low albumin level, use of antibiotics, steroids, or vasopressor drugs have been reported in recent studies examining IAD and the factors affecting it (20, 31, 33). In this study, no statistically significant difference was found between laboratory values such as age, gender, form of nutrition, movement level, type of incontinence, presence and duration of prior incontinence, HGB, HCT, and IAD development status in patients with chronic disease. However, in accordance with the literature, IAD development was higher in patients receiving antithrombotic and antidiabetic treatments in the intervention group. In the control group, IAD was higher in patients receiving antibiotic treatment. It is expected that the use of antibiotics may increase gastrointestinal motility and that the vascular structure of patients receiving antrombolytic and antidiabetic medications may be affected. According to these findings and the literature, it was predicted that taking into consideration the relevant risk variables would improve

diagnostic abilities and that persons in risk groups would be diagnosed more According to these findings and the literature, it was predicted that taking into consideration the relevant risk variables would improve diagnostic abilities and that persons in risk groups would be diagnosed more extensively.

IAD is caused by urine and/or faeces coming into contact with the skin in the perineal region (33). In this context, the type of incontinence is also the most critical factor influencing dermatitis development. It is claimed that in the development of IAD, faecal incontinence is the most important risk factor (19, 31) and that dermatitis develops more rapidly in patients with faecal incontinence than in individuals with urine incontinence. According to some studies, liquid stools increase the development of dermatitis by five times more than solid stools (6, 19, 28). This is explained by the fact that undigested nutrients and digestive enzymes (proteases and lipases) in the liquid stool cause damage to intercellular proteins and by the increased permeability of the skin (31). In their study, Campbell et al. showed that there was no difference between the development of dermatitis according to the incontinence type (faecal or urinary incontinence) despite the development of dermatitis in 10% of the sample group (9). In the same study, it was reported that dermatitis was observed in 50% of patients with liquid or soft stool consistency. Dermatitis occurs in 44.7% of the patients with 3 or more stools in a day. However, no significant relationship was found between the number of stools and incontinence-associated dermatitis (9). In their study conducted with intensive care patients, Chianca et al. showed that the development of IAD was higher in patients with liquid stools than in those without liquid stools (34). In the study in which Van Damme et al. examined the factors that may be effective in the development of severe IAD, they identified liquid stool as one of the most important factors in the development of IAD, reporting that 25.2% of patients with liquid stool of 1-3 days and 21.4% of patients with liquid stool of 4-6 days had IAD (31). This study's finding of a greater rate of IAD development in patients with liquid stool supports previous research.

Limitations

There are a few limitations to this study. The first of these is the fact that the study was conducted only with patients undergoing treatment and care in the neurology clinic and that the results are generalisable only for this group. The second limitation is that the prevalence and incidence studies were not conducted before the study.

CONCLUSION

Although no significant difference was observed statistically between the two products in terms of preventing IAD, the importance of nursing care in preventing IAD with frequent perineal care was identified in this study. This study is highly essential in terms of exposing the need for excellent nursing care at a time when nurses do not want to perform various care practises such as perineal care.

As a result of the findings, it may be advised that prevalence and incidence studies of IAD be conducted in high-risk groups in our nation, that nurses be made more aware of this issue, and that perineal care methods be compared.

Ethics Committee Approval: Ethics committee approval was received for this study from the ethics committee of İstanbul University-Cerrahpaşa University (Date: 02.12.2014, No:E-01).

Informed Consent: Written informed consent was obtained from families of the patients who participated in this study.

Peer Review: Externally peer-reviewed.

Author Contributions: Conception/Design of Study- G.Ö.A., H.K.; Data Acquisition- G.Ö.A.; Data Analysis/Interpretation- G.Ö.A.; Drafting Manuscript- G.Ö.A., H.K.; Critical Revision of Manuscript- G.Ö.A., H.K.; Final Approval and Accountability- G.Ö.A.

Acknowledgments: This study was funded by TUBITAK as part of the 3001- Start-Up R&D Projects Support Programme. The authors are grateful to TUBITAK (Project No: 215S944).

Conflict of Interest: The authors have no conflict of interest to declare.

Financial Disclosure: This research was supported by TUBITAK within the context of the 3001 Start-Up R&D Projects Support Programme (Project No: 215S944).

REFERENCES

1. Black JM, Gray M, Bliss DZ, Kennedy Evans KL, Logan S, Baharestani MM, et al. MASD Part 2: Incontinence-associated dermatitis and intertriginous dermatitis. J Wound Ostomy Continence Nurs 2011;38(3):303-15.
2. Bliss DZ, Savik K, Thorson MA, Ehman SJ, Lebak K, Beilman G. Incontinence-associated dermatitis in critically ill adults: time to development, severity, and risk factors. J Wound Ostomy Continence Nurs 2011;38(4):433-45.
3. Borchert K, Bliss D, Savik K, Radosevich DM. The incontinence-associated dermatitis and its severity instrument. J Wound Ostomy Continence Nurs 2010;37(5):527-35.
4. Langemo D, Hanson D, Hunter S, Thompson P, Oh IE. Incontinence and incontinence-associated dermatitis. Adv Skin Wound Care 2011;24(3):126-40.
5. Sugama J, Sanada H, Shigeta Y, Nakagami G, Konya C. Efficacy of an improved absorbent pad on incontinence-associated dermatitis in older women: cluster randomized controlled trial. BMC Geriatr 2012;12(1):1-7.
6. Bliss DZ, Savik K, Harms S, Fan Q, Wyman JF. Prevalence and correlates of perineal dermatitis in nursing home residents. Nurs Res 2006;55(4):243-51.
7. Beeckman D, Verhaeghe S, Defloor T, Schoonhoven L, Vanderwee K. A 3-in-1 perineal care wash cloth impregnated with dimethicone 3% versus water and pH neutral soap to prevent and treat incontinence-associated dermatitis: a randomized, controlled

clinical trial. J Wound Ostomy Continence Nurs 2011;38(6):627-34.
8. Gray M, Black JM, Baharestani MM, Bliss DZ, Colwell JC, Goldberg M, et al. Moisture-associated skin damage: overview and pathophysiology. J Wound Ostomy Continence Nurs 2011;38(3):233-41.
9. Campbell JL, Coyer FM, Osborne SR. Incontinence-associated dermatitis: a cross-sectional prevalence study in the Australian acute care hospital setting. Int Wound J 2014;13(3):403-11.
10. National Clinical Guideline Centre (UK). Urinary incontinence in neurological disease: management of lower urinary tract dysfunction in neurological disease. London: Royal College of Physicians (UK); 2012 Aug. https://www.ncbi.nlm.nih.gov/pubmedhealth/PMH0055279/pdf/PubMedHealth_PMH0055279.pdf.
11. Wiesel PH, Norton C, Roy AJ, Storrie JB, Bowers J, Kamm MA. Gut focused behavioural treatment (biofeedback) for constipation and faecal incontinence in multiple sclerosis. J Neurol Neurosurg Psychiatry Res 2000;69(2):240-3.
12. Tülek Z. Mesane ve Bağırsak Sorunlarının Değerlendirilmesi ve Yönetimi. İçinde: Topçuoğlu M, Durna Z, Karadakovan A, editors. Nörolojik Bilimler Hemşireliği Kanıta Dayalı Uygulamalar. İstanbul: Nobel Tıp Kitapevleri 2013.p.283-99.
13. Leandro TA, Araujo TLD, Cavalcante TF, Lopes MVDO, Oliveira TMFD, Lopes ACM. Urinary incontinence nursing diagnoses in patients with stroke. Rev Esc Enferm USP 2015;49(6):923-30.
14. Uraloğlu G, Selçuk B, Kurtaran A, Yalcin E, Inanir M, Sade I, Akyüz M. Assessment of the bowel dysfunctions in stroke patients. Turk J Geriatr 2014;17(4):330-7.
15. Hall KD, Clark RC. A prospective, descriptive, quality improvement study to decrease incontinence-associated dermatitis and hospital-acquired pressure ulcers. Ostomy/Wound Manag 2015;61(7):26-30.
16. Nix DH. Validity and reliability of the perineal assessment tool. Ostomy/Wound Manag 2002;48(2):43-9.
17. Beeckman D, Woodward S, Gray M. Incontinence-associated dermatitis: step-by-step prevention and treatment. Br J Nurs 2011;16(8):382-9.
18. Johnson D, Lineweaver L, Maze LM. Patients' bath basins as potential sources of infection: a multi center sampling study. Am J Crit Care 2009;18(1):31-40.
19. Beeckman D, Van Damme N, Schoonhoven L, Van Lancker A, Kottner J, Beele H, et al. Interventions for preventing and treating incontinence-associated dermatitis in adults. Cochrane Database Syst Rev 2016;11:1-72.
20. Coyer F, Campbell J. Incontinence-associated dermatitis in the critically ill patient: an intensive care perspective. Intensive Crit Care Nurs 2017;23(4):198-206.
21. Ma ZZ, Song JY, Wang M. Investigation and analysis on occurrence of incontinence-associated dermatitis of ICU patient with fecal incontinence. Int J Clin Exp Med 2017;10(5):7443-9.
22. Denat Y, Khorshid L. The effect of 2 different care products on incontinence-associated dermatitis in patients with fecal incontinence. J Wound Ostomy Continence Nurs 2011;38(2):171-6.
23. Aydın GÖ, Kaya H. Incontinence associated dermatitis assessment scale: study of inter-observer compliance. Florence Nightingale J Nurs 2017;25(2):111-8.
24. Avşar P, Karadağ A. Efficacy and cost-effectiveness analysis of evidence-based nursing interventions to maintain tissue integrity to prevent pressure ulcers and incontinence-associated dermatitis. Worldviews Evid Based Nurs 2018;15(1):54-61.
25. Demarre L, Verhaeghe S, Van Hecke A, Clays E, Grypdonck M, Beeckman D. Factors predicting the development of pressure ulcers in an at-risk population who receive standardized preventive care: secondary analyses of a multicentre randomised controlled trial. J Adv Nurs 2015;71(2):391-403.
26. Gray M, Giuliano KK. Incontinence-associated dermatitis, characteristics and relationship to pressure injury: a multisite epidemiologic analysis. J Wound Ostomy Continence Nurs 2018;45(1):63-7.
27. Kottner J, Beeckman D. Incontinence-associated dermatitis and pressure ulcers in geriatric patients. Giornale italiano di dermatologia e venereologia: organo ufficiale. G Ital Dermatol Venereol 2015;150(6):717-29.
28. Kottner J, Blume-Peytavi U, Lohrmann C, Halfens R. Associations between individual characteristics and incontinence-associated dermatitis: A secondary data analysis of a multi-centre prevalence study. Int J Nurs Stud 2014;51(10):1373-80.
29. Coyer F, Gardner A, Doubrovsky A. An interventional skin care protocol (InSPiRE) to reduce incontinence-associated dermatitis in critically ill patients in the intensive care unit: A before and after study. Intensive Crit Care Nurs 2017;40:1-10.
30. Boronat-Garrido X, Kottner J, Schmitz G, Lahmann N. Incontinence-associated dermatitis in nursing homes: prevalence, severity, and risk factors in residents with urinary and/or fecal incontinence. J Wound Ostomy and Continence Nurs 2016;43(6):630-5.
31. Van Damme N, Clays E, Verhaeghe S, Van Hecke A, Beeckman D. Independent risk factors for the development of incontinence-associated dermatitis (category 2) in critically ill patients with fecal incontinence: A cross-sectional observational study in 48 ICU units. Int J Nurs Stud 2018;81:30-9.
32. Arnold-Long M, Reed L, Dunning K, Ying J. Incontinence-associated dermatitis (IAD) in a long-term acute care (LTAC) facility: findings from a 12 week prospective study. J Wound Ostomy Continence Nurs 2012;39(3):318-27.
33. Beeckman D. A decade of research on Incontinence-Associated Dermatitis (IAD): Evidence, knowledge gaps and next steps. J Tissue Viability 2017;26(1):47-56.
34. Chianca TCM, Gonçales PC, Salgado PO, Machado BDO, Amorim GL, Alcoforado CLGC. Incontinence-associated dermatitis: a cohort study in critically ill patients. Rev Lat Am Enfermagem. 2016;37:68075.

RESEARCH ARTICLE / ARAŞTIRMA MAKALESİ
Journal of Advanced Research in Health Sciences /
Sağlık Bilimlerinde İleri Araştırmalar Dergisi 2024
DOI: 10.26650/JARHS2024-1424470

COMPARISON OF PERFORMANCE CHARACTERISTICS OF GAMMA CAMERAS WITH SCINTILLATION NaI(TI) AND SEMICONDUCTOR CdZnTe DETECTORS

NaI(TI) SİNTİLASYON VE CdZnTe YARI İLETKEN DEDEKTÖRLÜ GAMA KAMERALARIN PERFORMANS ÖZELLİKLERİNİN KARŞILAŞTIRILMASI

Armağan AYDIN[1,3], Füsun ÇETİN[2], Mustafa DEMİR[1,3]

[1]İstanbul University-Cerrahpaşa, Institute of Graduate Studies, Health Physics PhD Program, İstanbul, Türkiye
[2]İstanbul Aydın University, Institute of Health Sciences, Department of Health Physics, İstanbul, Türkiye
[3]İstanbul University-Cerrahpaşa, Cerrahpaşa Faculty of Medicine, Department of Nuclear Medicine, İstanbul, Türkiye

ORCID ID: A.A. 0000-0002-9126-8381; F.Ç. 0000-0001-9135-2615; M.D. 0000-0002-9813-1628

Citation/Atıf: Aydın A, Çetin F, Demir M. Comparison of performance characteristics of gamma cameras with scintillation NaI(TI) and semiconductor CdZnTe detectors. Journal of Advanced Research in Health Sciences 2024;7(3):174-179. https://doi.org/10.26650/JARHS2024-1424470

ABSTRACT

Objective: In recent years, gamma cameras with semiconductor detectors (CdZnTe) have entered routine practise diagnostic scintigraphic imaging in nuclear medicine. In this study, we aimed to compare the performance characteristics of a gamma camera with a semiconductor detector (CdZnTe) and a conventional gamma camera with a NaI(Tl) detector.

Material and Methods: In our experimental studies, spatial resolution, energy resolution, and linearity tests were performed using 3 capillary tubes of the same length and thickness, into which the Tc-99m radioisotope with different activities was placed. Sensitivity tests were performed by placing Tc-99m in a plastic Petri dish with a diameter of 3 cm. Scintigraphic images of the capillary tubes and the Petri dish were taken with both gamma cameras under equal geometric conditions. Regions of interest (ROI) were drawn on the images. The activity amount corresponding to the counts in the ROI was determined.

Results: The spatial resolution, energy resolution, and sensitivity values of the gamma camera with the CdZnTe detector and the gamma camera with NaI(Tl) detector are respectively: 7.16 mm, 5.1% and 17.5 cps/µCi for CdZnTe, and 13.2 mm, 9.4% and 3.9 cps/µCi for NaI(Tl) µCi respectively.

Conclusion: According to the results of our study, it was concluded that the energy resolution, spatial resolution, sensitivity, and linearity properties of the gamma camera with the semiconductor CdZnTe detector are superior to those of the gamma camera with the NaI(Tl) detector.

Keywords: Gamma camera, semiconductor detector, CdZnTe, energy resolution, spatial resolution

ÖZ

Amaç: Son yıllarda yarı iletken dedektörlere (CdZnTe) sahip gama kameralar, nükleer tıpta tanısal sintigrafik görüntülemede rutin uygulamaya girmiştir. Bu çalışmasında, yarı iletken dedektörlü (CdZnTe) bir gama kamera ile NaI(Tl) dedektörlü konvansiyonel bir gama kameranın performans özelliklerinin karşılaştırılması amaçlanmıştır.

Gereç ve Yöntemler: Deneysel çalışmalarımızda, farklı aktivitelerde Tc-99m radyoizotopu yerleştirilen aynı uzunluk ve kalınlığa sahip 3 kapiller tüp kullanılarak uzaysal çözünürlük, enerji çözünürlüğü ve doğrusal testler yapılmıştır. Duyarlılık testleri ise 3 cm çapında plastik petri kabına yerleştirilen Tc-99m ile gerçekleştirilmiştir. Kapiler tüplerin ve petri kabının sintigrafik görüntüleri her iki gama kamera ile eşit geometrik koşullar altında alınmıştır. Görüntüler üzerinde ilgi bölgeleri (ROI) çizilmiştir. ROI'deki sayımlara karşılık gelen aktivite miktarı belirlenmiştir.

Bulgular: CdZnTe dedektörlü gama kamera ile NaI(Tl) dedektörlü gama kameranın uzaysal çözünürlük, enerji çözünürlüğü ve duyarlılık değerleri sırasıyla; CdZnTe için 7,16 mm, %5,1 ve 17,5 cps/µCi, NaI(Tl) için ise 13,2 mm, %9,4 ve 3,9 cps/µCi olarak bulunmuştur.

Sonuç: Çalışmamızın sonuçlarına göre, yarı iletken CdZnTe dedektörlü gama kameranın enerji çözünürlüğü, uzaysal çözünürlüğü, duyarlılığı ve doğrusal özelliklerinin NaI(Tl) dedektörlü gama kameraya göre üstün olduğu sonucuna varılmıştır.

Anahtar Kelimeler: Gama kamera, yarı iletken dedektör, CdZnTe, enerji çözünürlüğü, uzaysal çözünürlük

Corresponding Author/Sorumlu Yazar: Armağan AYDIN **E-mail:** armanaydin@gmail.com

Submitted/Başvuru: 23.01.2024 • **Revision Requested/Revizyon Talebi:** 12.02.2024 • **Last Revision Received/Son Revizyon:** 05.08.2024 • **Accepted/Kabul:** 09.09.2024 • **Published Online/Online Yayın:** 24.10.2024

INTRODUCTION

Nuclear medicine is a scientific discipline in which the diagnosis and treatment of diseases are conducted through the administration of radiopharmaceuticals into the body. Distinguishing itself from anatomical imaging systems, its primary advantage lies in providing images that reflect the biological processes of organs at the cellular and molecular levels. Nuclear medicine also encompasses significant complementary methods for conventional radiological imaging. One of the scintigraphic imaging devices used in nuclear medicine is the gamma camera. The more advanced version of these devices, allowing for tomographic imaging, is referred to as Single Photon Emission Computerised Tomography (SPECT) gamma cameras. In evaluating the operational performance of a gamma camera, the homogeneity, linearity, energy resolution, spatial resolution, system sensitivity (or efficiency), and count rate performances are assessed (1, 2).

The primary aim of developing CZT gamma cameras has been to enhance image contrast by achieving better energy resolution while maintaining a spatial resolution comparable to that of scintillation cameras equipped with a low-energy high-resolution (LEHR) collimator, typically yielding 8–9-mm FWHM at a distance of 10 cm from the collimator face, a scenario common in most clinical examinations. In addition to designing the imaging system, automatic handling and assembly methods were developed to ensure detector positioning accuracy and enable cost-effective manufacturing and maintenance in the long term (3).

Following the recognition of the superior characteristics of semiconductor technology in ionising radiation detection, it has also been incorporated into gamma cameras. CdZnTe detector-based gamma cameras have been particularly employed for cardiac scintigraphy, and their usage is progressively expanding in contemporary practise (4).

The spatial resolution performance of the CZT is ultimately constrained by the size of the electron cloud and the diffusion of electrons within it. Resolution refers to the full width at half maximum (FWHM) of the camera's response to full photopeak radiation emitted from a line source positioned with its longitudinal axis aligned along a major axis of the crystal. While other parameters also contribute to describing the resolution, such as those outlined below, FWHM is commonly used to characterise scanning collimators. It proves valuable in illustrating performance fluctuations concerning differing gamma-ray energies, source-collimator distances, and variations across the crystal's surface (5).

The CZT detector offers a significant advantage in terms of enhanced energy resolution. The determination of energy resolution hinges upon several factors: (a) Electronic noise stemming from the input stage of the preamplifier, inclusive of the capacitance and leakage current inherent to the detector; (b) Linewidth attributed to the stochastic characteristics of charge generation; and (c) Fluctuations arising from the trapping of charge carriers within the detector. Linearity is the characteristic of a gamma camera that dictates its capacity to accurately replicate the spatial distribution of an isotope (6).

Sensitivity is quantified as the proportion of gamma rays that interact within the detector compared to the total number incident upon it. It serves as a crucial determinant of the camera system's efficacy. Inadequate detector design can lead to subpar overall performance (4).

This study aims to compare the performance characteristics of spatial resolution, linearity, energy resolution, and sensitivity between conventional gamma cameras with NaI(Tl) detector material and gamma cameras with the CdZnTe (semiconductor) detector material of the same brand.

MATERIALS AND METHODS

Experimental materials and radionuclide activities

Tc-99m activities were measured using a dose calibrator, and the solutions were prepared in separate vials at concentrations of 1 mCi/5ml, 2 mCi/10ml, and 3 mCi/15ml, respectively. From each vial, Tc-99m solutions were drawn into capillary tubes with internal diameters of 1 mm, lengths of 7.5 cm, and volumes of 0.8 ml. The tube ends were sealed with putty. The activity within the tubes was measured using a dose calibrator, and the net Tc-99m activities were determined after the background count corrections. The measurement times were recorded. The tubes were placed on a cardboard surface with a 4- cm spacing between them and were securely fixed in preparation for imaging.

Gamma cameras and imaging techniques

The experiments were conducted on two different gamma ca-

Table 1: GE Brand Discovery NM 530c Brand CdZnTe Detector and GE Tandem Discovery 630 NaI(Tl) detector gamma camera physical properties

Physical properties	GE discovery NM 530c	GE Tandem discovery 630
Crystal thickness	5 mm	12.4 mm
Detector material	CdZnTe	NaI(Tl)
Gamma camera type	SPECT	SPECT
Collimator type	Pin Hole	Parallel Hole (LEHR)
Detector density	5.78 g/cm^3	3.76 g/cm^3
Light transformation	100%	13%
Dead time	No	>20000 counts

GE: General Electric, NM: Nuclear Medicine, CdZnTe: Cadmium Zinc Tellure, NaI(Tl): Sodium Iodure (Thallium), SPECT: Single Photon Emission Tomography

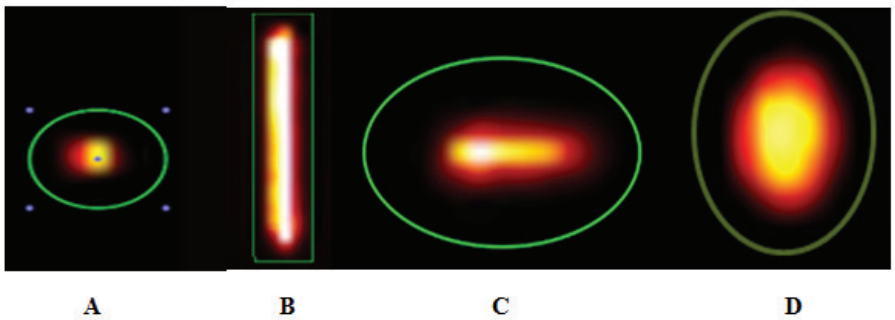

Figure 1: Capillary tube in different planar section images (A) short axis (axial) section (B) long axis (sagittal) section (C) long axis (coronal) section D) petri dish. (outer contours are ROI plots)

meras. One of them is the GE brand, Discovery NM 530c model, with a CdZnTe detector Gamma Camera. The detector assembly consists of a multi-pinhole collimator. Each pinhole in the block illuminates a solid-state pixellated gamma-ray detector made of CZT. Similarly, each pinhole and detector creates a complete miniature gamma camera. The other is the GE brand, Tandem Discovery 630 model, with a NaI(Tl) detector and LEHR collimator gamma camera. The technical specifications of these gamma cameras are provided in Table 1.

The capillary tubes were imaged under identical geometric conditions in two different gamma cameras. The distance between the detector and the tube was kept constant at 18 cm. Image acquisitions were performed based on the total counts according to the clinical imaging procedure. The imaging durations for the Discovery NM 530c and Tandem Discovery 630 devices were 7 min and 6.04 min, respectively.

Image quantifications

Image quantifications were conducted on the gamma camera workstations. Images were transferred to the workstation, and regions of interest (ROIs) were drawn around the tubes. Total counts within the ROIs were determined. Activity loss corrections were applied separately for each capillary tube. Count/activity quantities were determined for each of the three tubes.

Spatial resolutions for gamma cameras were extracted separately for tubes with three different activities. Count variation data between 0 and 40 mm in SPECT axial section images of the tubes were determined. These position-count data were transformed into a Gaussian fit graph using the mathematical formulas below, allowing the calculation of spatial resolutions and energy resolutions (7).

$$Spatial\ resolution, FWHM\ = 2.d.\sqrt{2.ln2}$$

$$Energy\ resolution, FWHM\ \% = \frac{Spatial\ resolution}{Gamma\ Energy\ of\ Radionuclide}\ x100$$

$$FWHM\ \% = \frac{2.d.\sqrt{2.ln2}}{140\ keV}.100$$

The linearity measurements were derived from the count measurements of the capillary tubes with three different activities. Linearity was determined by plotting the count-activity variations of tubes separately imaged and the ROIs drawn in the gamma cameras.

For sensitivity measurements, a 0.5 mCi/3ml Tc-99m solution was placed in a 3 cm diameter plastic Petri dish. The net activity was first measured in the dose calibrator, and the measurement time was recorded. The Petri dish was imaged for a duration of 7 min with a fixed geometry in both gamma cameras. The images were transferred to the workstation, and ROIs were drawn to determine the count/activity (cps/mCi) quantities.

RESULTS

Energy resolution and spatial resolution

The count variations in the axial section (short axis) images of three separate capillary tubes in the Tandem Discovery 630 device were determined by drawing ROIs in the 0-4 mm length region (Figure 1). Counts were transferred to the ImageJ programme, and the position-count variations were subtracted in ImageJ. Gaussian position-count variation graphs were obtained using these graphs. Spatial resolutions (mm) and energy resolutions (%) for each gamma camera were then calculated

Table 2: Spatial Resolution (mm) and percentage Energy Resolution Values of the Tandem Discovery 630 Model Gamma Camera with NaI(Tl) Detector and the GE Brand Discovery NM 530c Model (CdTeZn) Gamma Camera with the Detector

	Tandem Discovery 630				Discovery NM 530c			
	1. Tube	2. Tube	3. Tube	Mean	1. Tube	2. Tube	3. Tube	Mean
Activity (mCi)	1.015	2.08	3.09	2.06	1.015	2.08	3.09	2.06
Spatial resolution (mm)	14.221	12.724	12.683	13.210	6.854	7.267	7.377	7.166
Energy resolution (%)	10.158	9.089	9.060	9.435	4.896	5.191	5.269	5.119

NM: Nuclear Medicine, mCi: millicurie

Table 3: Sensitivity Values of the Discovery NM 530c Gamma Camera and the Discovery NM 630 Gamma Camera

	Discovery NM 530c	Tandem discovery 630
Activity (µCi)	44	40
Counts (cps)	7760.6	1534.7
Sensitivity (cps/µCi)	17.5	3.9

NM: Nuclear medicine, µCi: microCurie, cps: Count per second

for three different tubes and three different Tc-99m activities. Average values were subsequently obtained. Table 2 provides the spatial resolution (mm) and % energy resolution values for the GE Tandem Discovery 630 model NaI(Tl) detector gamma camera, while Table 3 presents the spatial resolution (mm) and % energy resolution values for the GE Discovery NM 530c model (CdTeZn) detector gamma camera.

Linearity

Variations between the ROI counts of the capillary tubes with three different Tc-99m activities and the measured net activity quantities (µCi) in the dose calibrator were plotted (Figure 2 and Figure 3). In Figure 3, it is observed that the linearity of the semiconductor gamma camera with the CdZnTe detector material perfectly coincides with the x = y (first bisector) line and

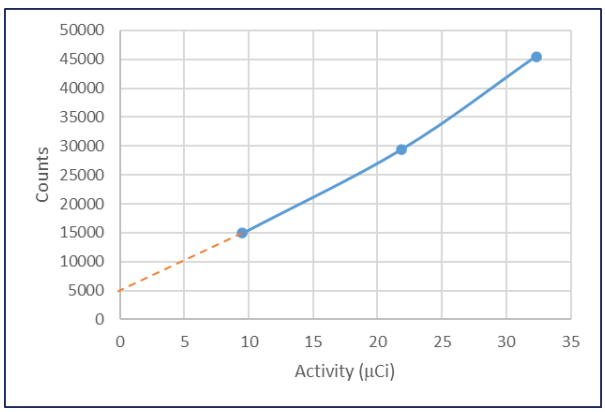

Figure 2: Count-activity linearity graph of the Discovery Tandem 630 model gamma camera

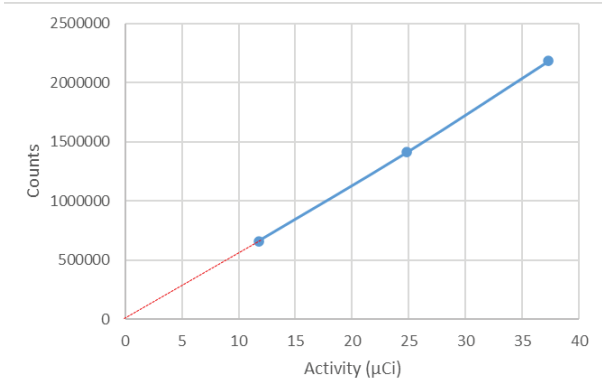

Figure 3: Count-activity linearity graph of the Discovery NM 530c model gamma camera

passes through the origin. The linearity curve of the conventional gamma camera with NaI(Tl) detector material, however, deviates from the origin to some extent, and the linearity is disrupted at count rates >20 cps/µCi.

Sensitivity

The sensitivity values calculated using the petri dish (cps/µCi) for the Discovery NM 530c CdZnTe detector gamma camera are presented in Table 3 and those for the Tandem Discovery 630 NaI(Tl) detector gamma camera are presented in Table 3 The sensitivity values for the Discovery NM 530c and Tandem Discovery 630 gamma cameras were found to be 17.52 cps/µCi and 3.905 cps/µCi, respectively.

DISCUSSION

Semiconductor-based gamma cameras are preferred in nuclear medicine clinics over gamma cameras using NaI(Tl) detector material due to their superior spatial resolution, energy resolution, higher sensitivity, and better linearity. Because of these superior performance characteristics, scintigraphic images of higher quality can be obtained in a shorter time and with lesser number of radiopharmaceuticals. In his study, Barber HB emphasised that semiconductor (CdZnTe) detectors yield good results in terms of spatial resolution and energy resolution in the field of nuclear medicine. He reported that the energy resolution of semiconductor gamma cameras with a CdZnTe detector material is 8% at 140 keV, while conventional gamma cameras with NaI(Tl) detectors have an energy resolution of 11% (8). John K. Hartwell reported an energy resolution of 7.6% for the CZT cameras and 14% for NaI(Tl) detector gamma cameras at 140 keV (9). Oliver Gal et al. found an energy resolution of 4.5% for semiconductor detector gamma cameras and 13% for NaI(Tl) detector gamma cameras at 662 keV (10). Agostini et al. reported an energy resolution of 6% for CZT cameras at 140 keV and 10% for conventional gamma cameras with NaI(Tl) detectors (11). Our results, with an energy resolution of 5.1% for the CdZnTe detector gamma camera and 9.4% for the NaI(Tl) detector gamma camera at 140 keV, are consistent with the literature data.

Analysing recent publications, Hugg et al. reported an energy resolution of 3.6% at 140 keV, a system spatial resolution of 6.8 mm, and a sensitivity of 11.4 cps/µCi for semiconductor CZT cameras (12). When compared to our results, it appears that the spatial resolution, energy resolution, and sensitivity values reported in recent studies are superior. This improvement in the performance parameters may be interpreted as ongoing advancement in the detector and gamma camera technology over time.

The spatial resolution test results investigated by Abe, A. et al. found a system spatial resolution of 2.2 mm at the FOV centre and a sensitivity of 11,052 cpm/MBq (13). In our results, the spatial resolution was 7.16 mm for the CdZnTe detector gamma camera and 13.21 mm for the NaI(Tl) detector gamma camera. Our sensitivity values were 17.518 cps/µCi for the Discovery NM 530c gamma camera and 3.905 cps/µCi for the Discovery

NM 630 gamma camera.

The sensitivity of the CZT camera was assessed in comparison to a 3/8" NaI(Tl) spot crystal Anger camera employing identical geometrical configurations. Energy windows of 6% and 10% were applied to the CZT and NaI detectors, respectively. The sensitivity of the CZT camera was determined to be 70% of that of the 3/8" NaI camera. This implies that approximately 60% of the incident 140 keV gamma photons were detected within the photopeak in the CZT (14). According to our results, the sensitivity of the semiconductor gamma camera was determined to be 77.5% better than that of the NaI(Tl) detector gamma camera.

When the response variations of gamma cameras to activity increases (linearity) were examined; it was found that in Figure 2, when sensitivity is >20 cps/µCi, linearity is disrupted due to the dead time related to the activity increase. In contrast, it was observed that the linearity of the CdZnTe detector gamma camera perfectly coincides with the x=y (first bisector) line and passes through the origin. Additionally, no linearity disruption due to the activity increase was observed in the examined range. This indicates that the linearity of the semiconductor detector gamma camera is more stable.

In addition to the advantages of semiconductor detectors, there are some disadvantages. One of the most significant is their limited field of view (FOV), making them unsuitable for scintigraphic imaging of organs other than the heart due to their small FOV. Nowadays, wider FOV semiconductor detector gamma cameras are also used. However, their high prices are a disadvantage for cameras with semiconductor detectors.

CONCLUSION

In this study, the technical performance of two gamma cameras based on different technologies from the same manufacturer was experimentally measured. According to our results, the sensitivity of the CdZnTe camera was found to be 4.48 times higher than that of the other camera. Consequently, it would be possible to reduce the amount of Tc-99m activity used in myocardial perfusion scintigraphy by the same factor. It was determined that using the CdZnTe camera for myocardial perfusion scintigraphy would reduce the patient's radiation dose by a factor of 4.48. Additionally, the study demonstrated that the radiation exposure to the personnel performing the procedure would decrease, the cost of radiopharmaceuticals would be reduced, and the number of procedures performed daily could be significantly increased.

Ethics Committee Approval: Since this is a phantom study, ethics committee approval is not required.

Peer Review: Externally peer-reviewed.

Author Contributions: Conception/Design of Study- M.D., A.A., F.Ç.; Data Acquisition- M.D., A.A., F.Ç.; Data Analysis/Interpretation- M.D., A.A., F.Ç.; Drafting Manuscript- M.D., A.A., F.Ç.; Critical Revision of Manuscript- M.D., A.A., F.Ç.; Final Approval and Accountability- M.D., A.A., F.Ç.; Material and Technical Support- M.D.; Supervision- M.D.

Conflict of Interest: The authors declare that there is no conflict of interest.

Financial Disclosure: The authors declared that this study has received no financial support.

REFERENCES

1. National Electrical Manufacturers Association. Performance Measurements of Gamma Cameras NEMA NU 1-2018. Rosslyn, VA: National Electrical Manufacturers Association. https://www.nema.org/docs/default-source/standards-document-library/nema_nu_1_2018-contents-and-scope.pdf?sfvrsn=d93985ea_1
2. Koppert WJ, Dietze MM, Van der Velden S, Steenbergen JL, De Jong HW. A comparative study of NaI (Tl), CeBr3, and CZT for use in a real-time simultaneous nuclear and fluoroscopic dual-layer detector. Physics in Medicine & Biology 2019;64(13):135012.
3. Verger L, Gentet MC, Gerfault L, Guillemaud R, Mestais C, Monnet O, et al. Performance and perspectives of a CdZnTe-based gamma camera for medical imaging. IEEE Transactions on Nuclear Science 2004;51(6):3111-7.
4. Amrami R, Shani G, Hefetz Y, Blevis I, Pansky A. A comparison between the performance of a pixellated CdZnTe based gamma camera and Anger NaI (TI) scintillator gamma camera. In Proceedings of the 22nd Annual International Conference of the IEEE Engineering in Medicine and Biology Society. 2000;1:352-5.
5. Zheng X, Cheng Z, Deen MJ, Peng H. Improving the spatial resolution in CZT detectors using charge sharing effect and transient signal analysis: Simulation study. NIMA 2016;808:60-70.
6. Montémont G, Lux S, Monnet O, Stanchina S, Verger L. Studying spatial resolution of CZT detectors using sub-pixel positioning for SPECT. IEEE Transactions on Nuclear Science 2014;61(5):2559-66.
7. Coman E, Brewster MW, Popuri SK, Andrew MR, Matthias KG. A comparative evaluation of Matlab, Octave, FreeMat, Scilab, R, and IDL on Tara. 2012 Oct. Technical Report HPCF–2012–15.
8. Barber H B. Applications of semiconductor detectors to nuclear medicine. NIMA 1999;436(1-2):102-10.
9. Agostinelli S, Allison J, Amako K, Apostolakis J, Araujo H, Arce P, et al. A comparative evaluation of Matlab, Octave, FreeMat, Scilab, R, and IDL on Tara. NIMA 2003;506:250-303.
10. Gal O, Gmar M, Ivanov OP, Laine F, Lamadie F, Le Goaller C, et al. Development of a portable gamma camera with coded aperture, nuclear instruments and methods in physics research section a: accelerators, spectrometers, detectors and associated equipment. NIMA 2006;563(1):233-7.
11. Agostini D, Marie PY, Ben-Haim S, Rouzet F, Songy B, Giordano A, et al. Performance of cardiac cadmium-zinc-telluride gamma camera imaging in coronary artery disease: A review from the Cardiovascular Committee of the European Association of Nuclear Medicine (EANM). EJNMMI 2016;43(13):2423-32.
12. Hugg J, Harris B, Tomita H. Evaluation of CZT Gamma Cameras for Human SPECT and Small FOV Imaging. J Nuclear Med 2018;59(supplement 1):220.

13. Abe A, Takahashi N, Lee J, Oka T, Shizukuishi K, Kikuchi T, et al. Performance evaluation of a hand-held, semiconductor (CdZnTe)-based gamma camera. Eur J Nuclear Med Molecular Imaging 2003;30(6):805-11.
14. Wagenaar D J, Parnham K, Sundal B, Maehlum G, Chowdhury S, Meier D, et al. Advantages of semiconductor CZT for medical imaging. In Penetrating Radiation Systems and Applications 2007;6707:144-53.

İSTANBUL UNIVERSITY PRESS

RESEARCH ARTICLE / ARAŞTIRMA MAKALESİ
Journal of Advanced Research in Health Sciences /
Sağlık Bilimlerinde İleri Araştırmalar Dergisi 2024
DOI: 10.26650/JARHS2024-1496234

INVESTIGATION OF THE PREVALENCE OF PATHOGENIC INTESTINAL PROTOZOANS IN PATIENTS WITH GASTROINTESTINAL COMPLAINTS VIA MICROSCOPY AND MULTIPLEX REAL-TIME PCR

GASTROİNTESTİNAL ŞİKÂYETİ OLAN HASTALARDA BAĞIRSAK PATOJENİ PROTOZOONLARIN PREVALANSININ MİKROSKOPİ VE MULTİPLEKS REAL-TIME PCR İLE ARAŞTIRILMASI

Burak KARACAN[1,2], Özden BÜYÜKBABA BORAL[3], Gülay İMADOĞLU YETKİN[2], Aslı ÇİFCİBAŞI ÖRMECİ[4], Ozan ÖZKAYA[5], Murat SÜTÇÜ[5], Muradiye ACAR[6], Bülent EDİZ[7]

[1]İstanbul University, Institute of Graduate Studies in Health Sciences, Department of Medical Microbiology, İstanbul, Türkiye
[2]İstinye University, Faculty of Medicine, Department of Microbiology and Clinical Microbiology, İstanbul, Türkiye
[3]İstanbul University, İstanbul Faculty of Medicine, Department of Medical Microbiology, İstanbul, Türkiye
[4]İstanbul University, İstanbul Faculty of Medicine, Department of Internal Diseases, İstanbul, Türkiye
[5]İstinye University, Faculty of Medicine, Department of Pediatrics, İstanbul, Türkiye
[6]İstinye University, Faculty of Medicine, Department of Medical Genetics, İstanbul, Türkiye
[7]İstinye University, Faculty of Medicine, Department of Biostatistics and Medical Information, İstanbul, Türkiye

ORCID ID: B.K. 0000-0003-1166-3101; Ö.B.B. 0000-0001-7144-1418; G.İ.Y. 0000-0002-6115-3583; A.Ç.Ö. 0000-0001-6297-8045; O.Ö. 0000-0002-0198-1221; M.S. 0000-0002-2078-9796; M.A. 0000-0003-4357-5229; B.E. 0000-0001-7337-2372

Citation/Atıf: Karacan B, Büyükbaba Boral Ö, İmadoğlu Yetkin G, Çifcibaşı Örmeci A, Özkaya O, Sütçü M, et al. Investigation of the prevalence of pathogenic intestinal protozoans in patients with gastrointestinal complaints via microscopy and multiplex real-time PCR. Journal of Advanced Research in Health Sciences 2024;7(3):180-184. https://doi.org/10.26650/JARHS2024-1496234

ABSTRACT

Objective: This study aimed to contribute to surveillance data by determining the prevalence of pathogenic intestinal protozoans in patients with gastrointestinal complaints and to comparatively evaluate the performance of microscopy and multiplex real-time PCR methods.

Materials and Methods: Forty adults (18 years or older) and 40 children (aged 5 to 12 years) who volunteered patients with at least one gastrointestinal complaint were included in the study. Stool samples collected three times every other day from each patient were examined under a light microscope using Native-Lugol, modified formol-ether concentration, Wheatley's modified trichrome staining, and Modified Ziehl-Neelsen staining techniques. In addition, the first stool samples were tested using multiplex real-time PCR with the Allplex™ GI Parasite Assay panel after DNA extraction. Differences between the sensitivities and specificities between the methods were analysed using Fisher's exact test. A p-value of <0.05 was considered statistically significant.

Results: The prevalence of pathogenic intestinal protozoans was 25% in adults and 35% in children. Differences in the sensitivities and specificities of the methods were not found to be statistically significant (p=0.999).

Conclusion: Multiplex real-time PCR method performed using the Allplex™ GI Parasite Assay panel was effective even when only the first sample tested, suggesting that this method would be used for the routine diagnosis of pathogenic intestinal protozoans.

Keywords: Pathogen, intestinal, protozoon, prevalence, microscopy, PCR

ÖZ

Amaç: Bu çalışmanın amacı, hem gastrointestinal şikâyeti olan hastalarda bağırsak patojeni protozoonların prevalansını tespit ederek sürveyans verilerine katkı sağlamak hem de mikroskopi ve multipleks real-time PCR yöntemlerinin performanslarını karşılaştırmalı olarak değerlendirmektir.

Gereç ve Yöntem: Çalışmaya, en az bir gastrointestinal şikâyeti olan 40 yetişkin (18 yaş ve üzerinde) ve 40 çocuk (5-12 yaş arasında) gönüllü hasta dâhil edildi. Her hastadan günaşırı olarak 3 kez alınan gaita örnekleri; Nativ-Lugol, modifiye formol-eter çöktürme, Wheatley'in trikrom boyama ve modifiye Ziehl-Neelsen boyama teknikleri uygulandıktan sonra ışık mikroskobunda incelendi. Ayrıca, yalnızca ilk olarak alınan gaita örnekleri; DNA ekstraksiyonundan sonra, Allplex™ GI Parasite Assay paneli kullanılarak multipleks real-time PCR yöntemiyle test edildi. Yöntemlerin duyarlılıkları ve özgüllükleri arasındaki farklılıklar, Fisher'in kesin testi ile analiz edildi. p değerinin <0,05 olması, istatistiksel olarak anlamlı kabul edildi.

Bulgular: Bağırsak patojeni protozoonların prevalansının yetişkin grubunda %25, çocuk grubunda ise %35 olduğu tespit edildi. Yöntemlerin duyarlılıkları ve özgüllükleri arasındaki farklılıklar, istatistiksel olarak anlamlı bulunmadı (p=0,999).

Sonuç: Allplex™ GI Parasite Assay paneli kullanılarak gerçekleştirilen multipleks real-time PCR yönteminin yalnızca ilk örnek test edildiğinde bile etkili olması; bu yöntemin, bağırsak patojeni protozoonların rutin tanısında kullanılabileceğini düşündürmektedir.

Anahtar Kelimeler: Patojen, bağırsak, protozoon, prevalans, mikroskopi, PCR

Corresponding Author/Sorumlu Yazar: Burak KARACAN **E-mail:** burak.karacan@istinye.edu.tr

Submitted/Başvuru: 05.06.2024 • **Revision Requested/Revizyon Talebi:** 09.07.2024 • **Published Online/Online Yayın:** 23.10.2024

INTRODUCTION

Gastrointestinal infections are a major cause of morbidity and mortality worldwide, posing a serious threat to public health (1, 2). In tropical and subtropical climate zones, including Türkiye, parasites are responsible for a significant proportion of gastrointestinal infections (2, 3). Pathogenic intestinal protozoans are the most common parasites causing gastrointestinal infections.

The diagnosis of pathogenic intestinal protozoans is generally made via microscopy. This method requires at least three stool samples every other day, along with experience, proper concentration, and permanent staining techniques for optimal results. Because the implementation of this method is both difficult and time-consuming, patients who can benefit from antiparasitic drugs or antibiotics may not receive appropriate treatment on time or at all (4-6). In addition, patients with chronic diseases/comorbidities may be unnecessarily hospitalized and may undergo extra examinations, such as gastroscopy and colonoscopy, until a diagnosis is complete (7-9). The Centers for Disease Control and Prevention (CDC) recommends that patients with suspected infectious diarrhea use contact precautions (10, 11). Thus, patients may be unnecessarily isolated and psychologically affected if diagnosis is delayed. Rapid and accurate diagnosis of gastrointestinal infections is crucial for infection control and prevention plans, public health interventions, and case management (1, 9, 12, 13). Therefore, a sensitive and specific method to rapidly and simultaneously detect protozoans that cause gastrointestinal infections is urgently needed. The Allplex™ Gastrointestinal (GI) Parasite Assay is the most comprehensive multiplex real-time panel for detecting pathogenic intestinal protozoans. The multiplex real-time Polymerase Chain Reaction (PCR) method performed using this panel may rapidly and accurately identify protozoans causing gastrointestinal complaints, ensuring timely initiation of appropriate treatment. Thus, the unnecessary and incorrect use of antiparasitic drugs and antibiotics, the development of resistance to antiparasitic drugs and antibiotics, needless isolation, redundant use of other diagnostic tests, length of hospital stays, and healthcare costs may be reduced.

In this study, we aimed to contribute to surveillance data by detecting the prevalence of pathogenic intestinal protozoans in patients with gastrointestinal complaints, and to comparatively evaluate the performances of microscopy and multiplex real-time PCR.

MATERIALS and METHODS

This study was conducted at İstanbul University İstanbul Faculty of Medicine Hospital, İstinye University Liv Hospital Bahçeşehir, and İstinye University Faculty of Medicine, after receiving approval from the İstanbul Medical Faculty Clinical Research Ethics Committee (Date: 24.09.2021, No: 17) and the İstinye University Clinical Research Ethics Committee (Date: 14.10.2021, No: 2/2021.K-75). The study was conducted in accordance with the Declaration of Helsinki. Written informed consent was obtained from all participants or their legal representatives.

Inclusion criteria

We focused on a specific age range for pediatric patients, in contrast to adult patients. In total, 80 volunteer patients who agreed to participate in the study, or whose legal representatives consented, and who met the criteria on items A-1, A-2, B-1, and B-2, were included in the study:

A-1: Twenty immunocompetent adults (≥18 years old) who applied to the Department of Internal Diseases at İstanbul University İstanbul Faculty of Medicine Hospital with at least one gastrointestinal complaint;

A-2: Twenty immunosuppressed adults (≥18 years old) who applied to the Department of Internal Diseases at İstanbul University İstanbul Faculty of Medicine Hospital with at least one gastrointestinal complaint;

B-1: Twenty immunocompetent children (aged 5 to 12 years) who applied to the Department of Pediatrics at İstinye University Liv Hospital Bahçeşehir with at least one gastrointestinal complaint;

B-2: Twenty immunosuppressed children (aged 5 to 12 years) who applied to the Department of Pediatrics at İstinye University Liv Hospital Bahçeşehir with at least one gastrointestinal complaint.

Sample collection

Stool samples were collected from adult patients between April 4 and May 8, 2022, and from pediatric patients between May 10 and June 16, 2022, three times every other day. Following the collection of the first stool sample from each patient, blood samples were also obtained.

Microscopic examination

Stool samples were examined under a binocular microscope (Nikon, Tokyo, Japan; Olympus, Tokyo, Japan) after applying Native-Lugol, modified formol-ether concentration (MF), Wheatley modified trichrome staining (WS), and modified Ziehl-Neelsen staining (ZN) techniques.

DNA extraction

DNA was extracted from the first samples using a QIAamp Fast DNA Stool Mini Kit (Qiagen, Hilden, Germany) according to the manufacturer's instructions. For amplification with the Allplex™ GI Parasite Assay (Seegene®, Seoul, South Korea), 10 µl of internal control (IC) DNA was added to the samples prior to extraction, as recommended by the manufacturer. After completing the DNA extraction procedure, samples were stored at -20°C until multiplex real-time PCR analysis.

Multiplex real-time PCR

Multiplex real-time PCR was performed using a CFX96 Touch real-time PCR detection system (Bio-Rad, Marnes-La-Coquette, France) and the Allplex™ GI Parasite Assay (Seegene®, Seoul, South Korea) panel, following the manufacturer's instructions. Amplifications were managed using the CFX Maestro Software (Seegene®, Seoul, South Korea), and results were analysed using the Seegene Viewer Software (v3 (Seegene®, Seoul, South

Korea). Samples with a Cycle threshold (Ct) value of ≤43 were interpreted as positive. A test that did not meet the positive and negative control criteria was repeated. In addition, the DNA extraction process and multiplex real-time PCR testing were repeated for four samples with IC Ct values interpreted as N/A.

Statistical analysis

All data were entered into an Excel (Microsoft Excel 2019) database, and statistical analysis was performed using IBM SPSS Statistics v26 (IBM SPSS Corp., Armonk, NY, USA). Differences in sensitivities and specificities between the methods were analysed using Fisher's exact test. A p-value of <0.05 was considered statistically significant.

RESULTS

Upon evaluating the results and all clinical parameters, 21 out of 80 samples were found to be positive. Among these positive samples, three exhibited co-infection: two samples were positive for both *Blastocystis* spp. and *D. fragilis*, and one sample was positive for both *Blastocystis* spp. and *G. lamblia*. The overall prevalence rates were 25% in adults and 35% in children. Detailed information on the prevalence of pathogenic intestinal protozoans is presented in Table 1.

Table 1: Information on the prevalence of pathogenic intestinal protozoans identified in this study

	Group			
	Adults (≥18 years)		Children (5-12 years)	
Pathogenic intestinal protozoans	**A-1**	**A-2**	**B-1**	**B-2**
Giardia lamblia	-	-	5%	5%
Dientamoeba fragilis	10%	10%	10%	15%
Entamoeba histolytica	-	5%	-	-
Cryptosporidium spp.	-	-	-	5%
Blastocystis spp.	10%	15%	15%	15%

It was found that the microscopy method yielded one false-negative result and three false-positive results for *Blastocystis* spp., as well as two false-negative results for *D. fragilis*. On the other hand, multiplex real-time PCR method yielded one false-negative result, besides two false-positive results with high Ct values (42.87 and 42.91) for *Blastocystis* spp., which were very close to the limit. The sensitivities and specificities of the methods are compared in Tables 2 and 3, respectively.

Compared with the examination of the first stool sample via microscopy, testing of the same sample via multiplex real-time PCR demonstrated remarkably higher sensitivity (45.83% vs. 95.83%), and the performance difference was statistically significant (p=0.0003). Compared with the examination of the first and second stool samples via microscopy, testing of the first stool sample via multiplex real-time PCR again demonstrated higher sensitivity (70.83% vs. 95.83%), and the performance difference remained statistically significant (p=0.049). Compared with the examination of the three stool samples via microscopy, testing of the first stool sample via multiplex real-time PCR also exhibited higher sensitivity (87.5% vs. 95.83%), but the performance difference was not statistically significant (p=0.6085). Compared with microscopy, multiplex real-time PCR showed higher specificity (94.92% vs 96.56%), but the performance difference was not statistically significant (p=0.999).

Table 2: Comparison of the sensitivities of the methods based on species level

	Sensitivity	
Pathogenic intestinal protozoan	**Microscopy (After examining the three samples)**	**Multiplex real-time PCR (After testing the first sample)**
Giardia lamblia	100% (2/2)	100% (2/2)
Dientamoeba fragilis	77.78% (7/9)	100% (9/9)
Entamoeba histolytica	100% (1/1)	100% (1/1)
Cryptosporidium spp.	100% (1/1)	100% (1/1)
Blastocystis spp.	90.91% (10/11)	90.91% (10/11)

Table 3: Comparison of the specificities of the methods based on species level

	Specificity	
Pathogenic intestinal protozoan	**Microscopy (After examining the three samples)**	**Multiplex real-time PCR (After testing the first sample)**
Giardia lamblia	100% (78/78)	100% (78/78)
Dientamoeba fragilis	100% (71/71)	100% (71/71)
Entamoeba histolytica	100% (79/79)	100% (79/79)
Cryptosporidium spp.	100% (79/79)	100% (79/79)
Blastocystis spp.	95.83% (69/72)	97.18% (69/71)

DISCUSSION

In our study, *Blastocystis* spp. was the pathogenic intestinal protozoan with the highest prevalence in both adults and children, followed by *Dientamoeba fragilis*. Our study supports the literature indicating that the most common protozoan causing gastrointestinal complaints in humans is *Blastocystis* spp., followed by *D. fragilis* (14).

The testing of the first stool sample via multiplex real-time PCR was statistically superior to the examination of two stool samples via microscopy. The testing of the first stool sample via multiplex real-time PCR was statistically equivalent to the examination of three stool samples via microscopy. For each case, examining three stool samples every other day using microscopy took approximately 5 days, while multiplex real-time PCR, including the DNA extraction procedure, took approximately 4.5 hours. Pathogenic intestinal protozoans can lead to epidemics, particularly in crowded areas. Co-infections may increase the likelihood of false-negative and false-positive results via microscopic diagnoses. Conversely, multiplex real-time PCR can rapidly detect multiple microorganisms simultaneously with high sensitivity and specificity, effectively overcoming the limitations of microscopy-based diagnosis.

In addition to Native-Lugol and MF, permanent staining techniques, such as WS (for *D. fragilis*, *E. histolytica and Blastocystis* spp.) and ZN (for *Cryptosporidium* spp.), were found to enhance the performance of the microscopy method. All *D. fragilis*, which were observed in 7 out of 9 cases via microscopy, could be detected using the WS technique. Thanks to the WS technique, we were able to observe erythrophagocytosis by *E. histolytica* trophozoites; the *E. histolytica*/*E. dispar* group could be separated as *E. histolytica* in one case and the *E. dispar* group in four cases. Separation of the *E. histolytica* and *E. dispar* group is crucial; treatment is unnecessary when the *E. dispar* group is diagnosed, while urgent treatment is required if *E. histolytica* is diagnosed (15). *Blastocystis* spp. were identified in 10 of 11 cases via microscopy, with 2 of these detected using the WS technique. *Cryptosporidium* spp. can lead to life-threatening complications, especially in immunosuppressed patients (16). *Cryptosporidium* spp. oocysts were detected in the first sample using the WS technique, and the immunosuppressed patient was immediately treated. However, these permanent staining techniques are not routinely utilized in many diagnostic laboratories worldwide. Their implementation is laborious and time-consuming, and successful results are not always achieved. In addition, no consensus has been reached on a complementary diagnostic test for the detection of pathogenic intestinal protozoans. Differences in the performance of various diagnostic methods and techniques can affect the reported prevalence rates (17). Therefore, multiplex real-time PCR should be employed as a first-line diagnostic method to ensure standardization in the diagnosis of pathogenic intestinal protozoans.

In our study, no infections caused by *Cyclospora cayetanensis*, *Cystoisospora* spp., *Sarcocystis* spp., or *Balantioides coli* were detected. *Cyclospora cayetanensis,* and *Cystoisospora* spp. are opportunistic protozoans that are especially prevalent in HIV/AIDS patients. A limitation of our study is that no HIV/AIDS patients or legal representatives participated in groups A-2 and B-2, which comprise the immunosuppressed groups. *Sarcocystis* spp. and *Balantioides coli* are commonly found in regions characterized by animal farming (especially pigs), poor sanitation, and the consumption of raw or undercooked meat (particularly pork). These pathogenic intestinal protozoans are rare in Türkiye. Although the panel used in our research is the most comprehensive multiplex real-time PCR panel for detecting pathogenic intestinal protozoans, and no cases caused by *Cystoisospora* spp., *Sarcocystis* spp., or *B. coli* were identified in our study, the panel must still be designed to detect these pathogenic intestinal protozoans for use in routine diagnosis. Since no cases of *C. cayetanensis* were identified, which is included in the Allplex™ GI Parasite Assay, we could not evaluate the sensitivities of either microscopy or multiplex real-time PCR methods for this pathogen. However, since no false-positive results were detected with either method, their specificity for detecting this pathogen was determined to be 100%.

By integrating automated DNA isolation, multiplex real-time PCR can be considered an almost entirely robotic process. This advancement facilitates the application of multiplex real-time PCR, saves extra time, and reduces staff costs. Recently, the manufacturer of the panel recommended the automated Seegene STARlet (Seegene®, Seoul, South Korea) device for DNA isolation. They stated that DNA isolation from 94 samples takes 155 minutes using this device.

Multiplex real-time PCR, which requires high-quality molecular laboratories, specialized equipment, and regular consumable supplies, is a more expensive method than microscopy. However, it may provide financial advantages by reducing unnecessary and incorrect use of antiparasitic drugs and antibiotics, decreasing the need for other diagnostic tests, and lowering overall healthcare costs. At this point, there is a need for studies evaluating the financial impacts of the multiplex real-time PCR in the diagnosis of pathogenic intestinal protozoans.

Apart from our study, only one prospective study (5) has comparatively evaluated the performance of microscopy and multiplex real-time PCR methods using Allplex™ GI Parasite Assay panel. However, unlike our study, the WS technique was not utilized in that research. The sensitivity value obtained in our study (95.83%) higher than that found in a prospective study (91.83%) conducted by Autier et al. (5). Two retrospective studies (5, 18) have evaluated the performance of multiplex real-time PCR using the Allplex™ GI Parasite Assay panel. The sensitivity value obtained in our study (95.83%) was higher than that found in a retrospective (90.35%) conducted by Autier et al. (5). Unlike our study, a comparison of specificity could not be performed in the study by Autier et al. (5) because specificity values were not stated. The sensitivity (95.83%) and specificity (96.56%) in our study were lower than the sensitivity (96.45%) and specificity (98.33%) reported by Argy et al. (18). These differences may arise from variations in the numbers of tested cases or the compatibility of the DNA extraction kit with the panel used. The sensitivity performance of the Allplex™ GI Parasite Assay against the most common *Cryptosporidium* species in human cases, as well as *C. cayetanensis*, was investigated by Autier et al. (5), and the panel's performance against these pathogens was found to be perfect. However, the performance against other *Cryptosporidium* species must also be evaluated to ensure that the method accurately detects all *Cryptosporidium* species.

CONCLUSION

The performance of multiplex real-time PCR performed using the Allplex™ GI Parasite Assay panel was effective even when only the first sample was tested. However, pathogenic intestinal protozoans not included in the panel, (*Cystoisospora* spp., *Sarcocystis* spp., and *B. coli*) must be added. In addition, it must be verified that the panel accurately detects all *Cryptosporidium* species. Additionally, an automated DNA isolation method should be integrated to maximize yield as soon as possible. We believe that if the panel demonstrates excellent performance in large-scale studies following these enhancements, the multiplex real-time PCR method would be used for the routine diagnosis of pathogenic intestinal protozoans.

Ethics Committee Approval: This study was approved by the İstanbul Medical Faculty Clinical Research Ethics Committee (Date: 24.09.2021, No: 17) and the İstinye University Clinical Research Ethics Committee (Date: 14.10.2021, No: 2/2021.K-75).

Informed Consent: Written informed consent was obtained from all study participants or their legal representatives.

Peer Review: Externally peer-reviewed.

Author Contributions: Conception/Design of Study- B.K., Ö.B.B., G.İ.Y.; Data Acquisition- B.K., Ö.B.B., G.İ.Y., A.Ç.Ö., O.Ö., M.S., M.A.; Data Analysis/Interpretation- B.K., Ö.B.B., G.İ.Y., A.Ç.Ö, O.Ö., M.S., M.A., B.E.; Drafting Manuscript- B.K., Ö.B.B., G.İ.Y.; Critical Revision of Manuscript- B.K., Ö.B.B., G.İ.Y., A.Ç.Ö., O.Ö., M.S., M.A., B.E.; Final Approval and Accountability- B.K., Ö.B.B., G.İ.Y, A.Ç.Ö., O.Ö., M.S., M.A., B.E.; Material or Technical Support- B.K., Ö.B.B., G.İ.Y., O.Ö., M.S., M.A, B.E; Supervision- B.K., Ö.B.B., G.İ.Y.

Conflict of Interest: The authors have no conflict of interest to declare.

Financial Disclosure: This work was supported by Scientific Research Projects Coordination Unit of İstanbul University (Project number: 38270).

REFERENCES

1. Axelrad JE, Freedberg DE, Whittier S, Greendyke W, Lebwohl B, Green DA. Impact of Gastrointestinal Panel Implementation on Health Care Utilization and Outcomes. J Clin Microbiol 2019;57(3):e01775-18.
2. Faria CP, Zanini GM, Dias GS, da Silva S, de Freitas MB, Almendra R, et al. Geospatial distribution of intestinal parasitic infections in Rio de Janeiro (Brazil) and its association with social determinants. PLoS Negl Trop Dis 2017;11(3):e0005445.
3. Short EE, Caminade C, Thomas BN. Climate Change Contribution to the Emergence or Re-Emergence of Parasitic Diseases. Infect Dis (Auckl) 2017;10:1178633617732296.
4. McHardy IH, Wu M, Shimizu-Cohen R, Couturier MR, Humphries RM. Detection of intestinal protozoa in the clinical laboratory. J Clin Microbiol 2014;52(3):712-20.
5. Autier B, Gangneux JP, Robert-Gangneux F. Evaluation of the AllplexTM Gastrointestinal Panel-Parasite Assay for protozoa detection in stool samples: A retrospective and prospective study. Microorganisms 2020;8(4):569.
6. Ghoshal U, Tejan N. Rationale of using multiplex polymerase chain reaction (PCR) panels for etiological diagnosis of infective diarrhea in the tropics. Indian J Gastroenterol 2018;37(5):381-4.
7. Goldenberg SD, Bacelar M, Brazier P, Bisnauthsing K, Edgeworth JD. A cost benefit analysis of the Luminex xTAG Gastrointestinal Pathogen Panel for detection of infectious gastroenteritis in hospitalised patients. J Infect 2015;70(5):504-11.
8. Beal SG, Tremblay EE, Toffel S, Velez L, Rand KH. A Gastrointestinal PCR Panel Improves Clinical Management and Lowers Health Care Costs. J Clin Microbiol 2017;56(1):e01457-17.
9. Machiels JD, Cremers AJH, van Bergen-Verkuyten MCGT, Paardekoper-Strijbosch SJM, Frijns KCJ, Wertheim HFL, et al. Impact of the BioFire FilmArray gastrointestinal panel on patient care and infection control. PLoS One 2020;15(2):e0228596.
10. https://www.cdc.gov/disasters/disease/diarrhea-evac.html (Access date: January 2, 2021).
11. https://www.cdc.gov/infectioncontrol/guidelines/isolation/precautions.html, (Access date: January 2, 2021).
12. Buss SN, Leber A, Chapin K, Fey PD, Bankowski MJ, Jones MK, et al. Multicenter evaluation of the BioFire FilmArray gastrointestinal panel for etiologic diagnosis of infectious gastroenteritis. J Clin Microbiol 2015;53(3):915-25.
13. Binnicker MJ. Multiplex molecular panels for diagnosis of gastrointestinal infection: performance, result interpretation, and cost-effectiveness. J Clin Microbiol 2015;53:3723-8.
14. Garcia LS. *Dientamoeba fragilis*, One of the Neglected Intestinal Protozoa. J Clin Microbiol 2016;54(9):2243-50.
15. uncay S, Inceboz T, Over L, Yalçin G, Usluca S, Şahin S, et al. Dışkıda *Entamoeba histolytica*'nın saptanmasında kullanılan yöntemlerin birlikte değerlendirilmesi. Turkiye Parazitol Derg 2007;31(3):188-93.
16. Acikgoz Y, Ozkaya O, Bek K, Genc G, Sensoy SG, Hokelek M. Cryptosporidiosis: a rare and severe infection in a pediatric renal transplant recipient. Pediatr Transplant 2012;16(4):E115-9.
17. Büyükbaba-Boral Ö, Çelik DG, İliaz R, Akgül A, İşsever H, Akyüz F. İnflamatuar Barsak Hastalığı Olan Hastalarda *Blastocystis* spp.'nin Farklı Tanı Yöntemleri ile Araştırılması. İst Tıp Fak Derg 2017;80(1):38-44.
18. Argy N, Nourrisson C, Aboubacar A, Poirier P, Valot S, Laude A, et al. Selecting a multiplex PCR panel for accurate molecular diagnosis of intestinal protists: a comparative study of Allplex® (Seegene®), G-DiaParaTrio (Diagenode®), and RIDA®GENE (R-Biopharm®) assays and microscopic examination. Parasite 2022;29:5.

İSTANBUL UNIVERSITY PRESS

RESEARCH ARTICLE / ARAŞTIRMA MAKALESİ
Journal of Advanced Research in Health Sciences /
Sağlık Bilimlerinde İleri Araştırmalar Dergisi 2024
DOI: 10.26650/JARHS2024-1498523

INVESTIGATION OF THE RELATIONSHIP BETWEEN HEPATITIS C AND LIVER CANCER DATABASES

HEPATİT C İLE KARACİĞER KANSERİ ARASINDAKİ İLİŞKİNİN VERİ TABANLARI ÜZERİNDEN ARAŞTIRILMASI

Gözde ÖZTAN[1], Halim İŞSEVER[2]

[1]İstanbul University, İstanbul Faculty of Medicine, Department of Medical Biology, İstanbul, Türkiye
[2]İstanbul University, İstanbul Faculty of Medicine, Department of Public Health, İstanbul, Türkiye

ORCID ID: G.Ö. 0000-0002-2970-1834; H.İ. 0000-0002-5435-706X

Citation/Atıf: Öztan G, İşsever H. Investigation of the relationship between hepatitis C and liver cancer databases. Journal of Advanced Research in Health Sciences 2024;7(3):185-200. https://doi.org/10.26650/JARHS2024-1498523

ABSTRACT

Objective: The global prevalence of hepatitis C virus (HCV) infections has recently reached epidemic levels. Liver cancer, known as hepatocellular carcinoma (HCC), is extremely lethal once detected and is common in those with persistent HCV infection without access to appropriate therapy. Recent studies have shown that HCV-encoded proteins contribute to cancer development in infected hepatocytes. To develop treatments for HCC and liver cancer, it is essential to understand how viral proteins interact with host cell proteins.

Material and Methods: We used the Reactive, WikiPathways, KEGG, and Biocarta databases to identify common DEG pathways associated with HCC and HCV.

Results: Through bioinformatics approaches, this study identified common differential genes and related pathways to determine the molecular mechanisms underlying the pathogenesis of hepatitis C-related liver cancer. Investigating gene-gene interactions may lead to more effective treatment approaches. The liver cancer transcriptome identified 708 genes associated with HCC. Data on hepatitis C infection revealed 1768 genes linked to HCV. The Venn diagram then identified 152 DEGs common to HCV and HCC.

Conclusion: We believe that hepatitis C-related liver cancer can be predicted using the first 20 target genes identified through PPI analysis.

Keywords: Hepatocellular carcinoma, hepatitis C virus, databases, genes, bioinformatics, pathways

ÖZ

Amaç: Hepatit C virüsü (HCV) enfeksiyonlarının küresel prevalansı son zamanlarda epidemik seviyelere ulaşmıştır. Hepatoselüler karsinom (HCC) olarak bilinen karaciğer kanseri, tespit edildiğinde çok öldürücüdür ve tedaviye erişimi olmayan, kalıcı HCV enfeksiyonu olan kişilerde yaygındır. Son çalışmalar, HCV tarafından kodlanan proteinlerin, enfekte hepatositlerde kanser gelişimine katkıda bulunduğunu göstermiştir. HCC ve karaciğer kanserine yönelik tedaviler geliştirmek için viral proteinlerin konak hücre proteinleriyle nasıl etkileşime girdiğini anlamak önemlidir.

Gereç ve Yöntemler: HCC ve HCV ile ilişkili yaygın DEG'lerin yolaklarını tanımlamak için Reactome, WikiPathways, KEGG ve Biocarta veritabanlarını kullandık.

Bulgular: Biyoenformatik yaklaşımlar aracılığıyla bu çalışmada, hepatit C ile ilişkili karaciğer kanserinin patogenezinin altında yatan moleküler mekanizmaları belirlemek için ortak diferansiyel genler ve ilgili yolaklar keşfedildi. Gen-gen etkileşimlerinin araştırılması daha etkili tedavi yaklaşımlarına yol açabilir. Karaciğer kanseri transkriptom verileri, 708 genin HCC ile ilişkili olduğunu tanımladı. Hepatit C enfeksiyonuna ilişkin veriler, HCV ile bağlantılı 1768 gen ortaya çıkardı. Daha sonra Venn diyagramı HCV ve HCC'de ortak olan 152 DEG'i tanımladı.

Sonuç: Hepatit C ile ilişkili karaciğer kanserinde, PPI analizi yoluyla belirlediğimiz ilk 20 hedef genin biyobelirteç olarak kullanabileceğine inanıyoruz.

Anahtar Kelimeler: Hepatoselüler karsinom, hepatit C virüsü, veritabanları, genler, biyoinformatik, yolaklar

Corresponding Author/Sorumlu Yazar: Gözde ÖZTAN **E-mail:** gozdeoztan@istanbul.edu.tr

Submitted/Başvuru: 10.06.2024 • **Revision Requested/Revizyon Talebi:** 04.07.2024 • **Last Revision Received/Son Revizyon:** 05.07.2024 • **Accepted/Kabul:** 25.07.2024 • **Published Online/Online Yayın:** 23.10.2024

INTRODUCTION

Globally, liver cancer (LC) is the second-leading cause of cancer-related mortality. Hepatocellular carcinoma (HCC) originates in liver cells and is the most common histological subtype (1). HCC is the second most common type of cancer worldwide, and it is frequently discovered late in development. As a result, early detection of the disease is critical for improving the prognosis of patients with HCC. Blood alpha-fetoprotein detection and liver ultrasonography are the current early clinical screening modalities for HCC. Hence, it is imperative that we promptly develop a more efficient and precise technique for detecting liver cancer. With advancements in our understanding of cancer biology, liquid biopsy will increasingly emerge as a valuable method for early detection of HCC. HCC is associated with many risk factors, including cirrhosis, aflatoxin B ingestion, alcohol use, infection with the hepatitis B virus (HBV), and infection with the hepatitis C virus (HCV) (2).

HCC is a type of cancer that is associated with ongoing inflammation, even in the absence of infectious agents or exposure to harmful substances. Abnormal microenvironment is a significant factor in HCC progression. Endothelial cells, pericytes, dendritic cells, stem/progenitor cells, extracellular matrix components, growth factors, cytokines, and inflammatory cells constitute the HCC microenvironment (3). It is interesting that these factors that cause cancer and HCC are linked to problems in the MDM2-p53 axis, which show up as p53 being turned off and *MDM2* (a transcriptional target and negative regulator of p53) being turned on too much. Mechanistically, dysregulation of the MDM2-p53 feedback loop in HCC tissues controls the initiation and progression of HCC (1).

HCV is a leading cause of liver cancer. As an RNA virus, HCV cannot incorporate itself into the host genome, in contrast to the hepatitis B virus. HCV infection may trigger the progression of HCC, with the intricate interplay between viral and host proteins causing the body to react, leading to inflammation, fibrosis, and eventually cirrhosis. HCV facilitates the oncogenic process by activating cellular oncogenes, inactivating tumour suppressor genes, and deregulating several signal transduction pathways. Epigenetic modifications and alterations are also involved in this process. Recent developments in genetics and gene expression profiling have enhanced our knowledge of the mechanisms underlying the progression of HCV-associated liver cancer (4).

The *TP53* tumour suppressor gene is one of the most frequently identified genetic abnormalities in a wide variety of human cancers, including liver cancer. Both HBV- and HCV-associated HCCs localised more than 60% of the nucleotide changes to the untranscribed strand, according to analysis of mutated TP53 nucleotides. G to A nucleotide changes and C to T mirror transitions were more abundant in the HCV-associated group (36%), compared to HBV-associated HCC (25%). Various forms of cancer, including HCC, have been shown to exhibit abnormal Wnt signalling activity and nuclear β-catenin accumulation. Most of the extra β-catenin in HCC arises from changes in the *CTNNB1* gene, which is found in 20%–40% of liver tumours, and in genes that encode the AXIN and AXIN2 proteins, which are part of the β-catenin degradation complex (5).

Growth hormone (GH) activates signal transducer and activator of transcription 5b (STAT5b), a transcription factor that regulates the expression of genes associated with sexual differences in the liver. If the GH hypothalamo-pituitary-liver axis does not turn on STAT5b, metabolic problems, steatosis, and liver cancer (6). Regardless of liver function, decreased expression of the GHR/STAT5/IGF-1 signalling pathway may influence the development, aggressiveness, and prognosis of HCV-associated HCC (7). Phosphatase and tensin homologue (*PTEN*) deletion on chromosome 10, a tumour suppressor, is frequently mutated or deleted in HCC tumours. *PTEN* has been shown to inhibit HCV secretion (8). They found that lower *PTEN* expression was associated with disease stage, tumour grade, and higher expression of alpha-fetoprotein, a tumour marker for HCC (9).

Bioinformatics methods are rapidly developing to identify genes that enable the detection of the relationship between disease and disease through genomic databases. These bioinformatics methods can identify candidate disease genes. In our study, the relationship between hepatitis C virus and liver cancer was integrated with different bioinformatic strategies by performing gene ontology (GO) and pathway enrichment analyses using various databases. Thus, this study aimed to identify candidate disease genes that will reveal the relationship between these two diseases and use them as possible biomarkers.

MATERIAL AND METHODS

Working area

The study was conducted between February and March 2024 using data analysis techniques.

TCGA and DisGeNET databases

Liver cancer transcriptome data were obtained from the Cancer Genome Atlas (TCGA) database (https://portal.gdc.cancer.gov/) (10). The study identified 708 genes associated with liver cancer.

Hepatitis C infection data were obtained through the DisGeNET database. A total of 1,768 genes were found to be associated with Hepatitis C. Then, 152 differentially expressed genes (DEGs) common to Hepatitis C and LC were identified by Venn diagram using the Bioinformatics & Evolutionary Genomics database (https://bioinformatics.psb.ugent.be/webtools/Venn/) (11).

Gene ontology (GO) and pathway enrichment analyses

An important goal of gene set enrichment analysis is to sort basic biological data into groups, like the molecular pathways of chromosomal areas linked to a group of diseases. We performed gene ontology and functional enrichment analyses using the Enrichr tool (https://maayanlab.cloud/Enrichr/) (12), specifically focusing on cellular components (CC), biological processes (BP), molecular functions (MF), and pathway en-

richment. Enrichr, a web-based programme, enhances gene sets to evaluate biological processes and signalling pathways associated with common genes. We searched four repositories for this research: WikiPathways, BioCarta, Reactive, and the Kyoto Encyclopaedia of Genes and Genomes (KEGG). We used these data repositories to identify the pathways that LC and hepatitis C share. The KEGG pathway identified overlapping genes associated with HCV-related LC.

PPI network analysis and hub protein detection

Subsequently, the study investigated the interaction associations among proteins using STRING (Search Tool for Retrieval of Interaction Genes and Proteins), a web-based application available at https://string-db.org/ (13). Using STRING to analyse the PPI DEG network, you can learn more about the connections among genes. We constructed the PPI protein network from common DEGs using the STRING repository to identify the physical and functional relationships between liver cancer and hepatitis C. Edges, nodes, and the relationships that connect them comprise the PPI network. In this context, the most common nodes are called hub genes. The STRING database presents the interactions between genes in tabular form, starting with the highest scores.

Evaluation of data using statistical methods

Bioinformatics analysis was performed using the R/Bioconductor package, which allows querying, downloading, and performing integrative analyses of TCGA data through the Cancer Genomic Atlas (TCGA) portal. P<0.05 values were used as the standard threshold to evaluate the pathways mentioned in gene ontology (GO) and pathway enrichment analyses. The STRING method was used to examine DEG interactions. Interaction scores >0.7 were considered to indicate high confidence significance and were used to prevent unclear PPIs.

RESULTS

Identification of hepatitis C-associated liver cancer target genes

By comparing genes associated with hepatitis C and liver cancer, we identified 152 DEGs as common therapeutic targets (Figure 1 and Table 1).

GO and KEGG enrichment analyses

Enrichr was used to perform GO and KEGG enrichment analyses to assess the biological values of common genes and their enriched pathways. Three categories emerged from the GO analysis: biological processes (BS), molecular function (MF), and cellular component (HB). We used the GO database as a source to annotate the data. Table 2 provides a concise overview of the 10 most significant terms in the BS, MF, and HB categories. For each of the distinct categories, the bar chart in Figure 2 presents a comprehensive ontological study in a linear manner. The bar chart in Figure 3 presents the top ten terms across the WikiPathways, BioCarta, Reactive, and KEGG pathways.

The Reactome, WikiPathways, KEGG, and Biocarta databases were used to identify pathways of common DEGs associated with liver cancer and hepatitis C. Table 3 summarises the most important pathways identified via analysis of the Reactive, WikiPathways, KEGG, and Biocarta datasets. Figure 3 presents the pathway enrichment analysis results as a bar graph. Hepatitis C and Hepatocellular Carcinoma WP3646 (p=1.014e-20) are included in term 38 via WikiPathways (Figure 3a). Although there are cancer-related pathways in BioCarta (Figure 3a) and Reactome (Figure 3b), none are directly related to hepatitis or HCC. In the KEGG pathway, hepatocellular carcinoma (p=2.101e-34) was found in the 11th term, whereas hepatitis C (p=3.949e-26) was found in the 31st term. The following list includes other cancers linked to HCC associated with HCC (Figure 3d).

Identification of Hub proteins using STRING analysis

We used STRING with Cytoscape to construct a differential gene interaction network through protein-protein interaction (PPI) analysis. A total of 152 nodes and 3077 edges make up the network's final topology (Figure 4). Using the STRING v12.0 analysis (https://string-db.org/), we could construct gene-gene and network relationships.

Our evaluation of hepatitis C-associated liver cancer identified 152 genes with altered expression levels. Using STRING, a web-based tool for network analysis, the possible connections between these 152 genes showed that there were more physiologically important links in the final network (PPI enrichment p value: < 1.0e-16).

We selected the 20 hub genes (Tumour Protein P53 *(TP53)*, Murine double minute 2 *(MDM2)*, E1A Binding Protein P300 *(EP300)*, Heat Shock Protein 90 Alpha Family Class A Member 1 *(HSP90AA1)*, ATM serine/threonine kinase *(ATM)*, Murine double minute 4 *(MDM4)*, B Cell Leukaemia /Lymphoma 2 *(BCL2)*, Breast cancer 1 *(BRCA1)*, Cyclin-dependent kinase inhibitor 1

Table 1: Comparison of two gene expression datasets for identifying co-expressed genes

Features	Total	Target genes
Coexpressed genes of X and Y	152	*CNBP CXCR4 EP300 MET BRCA1 ACSL3 FEV ALDH2 NFKB2 BCL2 PIK3CB NPM1 HLF APOBEC3B FUBP1 NFE2L2 BRD4 VTI1A SET KIT FHIT B2M CTNNB1 CCND1 NOTCH2 ESR1 PRF1 CDK4 ARHGAP26 HRAS BCL6 MYC ARID2 FOXO1 CCR7 PTPRC EXT1 SMAD2 MAPK1 MDM2 AKT2 EGFR NDRG1 ERBB2 CREB1 CD28 STAT5B MYCN TERT SOCS1 RB1 PTPN6 SRC FBXW7 CD209 TP53 CASP9 CDKN1A FAT1 PIK3R1 GPC3 CDKN2C PER1 POU5F1 PDCD1LG2 LMO1 MLH1 APC TPR PAX5 ERC1 SOX2 ROS1 BCL2L12 PTEN FCGR2B PTPN11 SMAD3 FAS CDKN1B MUC1 BCL9 SND1 CASP8 KRAS PPARG NRAS KLF6 MTOR CBLB LCK RAF1 SDC4 HLA-A STAT3 TRIM27 WAS ATM SPECC1 SMAD4 STAT6 TFRC CLTC HSP90AA1 CASP3 HNF1A EPHA3 RARA TNC MYD88 PML PIK3CA IL2 SYK DDIT3 CDH1 DDX6 IL6ST FCRL4 WRN BAP1 MSH2 NCKIPSD CEBPA SALL4 IL7R SDHC NFKBIE TCF7L2 JAK1 CCND2 AKT1 EIF4A2 CUX1 RAD21 MAP2K1 CLIP1 DCC FOXO3 CDKN2A JUN NF2 NRG1 DDX3X FLNA NOTCH1 CD274 TP63 MDM4 ERCC2 PMS2 TOP*1

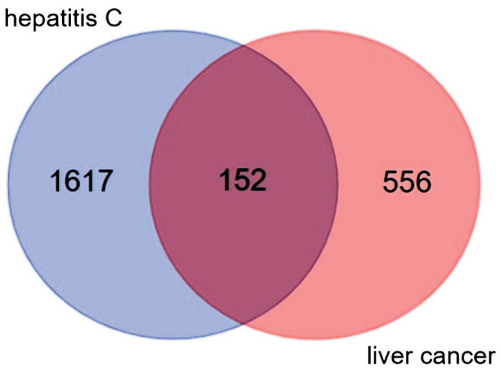

Figure 1: 152 DEGs identified in liver cancer and hepatitis C target genes

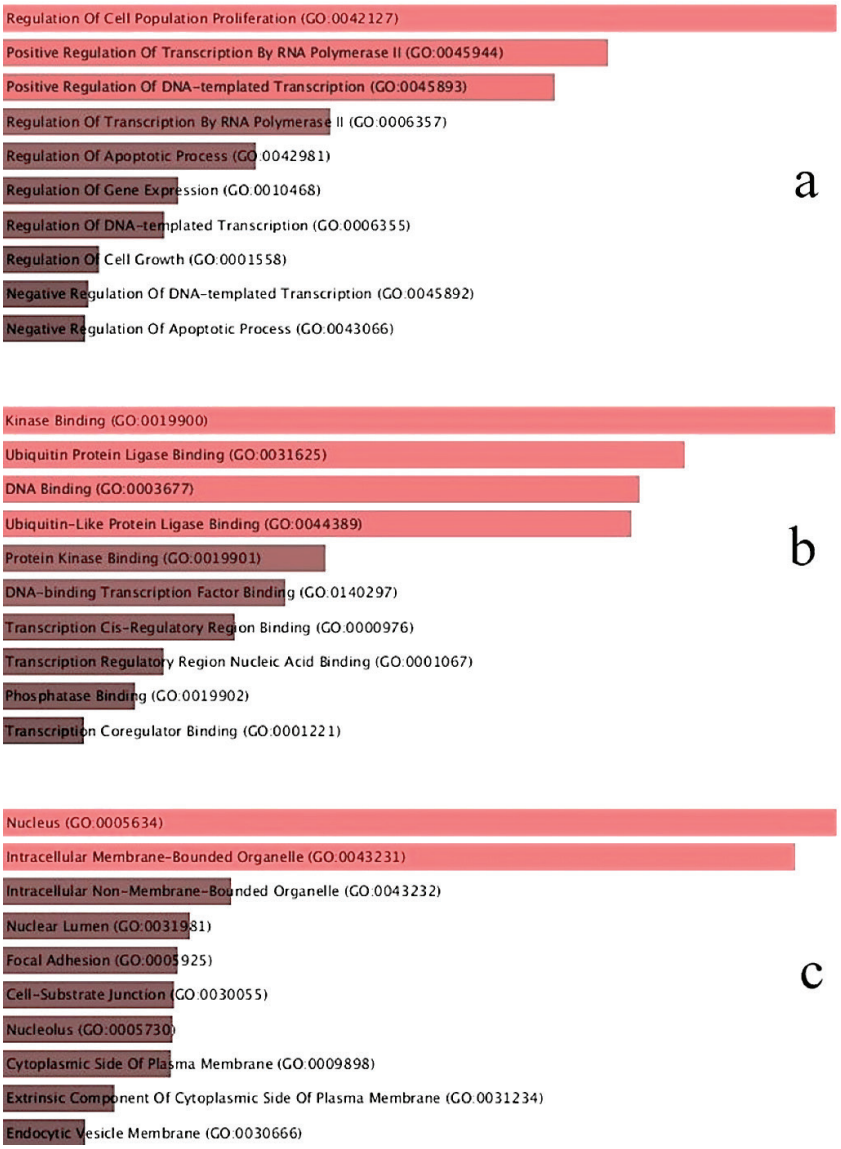

Figure 2: The Enrichr online programme was used to create bar graphs showing the ontological evaluation of shared DEGs between hepatitis C and liver cancer for (a) biological processes, (b) molecular function, and (c) cellular components

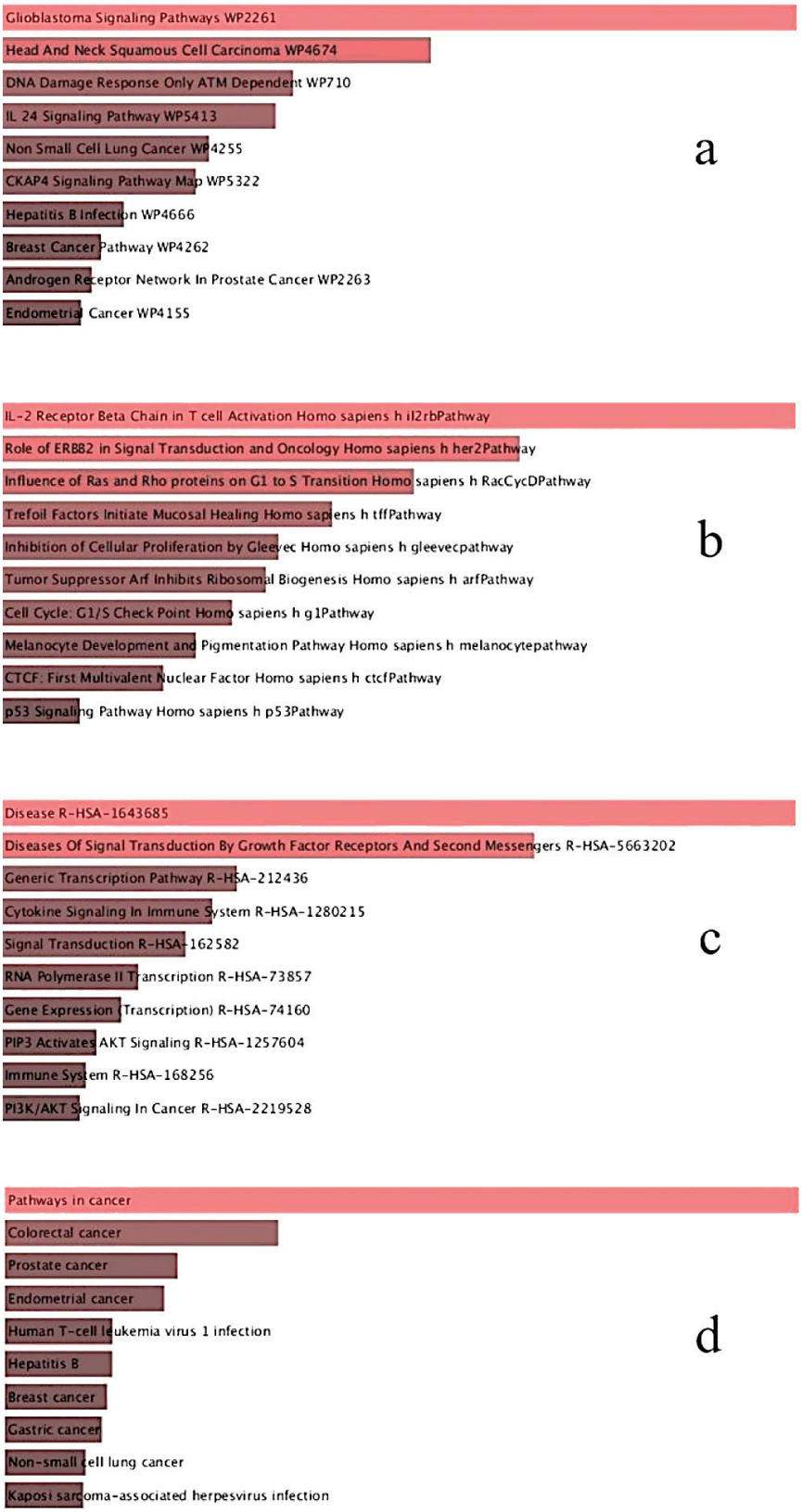

Figure 3: Bar graphs showing the pathway enrichment findings for shared differentially expressed genes (DEGs) between HCV and liver cancer. The data were gathered from four databases: (a) WikiPathways, (b) BioCarta, (c) Reactive, and (d) Enrichr database for KEGG

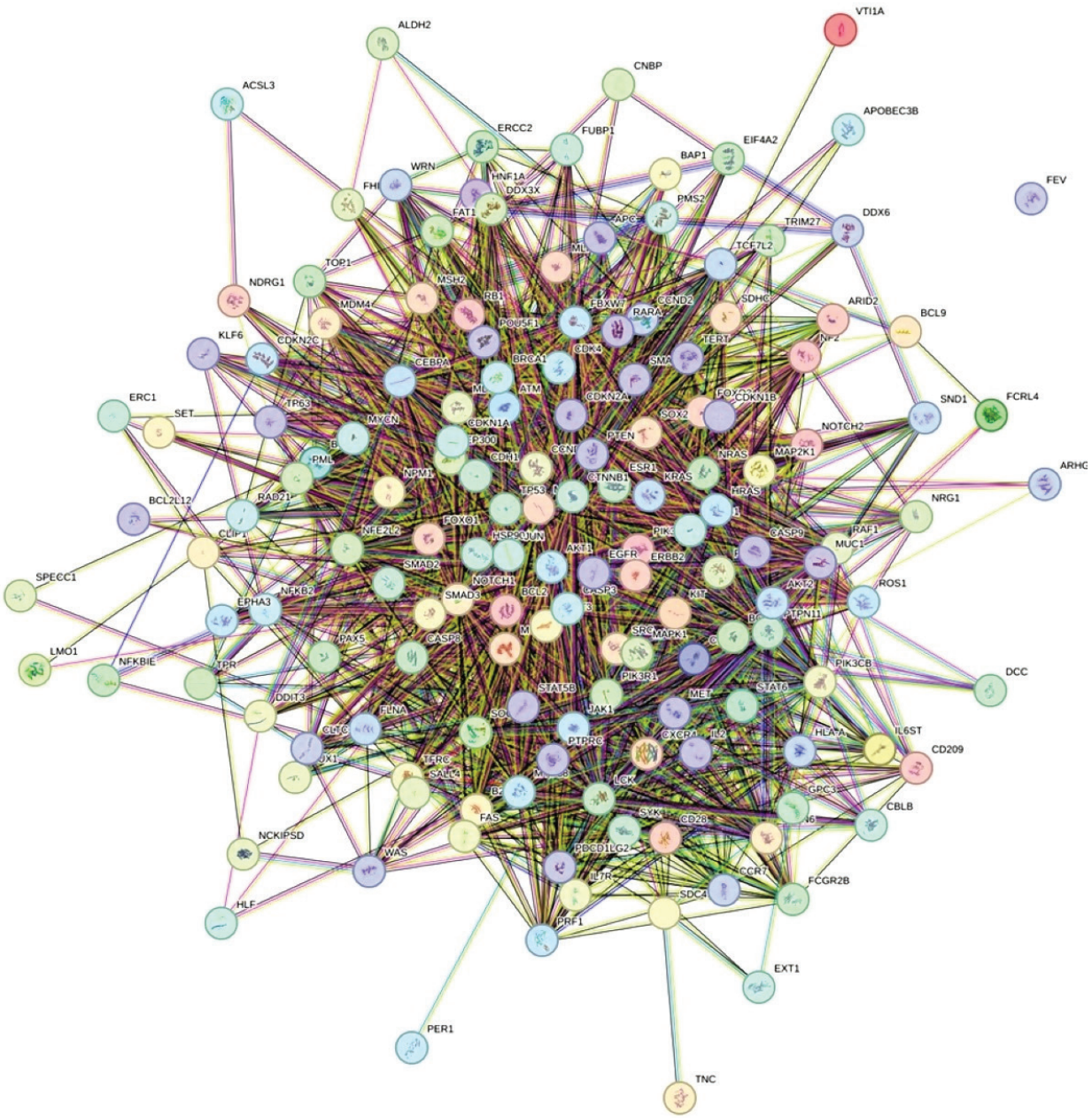

Figure 4: Interaction diagram showing 152 co-expressed genes associated with liver cancer and hepatitis C using the String v12.0 database

(CDKN1A), Cyclin-dependent kinase inhibitor 2A *(CDKN2A)*, Phosphatase and tensin homologue *(PTEN)*, Transcription factor 7-like 2 *(TCF7L2)*, Katenin beta 1 *(CTNNB1)*, Spleen Associated Tyrosine Kinase *(SYK)*, SRC Proto-Oncogene, Non-Receptor Tyrosine Kinase *(SRC)*, Signal transducer and activator of transcription 5B *(STAT5B)*, Janus kinase 1 *(JAK1)*, Signal transducer and activator of transcription 3 *(STAT3)*, Erb-B2 Receptor Tyrosine Kinase 2 *(ERBB2)*, Epidermal growth factor receptor *(EGFR)*) with the highest score from the network using the genomic association method via the Cytoscape plugin (Table 4). New therapeutic approaches may be possible because of the discovery of hub genes, which may also serve as biomarkers for diseases currently under investigation.

DISCUSSION

In this study, common differentially expressed genes for liver cancer and HCV infection were identified using bioinformatics techniques. Furthermore, PPI analysis of common differential genes identified the top 20 target genes. These target genes can guide potential treatment options and serve as biomarkers for liver cancer and hepatitis C infection.

Table 2: Ontology assessment of shared DEGs in liver cancer and hepatitis C

Category	GO ID	Term	P value	Genes
GO biological process	GO:0042127	Regulation of cell population proliferation	1.030e-26	*CEBPA;CDKN1A;NOTCH1;CDKN1B;TFRC;PTEN;EGFR;CCND2;MYC;AKT2;ERBB2;AKT1;STAT6;ARID2;HRAS;STAT5B;TCF7L2;MAP2K1;JUN;NPM1;SMAD3;CDKN2C;CDKN2A;CNBP;STAT3;NRG1;IL2;PML;BCL6;APC;CDK4;KIT;BCL2;MDM2;RARA;CTNNB1;MDM4;PTPN6;KRAS;NF2;RAF1;IL6ST;IL7R;TP53*
	GO:0045944	Positive regulation of transcription by RNA polymerase II	4.227e-24	*CEBPA;NOTCH1;DDX3X;WAS;PIK3R1;BRCA1;FOXO3;FOXO1;EGFR;SOX2;BCL2L12;MUC1;MYC;EP300;STAT6;HRAS;TP63;BRD4;LMO1;SMAD2;STAT5B;TCF7L2;SMAD4;JUN;NPM1;SMAD3;CNBP;STAT3;HNF1A;ESR1;POU5F1;NFKB2;BCL9;PER1;KLF6;MYCN;CREB1;DDIT3;RARA;CTNNB1;ATM;PPARG;TP53;MET;NFE2L2*
	GO:0045893	Positive regulation of DNA-templated transcription	1.724e-23	*DDX3X;BRCA1;SOX2;CDH1;MYC;EP300;AKT1;HRAS;TP63;LMO1;MAP2K1;HNF1A;POU5F1;MYCN;CREB1;DDIT3;RARA;PPARG;TP53;MET;CEBPA;NOTCH1;WAS;PIK3R1;FOXO3;FOXO1;EGFR;BCL2L12;TERT;ERBB2;STAT6;BRD4;SMAD2;STAT5B;TCF7L2;SMAD4;JUN;NPM1;SMAD3;CNBP;STAT3;ESR1;MTOR;NFKB2;BCL9;PER1;KLF6;CTNNB1;ATM;NFE2L2*
	GO:0006357	Regulation of transcription by RNA polymerase II	6.412e-21	*RB1;DDX3X;BRCA1;SOX2;CCND1;MYC;SALL4;EP300;TRIM27;ARID2;HRAS;TP63;LMO1;HNF1A;PAX5;POU5F1;MYCN;CREB1;DDIT3;RARA;PPARG;TP53;MET;CEBPA;NOTCH1;WAS;PIK3R1;FOXO3;FOXO1;EGFR;BCL2L12;MUC1;CUX1;RAD21;TPR;STAT6;BRD4;SMAD2;STAT5B;TCF7L2;SMAD4;JUN;NPM1;SMAD3;CNBP;STAT3;ESR1;NFKB2;BCL9;PER1;KLF6;BCL6;CDK4;FEV;MDM2;CTNNB1;ATM;MDM4;NFE2L2*
	GO:0042981	Regulation of the apoptotic process	4.578e-20	*NOTCH2;DDX3X;TFRC;SRC;PIK3R1;FOXO3;FOXO1;EGFR;CASP9;CCND2;CASP8;MYC;AKT2;CASP3;ERBB2;AKT1;FLNA;JUN;HSP90AA1;NPM1;NRG1;IL2;MTOR;BCL6;APC;BCL2;MDM2;CD28;CTNNB1;FAS;ATM;PTPN6;NF2;RAF1;IL6ST;TP53*
	GO:0010468	Regulation of gene expression	3.531e-19	*RB1;NOTCH2;CEBPA;NOTCH1;DDX3X;TFRC;TNC;BRCA1;PIK3CB;SOX2;CASP8;TERT;CDH1;MYC;AKT1;ERC1;HRAS;MAP2K1;SMAD3;FBXW7;CNBP;STAT3;NRG1;ESR1;POU5F1;MTOR;PML;NFKB2;PER1;MYCN;PTPRC;BCL6;CDK4;DDIT3;FUBP1;MDM2;CD28;ATM;PPARG;KRAS;TP53;MYD88;NFE2L2*
	GO:0006355	Regulation of DNA-templated transcription	5.111e-19	*RB1;CDKN1B;BRCA1;SOX2;CDH1;MYC;SALL4;EP300;AKT1;ERC1;ARID2;HRAS;TP63;MAP2K1;NRG1;HNF1A;PAX5;POU5F1;MYCN;CREB1;DDIT3;RARA;PPARG;TP53;CEBPA;SET;NOTCH1;FOXO3;FOXO1;EGFR;CUX1;RAD21;STAT6;BRD4;SMAD2;STAT5B;TCF7L2;SMAD4;JUN;NPM1;SMAD3;CDKN2A;CNBP;STAT3;ESR1;PML;NFKB2;PER1;KLF6;BCL6;FEV;MDM2;CTNNB1;MDM4;NFE2L2*
	GO:0001558	Regulation of cell growth	2.860e-18	*RB1;SMAD4;CDKN1A;SMAD3;CDKN1B;DDX3X;CDKN2C;TFRC;CDKN2A;TNC;NRG1;BRCA1;IL2;EGFR;MTOR;PML;BCL6;ERBB2;BCL2;AKT1;ROS1;TP53*
	GO:0045892	Negative regulation of DNA-templated transcription	3.784e-18	*RB1;CEBPA;SET;NOTCH1;CDKN1B;BRCA1;FOXO3;FOXO1;SOX2;MUC1;CCND1;CUX1;MYC;TPR;EP300;FLNA;TRIM27;TP63;SMAD2;TCF7L2;SMAD4;JUN;SMAD3;CDKN2A;CNBP;STAT3;NRG1;ESR1;POU5F1;PML;PER1;CREB1;BCL6;DDIT3;MDM2;RARA;CTNNB1;MDM4;PPARG;TP53*
	GO:0043066	Negative regulation of the apoptotic process	4.117e-18	*RB1;NOTCH2;SET;NOTCH1;DDX3X;TFRC;SRC;PIK3R1;FOXO1;EGFR;CCND2;MYC;AKT2;ERBB2;AKT1;FLNA;NPM1;IL2;MTOR;MSH2;PIK3CA;BCL2;MDM2;CD28;CTNNB1;FAS;RAF1;IL6ST;TP53*

Table 2: Ontology assessment of shared DEGs in liver cancer and hepatitis C (Continue)

Category	GO ID	Term	P value	Genes
	GO:0005634	Nucleus	6.773e-28	*RB1;SOX2;CCND2;CCND1;MYC;AKT2;SALL4;EP300;AKT1;TRIM27;TP63;LMO1;MAP2K1;FBXW7;HNF1A;SND1;CLIP1;MYCN;MSH2;DDIT3;TP53;NOTCH2;DDX6;SET;NOTCH1;PIK3R1;FOXO3;FHIT;NDRG1;FOXO1;BCL2L12;TERT;RAD21;TPR;SMAD2;STAT5B;SMAD4;JUN;SMAD3;ESR1;NFKB2;BCL6;CDK4;FEV;FUBP1;BCL2;MDM2;FAT1;ATM;MDM4;NF2;MYD88;APOBEC3B;NFE2L2;CDKN1A;CDKN1B;DDX3X;PTEN;BRCA1;PIK3CB;CASP3;JAK1;HSP90AA1;SYK;POU5F1;CREB1;RARA;PPARG;TOP1;CEBPA;WAS;CXCR4;EGFR;WRN;CUX1;ERBB2;MAPK1;FLNA;PMS2;STAT6;BRD4;TCF7L2;NPM1;CDKN2C;CDKN2A;CNBP;STAT3;PTPN11;MLH1;MTOR;PML;PER1;KLF6;APC;ERCC2;CTNNB1;PTPN6*
	GO:0043231	Intracellular membrane-bound organelles	1.320e-26	*RB1;TFRC;SOX2;CCND2;CCND1;MYC;AKT2;SALL4;EP300;AKT1;TRIM27;TP63;LMO1;MAP2K1;FBXW7;HNF1A;SND1;CLIP1;MYCN;MSH2;DDIT3;TP53;NOTCH2;DDX6;SET;NOTCH1;PIK3R1;FOXO3;FHIT;NDRG1;FOXO1;BCL2L12;TERT;RAD21;TPR;VTI1A;SMAD2;SPECC1;STAT5B;SMAD4;JUN;SMAD3;ESR1;NFKB2;BCL9;BCL6;CDK4;FEV;FUBP1;BCL2;MDM2;FAT1;ATM;MDM4;NF2;MYD88;APOBEC3B;NFE2L2;CDKN1A;CDKN1B;DDX3X;PTEN;BRCA1;PIK3CB;CASP3;JAK1;HSP90AA1;SYK;POU5F1;CREB1;RARA;PPARG;TOP1;CEBPA;WAS;CXCR4;EGFR;MUC1;WRN;CUX1;ERBB2;MAPK1;FLNA;PMS2;STAT6;BRD4;TCF7L2;NPM1;CDKN2C;CDKN2A;CNBP;STAT3;PTPN11;MLH1;MTOR;PML;PER1;KLF6;APC;ERCC2;CTNNB1;PTPN6*
GO Cellular Component	GO:0043232	Intracellular Non-membrane-bound organelles	5.826e-9	*CDKN1A;SET;CLTC;BRCA1;PIK3CB;WRN;CCND2;CASP8;TERT;MYC;RAD21;MAPK1;FLNA;TRIM27;NPM1;ACSL3;MLH1;PML;KLF6;MYCN;BCL6;CDK4;ERCC2;MDM2;RARA;ATM;PTPN6;NF2;TOP1;TP53*
	GO:0031981	Nuclear lumen	1.128e-7	*JUN;CDKN1A;NPM1;PIK3CB;PML;WRN;KLF6;CCND2;MYCN;TERT;BCL6;CDK4;MYC;MDM2;RARA;FLNA;ATM;PTPN6;TRIM27;NF2;TOP1;TP53*
	GO:0005925	Focal adhesion	2.747e-7	*MAP2K1;NPM1;SRC;CLTC;TNC;CXCR4;EGFR;PTPRC;FAT1;MAPK1;FLNA;CTNNB1;KRAS;B2M;JAK1*
	GO:0030055	Cell-substrate junction	3.565e-7	*MAP2K1;NPM1;SRC;CLTC;TNC;CXCR4;EGFR;PTPRC;FAT1;MAPK1;FLNA;CTNNB1;KRAS;B2M;JAK1*
	GO:0005730	Nucleolus	4.006e-7	*CDKN1A;NPM1;PIK3CB;PML;WRN;KLF6;CCND2;MYCN;TERT;BCL6;CDK4;MYC;MDM2;RARA;FLNA;ATM;PTPN6;TRIM27;NF2;TOP1;TP53*
	GO:0009898	Cytoplasmic side of the plasma membrane	4.498e-7	*PTPRC;SYK;CDH1;LCK;SRC;PTEN;KRAS;MYD88;JAK1*
	GO:0031234	Extrinsic component of the cytoplasmic side of a plasma membrane	0.00002653	*SYK;LCK;SRC;KRAS;MYD88;JAK1*
	GO:0030666	Endocytic vesicle membrane	0.0002169	*TFRC;CLTC;MDM2;HLA-A;IL7R;B2M;EGFR*

Table 2: Ontology assessment of shared DEGs in liver cancer and hepatitis C (Continue)

Category	GO ID	Term	P value	Genes
	GO:0019900	Kinase binding	9.156e-21	*RB1;CEBPA;CDKN1A;CDKN1B;TFRC;CLTC;WAS;FOXO3;EGFR;CASP9;CCND2;SOCS1;CCND1;FLNA;TCF7L2;NPM1;SMAD3;CDKN2C;CDKN2A;STAT3;PTPN11;ACSL3;ESR1;PER1;MYCN;PTPRC;APC;LCK;CTNNB1;FAS;PTPN6*
	GO:0031625	Binding of ubiquitin protein ligase	6.171e-19	*RB1;SMAD2;JUN;CDKN1A;HSP90AA1;SMAD3;CDKN1B;FBXW7;CXCR4;BRCA1;FHIT;FOXO1;POU5F1;EGFR;PML;PER1;CASP8;APC;BCL2;MDM2;CTNNB1;TP53;NFE2L2;JAK1*
	GO:0003677	DNA binding	2.197e-18	*CEBPA;DDX3X;BRCA1;FOXO3;FOXO1;EGFR;SOX2;WRN;TERT;CUX1;MYC;EP300;PMS2;TP63;SMAD2;TCF7L2;SMAD4;JUN;SMAD3;CNBP;STAT3;HNF1A;MLH1;POU5F1;PER1;MYCN;MSH2;BCL6;DDIT3;FUBP1;ERCC2;BCL2;RARA;PPARG;TOP1;TP53;NFE2L2*
	GO:0044389	Ubiquitin-like protein ligase binding	2.761e-18	*RB1;SMAD2;JUN;CDKN1A;HSP90AA1;SMAD3;CDKN1B;FBXW7;CXCR4;BRCA1;FHIT;FOXO1;POU5F1;EGFR;PML;PER1;CASP8;APC;BCL2;MDM2;CTNNB1;TP53;NFE2L2;JAK1*
GO-Molecular Function	GO:0019901	Protein kinase binding	1.443e-14	*CDKN1A;CDKN1B;TFRC;CLTC;WAS;FOXO3;CASP9;CCND2;SOCS1;CCND1;TPR;TCF7L2;HSP90AA1;NPM1;SMAD3;CDKN2C;CDKN2A;STAT3;PTPN11;ACSL3;ESR1;PTPRC;APC;LCK;RARA;PTPN6*
	GO:0140297	DNA-binding transcription factor binding	4.472e-14	*RB1;LMO1;SMAD2;CEBPA;TCF7L2;JUN;NPM1;SMAD3;STAT3;CREB1;BCL6;MYC;DDIT3;BCL2;EP300;FLNA;CTNNB1;PPARG;TP53;NFE2L2*
	GO:0000976	Transcription of Cis regulatory region binding	1.842e-13	*RB1;SMAD2;CEBPA;TCF7L2;SMAD4;JUN;NPM1;SMAD3;STAT3;HNF1A;BRCA1;FOXO3;POU5F1;SOX2;PER1;CUX1;MYC;DDIT3;RARA;PPARG;STAT6;TP53;NFE2L2;BRD4*
	GO:0001067	Transcription regulatory region nucleic acid binding	1.346e-12	*CEBPA;TCF7L2;SMAD4;JUN;SMAD3;STAT3;HNF1A;BRCA1;FOXO3;POU5F1;SOX2;PER1;DDIT3;PPARG;TP53;NFE2L2;BRD4*
	GO:0019902	Phosphatase binding	2.988e-12	*SMAD2;SMAD3;CDKN1B;STAT3;PIK3R1;EGFR;LCK;MAPK1;CTNNB1;STAT6;ROS1;MET;JAK1*
	GO:0001221	Transcription coregulator binding	1.254e-11	*PER1;SMAD4;SMAD3;TERT;BCL6;MYC;RARA;EP300;CTNNB1;PPARG;STAT6;ESR1*

GO: gene ontology, p value: probability value

Table 3: Evaluation of common differentially expressed genes between liver cancer and hepatitis C according to pathway enrichment analysis

Category	Term	P value	Genes
WikiPathways	Glioblastoma signalling pathway WP2261	2.063e-47	*RB1;CDKN1A;CDKN1B;SRC;PTEN;PIK3CB;BRCA1;PIK3R1;FOXO3;FOXO1;EGFR;NRAS;CCND2;CCND1;AKT2;ERBB2;AKT1;EP300;MAPK1;HRAS;MAP2K1;CDKN2C;CDKN2A;PIK3CA;CDK4;MDM2;KRAS;MDM4;ATM;RAF1;MET;TP53*
	Head and neck squamous cell carcinoma (WP4674)	3.077e-41	*RB1;NOTCH2;CDKN1A;NOTCH1;PTEN;PIK3CB;PIK3R1;EGFR;NRAS;CASP8;CCND1;TERT;AKT2;ERBB2;AKT1;HRAS;TP63;SMAD4;CDKN2A;MTOR;NFKB2;PIK3CA;CDK4;FAT1;CTNNB1;KRAS;TP53;NFE2L2*
	DNA damage response of ATM-dependent WP710	6.551e-39	*CDKN1A;CDKN1B;PTEN;PIK3R1;PIK3CB;FOXO3;NRAS;CCND2;CCND1;MYC;AKT2;ERBB2;AKT1;MAPK1;HRAS;TCF7L2;JUN;SMAD4;SMAD3;CDKN2A;NFKB2;BCL6;PIK3CA;APC;BCL2;MDM2;CTNNB1;ATM;KRAS;TP53*
	IL-24 signalling pathway WP5413	1.301e-38	*RB1;CDKN1A;CDKN1B;SRC;PRF1;PTEN;CXCR4;PIK3R1;NDRG1;EGFR;SOX2;CASP9;CASP8;CCND1;CDH1;MYC;CASP3;AKT1;MAPK1;JAK1;JUN;HSP90AA1;CDKN2A;STAT3;IL2;MTOR;PTPRC;BCL6;PIK3CA;APC;DDIT3;BCL2;CTNNB1;FAS;ATM;TP53;NFE2L2*
	Nonsmall cell lung cancer WP4255	1.739e-37	*RB1;CDKN1A;PIK3CB;PIK3R1;FOXO3;FHIT;EGFR;CASP9;NRAS;CASP8;CCND1;AKT2;CASP3;ERBB2;AKT1;MAPK1;HRAS;STAT5B;MAP2K1;CDKN2A;STAT3;PIK3CA;CDK4;KRAS;RAF1;TP53*
	CKAP4 signalling pathway map of WP5322	2.892e-37	*CDKN1B;SRC;PTEN;BRCA1;EGFR;SOX2;CASP9;CASP8;CCND1;CDH1;MYC;CASP3;AKT1;MAPK1;MAP2K1;JUN;SMAD4;SMAD3;FBXW7;ESR1;POU5F1;MYCN;PIK3CA;CDK4;MDM2;FAS;CTNNB1;ATM;TP53*
	Hepatitis B infection with WP4666	4.753e-36	*CDKN1A;DDX3X;SRC;PIK3R1;PIK3CB;CASP9;NRAS;CASP8;MYC;AKT2;CASP3;EP300;AKT1;MAPK1;STAT6;HRAS;JAK1;SMAD2;STAT5B;MAP2K1;JUN;SMAD4;SMAD3;STAT3;CREB1;PIK3CA;BCL2;FAS;KRAS;RAF1;MYD88*
	Breast Cancer pathway WP4262	1.152e-35	*RB1;NOTCH2;CDKN1A;NOTCH1;PTEN;PIK3R1;BRCA1;EGFR;NRAS;CCND1;MYC;AKT2;ERBB2;AKT1;MAPK1;HRAS;TCF7L2;MAP2K1;JUN;ESR1;MTOR;NFKB2;PIK3CA;APC;CDK4;KIT;CTNNB1;ATM;KRAS;RAF1;TP53*
	Androgen receptor network in prostate Cancer WP2263	1.653e-35	*RB1;PTEN;BRCA1;NDRG1;CASP9;CASP8;CCND1;MYC;CASP3;AKT1;MAPK1;HRAS;JAK1;SMAD2;MAP2K1;JUN;SMAD3;STAT3;PTPN11;MTOR;MSH2;PIK3CA;CDK4;BCL2;MDM2;ATM;RAF1;TP53*
	Endometrial cancer WP4155	2.523e-35	*TCF7L2;CDKN1A;MAP2K1;PTEN;PIK3CB;PIK3R1;FOXO3;EGFR;CASP9;NRAS;CCND1;PIK3CA;APC;CDH1;AKT2;MYC;ERBB2;AKT1;MAPK1;CTNNB1;KRAS;RAF1;HRAS;TP53*

Table 3: Evaluation of common differentially expressed genes between liver cancer and hepatitis C according to pathway enrichment analysis (Continue)

Category	Term	P value	Genes
BioCarta	IL-2 receptor beta chain in t-cell activation homo sapiens h ıl2rb pathway	2.394e-26	*RB1;STAT5B;MAP2K1;PIK3R1;IL2;CCND2;SOCS1;CCND1;PIK3CA;MYC;BCL2;AKT1;MAPK1;FAS;PTPN6;RAF1;HRAS;JAK1*
	Role of ERBB2 in signal transduction and oncology of homo sapiens h her2 pathway	5.672e-21	*MAP2K1;STAT3;PIK3R1;ESR1;EGFR;PIK3CA;ERBB2;EP300;AKT1;MAPK1;RAF1;HRAS;JAK1*
	Influence of ras and rho proteins on g1-to-s transition in homo sapiens h raccycdpathway	6.538e-19	*RB1;CDKN1A;MAP2K1;CDKN1B;CCND1;PIK3CA;CDK4;AKT1;MAPK1;PIK3R1;RAF1;HRAS*
	Trefoil factors ınitiate mucosal healing by homo sapiens h off pathway	2.554e-17	*CASP9;MAP2K1;PIK3CA;CASP3;ERBB2;AKT1;MAPK1;CTNNB1;PIK3R1;RAF1;HRAS;EGFR*
	Inhibition of cellular proliferation by the Gleevec Homo sapiens h Gleevec pathway	2.847e-16	*STAT5B;JUN;MAP2K1;PIK3CA;MYC;BCL2;AKT1;PIK3R1;RAF1;HRAS*
	Tumour suppressor arf ınhibits ribosomal biogenesis homo sapiens h arf pathways	5.005e-16	*RB1;HSP90AA1;PIK3CA;CDKN2A;MYC;MDM2;AKT1;ATM;PIK3R1;TP53*
	Cell Cycle: G1/S checkpoint pathway of Homo sapiens h g1	2.279e-15	*RB1;CDKN1A;SMAD4;CDKN1B;SMAD3;CCND1;CDKN2A;CDK4;ATM;TP53*
	Melanocyte development and pigmentation pathway of homo sapiens	1.151e-14	*MAP2K1;CREB1;KIT;BCL2;EP300;MAPK1;RAF1;HRAS*
	CTCF: First multivalent nuclear factor of homo sapiens h ctcf pathway	4.967e-14	*SMAD4;CDKN1B;PIK3CA;CDKN2A;MYC;PTEN;MDM2;PIK3R1;MTOR*
	p53 signalling pathway of homo sapiens h p53	2.104e-12	*RB1;CDKN1A;CCND1;CDK4;BCL2;MDM2;TP53*

Table 3: Evaluation of common differentially expressed genes between liver cancer and hepatitis C according to pathway enrichment analysis (Continue)

Category	Term	P value	Genes
Reactome	Disease R-HSA-1643685	1.661e-43	*RB1;CDKN1A;CDKN1B;CLTC;PTEN;BRCA1;PIK3CB;CASP9;CCND2;CASP8;CCND1;MYC;AKT2;EP300;AKT1;TRIM27;B2M;HRAS;JAK1;MAP2K1;HSP90AA1;SYK;FBXW7;NRG1;SND1;HLA-A;CREB1;MSH2;PIK3CA; LCK;KIT;TP53;NOTCH2;NOTCH1;SDC4;SRC;WAS;CXCR4;PIK3R1;FOXO3;FOXO1;EGFR;NCKIPSD;MUC1;NRAS;WRN;CUX1;TPR;ERBB2;GPC3;MAPK1;PMS2;BRD4;SMAD2;STAT5B;TCF7L2;SMAD4;JUN;NPM1;SMAD3;CDKN2A;CNBP;STAT3;PTPN11;MLH1;ESR1;MTOR;PML;NFKB2;EXT1;CDK4;ERCC2;MDM2;CD28;CTNNB1;ATM;PTPN6;MYD88;NFE2L2*
	Diseases of signal transduction via growth factor receptors and second messengers R-HSA-5663202	1.152e-37	*CDKN1A;NOTCH1;CDKN1B;SRC;CLTC;PTEN;PIK3R1;PIK3CB;FOXO3;FOXO1;EGFR;CASP9;NRAS;CUX1;MYC;AKT2;TPR;ERBB2;EP300;AKT1;MAPK1;HRAS;SMAD2;STAT5B;TCF7L2;MAP2K1;SMAD4;HSP90AA1;NPM1;SMAD3;FBXW7;STAT3;NRG1;PTPN11;ESR1;SND1;MTOR;CREB1;PIK3CA;LCK;KIT;MDM2;CD28;CTNNB1*
	Generic transcription pathway R-HSA-212436	5.144e-31	*RB1;CDKN1A;CDKN1B;PTEN;BRCA1;SOX2;CCND2;CCND1;MYC;AKT2;EP300;AKT1;ARID2;TP63;LMO1;FBXW7;HNF1A;PAX5;CREB1;MSH2;DDIT3;KIT;RARA;PPARG;TP53;NOTCH2;NOTCH1;SRC;FOXO3;NDRG1;FOXO1;EGFR;NRAS;WRN;ERBB2;MAPK1;PMS2;SMAD2;TCF7L2;SMAD4;JUN;NPM1;SMAD3;CDKN2A;PTPN11;MLH1;ESR1;IL2;MTOR;PML;BCL6;CDK4;ERCC2;MDM2;CTNNB1;ATM;MDM4*
	Cytokine signalling in immune system R-HSA-1280215	1.822e-30	*EIF4A2;CDKN1A;CDKN1B;PIK3R1;PIK3CB;FOXO3;FOXO1;SOX2;MUC1;NRAS;SOCS1;CASP8;CCND1;MYC;AKT2;CASP3;TPR;AKT1;MAPK1;FLNA;STAT6;B2M;HRAS;JAK1;STAT5B;MAP2K1;JUN;HSP90AA1;SMAD3;SYK;STAT3;PTPN11;IL2;PML;HLA-A;NFKB2;CREB1;BCL6;PIK3CA;LCK;BCL2;PTPN6;IL6ST;IL7R;TP53;MYD88*
	Signal transduction R-HSA-162582	7.225e-30	*CDKN1A;CDKN1B;TFRC;CLTC;PTEN;PIK3CB;SOX2;CASP9;CASP8;CCND1;MYC;AKT2;SALL4;CASP3;EP300;AKT1;CCR7;TRIM27;HRAS;JAK1;MAP2K1;HSP90AA1;SYK;FBXW7;NRG1;CLIP1;-MYCN;CREB1;PIK3CA;LCK;KIT;RARA;PPARG;IL6ST;TP53;NOTCH2;CD274;NOTCH1;SRC;WAS;CXCR4;PIK3R1;FOXO3;FOXO1;EGFR;NCKIPSD;NRAS;SOCS1;TERT;RAD21;ERBB2;MAPK1;FLNA;STAT6;SMAD2;STAT5B;TCF7L2;SMAD4;JUN;SMAD3;STAT3;PTPN11;ARHGAP26;ESR1;IL2;MTOR;PML;BCL9;CDK4;BCL2;MDM2;CD28;CTNNB1;PTPN6;NF2;MYD88*
	RNA Polymerase II Transcription R-HSA-73857	8.311e-29	*RB1;CDKN1A;CDKN1B;PTEN;BRCA1;SOX2;CCND2;CCND1;MYC;AKT2;EP300;AKT1;ARID2;TP63;LMO1;FBXW7;HNF1A;PAX5;CREB1;MSH2;DDIT3;KIT;RARA;PPARG;TP53;NOTCH2;NOTCH1;SRC;FOXO3;NDRG1;FOXO1;EGFR;NRAS;WRN;ERBB2;MAPK1;PMS2;SMAD2;TCF7L2;SMAD4;JUN;NPM1;SMAD3;CDKN2A;PTPN11;MLH1;ESR1;IL2;MTOR;PML;BCL6;CDK4;ERCC2;MDM2;CTNNB1;ATM;MDM4*
	Gene expression (Transcription) R-HSA-74160	1.993e-28	*RB1;CDKN1A;CDKN1B;PTEN;BRCA1;SOX2;CCND2;CCND1;MYC;AKT2;EP300;AKT1;ARID2;TP63;LMO1;HSP90AA1;FBXW7;HNF1A;PAX5;CREB1;MSH2;DDIT3;KIT;RARA;PPARG;TP53;NOTCH2;NOTCH1;SRC;FOXO3;NDRG1;FOXO1;EGFR;NRAS;WRN;TPR;ERBB2;MAPK1;PMS2;SMAD2;TCF7L2;SMAD4;JUN;NPM1;SMAD3;CDKN2A;PTPN11;MLH1;ESR1;IL2;MTOR;PML;BCL6;CDK4;ERCC2;MDM2;CTNNB1;ATM;MDM4*
	PIP3 activates AKT signalling R-HSA1257604	7.098e-28	*CDKN1A;CDKN1B;SRC;PTEN;PIK3R1;PIK3CB;FOXO3;FOXO1;EGFR;CASP9;AKT2;SALL4;ERBB2;AKT1;MAPK1;TRIM27;JUN;NRG1;PTPN11;ESR1;MTOR;PML;CREB1;PIK3CA;LCK;KIT;MDM2-;CD28;PPARG;TP53;MYD88*
	Immune System R-HSA-168256	1.230e-27	*EIF4A2;CDKN1A;CDKN1B;DDX3X;CLTC;PTEN;CBLB;PIK3CB;SOX2;CASP9;CASP8;CCND1;MYC;AKT2;CASP3;EP300;AKT1;B2M;HRAS;JAK1;MAP2K1;HSP90AA1;SYK;FBXW7;HLA-A;PDCD1LG2;CREB1;PIK3CA;LCK;IL6ST;TP53;CD274;SRC;WAS;PIK3R1;FOXO3;FOXO1;NCKIPSD;MUC1;NRAS;SOCS1;TPR;MAPK1;FLNA;STAT6;STAT5B;JUN;SMAD3;STAT3;PTPN11;IL2;MTOR;PML;NFKB2;PTPRC;BCL6;CD209;BCL2;CD28;CTNNB1;PTPN6;NF2;IL7R;NFKBIE;FCGR2B;MYD88*
	PI3K/AKT signalling in cancer R-HSA-2219528 Cells	1.679e-27	*CDKN1A;CDKN1B;SRC;PTEN;NRG1;PTPN11;PIK3R1;PIK3CB;FOXO3;ESR1;FOXO1;EGFR;MTOR;CASP9;CREB1;PIK3CA;LCK;AKT2;KIT;ERBB2;CD28;MDM2;AKT1*

Table 3: Evaluation of common differentially expressed genes between liver cancer and hepatitis C according to pathway enrichment analysis (Continue)

Category	Term	P value	Genes
KEGG	Pathways in cancer	6.708e-62	*RB1;CDKN1A;CDKN1B;PTEN;PIK3CB;CASP9;CCND2;CASP8;CCND1;CDH1;MYC;AKT2;CASP3;EP300;AKT1;HRAS;JAK1;MAP2K1;HSP90AA1;DCC;MSH2;PIK3CA;KIT;RARA;PPARG;RAF1;IL6ST;TP53;MET;NOTCH2;CEBPA;NOTCH1;CXCR4;PIK3R1;FOXO1;EGFR;NRAS;TERT;TPR;ERBB2;MAPK1;STAT6;SMAD2;STAT5B;TCF7L2;SMAD4;JUN;SMAD3;CDKN2A;STAT3;MLH1;ESR1;IL2;MTOR;PML;NFKB2;APC;CDK4;BCL2;MDM2;CTNNB1;FAS;KRAS;IL7R;NFE2L2*
	Colorectal cancer	1.159e-42	*CDKN1A;PIK3CB;PIK3R1;EGFR;CASP9;NRAS;CCND1;AKT2;CASP3;MYC;AKT1;MAPK1;HRAS;SMAD2;TCF7L2;MAP2K1;JUN;SMAD4;SMAD3;DCC;MLH1;MTOR;MSH2;PIK3CA;APC;BCL2;CTNNB1;KRAS;RAF1;TP53*
	Prostate cancer	5.973e-39	*RB1;CDKN1A;CDKN1B;PTEN;PIK3R1;PIK3CB;FOXO1;EGFR;CASP9;NRAS;CCND1;AKT2;ERBB2;AKT1;EP300;MAPK1;HRAS;TCF7L2;MAP2K1;HSP90AA1;MTOR;CREB1;PIK3CA;BCL2;MDM2;CTNNB1;KRAS;RAF1;TP53*
	Endometrial cancer	1.870e-38	*CDKN1A;PTEN;PIK3CB;PIK3R1;FOXO3;EGFR;CASP9;NRAS;CCND1;CDH1;AKT2;MYC;ERBB2;AKT1;MAPK1;HRAS;TCF7L2;MAP2K1;MLH1;PIK3CA;APC;CTNNB1;KRAS;RAF1;TP53*
	Human T-cell leukaemia virus 1 infection	1.549e-36	*RB1;CDKN1A;PTEN;PIK3R1;PIK3CB;NRAS;CCND2;CCND1;TERT;MYC;AKT2;EP300;AKT1;MAPK1;B2M;HRAS;JAK1;SMAD2;STAT5B;MAP2K1;SMAD4;JUN;SMAD3;CDKN2C;CDKN2A;IL2;HLA-A;NFKB2;CREB1;PIK3CA; CDK4; LCK;ATM;KRAS;TP53*
	Hepatitis B	1.573e-36	*RB1;CDKN1A;DDX3X;SRC;PIK3R1;PIK3CB;CASP9;NRAS;CASP8;MYC;AKT2;CASP3;EP300;AKT1;MAPK1;STAT6;HRAS;JAK1;STAT5B;MAP2K1;SMAD4;JUN;SMAD3;STAT3;CREB1;PIK3CA;BCL2;FAS;KRAS;RAF1;TP53;MYD88*
	Breast cancer	2.403e-36	*RB1;NOTCH2;CDKN1A;NOTCH1;PTEN;PIK3R1;BRCA1;PIK3CB;EGFR;NRAS;CCND1;AKT2;MYC;ERBB2;AKT1;MAPK1;HRAS;TCF7L2;MAP2K1;JUN;ESR1;MTOR;NFKB2;PIK3CA;APC;CDK4;KIT;CTNNB1;KRAS;RAF1;TP53*
	Gastric cancer	3.793e-36	*RB1;CDKN1A;CDKN1B;PIK3R1;PIK3CB;EGFR;NRAS;CCND1;TERT;CDH1;AKT2;MYC;ERBB2;AKT1;MAPK1;HRAS;SMAD2;TCF7L2;MAP2K1;SMAD4;SMAD3;MLH1;MTOR;PIK3CA;APC;BCL2;CTNNB1;KRAS;RAF1;TP53;MET*
	Nonsmall cell lung cancer	1.502e-35	*RB1;CDKN1A;PIK3CB;PIK3R1;FOXO3;FHIT;EGFR;CASP9;NRAS;CCND1;AKT2;ERBB2;AKT1;MAPK1;HRAS;STAT5B;MAP2K1;CDKN2A;STAT3;PIK3CA;CDK4;KRAS;RAF1;MET;TP53*
	Kaposi sarcoma-associated herpesvirus infection	1.848e-35	*RB1;CDKN1A;SRC;PIK3R1;PIK3CB;CASP9;NRAS;CASP8;CCND1;MYC;AKT2;CASP3;EP300;AKT1;MAPK1;HRAS;JAK1;TCF7L2;MAP2K1;JUN;SYK;STAT3;MTOR;HLA-A;CREB1;PIK3CA;CDK4-;CTNNB1;FAS;KRAS;RAF1; IL6ST;TP53*

WP: WikiPathways, R-HSA: Reactome Homo sapiens, KEGG: Kyoto Encyclopaedia of Genes and Genomes

Table 4: Identification of 20 highly linked genes based on Cytoscape score values

Node 1	Node 2	Node 1 access	Node 2 access	Score
TP53	*MDM2*	ENSP00000269305	ENSP00000258149	0.999
TP53	*EP300*	ENSP00000269305	ENSP00000263253	0.999
TP53	*HSP90AA1*	ENSP00000269305	ENSP00000335153	0.999
TP53	*ATM*	ENSP00000269305	ENSP00000278616	0.999
TP53	*MDM4*	ENSP00000269305	ENSP00000356150	0.999
TP53	*BCL2*	ENSP00000269305	ENSP00000381185	0.999
TP53	*BRCA1*	ENSP00000269305	ENSP00000418960	0.999
TP53	*CDKN1A*	ENSP00000269305	ENSP00000384849	0.999
TP53	*CDKN2A*	ENSP00000269305	ENSP00000418915	0.999
TP53	*PTEN*	ENSP00000269305	ENSP00000361021	0.999
TCF7L2	*CTNNB1*	ENSP00000486891	ENSP00000495360	0.999
SYK	*SRC*	ENSP00000364898	ENSP00000362680	0.999
STAT5B	*JAK1*	ENSP00000293328	ENSP00000499900	0.999
STAT3	*EP300*	ENSP00000264657	ENSP00000263253	0.999
STAT3	*JAK1*	ENSP00000264657	ENSP00000499900	0.999
STAT3	*SRC*	ENSP00000264657	ENSP00000362680	0.999
SRC	*STAT3*	ENSP00000362680	ENSP00000264657	0.999
SRC	*ERBB2*	ENSP00000362680	ENSP00000269571	0.999
SRC	*EGFR*	ENSP00000362680	ENSP00000275493	0.999
SRC	*HSP90AA1*	ENSP00000362680	ENSP00000335153	0.999

In the ontological evaluation between liver cancer and hepatitis C, *TP53, MDM2, MDM4, BCL2, CDKN1A, CDKN2A, PTEN, TCF7L2, CTNNB1, STAT5B, STAT3, ERBB2,* and *EGFR* genes are involved in the GO biological process and the regulation of cell population proliferation. *TP53, EP300, ATM, BRCA1, TCF7L2, CTNNB1, STAT5B, STAT3,* and *EGFR* genes play a role in the positive regulation of transcription by RNA polymerase II. While *TP53* and *EGFR* genes function in the positive regulation of DNA template transcription, *TP53, MDM2, EP300, ATM, MDM4, BRCA1, TCF7L2, CTNNB1, STAT5B, STAT3*, and *EGFR* genes are important in the regulation of transcription by RNA polymerase II. *MDM2, HSP90AA1, ATM, BCL2, CTNNB1, ERBB2,* and *EGFR* genes function in regulating the apoptotic process, and *MDM2, ATM, BRCA1,* and *STAT3* genes function in regulating gene expression. *MDM2, EP300, MDM4, BRCA1, CDKN2A, TCF7L2, CTNNB1, STAT5B, STAT3,* and *EGFR* genes are effective in regulating DNA templated transcription. In addition, *BCL2, BRCA1, CDKN1A, CDKN2A, ERBB2,* and *EGFR* genes play a role in the regulation of cell growth, MDM2 contributes to the negative regulation of DNA template transcription, and MDM2*, BCL2, CTNNB1, ERBB2,* and *EGFR* contribute to the negative regulation of apoptosis.

In terms of GO molecular functions, *MDM2, HSP90AA1, BCL2, BRCA1, CDKN1A,* and *EGFR* genes are important for ubiquitin protein ligase binding; *EP300, BCL2, BRCA1, TCF7L2, STAT3,* and *EGFR* genes are important for DNA binding; and *MDM2* and *HSP90AA1* genes are important for ubiquitin-like protein ligase binding. Additionally, EP300*, BCL2, TCF7L2,* and *STAT3* genes were associated with DNA-binding transcription factor binding, *BRCA1, TCF7L2,* and *STAT3* genes were associated with transcription cis-regulatory region binding, and *BRCA1, TCF7L2,* and *STAT3* genes were associated with transcription regulatory region nucleic acid binding.

Finding better treatments for the disease and understanding the underlying processes that cause disease progression are the main objectives of molecular research on HCC samples. Activated p53 triggers correct reactions in cells in response to biological stressors, including DNA repair, genetic stability, cell cycle arrest, and the elimination of DNA-damaged cells. The oncogenic protein MDM2 is a crucial cellular p53 antagonists. By stimulating the breakdown of p53, MDM2 inhibits p53 function. The processes underlying MDM2-p53 interactions are more intricate than initially believed, according to available research. Nutlin-3 may be useful for therapy because it stops p53 from binding to MDM2, which makes p53 more stable and increases its accumulation in cells (14).

Most research has focused on EP300's function as a histone acetyltransferase, which modifies chromatin structure to affect transcription. However, we still don't fully understand how EP300 functions as a transcriptional regulator of epithelial-to-mesenchymal transition (EMT). High EP300 expression in HCC tissues is associated with an increased risk of poor prognosis following EMT (15).

Hsp90a, encoded by the *HSP90AA1* gene, is the major cytosolic chaperone in eukaryotes. It functions in cell protection and intracellular signalling, controls protein homeostasis folding and the assembly of secretory polypeptides in the endoplasmic reticulum, and modulates the post-translational translocation of proteins across organelle membranes. Toraih et al. found that late HCC patients had statistically significantly higher *HSP90AA1* expression compared to early HCC patients (16). In response to DNA double-strand breaks, *ATM* acts as a crucial mediator. In their study, Patra et al. demonstrated that hepatocytes and chronic liver biopsy samples infected with HCV had greater ATM expression (17). Compared with HCC patients, those with wild-type TP53 and low p53 target expression have a notable increase in both copy number and expression of the p53 inhibitor protein MDM4 (18).

Bcl-2 suppressed programmed cell death and enhanced cell viability, conferring resistance to detrimental influences. Genes linked to *Bcl-2* are believed to control cell death and may contribute to the initiation and spread of cancer. Li et al. found that *STAT3, MMP-2, and Bcl-2* expression was significantly induced in peripheral blood mononuclear cells isolated from patients with HCV infection and in HCV-infected cell cultures. They also showed that HCV regulates *MMP-2* and *Bcl-2* by activating the STAT3 signalling cascade (19). Diao et al. found that distinct BRCA1-activated networks were identified in higher HCC tissues compared with lower tumour-free hepatitis/cirrhotic tissues arising from HBV or HCV infection (20). Researchers found a link between an unfavourable prognosis of HCC and reduced levels of breast cancer 2 *(BRCA2)* and cyclin-dependent kinase inhibitor 1A *(CDKN1A)* interacting protein (BCCIP) (21).

CDKN2A is a well-recognised gene that inhibits tumour growth and generates the p16-INK4a protein, which controls the cell cycle by preventing tumour progression. It hinders the activities of cyclin-dependent kinases 4 and 6, which are crucial in regulating the cell cycle by impeding the transition from G1 to S phase, thereby aiding in the prevention of cancer. Extensive CpG methylation downregulates CDKN2A expression in HCV-induced HCC (22). Ling et al. investigated the impact of *TCF7L2* gene polymorphisms on HCC risk in a cohort of patients with cirrhosis. This is significant because the *TCF7L2* gene is associated with cancer risk and plays a crucial role in the Wnt signalling pathway. Their research showed that differences in three single-nucleotide polymorphisms (rs290481, rs290487, and rs290489) near the 3' end of the *TCF7L2* gene may increase the risk of HCC. Three SNPs form the basis of a haplotype that significantly distinguishes between patients at low and high risk of HCC (23).

SYK is an innovative biomarker of HCC that plays a vital role in immune cell signalling pathways. Research indicates that HBV or HCV infection leads to significant increases in *SYK* and cytokine expression in hepatocytes. The two major isoform of SYK, SYK (L) and SYK (S), play different roles in HCC development. Healthy liver tissue contains SYK (L), but HCC significantly reduces it. On the other hand, non-tumour tissue showed significantly lower SYK (S) expression. Moreover, SYK (L) suppresses

the proliferation and invasion of HCC cells, whereas SYK (S) has oncogenic activities and promotes the invasion and metastasis of HCC cells (24).

Src is an oncogene, and its overexpression and high activity appear to be involved in the progression of various tumour types, including HCC (25). Physiological processes, such as cell survival and proliferation, rely on *Src* to maintain proper cellular homeostasis. Src regulates the cytoskeleton and cellular morphology, as well as preserving intercellular connections, cell-matrix adhesion, and mobility. Src signalling is essential for the regulation of cellular processes such as proliferation, invasion, migration, angiogenesis, and treatment resistance in liver cancer (26).

Hepatitis B infection is one of the most common differentially expressed genes linked to liver cancer and hepatitis C. Researchers have concluded that the KEGG pathway links it to gastrointestinal stromal tumours (GIST), including colorectal and stomach cancers, as well as various cancer pathways, including prostate, non-small cell lung, and endometrial cancers. According to pathway enrichment analysis data, finding that the Homo sapiens h gleevec pathway inhibits cell growth may help identify new drugs that can be used to improve treatment effectiveness, especially when gleevec (imatinib) is used to treat metastatic malignant GISTs.

In conclusion, our study investigated the roles of common differential genes in liver cancer and hepatitis C infection via bioinformatic analysis of publicly available databases. In hepatitis C-associated liver cancer, the expression and functions of genes related to biological processes, molecular functions, and cellular components were determined. Experimental studies are needed to determine whether these common genes are associated with liver cancer and hepatitis C. To validate our findings, experimental transcriptomic methods should investigate the expression of genes significantly upregulated in hepatitis C-related liver cancer, and proteomic methods should investigate changes in protein levels.

CONCLUSION

Our study found many hub genes, particularly *MDM2, TP53, EP300, HSP90AA1, ATM,* and *MDM4,* to be highly connected in HCC using the genomic association method in the context of the PPI network. These results are significant prognostic biomarkers of HCC and may offer guidance for HCC treatment.

Our study, which is based on bioinformatics results, can be supported by experimental studies that identify common DEGs and related pathways to detect the molecular mechanisms underlying the pathogenesis of HCC.

Ethics Committee Approval: The ethical review and approval for this study were waived due to the bioinformatics study.

Informed consent: This is not applicable.

Peer Review: Externally peer-reviewed.

Author Contributions: Conception/Design of Study- G.Ö., H.İ.; Data Acquisition- G.Ö., H.İ.; Data Analysis/Interpretation- G.Ö., H.İ.; Drafting Manuscript- G.Ö., H.İ.; Critical Revision of Manuscript- G.Ö.; Final Approval and Accountability- G.Ö., H.İ.; Supervision- G.Ö., H.İ.

Conflict of Interest: The authors have no conflict of interest to declare.

Financial Disclosure: The authors declared that this study has received no financial support.

REFERENCES

1. Cao H, Chen X, Wang Z, Wang L, Xia Q, Zhang W. Role of MDM2-p53 axis dysfunction in the hepatocellular carcinoma transformation. Cell Death Discovery 2020;6:53.
2. Chen G, Zhang W, Ben Y. Identification of Key Regulators of Hepatitis C Virus-Induced Hepatocellular Carcinoma by Integrating Whole-Genome and Transcriptome Sequencing Data. Frontiers in Genetics 2021;12:741608.
3. Huang LH, Hsieh TM, Huang CY, Liu YW, Wu SC, Chien PC, Hsieh CH. Disparity of Hepatocellular Carcinoma in Tumour Microenvironment-Related Genes and Infiltrating Immune Cells between Asian and Non-Asian Populations Genes (Basel) 2021;12(8):1274
4. Lin MV, King LY, Chung RT. Hepatitis C virus-associated cancer. Annu Rev of Pathol 2015;10:345-70.
5. Tornesello ML, Buonaguro L, Tatangelo F, Botti G, Izzo F, Buonaguro FM. Mutations in the TP53, CTNNB1, and PIK3CA genes of hepatocellular carcinoma associated with hepatitis B and hepatitis C virus infections. Genomics 2013;102(2):74-83.
6. Oshida K, Vasani N, Waxman DJ, Corton JC. Disruption of STAT5b-Regulated Sexual Dimorphism of the Liver Transcriptome by Diverse Factors Is a Common Event. PLoS One 2016;11(3):e0148308.
7. Abu El-Makarem MA, Kamel MF, Mohamed AA, Ali HA, Mohamed MR, Mohamed AEM, et al. Down-regulation of hepatic expression of GHR/STAT5/IGF-1 signalling pathway fosters development and aggressiveness of HCV-related hepatocellular carcinoma: Crosstalk with Snail-1 and type 2 transforming growth factor-beta receptor PLoS One 2022;17(11):e0277266.
8. Wu Q, Li Z, Mellor P, Zhou Y, Anderson DH, Liu Q. The role of PTEN-HCV core interaction in hepatitis C virus replication. Scientific Reports 2017;7(1):3695.
9. Khalid A, Hussain T, Manzoor S, Saalim M, Khaliq S. PTEN: A potential prognostic marker in virus-induced hepatocellular carcinoma. Tumour Biology 2017;39(6):1010428317705754.
10. National Cancer Enstitute, Genomic Data Commons, Data Portal. 09.06.2024 https://portal.gdc.cancer.gov Access Date: 09.06.2024
11. Bioinformatics & Evolutionary Genomics database. 09.06.2024. https://bioinformatics.psb.ugent.be/webtools/Venn/
12. Enrichr: comprehensive gene set enrichment analysis web server. 09.06.2024 https://maayanlab.cloud/Enrichr
13. STRING (Search Tool for Retrieval of Interaction Genes and Proteins), a web-based application 09.06.2024 https://string-db.org/
14. Azer SA. MDM2-p53 Interactions in Human Hepatocellular Carcinoma: What Is the Role of Nutlins and New Therapeutic

Options? J Clin Med 2018;7(4):64.
15. Ma C, Huang S, Xu L, Tian L, Yang Y, Wang J. Transcription coactivator P300 activates Elk1-aPKC-iota signalling mediated epithelial-to-mesenchymal transition and malignancy in hepatocellular carcinoma. Oncogenesis 2020;9(3):32.
16. Toraih EA, Alrefai HG, Hussein MH, Helal GM, Khashana MS, Fawzy MS. Overexpression of heat shock protein HSP90AA1 and translocase of the outer mitochondrial membrane TOM34 in HCV-induced hepatocellular carcinoma: A pilot study. Clin Biochemistr 2019;63:10-7.
17. Patra T, Meyer K, Ray RB, Ray R. Hepatitis C virus-mediated inhibition of miR-181c Activates ATM Signalling and Promotes Hepatocyte Growth. Hepatology 2020;71(3):780-93.
18. Cancer Genome Atlas Research Network. Electronic address: wbe, Cancer Genome Atlas Research N. Comprehensive and Integrative Genomic Characterisation of Hepatocellular Carcinoma. Cell 2017;169(7):1327-41.
19. Li Y, Zhang Q, Liu Y, Luo Z, Kang L, Qu J, et al. Hepatitis C virus activates Bcl-2 and MMP-2 expression through multiple cellular signalling pathways. J Virol 2012;86(23):12531-43.
20. Diao H, Wang L, Huang J, Jiang M, Zhou H, Li X, et al. BRCA1-mediated inflammation and growth activated and inhibited transition mechanisms between non-tumour hepatitis/cirrhotic tissues and HCC. J Cell Biochemistr 2014;115(4):641-50.
21. Lu H, Ye C, Feng X, Liu J, Bhaumik M, Xia B, et al. Spontaneous Development of Hepatocellular Carcinoma and B-Cell Lymphoma in Mosaic and Heterozygous Brca2 and Cdkn1a-Interacting Protein Knockout Mice. Am J Pathol 2020;190(6):1175-87.
22. Nomeir H, Elsheredy H, Nomeir A, Mostafa NR, El-Hamshary S. Diagnostic performance of RASSF1A and CDKN2A methylation versus -fetoprotein in hepatocellular carcinoma. Clin Experim Hepatol 2022;8(3):243-52.
23. Ling Q, Dong F, Geng L, Liu Z, Xie H, Xu X, Zheng S. Impacts of TCF7L2 gene polymorphisms on the susceptibility of hepatogenous diabetes and hepatocellular carcinoma in cirrhotic patients. Gene 2013;522(2):214-8.
24. Qu C, Zheng D, Li S, Liu Y, Lidofsky A, Holmes JA, et al. Tyrosine kinase SYK is a potential therapeutic target for liver fibrosis. Hepatology 2018;68(3):1125-39.
25. Zhao R, Wu Y, Wang T, Zhang Y, Kong D, Zhang L, et al. Elevated Src expression is associated with hepatocellular carcinoma metastasis in northern Chinese patients. Oncol Lett 2015;10(5):3026-34.
26. Ren H, Fang J, Ding X, Chen Q. Role and inhibition of Src signalling in the progression of liver cancer. Open Life Sciences 2016;11(1):513–8.

İSTANBUL UNIVERSITY PRESS

RESEARCH ARTICLE / ARAŞTIRMA MAKALESİ
Journal of Advanced Research in Health Sciences /
Sağlık Bilimlerinde İleri Araştırmalar Dergisi 2024
DOI: 10.26650/JARHS2024-1397075

LINKING METAL EXPOSURE TO ISCHAEMIC HEART DISEASE: A BIOINFORMATIC ANALYSIS

METAL MARUZİYETİNİN İSKEMİ KALP HASTALIĞIYLA BAĞLANTISI: BİYOİNFORMATİK ANALİZ

Fuat KARAKUŞ[1], Burak KUZU[2]

[1]Van Yüzüncü Yıl University, Faculty of Pharmacy, Department of Pharmaceutical Toxicology, Van, Türkiye
[2]Van Yüzüncü Yıl University, Faculty of Pharmacy, Department of Pharmaceutical Chemistry, Van, Türkiye

ORCID ID: F.K. 0000-0002-5260-3650; B.K. 0000-0002-7305-7177
Citation/Atıf: Karakuş F, Kuzu B. Linking metal exposure to ischaemic heart disease: A bioinformatic analysis. Journal of Advanced Research in Health Sciences 2024;7(3):201-208. https://doi.org/10.26650/JARHS2024-1397075

ABSTRACT

Objective: Cardiovascular disease causing the most deaths worldwide is ischaemic heart disease. In addition to modifiable and non-modifiable risk factors, there is a growing consideration that environmental factors, especially heavy metals, may also contribute to the risk of ischaemic heart disease. The study identified the potential molecular mechanisms associated with ischaemic heart disease induced by arsenic, cadmium, lead, and mercury.

Materials and Methods: In this study, we used toxicogenomic data and various bioinformatic databases and tools, including the Comparative Toxicogenomic Database, ToppGene Suite, GeneMANIA, String, Cytoscape, CHEA3, and MIENTURNET.

Results: We observed an overlap of the CRP, HMOX1, PON1, and PTGS2 genes among the metals and ischaemic heart disease. The most prevalent interactions among these genes were identified as physical interactions, constituting 77.64% of the total. Several pathways were determined as the principal molecular mechanisms that might be influenced by the examined metals involved in the aetiology of ischaemic heart disease (e.g., regulation of plasma lipoprotein particle levels, response to inorganic substances, blood circulation, circulatory system processes, and cellular response to metal ions). CRP and HMOX1 emerged as key genes, whereas CREB3L3 and ATF5 were identified as key transcription factors related to ischaemic heart disease caused by the combination of the examined metals. Furthermore, we identified two miRNAs (hsa-miR-128-3p and hsa-miR-1273g-3p) associated with ischaemic heart disease.

Conclusion: These observations make a substantial contribution to our understanding of the processes underlying ischaemic heart disease induced by arsenic, cadmium, lead, and mercury.

Keywords: Ischaemic heart disease, arsenic, cadmium, lead, mercury, big data

ÖZ

Amaç: Dünya çapında en çok ölüme neden olan kardiyovasküler hastalık iskemik kalp hastalığıdır. Değiştirilebilir ve değiştirilemez risk faktörlerinin yanı sıra, özellikle ağır metaller olmak üzere çevresel faktörlerin de iskemik kalp hastalığı riskine katkıda bulunabileceği düşünülmektedir. Çalışmamızın amacı, arsenik, kadmiyum, kurşun ve cıva tarafından indüklenen iskemik kalp hastalığı ile ilişkilendirilebilecek potansiyel moleküler mekanizmaları belirlemektir.

Gereç ve Yöntem: Bu çalışmada toksikogenomik verileri ve Comparative Toxicogenomic Database, ToppGene Suite, GeneMANIA, STRING, Cytoscape, ChEA3 ve MIENTURNET gibi biyoinformatik veritabanlarını ve araçları kullandık.

Bulgular: Çalışılan metaller ve iskemik kalp hastalığı ile ilişkili genlerden CRP, HMOX1, PON1 ve PTGS2'nin örtüştüğünü gözlemledik. Bu örtüşen genler arasında en yaygın etkileşim fiziksel etkileşimdi (%77,64). Çalışılan metallerin etkileyebilecekleri temel moleküler mekanizmalar olarak çeşitli yolaklar tanımlandı ve bunlar, iskemik kalp hastalığının etiyolojisinde rol oynayan yolakları içeriyordu (örneğin, plazma lipoprotein parçacık seviyelerinin düzenlenmesi, inorganik maddelere yanıt, kan dolaşımı, dolaşım sistemi süreçleri ve metal iyonlarına hücresel yanıt). Bu metallerin indüklediği iskemik kalp hastalığı ile ilişkili olarak temel genler CRP ve HMOX1 iken, ATF5 ve CREB3L3 de temel transkripsiyon faktörleri olarak belirlendi. Ayrıca, iskemik kalp hastalığıyla ilişkili iki miRNA da (hsa-miR-128-3p ve hsa-miR-1273g-3p) belirledik.

Sonuç: Bu gözlemler arsenik, kadmiyum, kurşun ve cıvanın neden olduğu iskemik kalp hastalığının altında yatan süreçleri anlamamıza önemli bir katkı sağlamaktadır.

Anahtar Kelimeler: İskemik kalp hastalığı, arsenik, kadmiyum, kurşun, cıva, büyük veri

Corresponding Author/Sorumlu Yazar: Fuat KARAKUŞ **E-mail:** fuatkarakus@yyu.edu.tr

Submitted/Başvuru: 28.11.2023 • **Revision Requested/Revizyon Talebi:** 03.03.2024 • **Last Revision Received/Son Revizyon:** 04.03.2024 • **Accepted/Kabul:** 19.04.2024 • **Published Online/Online Yayın:** 01.10.2024

INTRODUCTION

Ischaemic heart disease (IHD), alternatively referred to as coronary artery disease or coronary heart disease, refers to an insufficient blood supply to the myocardium due to blockage of the epicardial coronary arteries, typically caused by atherosclerosis. IHD accounts for 16% of global deaths, with a notable increase since 2000, reaching 8.9 million deaths in 2019 (1). Although factors such as age, gender, and family history are non-modifiable risks, there are also modifiable risks such as smoking, hypertension, increased cholesterol levels, physical inactivity, diabetes, obesity, an unhealthy diet, excessive alcohol consumption, and stress (2). Nevertheless, emerging evidence suggests that these factors alone may not entirely elucidate the complexities of IHD. Environmental factors, particularly heavy metal exposure, have been implicated as additional risk factors for IHD (3-5).

The widespread use of organic and inorganic chemicals in the past century has led to an escalation of environmental pollutants within the human body. Arsenic (As), cadmium (Cd), lead (Pb), and mercury (Hg) are extremely toxic metals linked to significant environmental contamination and health issues (6-9). Exposure to these heavy metals, either individually or in combination, is unavoidable because of their persistence in various environmental settings, such as industrial environments, food, water, air, and soil. The primary sources of human exposure include consuming contaminated water and foods, exposure to cigarette smoke, and inhaling polluted air in occupational or residential areas near industrial facilities. Recent studies have revealed that these metals may collectively induce IHD (10-14). Consequently, millions of people worldwide are exposed to elevated levels of these metals through various means.

The objectives of this study were to uncover the potential key genes, proteins, transcription factors, microRNAs, and molecular pathways that underlie heavy metal-linked IHD through the analysis of toxicogenomic data. These data were processed from databases that collect experimental and epidemiological data. Thus, inferences regarding the relationship between heavy metals and IHD were made using bioinformatics tools.

MATERIALS and METHODS

Identifying common genes for the metals and ischaemic heart disease

To investigate the potential relationship between the metals (As, Cd, Hg, and Pb) and IHD, we analysed data gathered from the Comparative Toxicogenomics Database (CTD; https://ctdbase.org) (15). The data were acquired from the "Direct Evidence" section of CTD, where "M" denotes "marker/mechanism" and "T" denotes "therapeutic." The data were downloaded on November 25, 2023, and the DiVenn tool was employed to identify common genes associated with both metals and IHD (16).

Determining the interplay between metals and overlapping genes in the context of IHD

To establish the correlation between genes linked to IHD and those connected to exposure to metals, we conducted a manual analysis using CTD (15). This involved scrutinising the "gene interaction" section in the CTD chemical profile and specifically identifying interactions between genes and metals from the array of interactions of protein activity, mRNA, and protein expression. The resulting table enumerates the interplay between the metals and the chosen genes, excluding interactions involving a combination of two or more chemicals and their collective impact on genes.

Enrichment analysis

Enrichment analysis for molecular functions and biological processes was conducted on annotated genes linked to IHD using the ToppGene Suite (17). This tool, available at https://toppgene.cchmc.org, serves as a platform for gene list enrichment analysis. ToppGene Suite offers ToppFun, accessible at https://toppgene.cchmc.org/enrichment.jsp, which facilitates the identification of functional enrichment within your gene list. It leverages diverse data sources, encompassing the transcriptome, proteome, regulate (TFBS and miRNA), ontologies (GO, Pathway), phenotype (human disease and mouse phenotype), pharmacome (Drug-Gene associations), literature co-citation, and additional features. The significance of the results can be determined by applying a false discovery rate (FDR) correction and adhering to a recommended p-value cut-off of 0.05, as suggested by the ToppGene Suite (17).

Exploring gene-gene and protein-protein interactions

GeneMANIA (http://genemania.org) was used to study the network of gene-gene interactions. The analysis focussed on *Homo sapiens* as the target organism (18).

The protein-protein interactions (PPI) associated with IHD induced by metals were investigated using String v.12 Database (https://string-db.org/cgi) by selecting a medium confidence threshold of 0.4 as the minimum required interaction score (19). Cytoscape version 3.10.1 (http://www.cytoscape.org/) was also utilised for the analysis (20). Additionally, to identify the core proteins contributing to the development of IHD caused by metals, the Network Analyser Cytoscape plugin was utilised to assess betweenness (BC), closeness (CC), and degree centralities (DC).

Analysis of transcription factors and microRNAs

We submitted overlapping genes linked to both the metals and IHD to ChIP-X Enrichment Analysis Version 3 (CHEA3) (https://maayanlab.cloud/chea3) to identify the transcription factors responsible for their regulation (21). Next, the genes were also subjected to the MIENTURNET tool (http://userver.bio.uniroma1.it/apps/mienturnet/) to determine potential miRNA networks from miRTarBase that were experimentally confirmed (22).

RESULTS

Overlapping genes between metals and IHD

The outcomes derived from the initial CTD data exploration showed that 38, 36, 10, 18, and 87 genes are related to As, Cd,

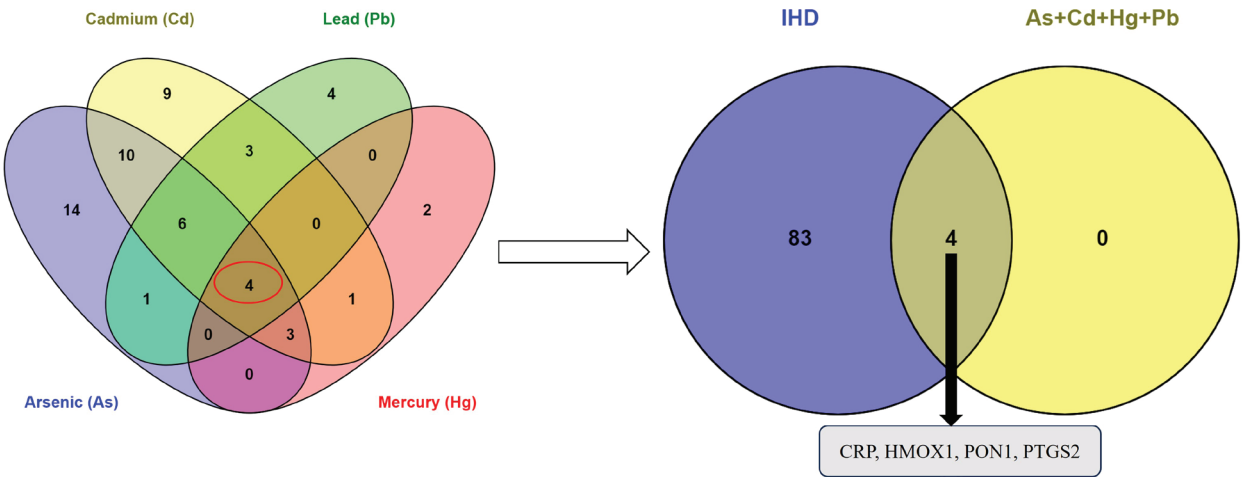

Figure 1: The Venn diagrams show the common genes between IHD and metals.

Hg, Pb, and IHD, respectively. Four genes (CRP, HMOX1, PON1, and PTGS2) were found to be common between the chemicals and IHD (Figure 1, Suppl. Table S1).

Overlapping gene alterations induced by metals

The results of the manually conducted gene interaction analysis are presented in Table 1, which provides detailed insights into the interactions between IHD and the studied chemicals. This includes information on the activity and expression of proteins and mRNA. Arsenic induced CRP and HMOX1 protein expression and increased HMOX1 mRNA expression. In contrast, it either increased or decreased PTGS2 mRNA expression. Cadmium increased both the protein and mRNA expression of HMOX1 and the protein activity of HMOX1. It decreased CRP mRNA expression. However, Cd increased PTGS2 protein expression while affecting mRNA expression in both an increase and a decrease. While lead and mercury decreased PON1 protein activity, they increased HMOX1 mRNA expression. Lead also increased CRP protein expression and PTGS2 mRNA and protein expression.

Molecular processes related to common genes between metals and IHD

The terms related to molecular function delineate actions occurring at the molecular level, typically aligning with activities achievable by individual gene products, such as proteins or RNA molecules. Gene ontology enrichment analysis showed that "lipoprotein particle binding", "protein-lipid complex binding", "protein homodimerization activity", "haem binding", and "tetrapyrrole binding" were among the molecular functions linked to genes induced by the metals and IHD (Table 2). The biological processes, or 'biological programmes' accomplished by multiple molecular activities. The five most significant biological processes involved in the aetiology of IHD induced by metals were "regulation of plasma lipoprotein particle levels", "response to inorganic substance", "blood circulation", "circulatory system process", and "cellular response to metal ion" (Table 3).

Analysis of core genes and proteins

The overlapping genes were input into the GeneMania online plug-in, generating a linked network. The analysis revealed that physical interactions (77.64%) were the predominant factors among the overlapping genes (Figure 2). In addition, the PPIs of four common genes (CRP, HMOX1, PON1, and PTGS2) showed four nodes and five edges, and the PPI enrichment p-value was $9.9e^{-05}$. The pivotal genes associated with both metals and IHD were also identified. CRP and HMOX1 were notably detected

Table 1: Overlapping gene alterations linked to the metals and ischaemic heart disease

Gene	Protein name	Arsenic (As)			Cadmium (Cd)			Lead (Pb)			Mercury (Hg)		
		Prot. act.	mRNA exp.	Prot. exp.	Prot. act.	mRNA exp.	Prot. exp.	Prot. act.	mRNA exp.	Prot. exp.	Prot. act.	mRNA exp.	Prot. exp.
CRP	C-reactive protein	-	-	↑	-	↓	-	-	-	↑	-	-	-
HMOX1	Haem oxygenase 1	-	↑	↑	↑	↑	↑	-	↑	-	-	↑	-
PON1	Paraoxonase/ arylesterase 1	-	-	-	-	-	-	↓	-	-	↓	-	-
PTGS2 (COX2)	Prostaglandin G/H synthase 2	-	↑↓	-	-	↑↓	↑	-	↑	↑	-	-	-

↑: Increase, ↓: Decrease, ↑↓: Either increase or decrease, Prot. act.: Protein activity, mRNA exp.: mRNA expression, Prot. exp.: Protein expression

Table 2: Top 5 molecular functions associated with the metals and ischaemic heart disease **(https://**toppgene.cchmc.org/output.jsp).

	ID	Name	pValue	Genes from the input	Genes used in annotation
1	GO:0071813	Lipoprotein particle binding	$1.797E^{-5}$	CRP, PON1	35
2	GO:0071814	Protein-lipid complex binding	$1.797E^{-5}$	CRP, PON1	35
3	GO:0042803	Protein homodimerization activity	$2.737E^{-4}$	HMOX1, PON1, and PTGS2	824
4	GO:0020037	Haem binding	$3.349E^{-4}$	HMOX1, PTGS2	150
5	GO:0046906	Tetrapyrrole binding	$3.809E^{-4}$	HMOX1, PTGS2	160

Table 3: Top 5 biological processes associated with the metals and ischaemic heart disease (https://toppgene.cchmc.org/output.jsp).

	ID	Name	pValue	Genes from the Input	Genes used in Annotation
1	GO:0097006	Regulation of plasma lipoprotein particle levels	$4.393E^{-7}$	CRP, HMOX1, and PON1	100
2	GO:0010035	Response to an inorganic substance	$1.699E^{-6}$	CRP, HMOX1, PON1, and PTGS2	747
3	GO:0008015	Blood circulation	$1.783E^{-6}$	CRP, HMOX1, PON1, and PTGS2	756
4	GO:0003013	circulatory system process	$2.746E^{-6}$	CRP, HMOX1, PON1, and PTGS2	842
5	GO:0071248	Cellular response to metal ions	$6.543E^{-6}$	CRP, HMOX1, and PTGS2	245

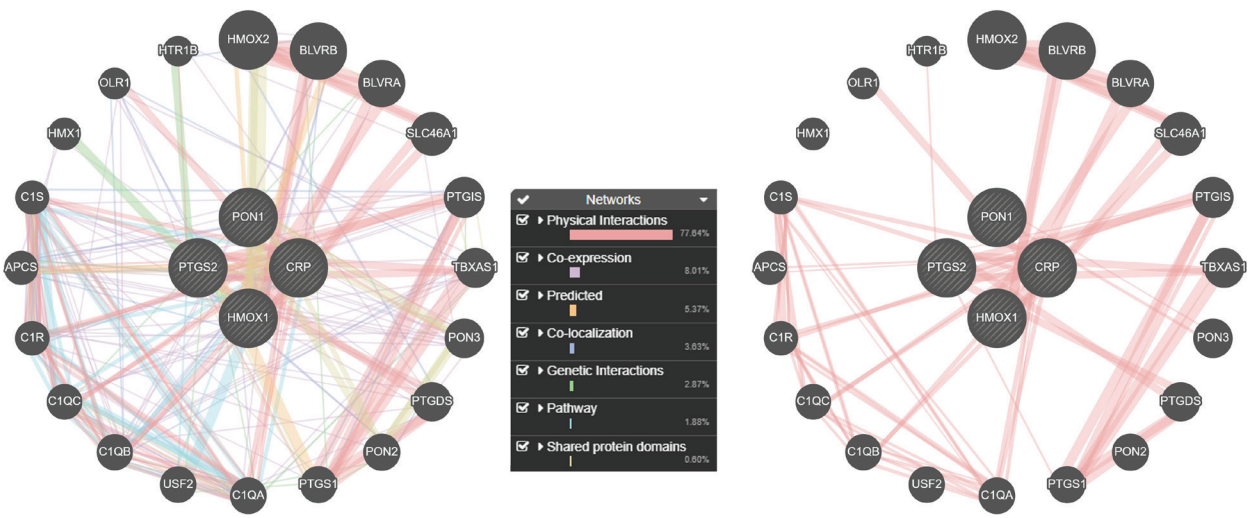

Figure 2: GeneMANIA-predicted gene-gene and physical interactions of the four common genes

in three centrality parameters: BC, CC, and DC (Figure 3a and Table 4).

Key transcription factors and miRNAs related to metals and IHD

To investigate the regulatory connexions between genes and transcription factors, the CHEA3 tool was employed. A total of 22 connexions were recognised between 10 transcription factors and 4 genes. As illustrated in Figure 3b, CREB3L3 and ATF5 regulated four genes, NR1H4 and NR1I3 regulated three genes, and ZNF267, NFE2L2, and NR4A3 regulated two genes each, with the others regulating one gene each. The primary transcription factors in this group were CREB3L3 and ATF5 (Suppl. Table S2).

Regarding miRNAs, we established connexions between miRNAs and target genes using the tool provided by MIENTURNET. We observed that the miRNAs displaying the most elevated

Table 4: Centrality analysis of overlapping genes related to the metals and ischaemic heart disease

Overlapping genes	Degree	Betweenness centrality	Closeness centrality
CRP	3	0.166	1.00
HMOX1	3	0.1667	1.00
PON1	2	0	0.75
PTGS2	2	0	0.75

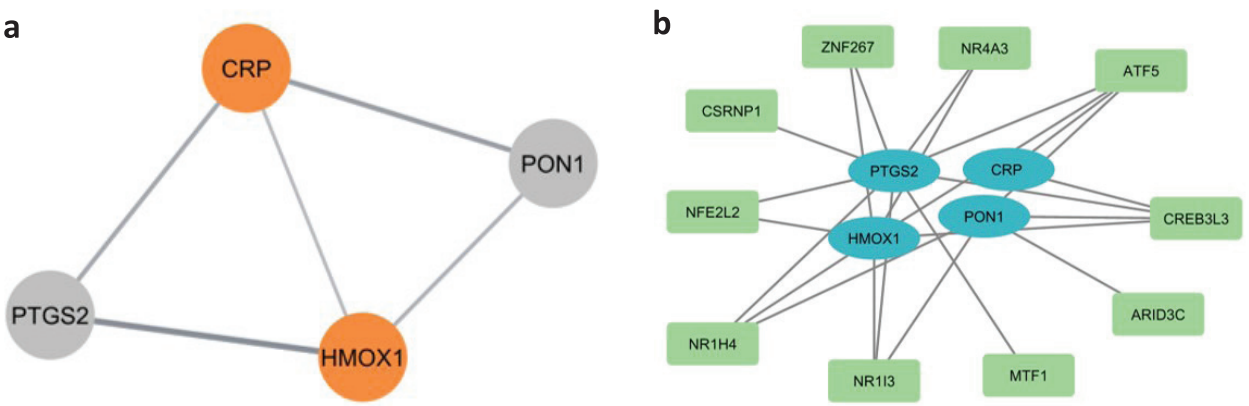

Figure 3: a) The centrality analysis of common genes reveals the core proteins/genes, shown as light brown nodes. b) The top 10 transcription factors related to the four common genes are highlighted, with green nodes indicating transcription factors. c) miRNA-target analysis shows the top 10 miRNAs related to the four common genes.

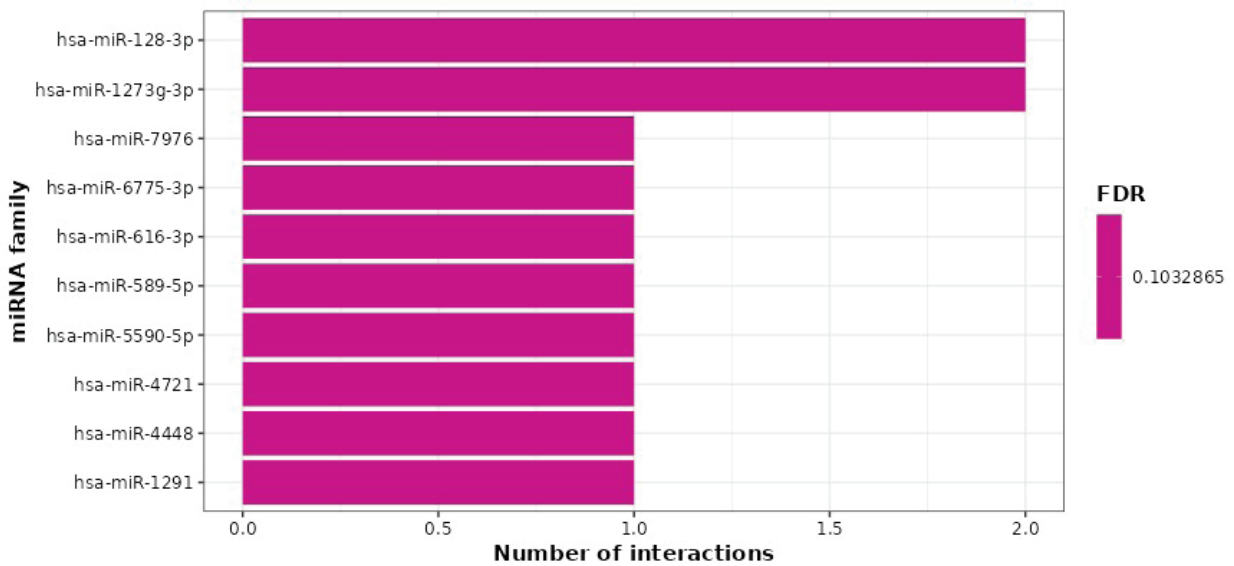

Figure 3: c) miRNA-target analysis shows the top 10 miRNAs related to the four common genes.

expression and interactions were hsa-miR-128-3p and hsa-miR-1273g-3p, which are related to four genes involved in the aetiology of IHD induced by metals (Figure 3c, Suppl. Table S3).

DISCUSSION

In this study, big data and toxicogenomic data mining were employed to illustrate a positive relationship between metals (As, Cd, Hg, and Pb) and ischaemic heart disease (IHD). *In silico* analysis of these metals revealed alterations in four genes (CRP, HMOX1, PON1, and PTGS2) involved in the aetiology of IHD. Lipoprotein particle binding emerged as the leading molecular function, whereas the regulation of plasma lipoprotein particle levels was identified as the foremost biological process related to IHD induced by these metals.

Centrality analysis revealed that CRP and HMOX1 are key genes in IHD induced by these metals. C-reactive protein (CRP) is encoded by the CRP gene and synthesised by the liver. CRP levels increase during inflammation in the body, which has been identified as a major risk factor for IHD (23-25). Manual CTD analysis indicated that As and Pb increased CRP protein expression (Table 1). Another core gene is haem oxygenase 1 (HMOX1), which degrades haem, generating CO and biliverdin, while simultaneously releasing iron. HMOX1 is critical for heart repair and survival. All studied metals upregulate HMOX1, although it is also frequently up-regulated in tumour tissues (26, 27) (Table 1).

ATF5 (Cyclic AMP-dependent transcription factor ATF5) and CREB3L3 (Cyclic AMP-responsive element-binding protein 3-like protein 3) were identified as the main transcription factors. Our findings align with those of prior research; for instance, ATF5 and CREB3L3 were identified as crucial transcription factors in cardiovascular diseases induced by cadmium, lead, and mercury. It has also been mentioned that the mitochondrial unfolded protein response, a cytoprotective signalling system, depends on ATF5 activation (28). Another core transcription factor is CREB3L3, which oversees various metabolic processes, including lipid metabolism, cholesterol absorption, and glucose. CREB3L3 performs a versatile protective function against atherosclerosis (29).

Regarding miRNAs, we observed that hsa-miR-128-3p and hsa-miR-1273g-3p were the predominant miRNAs triggered by the combination of metals associated with the aetiology of IHD. A study that reported the inhibition of hsa-miR-128-3p provides protection to human cardiomyocytes against ischaemia/reperfusion corroborates our results (30). However, there is no study in the literature regarding hsa-miR-1273g-3p.

In conclusion, our study highlights the crucial involvement of genes CRP and HMOX1, transcription factors ATF5 and CREB3L3, and miRNAs hsa-miR-128-3p and hsa-miR-1273g-3p in the development of IHD. ATF5 and CREB3L3, along with hsa-miR-128-3p and hsa-miR-1273g-3p, have the potential to open avenues for novel therapeutic targets in future IHD treatments.

Ethics Committee Approval: Since this study consists entirely of bioinformatics and in silico analyses, ethics committee approval is not required.

Peer Review: Externally peer-reviewed.

Author Contributions: Conception/Design of Study- F.K.; Data Acquisition- F.K., B.K. Data Analysis/Interpretation- F.K., B.K. Drafting Manuscript- F.K Critical Revision of Manuscript- F.K., B.K. Final Approval and Accountability- F.K., B.K. Material and Technical Support- F.K., B.K. Supervision- F.K.

Conflict of Interest: The authors declare that there is no conflict of interest.

Financial Disclosure: The authors declared that this study has received no financial support.

REFERENCES

1. Duggan JP, Peters AS, Trachiotis GD, Antevil JL. Epidemiology of coronary artery disease. Surg Clin North Am 2022;102(3):499-516.
2. Malakar AK, Choudhury D, Halder B, Paul P, Uddin A, Chakraborty S. A review on coronary artery disease, its risk factors, and therapeutics. J Cell Physiol 2019;234(10):16812-23.
3. Chen Z, Huo X, Chen G, Luo X, Xu X. Lead (Pb) exposure and heart failure risk. Environ Sci Pollut Res Int 2021;28(23):28833-47.
4. Wang Z, Xue K, Wang Z, Zhu X, Guo C, Qian Y, et al. Effects of e-waste exposure on biomarkers of coronary heart disease (CHD) and their associations with level of heavy metals in blood. Environ Sci Pollut Res Int 2022;29(33):49850-7.
5. Gump BB, Heffernan K, Brann LS, Hill DT, Labrie-Cleary C, Jandev V et al. Exposure to arsenic and subclinical cardiovascular disease in 9- to 11-year-old children, syracuse, new york. JAMA Netw Open 2023;6(6):e2321379.
6. Das S, Sultana KW, Ndhlala AR, Mondal M, Chandra I. Heavy metal pollution in the environment and its impact on health: exploring green technology for remediation. Environ Health Insights 2023;17:11786302231201259.
7. Xu L, Mondal D, Polya DA. Positive association of cardiovascular disease with chronic exposure to drinking water arsenic at concentrations below the who provisional guideline value: a systematic review and meta-Analysis. Int J Environ Res Public Health 2020;17(7):2536.
8. Glicklich D, Shin CT, Frishman WH. Heavy metal toxicity in chronic renal failure and cardiovascular disease: possible role for chelation therapy. Cardiol Rev 2020;28(6):312-8.
9. Hu XF, Lowe M, Chan HM. Mercury exposure, cardiovascular disease, and mortality: a systematic review and dose-response meta-analysis. Environ Res 2021;193:110538.
10. Tsuji JS, Perez V, Garry MR, Alexander DD. Association of low-level arsenic exposure in drinking water with cardiovascular disease: a systematic review and risk assessment. Toxicology 2014;323:78-94.
11. Ujueta F, Navas-Acien A, Mann KK, Prashad R, Lamas GA. Low-level metal contamination and chelation in cardiovascular disease-a ripe area for toxicology research. Toxicol Sci 2021;181(2):135-47.
12. Nigra AE, Moon KA, Jones MR, Sanchez TR, Navas-Acien A. Urinary arsenic and heart disease mortality in nhanes 2003-2014. Environ Res 2021;200:111387.
13. Liu J, Song W, Li Y, Wang Y, Cui Y, Huang J, et al. Burden of coronary heart disease and cancer from dietary exposure to inorganic arsenic in adults in china, 2016. Ann Glob Health 2022;88(1):28.
14. Liu J, Li Y, Li D, Wang Y, Wei S. The burden of coronary heart disease and stroke attributable to dietary cadmium exposure in chinese adults, 2017. Sci Total Environ 2022;825:153997.
15. Davis AP, Wiegers TC, Johnson RJ, Sciaky D, Wiegers J, Mattingly CJ. Comparative toxicogenomics database (ctd): update 2023. Nucleic Acids Res 2023;51(D1):D1257-62.
16. Sun L, Dong S, Ge Y, Fonseca JP, Robinson ZT, Mysore KS, Mehta P. Divenn: an interactive and integrated web-based visualization tool for comparing gene lists. Front Genet 2019;10:421.
17. Chen J, Bardes EE, Aronow BJ, Jegga AG. Toppgene suite for gene list enrichment analysis and candidate gene prioritization. Nucleic

Acids Res 2009;37:W305-11.
18. Franz M, Rodriguez H, Lopes C, Zuberi K, Montojo J, Bader GD, et al. Genemania update 2018. Nucleic Acids Res 2018;46(W1):W60-W64.
19. Szklarczyk D, Kirsch R, Koutrouli M, Nastou K, Mehryary F, Hachilif R, et al. The string database in 2023: protein-protein association networks and functional enrichment analyses for any sequenced genome of interest. Nucleic Acids Res 2023;51(D1):D638-46.
20. Shannon P, Markiel A, Ozier O, Baliga NS, Wang JT, Ramage D, et al. Cytoscape: a software environment for integrated models of biomolecular interaction networks. Genome Res 2003;13(11):2498-504.
21. Keenan AB, Torre D, Lachmann A, Leong AK, Wojciechowicz ML, Utti V, et al. Chea3: transcription factor enrichment analysis by orthogonal omics integration. Nucleic Acids Res 2019;47(W1):W212-24.
22. Licursi V, Conte F, Fiscon G, Paci P. Mienturnet: an interactive web tool for microrna-target enrichment and network-based analysis. BMC Bioinform 2019;20(1):545.
23. Kaptoge S, Di Angelantonio E, Lowe G, Pepys MB, Thompson SG, Collins R, et al. C-reactive protein concentration and risk of coronary heart disease, stroke, and mortality: an individual participant meta-analysis. Lancet 2010;375(9709):132-40.
24. Ridker PM. From c-reactive protein to interleukin-6 to interleukin-1: moving upstream to identify novel targets for atheroprotection. Circ Res 2016;118(1):145-56.
25. Amezcua-Castillo E, González-Pacheco H, Sáenz-San Martín A, Méndez-Ocampo P, Gutierrez-Moctezuma I, Massó F, et al. C-Reactive Protein: The quintessential marker of systemic inflammation in coronary artery disease-advancing toward precision medicine. Biomedicines 2023;11(9):2444.
26. Jozkowicz A, Was H, Dulak J. Heme oxygenase-1 in tumors: is it a false friend? Antioxid Redox Signal 2007;9(12):2099-117.
27. Otterbein LE, Foresti R, Motterlini R. Heme oxygenase-1 and carbon monoxide in the heart: the balancing act between danger signaling and pro-survival. Circ Res 2016;118(12):1940-59.
28. Nguyen HD, Kim MS. Effects of heavy metals on cardiovascular diseases in pre and post-menopausal women: from big data to molecular mechanism involved. Environ Sci Pollut Res Int 2022;29(51):77635-55.
29. Nakagawa Y, Wang Y, Han SI, Okuda K, Oishi A, Yagishita Y, et al. Enterohepatic transcription factor creb3L3 protects atherosclerosis via srebp competitive inhibition. Cell Mol Gastroenterol Hepatol 2021;11(4):949-71.
30. Chen GH, Xu CS, Zhang J, Li Q, Cui HH, Li XD, et al. Inhibition of mir-128-3p by tongxinluo protects human cardiomyocytes from ischemia/reperfusion injury via upregulation of p70s6k1/p-p70s6k1. Front Pharmacol 2017;8:775.

Table S1.

Chemical/Disease name	Inference network from Comparative Toxicogenomics Database
Arsenic (As)	*ABCG5 | APCS | ATP2B1 | CCL2 | CD40LG | CDKN2B |* ***CRP*** *| ESR1 | ESR2 | FES | FURIN | GDF15 | GFOD1 |* ***HMOX1*** *| IRS1 | JCAD | KCNE2 | LDLR | LTA | MAT2A | MIA3 | MRAS | NOS3 | PDGFD | PECAM1 | PLPP3 |* ***PON1*** *| PRDM16 | PROCR |* ***PTGS2*** *| TBX2 | TERT | TLR4 | TRAF6 | TRIB1 | TWIST1 | VAMP5 | VEGFA |*
Cadmium (Cd)	*ACE | ANGPTL4 | APCS | APOA1 | ATP2B1 | CCL2 | CDKN2B |* ***CRP*** *| CXCL12 | EPO | ESR1 | ESR2 | FURIN | GDF15 | GGCX |* ***HMOX1*** *| IRAK1 | IRS1 | KL | LDLR | LTA | MIR146A | MMP3 | NOS3 | PECAM1 | PHACTR1| PLPP3 |* ***PON1*** *| PSRC1 |* ***PTGS2*** *| SLC5A3 | TLR4 | TRAF6 | TRIB1 | VAMP5 | VEGFA |*
Mercury (Hg)	***CRP*** *| ESR2 | FURIN | GGCX |* ***HMOX1*** *| IRS1 | LIPA |* ***PON1*** *|* ***PTGS2*** *| WDR12 |*
Lead (Pb)	*ACE | APCS | APOA1 | CCL2 |* ***CRP*** *| HECTD4 |* ***HMOX1*** *| ICA1L | LDLR | LTA | MAT2A | MIR146A | NOS3 |* ***PON1*** *|* ***PTGS2*** *| SORT1 | TBC1D7 | TLR4 | VEGFA |*
Ischemic heart disease (IHD)	*ABCG5 | ABCG8 | ABO | ACE | ADAMTS7 | ADTRP | ANGPTL4 | ANKS1A | APCS | APOA1 | APOA5 | APOC3 | ATP2B1 | CARF | CCL2 | CD40LG | CDKN2B | CELSR2 |* ***CRP*** *| CXCL12 | DDAH2 | EPO | ESR1 | ESR2 | FES | FURIN | GDF15 | GFOD1 | GGCX | GNB3 | GUCY1A1 | HECTD4 | HHIPL1 |* ***HMOX1*** *| ICA1L | IRAK1 | IRS1 | JCAD | KCNE2 | KIAA1462 | KL | LDLR | LIPA | LMOD1 | LPA | LRP6 | LTA | MAT2A | MEF2A | MIA3 | MIR146A | MIR146B | MMP3 | MRAS | MRPS6 | NAT2 | NBEAL1 | NOS3 | NPPB | PAPPA | PCSK9 | PDGFD | PECAM1 | PHACTR1 | PLPP3 |* ***PON1*** *| PRDM16 | PROCR | PSRC1 |* ***PTGS2*** *| SARS1 | SH2B3 | SLC5A3 | SORT1 | TBC1D7 | TBX2 | TCF21 | TERT| TLR4 | TRAF6 | TRIB1 | TWIST1 | VAMP5 |VAMP8 | VEGFA | WDR12 | ZC3HC1*
As+Cd+Pb+Hg+ IHD	*CRP | HMOX1 | PON1 | PTGS2*

Table S2. The top 10 transcription factors (TF) related to the metals and ischemic heart disease (https://maayanlab.cloud/chea3/)

Transcription factors	Genes from input
CREB3L3	*CRP, PON1, HMOX1, PTGS2*
ATF5	*CRP, PON1, HMOX1, PTGS2*
NR1I3	*PON1, HMOX1, PTGS2*
NR1H4	*PON1, HMOX1, PTGS2*
ZNF267	*HMOX1, PTGS2*
NFE2L2	*HMOX1, PTGS2*
NR4A3	*HMOX1, PTGS2*
CSRNP1	*PTGS2*
ARID3C	*PON1*
MTF1	*PTGS2*

Table S3. The top 10 miRNAs related to the metals and ischemic heart disease (https://maayanlab.cloud/Enrichr/)

miRNAs	p-value	Genes from input
hsa-miR-1273g-3p	0.003705	*CRP, PON1*
mmu-miR-26b-5p	0.003994	*PTGS2*
hsa-miR-128-3p	0.004014	*HMOX1, PTGS2*
mmu-miR-101a-3p	0.005389	*PTGS2*
hsa-miR-6775-3p	0.009963	*HMOX1*
hsa-miR-616-3p	0.010559	*PON1*
mmu-miR-5098	0.010757	*CRP*
hsa-miR-1291	0.010955	*HMOX1*
hsa-miR-7976	0.011947	*HMOX1*
hsa-miR-5590-5p	0.014125	*HMOX1*

İSTANBUL UNIVERSITY PRESS

RESEARCH ARTICLE / ARAŞTIRMA MAKALESİ
Journal of Advanced Research in Health Sciences /
Sağlık Bilimlerinde İleri Araştırmalar Dergisi 2024
DOI: 10.26650/JARHS2024-1473193

ASSOCIATION BETWEEN GUSTATORY AND OLFACTORY DYSFUNCTIONS AND GHRELIN, IL-6, AND IL-10 LEVELS IN COVID-19 PATIENTS

COVID-19'LU HASTALARDA TAT VE KOKU ALMA BOZUKLUKLARI İLE GHRELİN, IL-6 VE IL-10 DÜZEYLERİ ARASINDAKİ İLİŞKİ

Gönül Şeyda SEYDEL[1], İnayet GÜNTÜRK[2], Cevat YAZICI[3], Füsun Ferda ERDOĞAN[4]

[1]Niğde Ömer Halisdemir University, Niğde Zübeyde Hanım Vocational School of Health Service, Department of Health Care Services, Niğde, Türkiye
[2]Niğde Ömer Halisdemir University, Zübeyde Hanım Faculty of Health Sciences, Department of Midwifery, Niğde, Türkiye
[3]Erciyes University, Faculty of Medicine, Department of Medical Biochemistry, Kayseri, Türkiye
[4]Erciyes University, Faculty of Medicine, Department of Neurology, Kayseri, Türkiye

ORCID ID: G.Ş.S. 0000-0001-9317-0719; İ.G. 0000-0002-8299-1359; C.Y. 0000-0003-0625-9542; F.F.E. 0000-0002-6315-7529

Citation/Atıf: Seydel GŞ, Güntürk İ, Yazıcı C, Erdoğan FF. Association between gustatory and olfactory dysfunctions and ghrelin, IL-6, and IL-10 levels in Covid-19 patients. Journal of Advanced Research in Health Sciences 2024;7(3):209-213. https://doi.org/10.26650/JARHS2024-1473193

ABSTRACT

Objective: The aim of this study was to examine the association between gustatory and olfactory dysfunctions and ghrelin, IL-6, and IL-10 levels in patients with COVID-19.

Materials and Methods: A total of 80 COVID-19 patients were enrolled in the study: 57 patients with gustatory and/or olfactory dysfunctions and 23 patients without gustatory or olfactory dysfunctions. The plasma ghrelin, IL-6, and IL-10 levels of all patients were determined using the ELISA method.

Results: COVID-19 patients with gustatory and/or olfactory dysfunctions had higher IL-6 and lower ghrelin and IL-10 levels compared with COVID-19 patients without gustatory or olfactory dysfunctions ($p<0.001$).

Conclusions: These results demonstrate that an inflammatory process mediated by ghrelin, IL-6, and IL-10 contributes to the development of gustatory and olfactory dysfunctions in COVID-19 patients.

Keywords: Ghrelin, IL-6, IL-10, COVID-19, Gustatory dysfunction, Olfactory dysfunction

ÖZ

Amaç: Bu çalışmanın amacı, COVID-19'lu hastalarda tat ve koku alma bozuklukları ile ghrelin, IL-6 ve IL-10 düzeyleri arasındaki ilişkiyi incelemekti.

Gereç ve Yöntemler: Çalışmaya tat ve/veya koku alma bozukluğu olan 57 hasta ve tat ve ya koku alma bozukluğu olmayan 23 hasta olmak üzere toplam 80 COVID-19 hasta dahil edildi. Tüm hastaların plazma ghrelin, IL-6 ve IL-10 düzeyleri ELISA yöntemi kullanılarak belirlendi.

Bulgular: Tat ve/veya koku alma bozukluğu olan COVID-19 hastaları, tat ve koku alma bozukluğu olmayan COVID-19 hastalarına kıyasla daha yüksek IL-6 ve daha düşük ghrelin ve IL-10 düzeylerine sahipti ($p<0.001$).

Sonuçlar: Bu sonuçlar, ghrelin, IL-6 ve IL-10'un aracılık ettiği inflamatuar bir sürecin, COVID-19 hastalarında tat ve koku alma bozukluklarının gelişimine katkıda bulunduğunu göstermektedir.

Anahtar Kelimeler: Ghrelin, IL-6, IL-10, COVID-19, tat alma bozukluğu, koku alma bozukluğu

INTRODUCTION

Coronavirus disease 2019 (COVID-19), a highly contagious disease caused by the spread of a coronavirus known as SARS-CoV-2, has primary clinical symptoms such as fever, dry cough, fatigue, headache, nasal congestion, and myalgia (1, 2). Besides these common symptoms, gustatory and olfactory dysfunctions have also been reported (3-5). A meta-analysis revealed that 47% of COVID-19 patients experienced gustatory and olfactory dysfunction, with the percentage rising to 67% in patients with mild to moderate symptoms (4).

The exact mechanisms underlying the impact of SARS-CoV-2 on gustatory and olfactory dysfunctions have not yet been clarified. However, it is considered that COVID-19 can lead to the dysfunction of these senses through various mechanisms, such as local inflammation. Infection with SARS-CoV-2 can trigger immune system dysfunction, leading to the overproduction of pro-inflammatory cytokines. This local excessive immune response and inflammation can further contribute to tissue damage and impair sensory functions (5, 6). Ghrelin is a hormone primarily recognised for its role in appetite regulation, food intake, and energy balance. Moreover, it has been demonstrated

Corresponding Author/Sorumlu Yazar: Gönül Şeyda SEYDEL **E-mail:** seydaseydel@hotmail.com

Submitted/Başvuru: 24.04.2024 • **Revision Requested/Revizyon Talebi:** 25.06.2024 • **Last Revision Received/Son Revizyon:** 26.07.2024 • **Accepted/Kabul:** 05.09.2024 • **Published Online/Online Yayın:** 25.10.2024

Table 1: Comparison of the demographic and biochemical data

	Group 1 (n=57)	Group 2 (n=23)	p
Age, years	49.81±17.36	48.09±15.86	0.682
Gender (F/M), n (%)	28 (49.1)/29 (50.9)	8 (34.8)/15 (65.12)	0.243
WBC (10^3/µL)	5.82 (4.99-8.57)	6.13 (4.18-8.22)	0.911
Neutrophil, (10^3/µL)	4.04 (2.95-6.39)	3.92 (2.97-5.75)	0.493
Lymphocyte (10^3/µL)	1.55 (1.07-2.10)	1.42 (0.79-1.87)	0.258
Platelet (10^3/µL)	250 (199-302)	218 (197-293)	0.361
CRP (mg/L)	11.74 (3.76-61.4)	4.78 (2.22-17.8)	0.214
Procalcitonin (ng/mL)	0.06 (0.02-0.12)	0.04 (0.02-0.16)	0.565
D-dimer (ng/mL)	400 (265-690)	500 (380-730)	0.066
LDH (U/L)	220 (180-302)	223 (184-271)	0.869
ALT (U/L)	21 (16.9-36.9)	22 (14.0-34.0)	0.562
AST (U/L)	22 (19.0-40.2)	21 (16.0-28.0)	0.253
BUN (mg/dL)	13.5 (10.0-18.2)	12.3 (9.20-16.8)	0.632
Creatinin (mg/dL)	0.89 (0.76-1.07)	0.77 (0.63-0.96)	0.042

ALT: Alanine transaminase, AST: Aspartate aminotransferase, BUN: Blood urea nitrogen, CRP: C-reactive protein, LDH: Lactate dehydrogenase, WBC: White blood cell

Table 2: Comparison of the plasma levels of ghrelin, IL-6, and IL-10

	Group 1 (n=57)	Group 2 (n=23)	p
Ghrelin (pg/mL)	165.00 (138.75-211.31)	206.70 (203.51-234.64)	<0.001
IL-6 (pg/mL)	15.09 (13.22-16.20)	11.78±1.05	<0.001
IL-10 (pg/mL)	73.77±28.27	110.03±25.64	<0.001

that this endogenous ligand possesses distinct properties, such as oxidative stress, inflammation, inhibition of cell proliferation, apoptosis, and involvement in metabolic processes. Ghrelin counteracts the effects of pro-inflammatory cytokines by acting as an anti-inflammatory mediator (7). Studies on COVID-19 have shown that ghrelin plays a crucial role in modulating the immune response and could be considered a potential treatment option to reduce complications associated with COVID-19 (7, 8). Interleukin-6 (IL-6), a potent pro-inflammatory cytokine, regulates a variety of physiological inflammatory and immunological processes (9). Increased IL-6 levels are related to complications, adverse outcomes, and disease severity in COVID-19 patients, according to current research. Furthermore, IL-6 has been considered a negative prognostic factor due to its involvement in the cytokine storm reported in severe COVID-19 patients (10-12). Interleukin-10 (IL-10), a pleiotropic cytokine, possesses immunosuppressive and anti-inflammatory properties (13). The role of this cytokine in COVID-19 is intricate and multifaceted, and it has been linked to the severity of the disease (14-16). Although the importance of these cytokines in the severity of COVID-19 disease has been reported, there are limited studies investigating their relationship with gustatory and/or olfactory dysfunctions. Therefore, in this study, we investigated the association between gustatory and olfactory dysfunctions and ghrelin, IL-6, and IL-10 levels in patients with COVID-19.

MATERIALS AND METHODS

Ethics and study design

Ethical approval was granted by the Non-Invasive Ethics Committee of Niğde Ömer Halisdemir University (Date: 08.04.2021, No: 2021/40) after obtaining approval for the study's scientific research from the Directorate General of Health Services of the Ministry of Health. All participants received written informed consent after being fully informed about the study.

This prospective study was conducted on 80 COVID-19 patients with RT-PCR-confirmed diagnosis admitted to the Department of Neurology, Faculty of Medicine, Niğde Ömer Halisdemir University between June 15 and December 15, 2021. The patients with COVID-19 were separated into two groups: those with gustatory and/or olfactory dysfunctions (Group 1) and those without gustatory or olfactory dysfunctions (Group 2). Blood samples from patients were collected within 24 h. World Health Organization (WHO) diagnostic criteria were used to classify the severity of COVID-19 (17). Because the patients had mild/moderate cases, they were conscious and able to communicate. Gustatory and/or olfactory dysfunctions were documented based on the patients' verbal statements. The demographic and biochemical data, including alanine transaminase (ALT), aspartate aminotransferase (AST), blood urea nitrogen (BUN), C-reactive protein (CRP), D-dimer, lactate dehydrogenase (LDH),

lymphocyte, neutrophil, platelet, procalcitonin, and white blood cell (WBC), were retrieved from the medical records of the patients.

The study inclusion criteria for both groups were as follows: (1) a laboratory-confirmed diagnosis of COVID-19, (2) age≥ 18 years, (3) no history of nasal surgery, and (4) no pre-existing conditions that affect gustatory and olfactory functions. The exclusion criteria for both groups were as follows: (1) the presence of a chronic inflammatory disease, (2) a metabolic disease, (3) an active upper respiratory tract infection other than COVID-19, (4) pregnant or lactating women, and (5) diseases affecting carbohydrate and lipid metabolism.

Blood sample collection and determination of ghrelin, IL-6, and IL-10 plasma levels

Blood samples of 5 mL were obtained from each patient and placed into tubes containing EDTA. The samples were centrifuged at 1500 x g at 4°C for 15 min and stored in aliquots at -80°C until enzyme-linked immunosorbent assay (ELISA) testing was conducted using a BioTek ELx800 absorbance microplate reader. Plasma levels of ghrelin, IL-6, and IL-10 were measured using commercial ELISA kits (USCN, Wuhan USCN Business Co., Ltd., China, Product No: CEA991Hu (Version: 13.0); SEA079Hu (Version: 13.0); SEA056Hu (Version: 13.0), respectively) according to the manufacturer's instructions.

Statistical analysis

The data analyses were conducted using the Statistical Package for the Social Sciences (SPSS) version 23.0 (IBM Corp, Armonk, NY, USA). The Shapiro-Wilk test was performed to assess the normality of the data. Mean±standard deviation (SD) and/or median [interquartile ranges (IQR; 25%-75%)] were used to analyse both normally and non-normally distributed data. For comparisons between groups, the Student's t-test was used for normally distributed data, and the Mann−Whitney U test was used for non-normally distributed data. Statistical significance was defined as a p-value <0.05.

RESULTS

In this study, 80 COVID-19 patients were enrolled. Group 1 included 57 patients with gustatory and/or olfactory dysfunctions; of these, 28 were male (49.1%) and 29 were female (50.9%), with a mean age of 49.81±17.36 years. Group 2 included 23 patients without gustatory or olfactory dysfunctions; of these, 8 were male (34.8%) and 15 were female (65.1%), with a mean age was 48.09±15.86 years. There were no significant differences between the groups in terms of age, gender, and laboratory parameters except for creatinine. Group 2 had significantly lower creatinine levels than Group 1 (Table 1).

In Group 1, the plasma ghrelin, IL-6, and IL-10 levels were 165.00 (138.75-211.31) pg/mL, 15.09 (13.22-16.20) pg/mL, and 73.77±28.27 pg/mL, respectively. In Group 2, ghrelin, IL-6, and IL-10 levels were 206.70 (203.51-234.64) pg/mL, 11.78±1.05 pg/mL, and 110.03±25.64 pg/mL, respectively. Data analysis showed that the IL-6 level was significantly higher in Group 1 than in Group 2 ($p<0.001$). Conversely, the levels of IL-10 and ghrelin were significantly lower in Group 1 than in Group 2 ($p<0.001$) (Table 2).

DISCUSSION

Gustatory and olfactory dysfunctions have been recognised as prevalent symptoms of COVID-19; however, the underlying pathological mechanisms remain unclear. A severe cytokine storm mediated by pro-inflammatory cytokines is thought to cause damage in cases of gustatory and olfactory dysfunctions resulting from COVID-19 infection (5, 6). Ghrelin, a ligand for the growth hormone secretagogue receptor 1A (GHSR1A), is predominantly produced by the P/D1-like cells in the human stomach (8, 18). Ghrelin and GHSR1A are also expressed in lymphoid tissues, immune cells, natural killer cells, and monocytes. Some studies show that ghrelin prevents the synthesis of pro-inflammatory cytokines. Furthermore, it increases the levels of the anti-inflammatory cytokine IL-10 and exhibits protective properties in various models of inflammatory diseases (7, 8, 19). Azizzadeh et al. demonstrated that in a rat model of inflammatory pain, ghrelin exerted analgesic effects by modulating the levels of IL-10 and TGF-β (19). In this regard, ghrelin is acknowledged as a hormone with anti-inflammatory and immunomodulatory properties. Because of these effects, ghrelin has recently become an attractive agent to mitigate the complications related to SARS-CoV-2. Additionally, by downregulating NF-κB expression and upregulating PPARγ, ghrelin is capable of reducing the uncontrolled production of cytokines that lead to acute lung injury (7). An in silico study by Russo et al. found that ghrelin exerts an immunomodulatory function during the progression of SARS-CoV-2 (8). There are only a few studies on the levels of ghrelin in COVID-19 patients. Kuliczkowska-Płaksej et al. demonstrated that ghrelin levels were notably elevated six months after a mild SARS-CoV-2 infection (20). In contrast, Hakami et al. found no significant changes in ghrelin levels in the blood samples of COVID-19 patients. Nonetheless, they speculate that ghrelin might exhibit potential changes in saliva rather than its effects in the blood (21). Ghrelin also influences sensory function and plays a notable role in taste sensation, sniffing, and olfaction (18). Ghrelin receptors have also been detected in the granule cell layers of the olfactory bulb, glomerular and mitral cells, and the piriform cortex (22). Recent research has indicated that ghrelin cells are chemosensory and possess taste receptors (23). In our study, we found that COVID-19 patients with gustatory and/or olfactory dysfunctions had lower levels of ghrelin compared with patients without gustatory or olfactory dysfunctions. There is only one study in COVID-19 patients on the relationship between ghrelin and these dysfunctions. Shanyoor et al. demonstrated that the ghrelin levels in COVID-19 patients with anosmia and ageusia were considerably lower than those without these symptoms (24). These findings consistent with our results.

IL-6 is a crucial cytokine involved in the immune response to infections. Numerous studies have shown that increased IL-6 levels are linked to the disease severity and adverse outcomes

in COVID-19 patients. Hence, increased IL-6 levels are considered a negative prognostic factor for COVID-19 (10-12). Research examining the relationship between this cytokine and gustatory and/or olfactory dysfunctions is relatively limited. Some studies have found a link between them, while others have not established a relationship (25-29). Henkin et al. showed that there were increased IL-6 levels in the saliva, plasma, and nasal mucus of patients with hyposmia and that these alterations can be attributed to systemic or local inflammatory processes, which may underlie or result in hyposmia pathology (25). Cazzolla et al. found a significant association between lower IL-6 levels and the improvement of olfactory and gustatory dysfunctions (26). Likewise, Liang et al. observed a significant relationship between increased IL-6 levels and an increased risk of olfactory dysfunction in patients infected with the Omicron variant. They also noted that groups with olfactory dysfunction displayed higher levels of IL-6 compared with the control group and proposed a hypothesis suggesting that elevated IL-6 levels might be considered a possible causal factor for initiating olfactory dysfunction following local or systemic infection, owing to immunological and inflammatory alterations (27). Chang et al. also showed that IL-6 levels were increased in nasal swab samples from COVID-19 patients with olfactory dysfunctions (29). A recent study conducted by De Melo et al. revealed that in patients with olfactory dysfunction, this infection was found to be connected to inflammation of the olfactory mucosa. Notably, the researchers observed pronounced pro-inflammatory conditions in both the nasal turbinates and olfactory bulb, with up-regulation of IL-6 (30). In line with previous studies, our study indicated that COVID-19 patients with gustatory and/or olfactory dysfunctions had higher IL-6 levels than those without. In line with previous studies, our study indicated that COVID-19 patients with gustatory and/or olfactory dysfunctions had higher IL-6 levels than those without. The findings of the current study were consistent with the literature data indicating a significant relationship between the increased IL-6 levels and gustatory and/or olfactory dysfunctions in COVID-19 patients.

IL-10 is primarily recognised for its anti-inflammatory and immunosuppressive properties (13). However, in the context of COVID-19, the role of IL-10 is intricate and multifaceted. Various studies have indicated that elevated levels of IL-10 are linked to severe cases of COVID-19 compared to mild or moderate cases, implying its potential pro-inflammatory effects (14-16). However, adequate research on the relationship between gustatory and/or olfactory dysfunctions and IL-10 levels has not been conducted, and only one study has been undertaken on this topic to date. In our study, we observed that COVID-19 patients with gustatory and/or olfactory dysfunctions had reduced IL-10 levels compared with patients without gustatory or olfactory dysfunctions. Similar to our findings, Locatello et al. showed that the recovery of gustatory dysfunction was linked to elevated IL-10 levels. Furthermore, they proposed that immunological parameters may be valuable in monitoring the progression of chemosensory impairments in patients with COVID-19, and the elevated IL-10 levels should be regarded as a marker of recovery (31).

The relatively small sample size was a limitation of this study. The results of our study demonstrate that ghrelin, IL-6, and IL-10 might play a significant role in the development of these dysfunctions in COVID-19 patients, indicating their involvement in an inflammatory process. Further research is needed to understand the association between ghrelin, IL-6, and IL-10 levels and gustatory and olfactory dysfunctions in patients with COVID-19.

Ethics Committee Approval: This study was approved by Non-Invasive Ethics Committee of Niğde Ömer Halisdemir University (Date: 08.04.2021, No: 2021/40).

Informed Consent: All participants received written informed consent after being fully informed about the study.

Peer Review: Externally peer-reviewed.

Author Contributions: Conception/Design of Study- G.Ş.S., İ.G.; Data Acquisition- F.F.E.; Data Analysis/Interpretation- G.Ş.S., İ.G., C.Y., F.F.E.; Drafting Manuscript- G.Ş.S.; Critical Revision of Manuscript- G.Ş.S., İ.G., C.Y., F.F.E.; Final Approval and Accountability- G.Ş.S., İ.G., C.Y., F.F.E.; Material and Technical Support- G.Ş.S., C.Y.; Supervision- G.Ş.S.

Conflict of Interest: The authors have no conflict of interest to declare.

Financial Disclosure: Financial Disclosure: This work was supported by the Niğde Ömer Halisdemir University under Grant [SAT 2021/10-HIDEP].

REFERENCES

1. Zhou M, Zhang X, Qu J. Coronavirus disease 2019 (COVID-19): a clinical update. Front Med 2020;14(2):126-35.
2. Huang C, Wang Y, Li X, Ren L, Zhao J, Hu Y, et al. Clinical features of patients infected with 2019 novel coronavirus in Wuhan, China. Lancet 2020;395(10223):497-506.
3. Lechien JR, Chiesa-Estomba CM, De Siati DR, Horoi M, Le Bon SD, Rodriguez A, et al. Olfactory and gustatory dysfunctions as a clinical presentation of mild-to-moderate forms of the coronavirus disease (COVID-19): a multicenter European study. Eur Arch Otorhinolaryngol 2020;277(8):2251-61.
4. Borsetto D, Hopkins C, Philips V, Obholzer R, Tirelli G, Polesel J, et al. Self-reported alteration of sense of smell or taste in patients with COVID-19: a systematic review and meta-analysis on 3563 patients. Rhinology 2020;58(5):430-6.
5. Eshraghi AA, Mirsaeidi M, Davies C, Telischi FF, Chaudhari N, Mittal R. Potential mechanisms for COVID-19 induced anosmia and dysgeusia. Front Physiol 2020;11:1039.
6. Khani E, Khiali S, Beheshtirouy S, Entezari-Maleki T. Potential pharmacologic treatments for COVID-19 smell and taste loss: A comprehensive review. Eur J Pharmacol 2021;912:174582.
7. Jafari A, Sadeghpour S, Ghasemnejad-Berenji H, Pashapour S, Ghasemnejad-Berenji M. Potential antioxidative, anti-inflammatory and Immunomodulatory effects of ghrelin, an endogenous peptide

from the stomach in SARS-CoV2 infection. Int J Pept Res Ther 2021;27(3):1875-83.
8. Russo C, Morello G, Mannino G, Russo A, Malaguarnera L. Immunoregulation of Ghrelin in neurocognitive sequelae associated with COVID-19: an in silico investigation. Gene 2022;834:146647.
9. Ataie-Kachoie P, Pourgholami MH, Richardson DR, Morris DL. Gene of the month: Interleukin 6 (IL-6). J Clin Pathol 2014;67(11):932-7.
10. Herold T, Jurinovic V, Arnreich C, Lipworth BJ, Hellmuth JC, von Bergwelt-Baildon M, et al. Elevated levels of IL-6 and CRP predict the need for mechanical ventilation in COVID-19. J Allergy Clin Immunol 2020;146(1):128-36.
11. Vaira LA, De Vito A, Deiana G, Pes C, Giovanditto F, Fiore V, et al. Correlations between IL-6 serum level and olfactory dysfunction severity in COVID-19 patients: a preliminary study. Eur Arch Otorhinolaryngol 2022;279(2):811-6.
12. Coomes EA, Haghbayan H. Interleukin-6 in Covid-19: A systematic review and meta-analysis. Rev Med Virol 2020 ;30(6):1-9.
13. Islam H, Chamberlain TC, Mui AL, Little JP. Elevated interleukin-10 levels in COVID-19: Potentiation of pro-Inflammatory responses or impaired anti-Inflammatory Action? Front Immunol 2021;12:677008.
14. Zhao Y, Qin L, Zhang P, Li K, Liang L, Sun J, et al. Longitudinal COVID-19 profiling associates IL-1RA and IL-10 with disease severity and RANTES with mild disease. JCI Insight 2020;5(13):e139834.
15. Tan M, Liu Y, Zhou R, Deng X, Li F, Liang K, Shi Y. Immunopathological characteristics of coronavirus disease 2019 cases in Guangzhou, China. Immunology 2020;160(3):261-8.
16. Han H, Ma Q, Li C, Liu R, Zhao L, Wang W, et al. Profiling serum cytokines in COVID-19 patients reveals IL-6 and IL-10 are disease severity predictors. Emerg Microbes Infect 2020;9(1):1123-30.
17. Baj J, Karakuła-Juchnowicz H, Teresiński G, Buszewicz G, Ciesielka M, Sitarz R, et al. COVID-19: Specific and Non-Specific Clinical Manifestations and Symptoms: The Current State of Knowledge. J Clin Med 2020;9(6):1753.
18. Akalu Y, Molla MD, Dessie G, Ayelign B. Physiological effect of ghrelin on body systems. Int J Endocrinol 2020;2020:1385138.
19. Azizzadeh F, Mahmoodi J, Sadigh-Eteghad S, Farajdokht F, Mohaddes G. Ghrelin exerts analgesic effects through modulation of IL-10 and TGF-β levels in a rat model of inflammatory pain. Iran Biomed J 2017;21(2):114-9.
20. Kuliczkowska-Płaksej J, Jawiarczyk-Przybyłowska A, Zembska A, Kolačkov K, Syrycka J, Kałużny M, et al. Ghrelin and leptin concentrations in patients after SARS-CoV2 infection. J Clin Med 2023;12(10):3551.
21. Hakami NY, Alhazmi WA, Taibah EO, Sindi M, Alotaibi OF, Al-Otaibi HM, et al. The effect of COVID-19 infection on human blood ghrelin hormone: A pilot study. J Pharm Res Int 2021;33(7):33-8.
22. Tong J, Mannea E, Aimé P, Pfluger PT, Yi CX, Castaneda TR, et al. Ghrelin enhances olfactory sensitivity and exploratory sniffing in rodents and humans. J Neurosci 2011;31(15):5841-6.
23. Müller TD, Nogueiras R, Andermann ML, Andrews ZB, Anker SD, Argente J, et al. Ghrelin. Mol Metab 2015;4(6):437-60.
24. Shanyoor SJ, Ali Naji ZM. Association of leptin and ghrelin serum levels with anosmia and ageusia in Iraqi COVID-19 infected patients. PJMHS 2022;16(5):832-5.
25. Henkin RI, Schmidt L, Velicu I. Interleukin 6 in hyposmia. JAMA Otolaryngol Head Neck Surg 2013;139(7):728-34.
26. Cazzolla AP, Lovero R, Lo Muzio L, Testa NF, Schirinzi A, Palmieri G, et al. Taste and smell disorders in COVID-19 patients: role of interleukin-6. ACS Chem Neurosci 2020;11(17):2774-81.
27. Liang Y, Mao X, Kuang M, Zhi J, Zhang Z, Bo M, et al. Interleukin-6 affects the severity of olfactory disorder: a cross-sectional survey of 148 patients who recovered from Omicron infection using the Sniffin' Sticks test in Tianjin, China. Int J Infect Dis 2022;123:17-24.
28. Sanli DET, Altundag A, Kandemirli SG, Yildirim D, Sanli AN, Saatci O, et al. Relationship between disease severity and serum IL-6 levels in COVID-19 anosmia. Am J Otolaryngol 2021;42(1):102796.
29. Chang K, Kallogjeri D, Piccirillo J, House SL, Turner J, Schneider J, et al. Nasal inflammatory profile in patients with COVID-19 olfactory dysfunction. Int Forum Allergy Rhinol 2022;12(7):952-4.
30. de Melo GD, Lazarini F, Levallois S, Hautefort C, Michel V, Larrous F, et al. COVID-19-related anosmia is associated with viral persistence and inflammation in human olfactory epithelium and brain infection in hamsters. Sci Transl Med 2021;13(596):eabf8396.
31. Locatello LG, Bruno C, Maggiore G, Cilona M, Orlando P, Fancello G, et al. The prognostic role of IL-10 in non-severe COVID-19 with chemosensory dysfunction. Cytokine 2021;141:155456.

RESEARCH ARTICLE / ARAŞTIRMA MAKALESİ
Journal of Advanced Research in Health Sciences /
Sağlık Bilimlerinde İleri Araştırmalar Dergisi 2024
DOI: 10.26650/JARHS2024-1407047

IN VITRO TOXIC EFFECTS OF AZOXYSTROBIN ON HUMAN NEUROBLASTOMA CELL LINE

AZOXYSTROBİN'İN İNSAN NÖROBLASTOMA HÜCRE HATTI ÜZERİNDEKİ *İN VİTRO* TOKSİK ETKİLERİ

Ayşenur BİLGEHAN[1,3], Gül ÖZHAN[2]

[1]İstanbul University, Institute of Graduate Studies in Health Sciences, İstanbul, Türkiye
[2]İstanbul University, Faculty of Pharmacy, Department of Pharmaceutical Toxicology, İstanbul, Türkiye
[3]University of Health Sciences, Faculty of Pharmacy, Department of Pharmaceutical Toxicology, İstanbul, Türkiye

ORCID ID: A.B. 0000-0002-7672-9127; G.Ö. 0000-0002-6926-5723

Citation/Atıf: Bilgehan A, Özhan G. In vitro toxic effects of azoxystrobin on human neuroblastoma cell line. Journal of Advanced Research in Health Sciences 2024;7(3):214-219. https://doi.org/10.26650/JARHS2024-1407047

ABSTRACT

Objective: Exposure to agricultural chemicals is associated with health issues such as autism, brain aging, and neurodegenerative diseases. Azoxystrobin (AZS), a strobilurin-derived fungicide, is a commonly used chemical. Although studies have demonstrated that AZS induces toxic effects on various tissues, there is a lack of clear understanding of the mechanisms underlying its neurotoxic effects. The mechanisms linking pesticide exposure to these health outcomes might be oxidative stress and apoptosis. Therefore, we conducted this study to investigate oxidative stress and cell death induction in human neuroblastoma SH-SY5Y cells, a widely established *in vitro* model for neurotoxicity experiments, after exposure to AZS.

Materials and Methods: SH-SY5Y cells were exposed to different concentrations of AZS for 24 h. Cytotoxicity was evaluated using the 3-[4,5-dimethylthiazol-2-yl]-2,5-diphenyl-tetrazolium bromide assay, the induction of reactive oxygen species (ROS) was determined using a fluorescent dye, and cell apoptosis was detected using the FITC Annexin V assay.

Results: The half-maximal inhibitory concentration value of AZS was 44.87 µM. The levels of ROS (at least 1.5-fold; p≤0.05) and apoptosis (at least 5-fold; p≤0.05) increased in a dose-dependent manner at AZS exposure concentrations of 6.25-25 µM.

Conclusion: AZS-induced neurotoxic effects may be a consequence of ROS generation and ROS-induced apoptosis. However, the mechanisms underlying AZS-induced neurotoxicity should be evaluated by further studies to gain a deeper understanding of its toxic capacity and conduct evaluations of occupational and environmental risks.

Keywords: Azoxystrobin, apoptosis, oxidative stress, neurotoxicity

ÖZ

Amaç: Çalışmalar, tarım ilaçlarına maruziyetin otizm, beyin yaşlanması ve nörodejeneratif hastalıklar gibi sağlık sorunları ile ilişkili olabileceğini bildirmektedir. Yaygın kullanılan tarım ilaçlarından biri de strobilurin türevi bir fungusit olan azoksistrobin (AZS)'dir. Araştırmalar, çeşitli dokularda AZS'nin toksik etkilerini gösterse de nörotoksik etkilerin altında yatan temel mekanizmalar halen tam olarak anlaşılamamıştır. Tarım ilaçlarına maruziyetin sebep olduğu sağlık sorunlarının oksidatif stres ve apoptoz ile ilişkili olabieceği bildirilmektedir. Bu nedenle, nörotoksisite değerlendirmelerinde yaygın kullanılan bir *in vitro* model olan insan nöroblastoma (SH-SY5Y) hücrelerinde AZS'nin oksidatif hasar oluşturma ve hücre ölümünü indükleme etkisinin değerlendirilmesi amaçlanmıştır.

Gereç ve Yöntem: SH-SY5Y hücreleri 24 saat boyunca AZS'nin farklı konsantrasyonlarına maruz bırakılmıştır. MTT testi ile sitotoksisite değerlendirilirken spesifik floresan boya ile reaktif oksijen türlerinin (ROS) oluşumu ve FITC Annexin V testi ile de hücresel apoptoz seviyeleri incelenmiştir.

Bulgular: AZS'nin IC_{50} değeri 44.87 µM olarak bulunmuştur. ROS (en az 1,5 kat; p≤0,05) ve apoptoz (en az 5 kat; p≤0,05) seviyeleri 6.25-25 µM AZS maruziyet aralığında doza bağlı artmıştır.

Sonuç: Bulgularımız, AZS'nin neden olduğu nörotoksik etkilerin ROS üretimi ve ROS ile indüklenen apoptozun bir sonucu olabileceğini düşündürmektedir. Ancak, AZS'nin toksik etki potansiyelinin daha iyi anlaşılması, mesleki ve çevresel risk faktörlerinin değerlendirilmesi, AZS kaynaklı nörotoksisiteye neden olan temel mekanizmaların aydınlatılması için ileri araştırmalara ihtiyaç duyulduğu da göz ardı edilmemelidir.

Anahtar Kelimeler: Azoksistobin, apoptoz, oksidatif stres, nörotoksisite

Corresponding Author/Sorumlu Yazar: Gül ÖZHAN **E-mail:** gulozhan@istanbul.edu.tr

Submitted/Başvuru: 19.12.2023 • **Revision Requested/Revizyon Talebi:** 31.01.2024 • **Last Revision Received/Son Revizyon:** 07.02.2024 • **Accepted/Kabul:** 15.03.2024 • **Published Online/Online Yayın:** 22.10.2024

INTRODUCTION

Fungicides are globally used to protect crops and plants from fungal diseases originating in the soil and to prevent spoilage after harvest. They are essential for ensuring food safety, maintaining healthy plant growth, increasing agricultural yields, and maintaining the quality of produce. The adverse effects of fungicides on the environment and human health have been reported in association with both occupational and consumer risks (1). The use of fungicides in agriculture poses a potential health threat because they can spread from the field and present a risk to the local people and children in addition to agricultural laborers due to contact with air, soil, and water. Exposure to these environmental chemicals can cause reproductive dysfunction, developmental toxicity, hepatotoxicity, and neurotoxicity (2-9).

Strobilurins, a class of fungicides derived from the fungus *Strobilurus tenacellus*, have gained considerable attention in the agricultural industry (8, 10). Strobilurin fungicides work by binding to cytochrome b1 in fungal mitochondrial membranes, inhibiting mitochondrial respiration and disrupting the electron transport chain. This results in the inhibition of fungal growth and control of disease (8).

AZS is a strobilurin-based, systemic fungicide with a broad spectrum of application for fruit and vegetable crops for the postharvest treatment of agricultural products. The fact that AZS is applied postharvest implies that the time between fungicide application and consumption is relatively short compared with that for other active ingredients used during cultivation. Studies have demonstrated that postharvest fungicides can contribute to > 95% of the total human toxicity effects (5-7, 11-13). Recently, AZS has been incorporated into certain types of mold-resistant wallboard to prevent fungal growth (14). Over the past decade, AZS has gained popularity as a patented ingredient in mold-resistant building materials such as wallboard. These products were formally registered with the EPA (United States Environmental Protection Agency) in 2004 (15). Human exposure to AZS, other than through dietary ingestion of products containing residues, may be due to the recent use of AZS in mold-resistant building materials, including wallboard, which can eventually accumulate in house dust and potentially be inhaled or come into contact with the skin. This raises concerns regarding the possibility of AZS exposure indoors (14).

The widespread use of AZS has led to the accumulation of residues in the environment, including air, water, and soil, posing a risk to nontarget organisms such as aquatic organisms, animals, and humans. AZS has the ability to endure in soil for more than 300 days and reach its highest concentration approximately 30 days after application, posing a potential risk of contamination to nearby ecosystems (8). The European Food Safety Authority (EFSA) report on pesticide residues in food indicated the presence of residues on honey and beekeeping products (16). Soydan et al. found AZS to be the most frequently detected fungicide in the range of 0.011-0.758 mg/kg in fruit samples collected between 2012 and 2016 in Turkey, commonly being found in dried apricot and fig, grapes, strawberries, and peach (16, 17). Cooper et al. reported that AZS was the most commonly detected strobilurin (93% of dust samples) and was found at the highest concentrations, ranging from < MDL (method detection limit) to 10.587 ng/g, in house dust samples from homes in North Carolina during 2014-2016 (14).

AZS exerts its mechanism of action by acting as a typical mitochondrial complex III inhibitor by binding to ubiquinone Qo site and disrupting mitochondrial function by inhibiting electron transport, preventing adenosine triphosphate production and promoting neuronal cell death in fungi (18, 19). AZS was found to be cytotoxic to human esophageal cancer cells through the mitochondrial pathway and cause mitochondrial dysfunction (20). Mitochondrial dysfunction is associated with degenerative diseases of the nervous system, including Parkinson's and Alzheimer's diseases. The potential neurotoxicity of AZS raises concerns regarding its impact on human health and the development of neurological disorders. Despite the potential risks, there has been limited research on its neurotoxic effects (5, 8, 21), and the mechanisms underlying the neurotoxic effects of AZS are not completely understood. Therefore, to address the existing knowledge gap regarding AZS-induced neurotoxicity, we investigated the potential neurotoxicity of AZS in SH-SY5Y cells, a widely established *in vitro* model of neurodegeneration (22).

MATERIAL AND METHODS

Chemicals

AZS (PESTANAL®, CAS # 131860–33–8) was purchased from Sigma-Aldrich (MO, USA), FITC Annexin V Apoptosis Detection Kit with PI was purchased from BioLegend (CA, USA), and MTT (3-[4,5-dimethylthiazol-2-yl]-2,5-diphenyl-tetrazolium bromide), 2',7'-dichlorodihydrofluorescein diacetate (H_2DCF-DA), and other chemicals were obtained from Sigma-Aldrich (MO, USA). Cell culture supplements were purchased from Multicell Wisent (QC, Canada).

Cell Culture and Treatment Conditions

The SH-SY5Y cell line (CRL-2266, American Type Culture Collection, Virginia, USA) was grown in Dulbecco's Modified Eagle Medium F-12 supplemented with fetal bovine serum (10%) and penicillin/streptomycin (100 U/100 µg/mL). Cells (1×10^6/mL) were exposed to AZS. The working solutions of AZS were prepared at concentrations of 3.125, 6.25, 12.5, and 25 µM (in dimethyl sulfoxide [DMSO]). The solvent and positive controls were DMSO (1%) and Triton X-100 (1%), respectively.

Evaluation of Cytotoxicity

The effect of AZS on cell viability was evaluated using the MTT assay. Cells (1×10^5/100 µL cell culture medium/well) were incubated overnight and then treated with AZS at concentrations of 50-400 µM for 24 h. Then, the cells were incubated with MTT for 3 h at 37°C in the dark, after which the medium was removed, and DMSO (100 µL) was added to each well. Optical densities were measured at 590 nm using a microplate spectrophotometer system (Biotech, Epoch, Vermont, USA).

The half-maximal inhibitory concentration (IC_{50}) was then calculated using the formula from the logarithmic curve of the inhibition concentration graph.

Total Reactive Oxygen Species Assay

The 2',7'-dichlorodihydrofluorescein diacetate (H_2DCF-DA) dye was used to evaluate the production of cellular ROS (23). After 24 h of exposure, the cells were trypsinized and rinsed with phosphate-buffered saline, followed by incubation with H_2DCF-DA dye (20 mM) for 30 min. The intensity of ROS-dependent fluorescence after rinsing was detected using an ACEA NovoCyte flow cytometer (California, USA). Data were analyzed using the Novoexpress software (ACEA, CA, USA). The median fluorescence intensity (MFI) was used to quantify changes in cellular ROS generation, which was obtained by dividing the MFI of the amount tested by the MFI of the control and then multiplying the result by 100. The MFI values of all treatment groups were normalized to the control group.

Cell Apoptosis Analysis

Early and late apoptotic and necrotic cells were identified using the FITC Annexin V Apoptosis Detection Kit with PI according to the manufacturer's guideline. After trypsinization and washing steps, the cells were incubated with Annexin V and PI dyes for 15 min at room temperature. The fluorescence intensities of 10,000 gated events per sample were measured at 488 nm on the ACEA NovoCyte flow cytometer (California, USA). Results were expressed as the percentage of the total number of cells from the quadrants.

Statistical Analysis

Statistical analysis was conducted using Graphpad Prism 9 (GraphPad Software Inc, CA, USA). Statistical differences were evaluated using one-way ANOVA followed by the Tukey test. Results were expressed as mean ± standard deviation (SD), and $p<0.05$ was considered significant. All experiments were performed multiple times for reproducibility.

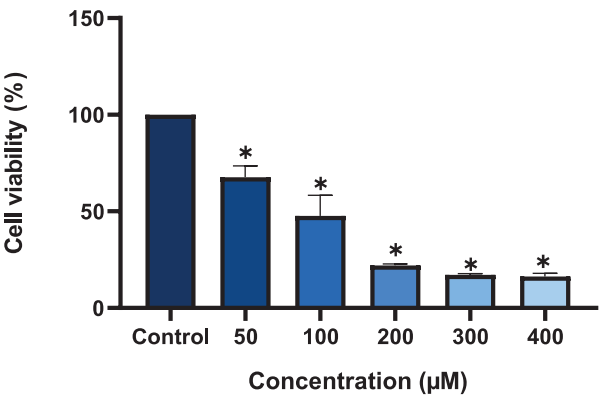

Figure 1: Effects of AZS (50-400 µM) on cell viability evaluated using the MTT assay in SH-SY5Y cells after 24 h of treatment. Data are expressed as mean ± SD. *p<0.05 indicates groups with significant differences from the control.

RESULTS

The cytotoxic effects of AZS on SH-SY5Y cells were evaluated using the MTT assay, which revealed a dose-dependent reduction in cell viability at concentration of up to 200 µM. At 300 and 400 µM, ≥ 95% cells died. The IC_{50} value of AZS was 44.87 µM (Figure 1).

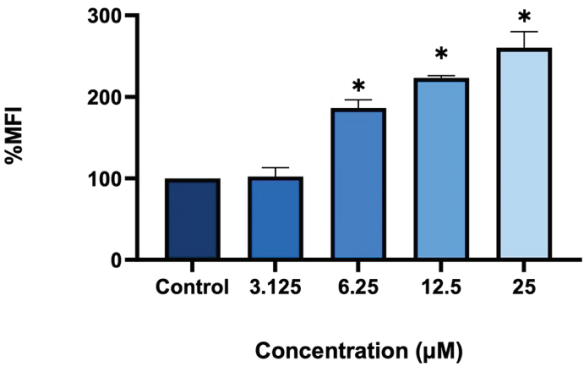

Figure 2: Effects of AZS (3.125-25 µM) on total ROS levels in SH-SY5Y cells after 24 h of treatment. Data are expressed as mean ± SD. *p<0.05 indicates groups with significant differences from the control.

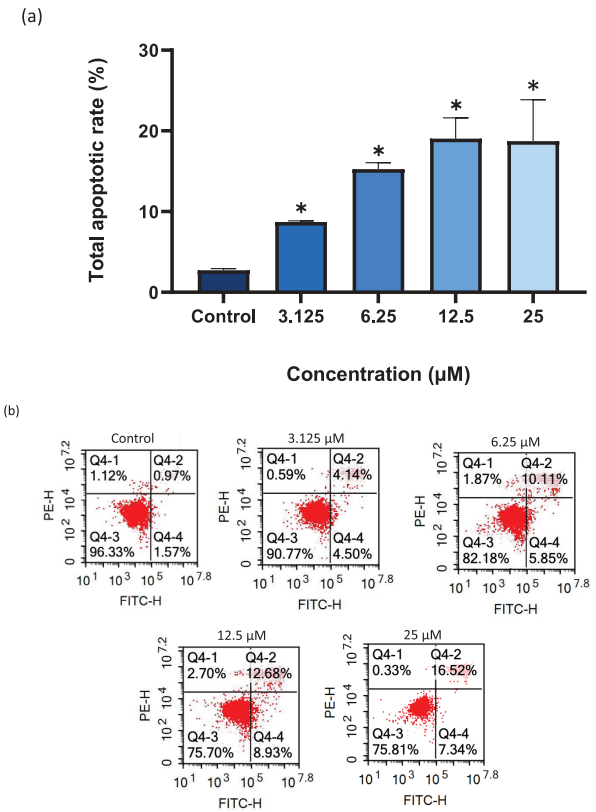

Figure 3: Effects of AZS (3.125-25 µM) on total apoptotic rate (a) and early and late apoptotic effects of AZS (b) measured using flow cytometer in SH-SY5Y cells after 24 h of treatment. Data are expressed as mean ± SD. *p<0.05 indicates groups with significant differences from the control. FITC-H: fluorescein isothiocyanate, PE-H: R-phycoerythrin.

Based on the results of the MTT assay, we decided to investigate concentrations less than the IC_{30} value for subsequent experiments. We observed that ROS levels increased significantly (at least 1.5-fold; p≤0.05) compared with that in the control cells after exposure to AZS at concentrations of 6.25-25 µM for 24 h (Figure 2).

The results of the Annexin V assay revealed that AZS exposure led to ROS-induced apoptosis in SH-SY5Y cells. The apoptosis levels increased significantly (at least 5-fold; p≤0.05) after AZS exposure at concentrations of 6.25-25 µM for 24 h (Figure 3a). At the highest concentration, late apoptosis levels increased up to 16.52%, and early apoptosis levels increased up to 8.93% (Figure 3b).

DISCUSSION

Numerous *in vitro* and *in vivo* studies have demonstrated that pesticides from various categories can exert toxic effects associated with oxidative stress caused by ROS generation. High levels of ROS production can cause damage to cellular components, potentially resulting in cell death (24). Furthermore, ROS can be highly reactive and harmful because they have the ability to alter the structure and function of cellular macromolecules, resulting in behavioral abnormalities, cytotoxicity, and even apoptosis formation (25). The neurotoxic effects of agricultural fungicides can result in neuronal cell damage through oxidative damage, mitochondrial dysfunction, neuroinflammation, and metabolic disorders. Although the ecotoxicological effects of certain strobilurin fungicides are well documented (4), the associated risks to animals and humans have not been investigated in detail. To address this knowledge gap, we explored the pathways that contribute to neurotoxicity in the SH-SY5Y cell line.

Our results demonstrated that AZS significantly reduced cell viability within 24 h of exposure, with an IC_{50} value of 44.87 µM. In a recent study that investigated neurotoxicity via the mitochondrial pathway in differentiated SH-SY5Y cells, the cells were differentiated and exposed to AZS at concentrations of 25-200 µM for up to 48 h to elucidate the mitochondrial mechanisms causing neurotoxicity. It was found that exposure to AZS at 25-200 µM resulted in reduced cell viability but not cytotoxicity after 48 h in differentiated SH-SY5Y cells (26).

In another study, the developing mouse brain was exposed to AZS both acutely and chronically (24 h and 7 days, respectively) to elucidate the neurotoxic effects (5). It was found that AZS was cytotoxic to the primary cortical neuron culture with an IC_{50} value of 30 µM after 24 h of exposure. The lower IC_{50} value was explained by the fact that primary cells are more sensitive than immortalized cells. Another study reported that AZS accumulated in the cerebral cortex of mice during embryonic and early postnatal stages at a concentration of approximately 10 nM after chronic exposure and caused cell death in cortical neurons cultured *in vitro* (21). Furthermore, Shi et al. found that AZS exhibited inhibitory effects on the proliferation of human esophageal squamous cell carcinoma KYSE150 cells with an IC_{50} value of 2.42 µg/mL after 48 h of treatment (20). Chen et al. also demonstrated that AZS inhibited cell viability in human oral squamous cell carcinoma CAL27 and SCC15 cells with IC_{50} values of 4.4 and 7.82 µg/mL, respectively (27).

Damage to mitochondria could cause excessive production of ROS in cells, leading to oxidative stress in organisms. An essential component in the production of ROS is mitochondrial complex III (28). Takahashi et al. investigated the levels of apoptosis and cell cycle arrest induced by AZS in the p53-negative human myelogenous leukemia cell line HL-60RG and p53-positive human T-cell leukemia cell line MOLT-4F (12). They reported AZS-induced cell death, but the mechanisms underlying the damage differed between the cell lines. Chen et al. demonstrated that treatment with 5 µg/mL AZS significantly suppressed the function of mitochondrial complex III and increased the levels of both mitochondrial and intracellular ROS in CAL27 cells, suggesting that AZS causes ROS accumulation by preventing mitochondrial complex III from functioning (27).

In the present study, AZS caused a significant increase in cellular ROS levels at concentrations of ≥ 6.25 µM. Similar to our results, Kang et al. demonstrated that 5 µM AZS caused ROS induction in primary cortical neuronal cultures in developing mouse embryos (5). However, Nguyen et al. indicated that there was no increase in ROS levels with AZS exposure up to 200 µM in differentiated SH-SY5Y cells (8). Cao et al. demonstrated that AZS increased the levels of ROS and MDA and triggered the activities of SOD and CAT in larval and adult zebrafish at a concentration of 0.20 mg/L (3). Furthermore, Wei et al. showed that AZS-induced oxidative stress in *Chironomus dilutus* by altering the levels of H_2O_2 and MDA in addition to the induction of SOD and CAT enzymes at a concentration of more than 0.07 ± 0.01 mg/L, which is almost similar to the environmentally relevant concentration for aquatic environments throughout the world (29).

Mitochondria are extremely important organelles involved in the generation of apoptosis in the cell. Elevated ROS levels trigger apoptotic pathways mediated by mitochondria, resulting in cellular death (30). Our results indicated that excessive cellular ROS generation induced the formation of apoptosis in SH-SY5Y cells. After exposure to AZS at concentrations of 6.25-25 µM, the apoptosis levels significantly increased compared with those in the control group, even at the lower AZS concentration of 6.25 µM. Similar to our results, Nguyen et al. demonstrated increased caspase-3/7 activity after exposure to AZS (50 µM) and trifloxystrobin (25 µM) in differentiated SH-SY5Y cells at 48 h, indicating autophagic apoptosis (8). Kang et al. claimed that AZS activated the intrinsic mitochondrial apoptosis pathway related to Bcl2/Bax and cleaved caspase 3, resulting in cell death (5). Neuronal cells were rescued from reduced viability after the addition of the ROS scavenger NAC in combination with AZS (5). Chen et al. suggested that treatment with AZS at 5 µg/mL for 48 h induced apoptosis of esophageal squamous cell carcinoma cells CAL27 and SCC15 (31). Another previous study showed that 0.20 mg/L AZS-induced an increase in p53,

bax, and apaf 1 levels in the zebrafish liver, which clearly confirmed the occurrence of apoptosis (3).

CONCLUSION

High levels of ROS can trigger mitochondrial-mediated apoptotic pathways, resulting in cell death (32). Our findings suggest that the AZS-induced neurotoxic effect is a consequence of ROS generation and ROS-induced apoptosis. Nonetheless, the mechanisms underlying AZS-induced neurotoxicity must be further investigated to determine the environmental and occupational risks as well as gain a better understanding of its potential toxicity.

Ethics Committee Approval: Since the study was an in vitro study, ethics committee approval was not required.

Peer Review: Externally peer-reviewed.

Author Contributions: Conception/Design of Study- A.B., G.Ö.; Data Acquisition- A.B.; Data Analysis/Interpretation- A.B., G.Ö.; Drafting Manuscript- A.B.; Critical Revision of Manuscript- A.B., G.Ö.; Final Approval and Accountability- A.B., G.Ö.; Material and Technical Support- G.Ö.; Supervision- G.Ö.

Conflict of Interest: The authors have no conflict of interest to declare.

Financial Disclosure: The authors declared that this study has received no financial support.

REFERENCES

1. Queirós L, Aguiar N, Pereira P, Gonçalves FJM, Alves A, Pereira JL. Recommended rates of azoxystrobin and tebuconazole seem to be environmentally safe but ineffective against target fungi. Ecotoxicology 2023;32(1):102-13.
2. Pearson BL, Simon JM, McCoy ES, Salazar G, Fragola G, Zylka MJ. Identification of chemicals that mimic transcriptional changes associated with autism, brain aging and neurodegeneration. Nat Commun 2016;7(1):1173.
3. Cao F, Wu P, Huang L, Li H, Qian L, Pang S, et al. Short-term developmental effects and potential mechanisms of azoxystrobin in larval and adult zebrafish (Danio rerio). Aquat Toxicol 2018;198:129-40.
4. Bartlett DW, Clough JM, Godwin JR, Hall AA, Hamer M, Parr-Dobrzanski B. The strobilurin fungicides. Pest Manag Sci 2002;58(7):649-62.
5. Kang J, Bishayee K, Huh SO. Azoxystrobin Impairs Neuronal Migration and Induces ROS Dependent Apoptosis in Cortical Neurons. Int J Mol Sci 2021;22(22):12495.
6. Cao F, Li H, Zhao F, Wu P, Qian L, Huang L, et al. Parental exposure to azoxystrobin causes developmental effects and disrupts gene expression in F1 embryonic zebrafish (Danio rerio). Sci Total Environ 2019;646:595-605.
7. Cao F, Martyniuk CJ, Wu P, Zhao F, Pang S, Wang C, et al. Long-Term Exposure to Environmental Concentrations of Azoxystrobin Delays Sexual Development and Alters Reproduction in Zebrafish (Danio rerio). Environ Sci Technol 2019;53(3):1672-9.
8. Nguyen K, Sanchez CL, Brammer-Robbins E, Pena-Delgado C, Kroyter N, El Ahmadie N, et al. Neurotoxicity assessment of QoI strobilurin fungicides azoxystrobin and trifloxystrobin in human SH-SY5Y neuroblastoma cells: Insights from lipidomics and mitochondrial bioenergetics. Neurotoxicology 2022;91:290-304.
9. Regueiro J, Olguín N, Simal-Gándara J, Suñol C. Toxicity evaluation of new agricultural fungicides in primary cultured cortical neurons. Environ Res 2015;140:37-44.
10. Olsvik PA, Kroglund F, Finstad B, Kristensen T. Effects of the fungicide azoxystrobin on Atlantic salmon (Salmo salar L.) smolt. Ecotoxicol Environ Saf 2010;73(8):1852-61.
11. Juraske R, Sanjuán N. Life cycle toxicity assessment of pesticides used in integrated and organic production of oranges in the Comunidad Valenciana, Spain. Chemosphere. 2011;82(7):956-62.
12. Takahashi S, Shinomiya T, Nagahara Y. Azoxystrobin Induces Apoptosis and Cell Cycle Arrest in Human Leukemia Cells Independent of p53 Expression. Anticancer Res 2022;42(3):1307-12.
13. Kumar N, Willis A, Satbhai K, Ramalingam L, Schmitt C, Moustaid-Moussa N, et al. Developmental toxicity in embryo-larval zebrafish (Danio rerio) exposed to strobilurin fungicides (azoxystrobin and pyraclostrobin). Chemosphere 2020;241:124980.
14. Cooper EM, Rushing R, Hoffman K, Phillips AL, Hammel SC, Zylka MJ, et al. Strobilurin fungicides in house dust: is wallboard a source? J Expo Sci Environ Epidemiol 2020;30(2):247-52.
15. U.S. EPA, Pesticide Product Label, Azoxystrobin Mold-Retardant 2.08 SC. 2004. 2024 March 23. https://www3.epa.gov/pesticides/chem_search/ppls/000100-01197-20041130.pdf
16. Carrasco Cabrera L, Medina Pastor P. The 2019 European Union report on pesticide residues in food. EFSA Journal 2021;19(4):89.
17. Kazar Soydan D, Turgut N, Yalçın M, Turgut C, Karakuş PBK. Evaluation of pesticide residues in fruits and vegetables from the Aegean region of Turkey and assessment of risk to consumers. Environ Sci Pollut Res Int. 2021;28(22):27511-9.
18. NCB (National Center for Biotechnology) PubChem Compound Summary for CID 3034285, Azoxystrobin. PubChem 2021. 2024 March 23. https://pubchem.ncbi.nlm.nih.gov/compound/Azoxystrobin.
19. Crupkin AC, Fulvi AB, Iturburu FG, Medici S, Mendieta J, Panzeri AM, et al. Evaluation of hematological parameters, oxidative stress and DNA damage in the cichlid Australoheros facetus exposed to the fungicide azoxystrobin. Ecotoxicol Environ Saf 2021;207:111286.
20. Shi XK, Bian XB, Huang T, Wen B, Zhao L, Mu HX, et al. Azoxystrobin Induces Apoptosis of Human Esophageal Squamous Cell Carcinoma KYSE-150 Cells through Triggering of the Mitochondrial Pathway. Front Pharmacol 2017;8:277.
21. Hu W, Liu CW, Jiménez JA, McCoy ES, Hsiao YC, Lin W, et al. Detection of Azoxystrobin Fungicide and Metabolite Azoxystrobin-Acid in Pregnant Women and Children, Estimation of Daily Intake, and Evaluation of Placental and Lactational Transfer in Mice. Environ Health Perspect 2022;130(2):27013.
22. Xicoy H, Wieringa B, Martens GJM. The SH-SY5Y cell line in Parkinson's disease research: a systematic review. Mol Neurodegener 2017;12(1):1-11.

23. Eruslanov E, Kusmartsev S. Identification of ROS using oxidized DCFDA and flow-cytometry. Methods Mol Biol 2010;594:57-72.
24. Ruiz-Yance I, Siguas J, Bardales B, Robles-Castañeda I, Cordova K, Ypushima A, et al. Potential Involvement of Oxidative Stress, Apoptosis and Proinflammation in Ipconazole-Induced Cytotoxicity in Human Endothelial-like Cells. Toxics 2023;11(10):839.
25. Barrios-Arpi L, Arias Y, Lopez-Torres B, Ramos-Gonzalez M, Ticli G, Prosperi E, et al. In Vitro Neurotoxicity of Flumethrin Pyrethroid on SH-SY5Y Neuroblastoma Cells: Apoptosis Associated with Oxidative Stress. Toxics 2022;10(3):131.
26. Nguyen K, Sanchez CL, Brammer-Robbins E, Pena-Delgado C, Kroyter N, El Ahmadie N, et al. Neurotoxicity assessment of QoI strobilurin fungicides azoxystrobin and trifloxystrobin in human SH-SY5Y neuroblastoma cells: Insights from lipidomics and mitochondrial bioenergetics. Neurotoxicology 2022;91:290-304.
27. Chen H, Li L, Lu Y, Shen Y, Zhang M, Ge L, et al. Azoxystrobin Reduces Oral Carcinogenesis by Suppressing Mitochondrial Complex III Activity and Inducing Apoptosis. Cancer Manag Res 2020;12:11573-83.
28. De Souza WR, Vessecchi R, Dorta DJ, Uyemura SA, Curti C, Vargas-Rechia CG. Characterization of Rubus fruticosus mitochondria and salicylic acid inhibition of reactive oxygen species generation at Complex III/Q cycle: potential implications for hypersensitive response in plants. J Bioenerg Biomembr 2011;43(3):237-46.
29. Wei F, Su T, Wang D, Li H, You J. Transcriptomic analysis reveals common pathways and biomarkers associated with oxidative damage caused by mitochondrial toxicants in Chironomus dilutus. Chemosphere 2020;254:126746.
30. Finkel T. Signal transduction by mitochondrial oxidants. Journal of Biological Chemistry 2012;287(7):4434-40.
31. Chen H, Wang J, Zhang C, Ding P, Tian S, Chen J, et al. Sphingosine 1-phosphate receptor, a new therapeutic direction in different diseases. Biomed Pharmacother 2022;153:113341.
32. Kang J, Bishayee K, Huh SO. Azoxystrobin Impairs Neuronal Migration and Induces ROS Dependent Apoptosis in Cortical Neurons. Int J Mol Sci 2021;22(22):12495.

İSTANBUL UNIVERSITY PRESS

RESEARCH ARTICLE / ARAŞTIRMA MAKALESİ
Journal of Advanced Research in Health Sciences /
Sağlık Bilimlerinde İleri Araştırmalar Dergisi 2024
DOI: 10.26650/JARHS2024-1405790

CYTOTOXIC AND GENOTOXIC EFFECTS OF NICKEL OXIDE NANOPARTICLES ON HeLa CELLS

NİKEL OKSİT NANOPARTİKÜLLERİNİN HeLa HÜCRELERİNDE SİTOTOKSİK VE GENOTOKSİK ETKİSİ

Onur PATAN[1,2], Özge Sultan ZENGİN[1,2], Mahmoud ABUDAYYAK[2]

[1]İstanbul University, Institute of Graduate Studies in Health Sciences, İstanbul, Türkiye
[2]İstanbul University, Faculty of Pharmacy, Department of Pharmaceutical Toxicology, İstanbul, Türkiye

ORCID ID: O.P. 0009-0002-3290-4525; Ö.S.Z. 0009-0006-9301-7371; M.A. 0000-0003-2286-4777

Citation/Atıf: Patan O, Zengin ÖS, Abudayyak M. Cytotoxic and genotoxic effects of nickel oxide nanoparticles on HeLa cells. Journal of Advanced Research in Health Sciences 2024;7(3):220-226. https://doi.org/10.26650/JARHS2024-1405790

ABSTRACT

Objective: Nickel oxide nanoparticles (NiO-NPs) are used invarious applications, and their increasing use has stimulated extensive studies both *in vivo* and *in vitro*. Nevertheless, their activity in cancer cells and thus the possibility of developing new anticancer drugs still remain controversial. Therefore, this study was conducted to specifically investigate the cytotoxicity and genotoxicity of NiO-NPs in human cervical carcinoma (HeLa) cells.

Material and Methods: The cytotoxicity of NiO-NPs was evaluated using 3-(4,5-dimethylthiazol-2-yl)-2,5-diphenyltetrazolium bromide (MTT), lactate dehydrogenase (LDH), and neutral red uptake (NRU) cytotoxicity assays. A comet assay was performed to determine the genotoxicity of NiO-NPs.

Results: The half maximal inhibitory concentration (IC_{50}) values were 419.6, 316.4, and 119.3 µg/mL in the MTT, NRU, and LDH assays, respectively. The comet assay revealed that NiO-NPs caused significant induction of DNA damage in the exposed HeLa cells. The tail intensity was 18.20% at 120 µg/mL.

Conclusion: NiO-NPs were cytotoxic and genotoxic to HeLa cells. Although NiO-NPs may be hazardous for a normal cell line, the effects observed on HeLa cells indicate that NiO-NPs can be proposed as a novel anticancer agent. However, the potential for NiO-NPs in cancer treatment will require additional and comprehensive studies on other cancer cell lines.

Keywords: HeLa cells, cytotoxicity, genotoxicity, NiO-NPs

ÖZ

Amaç: Nikel oksit nanopartikülleri (NiO-NP) endüstride geniş bir uygulama alanına sahiptir. Artan kullanım alanları ve miktarları ile birlikte kapsamlı araştırmalar ile araştırmacıların da ilgi odağı olmaktadır. Ancak, kanser hücrelerindeki etkinlikleri ve dolayısıyla yeni kanser ilaçları geliştirme olasılığı hala tartışmalıdır. Çalışmamızda NiO-NP'lerin insan servikal karsinom (HeLa) hücreleri üzerine sitotoksik ve genotoksik etki potansiyeli incelenmiştir.

Gereç ve Yöntem: NiO-NP'lerin sitotoksisitesi 3-(4,5-dimetiltiyazol-2-il)-2,5-difeniltetrazolyum bromür (MTT), laktat dehidrojenaz (LDH) ve nötral kırmızı alımı (NRU) testleri ile değerlendirilirken genotoksisitesi Comet testi ile araştırılmıştır.

Bulgular: Yarı maksimal inhibitör konsantrasyon (IC_{50}) değerleri MTT testi için 419,6 µg/mL, NRU testi için 316,4 µg/mL ve LDH testi için 119,3 µg/mL olarak bulunmuştur. Comet testi verilerine göre, NiO-NP'lerine maruz bırakılan hücrelerde DNA hasarı önemli ölçüde indüklenmiştir. Kuyruk yoğunluğunun 120 µg/mL maruziyet için %18,20 düzeylerinde olduğu tespit edilmiştir.

Sonuç: NiO-NP'ler HeLa hücrelerinde sitotoksik ve genotoksik etkili olduğu tespit edilmiştir. Normal bir hücre hattı için tehlikeli gibi görünse de kanser hücresi üzerine bu etkiler yeni bir antikanser ajan olarak NiO-NP'lerin umut verici olabileceğini göstermektedir. Ancak, NiO-NP'lerin kanser tedavisinde bir alternatif olma potansiyelini değerlendirmek üzere diğer kanser hücre hatlarında ve ileri çalışmalara ihtiyaç duyulmaktadır.

Anahtar Kelimeler: HeLa hücreleri, Sitotoksisite, Genotoksisite, Nikel oksit nanopartikülü

Corresponding Author/Sorumlu Yazar: Mahmoud ABUDAYYAK **E-mail:** mfirat.kenanoglu@istanbul.edu.tr

Submitted/Başvuru: 16.12.2023 • **Revision Requested/Revizyon Talebi:** 07.01.2024 • **Last Revision Received/Son Revizyon:** 18.02.2024 • **Accepted/Kabul:** 27.02.2024 • **Published Online/Online Yayın:** 22.10.2024

INTRODUCTION

Nickel oxide nanoparticles (NiO-NPs) are desired in various fields because of their advantageous chemical and physical properties, including large surface area, high surface energy, magnetic properties, and low-melting point. NiO-NPs are widely used in battery construction, alloys, pigmentation, and biomedical materials. Nevertheless, the particle size, which is an advantage in industrial applications, increases the risk of toxicity to biological systems; nanoparticles, due to their extremely small size, can be more easily transported to cells and tissues and accumulate in target organs (1, 2). Because of their widespread use, it has been questioned whether they pose a threat to humans, and there is also some research addressing this issue (2). Conversely, the super small size and easy passage through cell membranes, and the fact that NiO-NPs have been confirmed to exert a cytotoxic effect on some cancer cells, make it possible to use these NPs to kill cancer cells as a type of chemotherapy and suggest their use as anticancer agents. Hence, several studies have investigated the cytotoxic effect of different NPs in general and NiO-NPs in particular in different cell lines (3, 4). Nickel-based NPs, which are widely used in industries, pose a high risk for airborne dermal and respiratory toxicity to workers. In this regard, studies primary evaluate their effects after inhalation exposure. *In vivo* studies have explored their effects on the cardiovascular system, lungs, and other organs, whereas *in vitro* studies have generally focused on cellular mechanisms. The results of different studies indicate that NiO-NPs generally caused cytotoxicity, increase in reactive oxygen species (ROS) levels, apoptosis, and genotoxicity (1, 2).

In the present study, it was hypothesized that NiO-NPs could exert an anticancer effect, because they could exert cytotoxic effects on human cervical cancer cells. It was also hypothesized that DNA damage could be a mechanism of this effect. A well-known human cancer cell line, HeLa, was used in this study. HeLa cells are derived from the epithelial cells of human cervical cancer and are the first immortal human cells to be grown in culture. These cells possess an extraordinary capacity for continuous proliferation, rendering them immortal in laboratory cultures. Moreover, HeLa cells exhibit a high growth rate, dividing rapidly and facilitating the generation of large cell populations for experimentation. Hence, they are widely used in different research areas (5). Various cytotoxicity assays were then used in this study to investigate the affected cellular organelle and, in addition, to test whether DNA damage was a cytotoxicity mechanism. The NiO-NP-exposed cells were also evaluated using the comet assay.

MATERIAL AND METHODS

Particle size characterization

NiO-NPs (Sigma-Aldrich, MO, USA) were suspended in double-distilled water or complete cell culture medium. Then, they were subjected to sonication for 15 min before examination under a transmission electron microscope (TEM) (JEM-2100 HR, JEOL, USA). The image of more than 100 particles in arbitrary TEM fields was captured and analyzed by measuring their diameters. Dynamic light scattering (DLS) was also performed to determine the size of NPs using a ZetaSizer Nano-ZS instrument (Malvern, UK). For DLS analysis, the NiO-NPs (1 mg) were dissolved in cell culture medium and sonicated at 40 W for 15 min at room temperature, then, a 10 µg/mL freshly prepared suspension was used in the measurement.

Cell culture procedure and exposure conditions

HeLa cells, a human cervical carcinoma cell line (CCL-2, ATCC, USA), were cultured in Eagle's minimum essential medium supplemented with penicillin–streptomycin (1%) and fetal bovine serum (FBS, 10%). Subculturing was conducted when the cells reached 50% confluence.

For exposure, the NP suspension was freshly prepared before each experiment. For this, the NiO-NPs were dispersed in the complete cell culture medium and sonicated for 15 min at room temperature, from which different concentrations were prepared. The exposure concentrations were 0–1000 µg/mL for the 3-(4,5-dimethylthiazol-2-yl)-2,5-diphenyltetrazolium bromide (MTT), lactate dehydrogenase (LDH), and neutral red uptake (NRU) cytotoxicity assays and 15–120 µg/mL for the comet assay. The exposure time was set at 24 h. For the cytotoxicity assays, the percentage of cell viability was determined in comparison with the untreated cell group (negative control, NC).

Cytotoxicity

For the MTT assay, the MTT dye (5 mg/mL) was added to each well. After 3 h of incubation, the formazan crystals formed were dissolved using dimethyl sulfoxide (DMSO, 100 µL) per well. The optical density (OD) at 590 nm was measured using a microplate reader (Epoch, Germany) (6). For the NRU assay, the cells were treated with a neutral red solution (10 mg/mL NR dye in the cell culture medium) for 3 h. After incubation, the cells were washed with phosphate-buffered saline (PBS, 1×), and a dissolution reagent (100 µL/well) was added. OD was measured at 540 nm using the same microplate reader (7). For the LDH assay, the microplate was centrifuged at 250 *g* for 10 min. The supernatant was carefully transferred to new plates. LDH assay kit solutions were added and incubated according to the kit instructions, a stop solution was added, and the OD was measured at 490 nm using the same microplate reader (8).

Genotoxicity

Cells were cultured in 6-well plates (5×10^5 cells/well), incubated for 12 h, and then treated with NiO-NPs for 24 h. The cells were collected by trypsinization, centrifuged, washed, and suspended in PBS (1 mL). The cell suspension was mixed with prewarmed low-melting agarose and then applied to microscope slides previously coated with normal-melting agarose. After solidification at 4°C, the slides were incubated in a lysis solution at 4°C for at least 2 h. Then, the slides were transferred to fresh, cold electrophoresis buffer at 4°C for 20 min to dissolve the DNA strands. Electrophoresis was performed at 4°C for 20 min.

After electrophoresis, the slides were washed, neutralized, and then fixed in ethanol. DNA staining was performed using ethidium bromide, and the slides were examined under a fluorescence microscope (Olympus BX53, Tokyo, Japan) at 400X. The comet assay IV image analysis software (Perceptive Instruments, Suffolk, UK) was used to visualize and analyze the results. A minimum of 100 cells were scored for each sample, and the

amount of DNA damage in each cell was expressed as the tail intensity. The NC groups consisted of cells not treated with any chemical, whereas cells exposed to hydrogen peroxide (H_2O_2, 100 µM) were identified as the positive control (PC) group (9).

Statistical analysis

All assays were performed three times independently, each time in triplicate (n=9). One-way analysis of variance or Dunnett's test was used to examine the results, which were expressed as mean ± standard error. Statistical analyses were conducted using the SPSS software for Windows version 22.0, (IBM SPSS Corp., Armonk, NY, USA), and a *p* value cut-off of 0.05 indicated statistical significance.

RESULTS

According to the manufacturer, the nanoparticles are cubic, the mean particle size is ≤50 nm, and they are highly pure (99.8%). Based on TEM data, the particle size of NiO-NPs in water ranged from 4.2 to 38.1 nm, with a mean size of 15.0 nm. When the particles were dispersed in the cell culture medium, their average diameter increased to 21.4 nm, which could be due to agglomerated and aggregated NPs or adsorbed proteins from the medium. NiO-NPs have a size range of 7.70–194.1 nm and an average hydrodynamic size of 135.81 nm in the cell culture medium. The results of DLS revealed that 33% of NiO-NPs were smaller than 24.8 nm (Figure 1).

Cytotoxicity evaluation revealed that NiO-NPs caused cell death in a concentration-dependent manner. The half maximal inhibitory concentration (IC_{50}) values were 419.6, 316.4, and 119.3 µg/mL in the MTT, NRU, and LDH assays, respectively. Figure 2 depicts the relationship concentration and cell death (%).

The results of the comet assay revealed an accumulation of DNA damage according to the concentration of NiO-NPs, where the tail intensity was 3.78% (1.23-fold of NC) and 18.20% (5.92-fold of NC) at the lowest and highest concentrations, res-

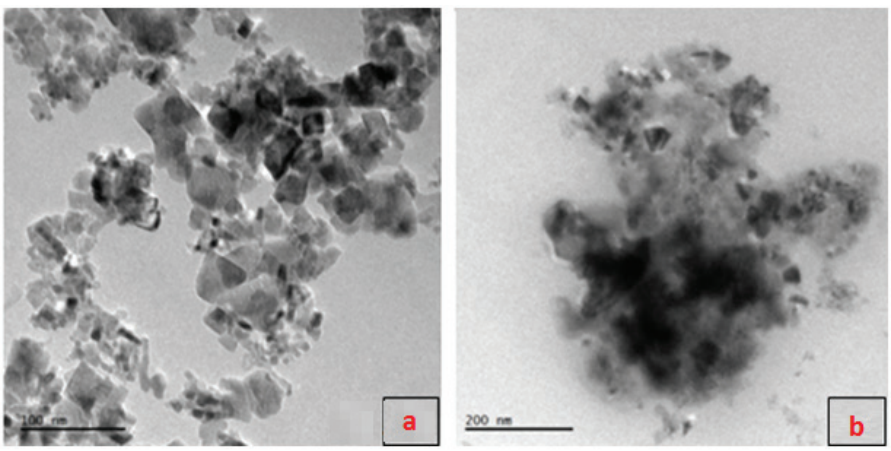

Figure 1: TEM images of NiO-NPs in water (a) and cell culture medium (b) (22)

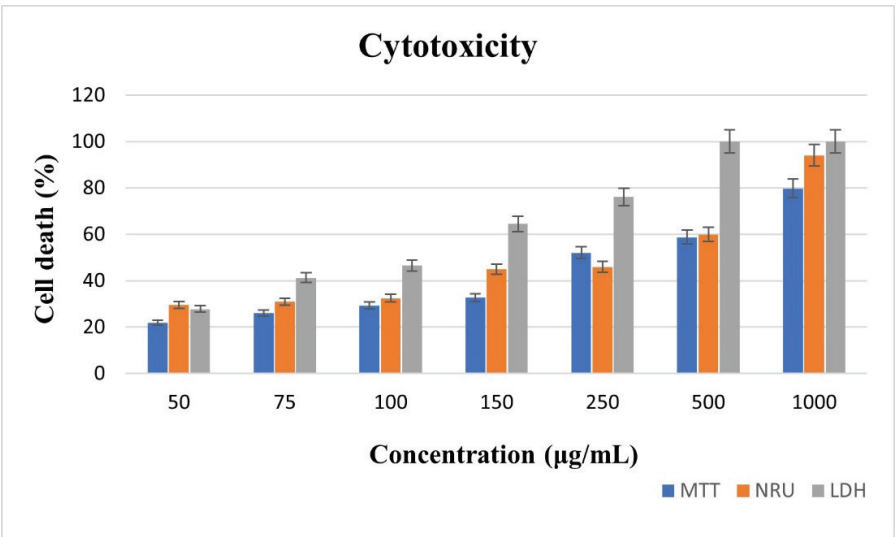

Figure 2: Cytotoxic potential of nickel oxide nanoparticles (NiO-NPs) evaluated using 3-(4,5-dimethylthiazol-2-yl)-2,5-diphenyltetrazolium bromide (MTT), neutral red uptake (NRU), and lactate dehydrogenase (LDH) assays. Cells were exposed to NiO-NPs at different concentrations for 24 h.

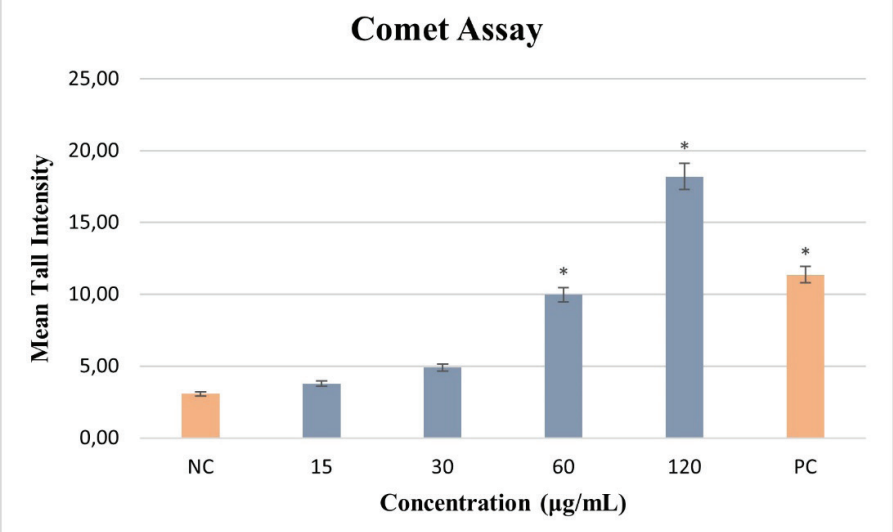

Figure 3: Genotoxic potential of nickel oxide nanoparticles (NiO-NPs) in HeLa cells evaluated using the comet assay. Cells were exposed to NiO-NPs at 15–120 µg/mL concentrations for 24 h. Unexposed cells and cells exposed to hydrogen peroxide (H_2O_2, 100 µM) served as negative control (NC) and positive control (PC), respectively

pectively. In the positive control, the tail intensity was 11.36% (3.7-fold of NC) (Figure 3). This increase in tail intensity was statistically significant ($p \leq 0.05$) for the 60 and 120 µg/mL groups but not for the 15 and 30 µg/mL groups.

DISCUSSION

NiO-NPs are one of the most widely utilized nanoparticles in various medical and commercial fields. In addition to their physicochemical properties, the possibility of their application as drugs has been evaluated by different research groups (1, 2). In particular, some studies have demonstrated that NiO-NPs cause cytotoxicity in several cancer cells, and other studies have explained their molecular and cellular effects such as ROS induction, lipid peroxidation, oxidative stress, apoptosis, necrosis, and DNA and chromosomal damage (Table 1). Based on these effects on cancer cells, we explored whether NiO-NPs might be a material that could be used in cancer treatment. For this purpose, we evaluated cytotoxicity and DNA damage induction in the well-known human cervical cancer cell line (HeLa) after 24 h of exposure.

The effects of NiO-NPs were evaluated in both normal and cancerous cells; previous studies have demonstrated low or no toxicity of NiO-NPs on normal cells. Khan et al. reported no cytotoxicity of NiO-NPs on normal splenic cells at concentrations up to 1000 µg/mL (10). Similarly, Abbaszadeh et al. reported low cytotoxicity for modified NiO-NPs in Hek293 normal cells, where the IC_{50} was 475 µg/mL (11). In human normal keratinocytes (HaCaT cells), the cytotoxic effects were also lower than those in the tested cancerous cells, with the IC_{50} being 312.5 µg/mL in the MTT test (12). No significant cytotoxicity was reported for NiO and other Ni-based salt NPs in human normal umbilical vein endothelial (HUVEC) cells at concentrations up to 1000 µg/mL (13). In contrast, NiO-NPs resulted in significant cell death in different cancerous cells, causing cytotoxicity in the leukaemia monocyte cell line THP-1 after 24 h of treatment, with the IC_{50} being 23.31 µg/mL (14). According to the studies of Horie et al., Ahamed et al., and Capasso et al., NiO-NPs are cytotoxic to A549 lung cancer cells (15-17). A549 cells were exposed to NiO-NPs at concentrations of 0–25 µg/mL for 24 and 48 h, which resulted in a gradual decrease in cell viability with increasing exposure concentrations and/or duration as evaluated using MTT and LDH assays. The oxidative stress caused by NiO-NPs was demonstrated by Horie et al. and Ahamed et al. Moreover, Horie et al. examined ROS production and lipid peroxidation in their study, and Ahamed et al. examined apoptosis as a cell death pathway in their study (16, 17).

Ahamed et al. and Ahmad et al. conducted studies demonstrating the cytotoxic and apoptotic effects of NiO-NPs on the HepG2 liver cancer cell line (18, 19). Ahamed et al. showed that exposure of HepG2 cells to NiO-NPs at concentrations of 0–200 µg/mL for 24 h resulted in cell viability of only 25% at 200 µg/mL concentration. Ahmad et al. exposed the cells to NiO-NPs (0–100 µg/mL) for the same duration and conducted MTT and NRU assays, which revealed a reduction in cell viability, decreasing to 50% at 100 µg/mL, in a concentration-dependent manner. Both studies concluded that NiO-NPs induced oxidative stress in a dose-dependent manner in addition to their observed cytotoxic effects (18, 19).

Siddiqui et al. conducted a study using Hep-2 cells containing HeLa marker chromosomes and observed that NiO-NPs at concentrations of 0–100 µg/mL induced dose-dependent cytotoxicity and apoptosis during 24-h exposure. Similar results were found in MCF-7 breast cancer cells in the same study. In the MTT assay, the viability of Hep-2 cells was 11% and that of MCF-7 cells was 9% at 100 µg/mL of NiO-NPs (4).

NiO-NP treatment for 24 h at different concentrations (0–640 µg/mL) induced cytotoxicity and apoptosis in HT-29 and SW620 colon cancer cell lines, with the IC_{50} values being 13.72 and

394.41 g/mL, respectively (3).

NiO-NPs have been demonstrated to cause cytotoxicity, apoptosis, DNA damage, and oxidative stress in SH-SY5Y neuroblastoma cell lines at concentrations of 50–500 µg/mL for 24 h. The IC_{50} values were 249.92 and 229.34 µg/mL in the MTT and NRU assays, respectively (20). In another study, treating Caco-2 colorectal adenocarcinoma cells with NiO-NPs (50–500 µg/mL) for 24 h resulted in apoptosis and cytotoxicity, with the IC_{50} values being 351.6 and 479.15 µg/mL in the MTT and NRU assays, respectively. At 30–150 µg/mL, NiO-NPs caused DNA and oxidative damage (21). In another study, Annexin V-FITC/PI apoptosis detection was used to determine whether NRK-52E kidney epithelial cells suffered necrosis or apoptosis. The results showed that the primary mechanism of cell death in NiO-NP-treated NRK-52E cells was apoptosis, wherein approximately 62.5% of the overall cell count at the maximum dose (300 g/mL) consisted of apoptotic cells and 14.4% of the overall cell count consisted of necrotic cells (22).

In the study by Ada et al., NiO-NPs were synthesized in an aqueous solution using a homogeneous precipitation method. Laboratory-synthesized NiO-NPs were evaluated for their cytotoxic, apoptotic, and necrotic effects on HeLa cells. For cytotoxicity, HeLa cells were exposed to NiO-NPs at 50–500 µl/mL concentrations for 2, 6, 12, and 16 h. Results showed that cytotoxicity increased with concentration and exposure time, and necrosis appeared to be the major cell death pathway at all concentrations for all exposure times (23).

Because the properties of NPs exert a significant influence on their biological effects, and the particle size, size distribution, chemical residues for synthesis process, and surface chemistry of NPs can impact the biological potential (1, 2), we believe that reference NiO-NPs should be evaluated in HeLa cells, so that the results could be compared with those of previous studies that used the same particles. The results of the present study indicated that NiO-NPs triggered cytotoxic effects in HeLa cells with IC_{50} values of 419.6, 316.4, and 119.3 µg/mL in the MTT, NRU, and LDH assays, respectively. Remarkably, although previous studies demonstrated a higher toxicity of antineoplastic agents that are already in use in HeLa cells compared with our study results related to NiO-NPs, some of those studies reported IC_{50} values not far from those of NiO-NPs or even lower than the IC_{50} of NiO-NPs. A previous study reported that 5-fluorouracil (5-FU) at 200 µM (26.016 µg/mL) decreased cell viability to 70% after 24 h of exposure (24), whereas another study reported that 7.8125 µg/mL of 5-FU did not induce any

Table 1: Previous studies that investigated the effects of NiO-NPs on cancer cells

Cell line	NiO-NP-induced toxicity	IC_{50} values by MTT	Reference
A549	ROS production, lipid peroxidation, oxidative stress	Not available	11
A549*	Cytotoxicity	38% cell viability at 10 µg/mL (24 h)	13
Caco-2*	Cytotoxicity, apoptosis, DNA damage	351.6 µg/mL (24 h)	17
HeLa	Cytotoxicity, apoptosis, necrosis	41% cell viability at 350 µg/mL (16 h)	19
HEPG2	Cytotoxicity, ROS production, apoptosis, oxidative stress	41% cell viability at 100 µg/mL (24 h)	14
HEp-2*	Cytotoxicity, apoptosis	43% cell viability at 25 µg/mL (24 h)	4
HT-29	Cytotoxicity, apoptosis	13.72 µg/mL (24 h)	3
MCF-7*	Cytotoxicity, apoptosis	42% cell viability at 10 µg/mL (24 h)	16
SH-SY5Y*	Cytotoxicity, apoptosis, DNA damage, oxidative stress	≥229.34 µg/mL (24 h)	16
SW620	Cytotoxicity	394.41 µg/mL (24 h)	3
THP-1	Cytotoxicity	23.31 µg/mL (24 h)	10

* The same nickel oxide nanoparticles (Sigma-Aldrich, Product No.: 637130) were used in this study. DNA: deoxyribonucleic acid, NiO-NPs: nickel oxide nanoparticles, IC_{50}: half maximal inhibitory concentration, MTT: 3-(4,5-dimethylthiazol-2-yl)-2,5-diphenyltetrazolium bromide, ROS: reactive oxygen species.

cytotoxicity to the cells, with the IC_{50} being approximately 125 µg/mL (25). Cisplatin treatment to the same cells caused cytotoxicity, with the IC_{50} being 34.2 µM (26). However, in another study, the IC_{50} of cisplatin was 0.5–1 µM (27).

The comet assay revealed a significant induction of DNA damage at 60 and 120 µg/mL of NiO-NPs, suggesting that DNA damage could be a mechanism by which NiO-NPs induced cell death in HeLa cells. Compared with studies that used the same NiO-NPs and assays but different cell lines, HeLa cells may be more resistant than some cell lines (Table 1).

In conclusion, different studies have reported different results on the toxicity of NiO-NPs to cancer cells. These inconsistencies can be attributed to differences in the cell lines used; the type, shape, and size of NPs; and the synthesis method of NPs. Our results showed that NiO-NPs caused cell death at moderate concentrations (IC_{50} 119.3–419.6 µg/mL). The observed increase in DNA damage in exposed cells suggests that DNA damage contributes to the death of HeLa cells after exposure to NiO-NPs. These data further support the notion that Ni-based NPs, particularly NiO-NPs, have the potential for targeted cancer treatment by eliminating cancerous tissue. Nevertheless, further *in vitro* and *in vivo* research is required to gain a better understanding of the underlying mechanism of action of NiO-NPs. Furthermore, such studies are essential to determine the safety profile and feasibility of NPs for use in cancer therapy.

Peer Review: Externally peer-reviewed.

Author Contributions: Conception/Design of Study- O.P., Ö.S.Z.; Data Acquisition- O.P., Ö.S.Z.; Data Analysis/Interpretation- O.P., Ö.S.Z., M.A.; Drafting Manuscript- O.P., Ö.S.Z.; Critical Revision of Manuscript- O.P., Ö.S.Z., M.A.; Final Approval and Accountability- M.A.; Material and Technical Support- M.A.; Supervision- M.A.

Conflict of Interest: The authors have no conflict of interest to declare.

Financial Disclosure: The author declared that this study has received no financial support.

REFERENCES

1. More SL, Kovochich M, Lyons-Darden T, Taylor M, Schulte AM, Madl AK. Review and evaluation of the potential health effects of oxidic nickel nanoparticles. Nanomaterials 2021;11(3):642.
2. Magaye R, Zhao J. Recent progress in studies of metallic nickel and nickel-based nanoparticles' genotoxicity and carcinogenicity. Environ Toxicol Pharmacol 2012;34(3):644-50.
3. Khan S, Ansari AA, Malik A, Chaudhary AA, Syed JB, Khan AA. Preparation, characterizations, and in vitro cytotoxic activity of nickel oxide nanoparticles on HT-29 and SW620 colon cancer cell lines. J Trace Elem Med Biol 2019;52(1):12-7.
4. Siddiqui MA, Ahamed M, Ahmad J, Khan MM, Musarrat J, Al-Khedhairy AA, et al. Nickel oxide nanoparticles induce cytotoxicity, oxidative stress, and apoptosis in cultured human cells that are abrogated by the dietary antioxidant curcumin. Food Chem Toxicol 2012;50(3-4):641-7.
5. American Type Culture Collection (ATTC). HeLa CCL-2. https://www.atcc.org/products/ccl-2 2022
6. Van Meerloo J, Kaspers GJ, Cloos J. Cell sensitivity assays: the MTT assay. Methods Mol Biol 2011;731:237-45.
7. Repetto G, Del Peso A, Zurita, JL. Neutral red uptake assay for the estimation of cell viability/cytotoxicity. Nature protocols 2008;3(7):1125-31.
8. Kumar P, Nagarajan A, Uchil PD. Analysis of cell viability by the lactate dehydrogenase assay. Cold Spring Harb Protoc 2018;6:465-8
9. Speit G, Hartmann A. The comet assay (Single-Cell Gel Test) a sensitive genotoxicity test for the detection of DNA damage and repair. Methods Mol Biol 1999;113:203-12.
10. Khan A, Shkir M, Ibrahim EH, Kilany M, AlFaify S, Sayed MA, Siddiquei MM. Effect of Bi contents on key physical properties of NiO NPs synthesized by flash combustion process and their cytotoxicity studies for biomedical applications. Ceram Int 2020;46(12):19691-700.
11. Abbaszadeh N, Jaahbin N, Pouraei A, Mehraban F, Hedayati M, Majlesi A, Salehzadeh A. Preparation of novel nickel oxide glutamic/thiosemicarbazide nanoparticles: Implications for cytotoxic and anti-cancer studies in MCF-7 breast cancer cells. J Clust Sci 2020;(10):1-9.
12. Rincon-Granados KL, Vázquez-Olmos AR, Rodríguez-Hernández AP, Prado-Prone G, Garibay-Febles V, et al. Bactericidal and Cytotoxic Study of Hybrid Films Based on NiO and NiFe2O4 Nanoparticles in Poly-3-Hydroxybutyrate. J Clust Sci 2023;35:167-78.
13. Zhang Y, Mahdavi B, Mohammadhosseini M, Rezaei-Seresht E, Paydarfard S, Qorbani M, et al. Green synthesis of NiO nanoparticles using Calendula officinalis extract: Chemical charactrization, antioxidant, cytotoxicity, and anti-esophageal carcinoma properties. Arab J Chem 2021;14(5):103-5.
14. Lanone S, Rogerieux F, Geys J, Dupont A, Maillot-Marechal E, Boczkowski J, Hoet P. Comparative toxicity of 24 manufactured nanoparticles in human alveolar epithelial and macrophage cell lines. Part Fibre Toxicol 2009;6(1):1-12.
15. Horie M, Fukui H, Nishio K, Endoh S, Kato H, Fujita K, Iwahashi H. Evaluation of acute oxidative stress induced by NiO nanoparticles *in vivo* and *in vitro*. J Occup Health 2011;53(2):64-74.
16. Ahamed M. Toxic response of nickel nanoparticles in human lung epithelial A549 cells. Toxicol In Vitro 2011;25(4):930-6.
17. Capasso L, Camatini M, Gualtieri M. Nickel oxide nanoparticles induce inflammation and genotoxic effect in lung epithelial cells. Toxicol Lett 2014;226(1):28-34.
18. Ahamed M, Ali D, Alhadlaq HA, Akhtar MJ. Nickel oxide nanoparticles exert cytotoxicity via oxidative stress and induce apoptotic response in human liver cells (HepG2). Chemosphere 2013;93(10):2514-22.
19. Ahmad J, Alhadlaq HA, Siddiqui MA, Saquib Q, Al-Khedhairy AA, Musarrat J, Ahamed M. Concentration-dependent induction of reactive oxygen species, cell cycle arrest and apoptosis in human liver cells after nickel nanoparticles exposure. Environ Toxicol 2015;30(2):137-48.
20. Abudayyak M, Guzel E, Özhan G. Nickel oxide nanoparticles

are highly toxic to SH-SY5Y neuronal cells. Neurochem Int 2017;108(1):7-14.

21. Abudayyak M, Güzel E, Özhan G. Cytotoxic, genotoxic, and apoptotic effects of nickel oxide nanoparticles in intestinal epithelial cells. Turk J Pharm Sci 2020;17(4):446.
22. Abudayyak M, Guzel E, Özhan G. Nickel oxide nanoparticles induce oxidative DNA damage and apoptosis in a kidney cell line (NRK-52E). Biol Trace Elem Res 2016;178:98-104.
23. Ada K, Turk M, Oguztuzun S, Kilic M, Demirel M, Tandogan N, Latif O. Cytotoxicity and apoptotic effects of nickel oxide nanoparticles in cultured HeLa cells. Folia Histochem Cytobiol 2010;48(4):524-9.
24. Mavrikou S, Tsekouras V, Karageorgou MA, Moschopoulou G, Kintzios S. Detection of superoxide alterations induced by 5-fluorouracil on HeLa cells with a cell-based biosensor. Biosensors 2019;9(4):126.
25. Arabnezhad S, Mani H, Gordi P, Ahmadi R. The Cytotoxic Effects of 5FU on Hek293 and HeLa Cells in vitro. Int J BioLife Sci 2022;1(3S)128-33.
26. Jurado R, Lopez-Flores A, Alvarez A, García-López P. Cisplatin cytotoxicity is increased by mifepristone in cervical carcinoma: an in vitro and in vivo study. Oncol rep 2009;22(5):1237-45.
27. Fathy M, Fawzy MA, Hintzsche H, Nikaido T, Dandekar T, Othman EM. Eugenol exerts apoptotic effect and modulates the sensitivity of HeLa cells to cisplatin and radiation. Molecules 2019;24(21):3979.

Aims and Scope

Journal of Advanced Research in Health Sciences (JARHS) is an international, scientific, open access periodical published in accordance with independent, unbiased, and double-blinded peer-review principles. The journal is the official publication of Institute of Health Sciences of İstanbul University and it is published every 4 months on February, June, and October. The publication language of the journal is English as of June 2023.

Journal of Advanced Research in Health Sciences (JARHS) aims to contribute to the literature by publishing manuscripts at the highest scientific level on all fields of medicine. The journal publishes original experimental and clinical research articles, reports of rare cases, reviews that contain sufficient amount of source data conveying the experiences of experts in a particular field, and letters to the editors as well as brief reports on a recently established method or technique or preliminary results of original studies related to all disciplines of medicine from all countries.

Editorial Policies and Peer Review Process

The editorial and publication processes of the journal are shaped in accordance with the guidelines of the International Council of Medical Journal Editors (ICMJE), the World Association of Medical Editors (WAME), the Council of Science Editors (CSE), the Committee on Publication Ethics (COPE), the European Association of Science Editors (EASE), and National Information Standards Organization (NISO). The journal conforms to the Principles of Transparency and Best Practice in Scholarly Publishing (doaj.org/bestpractice).

Originality, high scientific quality, and citation potential are the most important criteria for a manuscript to be accepted for publication. Manuscripts submitted for evaluation should not have been previously presented or already published in an electronic or printed medium. The journal should be informed of manuscripts that have been submitted to another journal for evaluation and rejected for publication. The submission of previous reviewer reports will expedite the evaluation process. Manuscripts that have been presented in a meeting should be submitted with detailed information on the organization, including the name, date, and location of the organization.

Manuscripts submitted to Journal of Advanced Research in Health Sciences will go through a double-blind peer-review process. Each submission will be reviewed by at least two external, independent peer reviewers who are experts in their fields in order to ensure an unbiased evaluation process. The editorial board will invite an external and independent editor to manage the evaluation processes of manuscripts submitted by editors or by the editorial board members of the journal. The Editor in Chief is the final authority in the decision-making process for all submissions.

An approval of research protocols by the Ethics Committee in accordance with international agreements (World Medical Association Declaration of Helsinki "Ethical Principles for Medical Research Involving Human Subjects," amended in October 2013, www.wma.net) is required for experimental, clinical, and drug studies and for some case reports. If required, ethics committee reports or an equivalent official document will be requested from the author(s). For manuscripts concerning experimental research on humans, a statement should be included that shows that written informed consent of patients and volunteers was obtained following a detailed explanation of the procedures that they may undergo. For studies carried out on animals, the measures taken to prevent pain and suffering of the animals should be stated clearly. Information on patient consent, the name of the ethics committee, and the ethics committee approval number should also be stated in the Materials and Methods section of the manuscript. It is the author(s)' responsibility to carefully protect the patients' anonymity. For photographs that may reveal the identity of the patients, signed releases of the patient or of their legal representative should be enclosed.

All submissions are screened by a similarity detection software (iThenticate by CrossCheck).

In the event of alleged or suspected research misconduct, e.g., plagiarism, citation manipulation, and data falsification/fabrication, the Editorial Board will follow and act in accordance with COPE guidelines.

Each individual listed as an author should fulfill the authorship criteria recommended by the International Committee of Medical Journal Editors

(ICMJE - www.icmje.org). The ICMJE recommends that authorship be based on the following 4 criteria:

1. Substantial contributions to the conception or

design of the work; or the acquisition, analysis, or interpretation of data for the work; AND

2. Drafting the work or revising it critically for important intellectual content; AND
3. Final approval of the version to be published; AND
4. Agreement to be accountable for all aspects of the work in ensuring that questions related to the accuracy or integrity of any part of the work are appropriately investigated and resolved.

In addition to being accountable for the parts of the work he/she has done, an author should be able to identify which co-authors are responsible for specific other parts of the work. In addition, authors should have confidence in the integrity of the contributions of their co-authors.

All those designated as authors should meet all four criteria for authorship, and all who meet the four criteria should be identified as authors. Those who do not meet all four criteria should be acknowledged in the title page of the manuscript.

The Editorial Board of the journal handles all appeal and complaint cases within the scope of COPE guidelines. In such cases, authors should get in direct contact with the editorial office regarding their appeals and complaints. When needed, an ombudsperson may be assigned to resolve cases that cannot be resolved internally. The Editor in Chief is the final authority in the decision-making process for all appeals and complaints.

Journal of Advanced Research in Health Sciences requires each submission to be accompanied by a Copyright Agreement Form (available for download at https://dergipark.org.tr/en/pub/sabiad). When using previously published content, including figures, tables, or any other material in both print and electronic formats, authors must obtain permission from the copyright holder. Legal, financial and criminal liabilities in this regard belong to the author(s).

Statements or opinions expressed in the manuscripts published in Journal of Advanced Research in Health Sciences reflect the views of the author(s) and not the opinions of the editors, the editorial board, or the publisher; the editors, the editorial board, and the publisher disclaim any responsibility or liability for such materials. The final responsibility in regard to the published content rests with the authors.

Publication Policy

The journal is committed to upholding the highest standards of publication ethics and pays regard to Principles of Transparency and Best Practice in Scholarly Publishing published by the Committee on Publication Ethics (COPE), the Directory of Open Access Journals (DOAJ), the Open Access Scholarly Publishers Association (OASPA), and the World Association of Medical Editors (WAME) on https://publicationethics.org/resources/guidelines-new/principles-transparency-and-best-practice-scholarly-publishing

The subjects covered in the manuscripts submitted to the Journal for publication must be in accordance with the aim and scope of the Journal. Only those manuscripts approved by every individual author and that were not published before in or sent to another journal, are accepted for evaluation.

Changing the name of an author (omission, addition or order) in papers submitted to the Journal requires written permission of all declared authors.

Plagiarism, duplication, fraud authorship/denied authorship, research/data fabrication, salami slicing/salami publication, breaching of copyrights, prevailing conflict of interest are unethical behaviors. All manuscripts not in accordance with the accepted ethical standards will be removed from the publication. This also contains any possible malpractice discovered after the publication.

Plagiarism

Submitted manuscripts that pass preliminary control are scanned for plagiarism using iThenticate software. If plagiarism/self-plagiarism will be found authors will be informed. Editors may resubmit manuscript for similarity check at any peer-review or production stage if required. High similarity scores may lead to rejection of a manuscript before and even after acceptance. Depending on the type of article and the percentage of similarity score taken from each article, the overall similarity score is generally expected to be less than 15 or 20%.

Double Blind Peer-Review

After plagiarism check, the eligible ones are evaluated by the editors-in-chief for their originality, methodology, the importance of the subject covered and compliance with the journal scope. The editor provides a fair double-blind peer review of the submitted articles and hands over the papers matching

the formal rules to at least two national/international referees for evaluation and gives green light for publication upon modification by the authors in accordance with the referees' claims.

Open Access Statement

The journal is an open access journal and all content is freely available without charge to the user or his/her institution. Except for commercial purposes, users are allowed to read, download, copy, print, search, or link to the full texts of the articles in this journal without asking prior permission from the publisher or the author. This is in accordance with the BOAI definition of open access.

The open access articles in the journal are licensed under the terms of the Creative Commons Attribution-NonCommercial 4.0 International (CC BY-NC 4.0) license. (https://creativecommons.org/licenses/by-nc/4.0/deed.en)

Copyright Notice

Authors publishing with the journal retain the copyright to their work licensed under the Creative Commons Attribution-NonCommercial 4.0 International license (CC BY-NC 4.0) (https://creativecommons.org/licenses/by-nc/4.0/) which permits unrestricted, non-commercial use, distribution, and reproduction in any medium, provided the original work is properly cited.

Manuscript Preparation

The manuscripts should be prepared in accordance with ICMJE-Recommendations for the Conduct, Reporting, Editing, and Publication of Scholarly Work in Medical Journals (updated in December 2015 - http://www.icmje.org/icmje-recommendations.pdf). Author(s) are required to prepare manuscripts in accordance with the CONSORT guidelines for randomized research studies, STROBE guidelines for observational original research studies, STARD guidelines for studies on diagnostic accuracy, PRISMA guidelines for systematic reviews and meta-analysis, ARRIVE guidelines for experimental animal studies, and TREND guidelines for non-randomized public behavior.

Manuscripts can only be submitted through the journal's online manuscript submission and evaluation system, available at https://dergipark.org.tr/tr/pub/sabiad Manuscripts submitted via any other medium will not be evaluated.

Manuscripts submitted to the journal will first go through a technical evaluation process where the editorial office staff will ensure that the manuscript has been prepared and submitted in accordance with the journal's guidelines. Submissions that do not conform to the journal's guidelines will be returned to the submitting author with technical correction requests.

Author(s) are required to submit the following:

• **Copyright Agreement Form,**

Title page: A separate title page should be submitted with all submissions and this page should include:

• The full title of the manuscript as well as a short title (running head) of no more than 50 characters,

• Name(s), affiliations, highest academic degree(s) and ORCID ID(s) of the author(s),

• Grant information and detailed information on the other sources of support,

• Name, address, telephone (including the mobile phone number) and fax numbers, and email address of the corresponding author,

• Acknowledgment of the individuals who contributed to the preparation of the manuscript but who do not fulfil the authorship criteria.

Abstract: A Turkish and an English abstract should be submitted with all submissions except for Letters to the Editor. Submitting a Turkish abstract is not compulsory for international authors. The abstract of Original Articles should be structured with subheadings (Objective, Materials and Methods, Results, and Conclusion). Abstracts of Case Reports and Reviews should be unstructured. Please check Table 1 below for word count specifications.

Keywords: Each submission must be accompanied by a minimum of three to a maximum of six keywords for subject indexing at the end of the abstract. The keywords should be listed in full without abbreviations. The keywords should be selected from the National Library of Medicine, Medical Subject Headings database (http://www.nlm.nih.gov/mesh/MBrowser.html).

Manuscript Types

Original Articles: This is the most important type of article since it provides new information based on original research. The main text of original articles should be structured with Introduction, Material and Method, Results, Discussion, and Conclusion

Table 1: Limitations for each manuscript type

Type of manuscript	Word limit	Abstract word limit	Reference limit	Table limit	Figure limit
Original Article	3500	250 (Structured)	50	6	7 or total of 15 images
Invited Review Article	5000	250	50	6	10 or total of 20 images
Case Report	1000	200	15	No tables	10 or total of 20 images
Technical Note	1500	No abstract	15	No tables	10 or total of 20 images
Letter to the Editor	500	No abstract	5	No tables	No media

subheadings. Please check Table 1 for the limitations for Original Articles.

Statistical analysis to support conclusions is usually necessary. Statistical analyses must be conducted in accordance with international statistical reporting standards (Altman DG, Gore SM, Gardner MJ, Pocock SJ. Statistical guidelines for contributors to medical journals. Br Med J 1983: 7; 1489-93). Information on statistical analyses should be provided with a separate subheading under the Materials and Methods section and the statistical software that was used during the process must be specified.

Units should be prepared in accordance with the International System of Units (SI).

Editorial Comments: Editorial comments aim to provide a brief critical commentary by reviewers with expertise or with high reputation in the topic of the research article published in the journal. Authors are selected and invited by the journal to provide such comments. Abstract, Keywords, and Tables, Figures, Images, and other media are not included.

Invited Review Articles: Reviews prepared by authors who have extensive knowledge on a particular field and whose scientific background has been translated into a high volume of publications with a high citation potential are welcomed. These authors may even be invited by the journal. Reviews should describe, discuss, and evaluate the current level of knowledge of a topic in clinical practice and should guide future studies. The main text should contain Introduction, Clinical and Research Consequences, and Conclusion sections. Please check Table 1 for the limitations for Review Articles.

Case Reports: There is limited space for case reports in the journal and reports on rare cases or conditions that constitute challenges in diagnosis and treatment, those offering new therapies or revealing knowledge not included in the literature, and interesting and educative case reports are accepted for publication. The text should include Introduction, Case Presentation, Discussion, and Conclusion subheadings. Please check Table 1 for the limitations for Case Reports.

Letters to the Editor: This type of manuscript discusses important parts, overlooked aspects, or lacking parts of a previously published article. Articles on subjects within the scope of the journal that might attract the readers' attention, particularly educative cases, may also be submitted in the form of a "Letter to the Editor." Readers can also present their comments on the published manuscripts in the form of a "Letter to the Editor." Abstract, Keywords, and Tables, Figures, Images, and other media should not be included. The text should be unstructured. The manuscript that is being commented on must be properly cited within this manuscript.

Tables should be included in the main document, presented after the reference list, and they should be numbered consecutively in the order they are referred to within the main text. A descriptive title must be placed above the tables. Abbreviations used in the tables should be defined below the tables by footnotes (even if they are defined within the main text). Tables should be created using the "insert table" command of the word processing software and they should be arranged clearly to provide easy reading. Data presented in the tables should not be a repetition of the data presented within the main text but should be supporting the main text.

Figures and Figure Legends

Figures, graphics, and photographs should be submitted as separate files (in TIFF or JPEG format) through the submission system. The files should not

be embedded in a Word document or the main document. When there are figure subunits, the subunits should not be merged to form a single image. Each subunit should be submitted separately through the submission system. Images should not be labeled (a, b, c, etc.) to indicate figure subunits. Thick and thin arrows, arrowheads, stars, asterisks, and similar marks can be used on the images to support figure legends. Like the rest of the submission, the figures too should be blind. Any information within the images that may indicate an individual or institution should be blinded. The minimum resolution of each submitted figure should be 300 DPI. To prevent delays in the evaluation process, all submitted figures should be clear in resolution and large in size (minimum dimensions: 100 × 100 mm). Figure legends should be listed at the end of the main document.

All acronyms and abbreviations used in the manuscript should be defined at first use, both in the abstract and in the main text. The abbreviation should be provided in parentheses following the definition.

When a drug, product, hardware, or software program is mentioned within the main text, product information, including the name of the product, the producer of the product, and city and the country of the company (including the state if in USA), should be provided in parentheses in the following format: "Discovery St PET/CT scanner (General Electric, Milwaukee, WI, USA)"

All references, tables, and figures should be referred to within the main text, and they should be numbered consecutively in the order they are referred to within the main text.

Limitations, drawbacks, and the shortcomings of original articles should be mentioned in the Discussion section before the conclusion paragraph.

Revisions

When submitting a revised version of a paper, the author(s) must submit a detailed "Response to the reviewers" that states point by point how each issue raised by the reviewers has been covered and where it can be found (each reviewer's comment, followed by the author's reply and line numbers where the changes have been made) as well as an annotated copy of the main document. Revised manuscripts must be submitted within 30 days from the date of the decision letter. If the revised version of the manuscript is not submitted within the allocated time, the revision option may be canceled. If the submitting author(s) believe that additional time is required, they should request this extension before the initial 30-day period is over.

Accepted manuscripts are copy-edited for grammar, punctuation, and format. Once the publication process of a manuscript is completed, it is published online on the journal's webpage as an ahead-of-print publication before it is included in its scheduled issue. A PDF proof of the accepted manuscript is sent to the corresponding author(s) and their publication approval is requested within 2 days of their receipt of the proof.

References

While citing publications, preference should be given to the latest, most up-to-date publications. If an ahead-of-print publication is cited, the DOI number should be provided. Authors are responsible for the accuracy of references. Journal titles should be abbreviated in accordance with the journal abbreviations in Index Medicus/ MEDLINE/PubMed. When there are six or fewer authors, all authors should be listed. If there are seven or more authors, the first six authors should be listed followed by "et al." In the main text of the manuscript, references should be cited using Arabic numbers in parentheses. The reference styles for different types of publications are presented in the following examples.

Journal Article: Blasco V, Colavolpe JC, Antonini F, Zieleskiewicz L, Nafati C, Albanèse J, et al. Long-term out come in kidneyrecipients from do norstreated with hydroxyethylstarch 130/0.4 and hydroxyethylstarch 200/0.6. Br J Anaesth 2015;115(5):797-8.

Book Section: Suh KN, Keystone JS. Malaria and babesiosis. Gorbach SL, Barlett JG, Blacklow NR, editors. Infectious Diseases. Philadelphia: Lippincott Williams; 2004.p.2290-308.

Books with a Single Author: Sweetman SC. Martindale the Complete Drug Reference. 34th ed. London: Pharmaceutical Press; 2005.

Editor(s) as Author: Huizing EH, de Groot JAM, editors. Functional reconstructive nasal surgery. Stuttgart-New York: Thieme; 2003.

Conference Proceedings: Bengisson S. Sothemin BG. Enforcement of data protection, privacy and security in medical informatics. In: Lun KC, Degoulet P, Piemme TE, Rienhoff O, editors. MEDINFO 92. Proceedings of the 7th World Congress on Medical

Informatics; 1992 Sept 6-10; Geneva, Switzerland. Amsterdam: North-Holland; 1992. pp.1561-5.

Scientific or Technical Report: Cusick M, Chew EY, Hoogwerf B, Agrón E, Wu L, Lindley A, et al. Early Treatment Diabetic Retinopathy Study Research Group. Risk factors for renal replacement therapy in the Early Treatment Diabetic Retinopathy Study (ETDRS), Early Treatment Diabetic Retinopathy Study KidneyInt: 2004. Report No: 26.

Thesis: Yılmaz B. Ankara Üniversitesindeki Öğrencilerin Beslenme Durumları, Fiziksel Aktivitelerive Beden Kitle İndeksleri Kan Lipidleri Arasındaki Ilişkiler. H.Ü. SağlıkBilimleriEnstitüsü, DoktoraTezi. 2007.

Manuscripts Accepted for Publication, Not Published Yet: Slots J. The microflora of black stain on human primary teeth. Scand J Dent Res. 1974.

Epub Ahead of Print Articles: Cai L, Yeh BM, Westphalen AC, Roberts JP, Wang ZJ. Adult living donor liver imaging. DiagnIntervRadiol. 2016 Feb 24. doi: 10.5152/dir.2016.15323. [Epub ahead of print].

Manuscripts Published in Electronic Format: Morse SS. Factors in the emergence of infectious diseases. Emerg Infect Dis (serial online) 1995 Jan-Mar (cited 1996 June 5): 1(1): (24 screens). Available from: URL: http:/ www.cdc.gov/ncidodlElD/cid.htm.

Submission Checklist

- **Cover letter to the editor**
  - The category of the manuscript
  - Confirming that "the paper is not under consideration for publication in another journal".
  - Including disclosure of any commercial or financial involvement.
  - Confirming that the statistical design of the research article is reviewed.
  - Confirming that the references cited in the text and listed in the references section are in line with NLM.
- **Copyright Agreement Form**
- **Author Form**
- **Permission of previous published material if used in the present manuscript**
  - Acknowledgement of the study "in accordance with the ethical standards of the responsible committee on human experimentation (institutional and national) and with the Helsinki Declaration.
  - Statement that informed consent was obtained after the procedure(s) had been fully explained. Indicating whether the institutional and national guide for the care and use of laboratory animals was followed as in "Guide for the Care and Use of Laboratory Animals".
- **Title page**
  - The category of the manuscript
  - The title of the manuscript both in Turkish and in English
  - Short title (running head) both in Turkish and in English
  - All authors' names and affiliations (institution, faculty/department, city, country), e-mail addresses
  - Corresponding author's email address, full postal address, telephone and fax number
  - ORCIDs of all authors.
- **Main Manuscript Document**
  - The title of the manuscript both in Turkish and in English
  - Abstracts both in Turkish and in English (250 words). (Case report's abstract limit is 200 words)
  - Key words: 3 - 6 words both in Turkish and in English
  - Main article sections
  - References
  - Acknowledgement (if exists)
  - All tables, illustrations (figures) (including title, description, footnotes)

İstanbul University
İstanbul Üniversitesi

Dergi Adı: Sağlık Bilimlerinde İleri Araştırmalar Dergisi
Journal Name: Journal of Advanced Research in Healt Sciences

Telif Hakkı Anlaşması Formu
Copyright Agreement Form

Sorumlu Yazar *Responsible/Corresponding Author*	
Makalenin Başlığı *Title of Manuscript*	
Kabul Tarihi *Acceptance Date*	
Yazarların Listesi *List of Authors*	

Sıra No	**Adı-Soyadı** *Name - Surname*	**E-Posta** *E-Mail*	**İmza** *Signature*	**Tarih** *Date*
1				
2				
3				
4				
5				

Makalenin türü (Araştırma makalesi, Derleme, v.b.) *Manuscript Type (Research Article, Review, etc.)*	

Sorumlu Yazar:
Responsible/Corresponding Author:

Çalıştığı kurum	*University/company/institution*	
Posta adresi	*Address*	
E-posta	*E-mail*	
Telefon no; GSM no	*Phone; mobile phone*	

Yazar(lar) aşağıdaki hususları kabul eder::
Sunulan makalenin yazar(lar)ın orijinal çalışması olduğunu ve intihal yapmadıklarını,
Tüm yazarların bu çalışmaya asli olarak katılmış olduklarını ve bu çalışma için her türlü sorumluluğu aldıklarını,
Tüm yazarların sunulan makalenin son halini gördüklerini ve onayladıklarını,
Makalenin başka bir yerde basılmadığını veya basılmak için sunulmadığını,
Makalede bulunan metnin, şekillerin ve dokümanların diğer şahıslara ait olan Telif Haklarını ihlal etmediğini kabul ve taahhüt ederler.
İSTANBUL ÜNİVERSİTESİ'nin bu fikri eseri, Creative Commons Atıf-GayrıTicari 4.0 Uluslararası (CC BY-NC 4.0) lisansı ile yayınlamasına izin verirler. Creative Commons Atıf-GayrıTicari 4.0 Uluslararası (CC BY-NC 4.0) lisansı, eserin ticari kullanım dışında her boyut ve formatta paylaşılmasına, kopyalanmasına, çoğaltılmasına ve orijinal esere uygun şekilde atıfta bulunmak kaydıyla yeniden düzenleme, dönüştürme ve eserin üzerine inşa etme dâhil adapte edilmesine izin verir.
Yazar(lar)ın veya varsa yazar(lar)ın işvereninin telif dâhil patent hakları, fikri mülkiyet hakları saklıdır.
Ben/Biz, telif hakkı ihlali nedeniyle üçüncü şahıslarca vuku bulacak hak talebi veya açılacak davalarda İSTANBUL ÜNİVERSİTESİ ve Dergi Editörlerinin hiçbir sorumluluğunun olmadığını, tüm sorumluluğun yazarlara ait olduğunu taahhüt ederim/ederiz.
Ayrıca Ben/Biz makalede hiçbir suç unsuru veya kanuna aykırı ifade bulunmadığını, araştırma yapılırken kanuna aykırı herhangi bir malzeme ve yöntem kullanılmadığını taahhüt ederim/ederiz.
Bu Telif Hakkı Anlaşması Formu tüm yazarlar tarafından imzalanmalıdır/onaylanmalıdır. Form farklı kurumlarda bulunan yazarlar tarafından ayrı kopyalar halinde doldurularak sunulabilir. Ancak, tüm imzaların orijinal veya kanıtlanabilir şekilde onaylı olması gerekir.

The author(s) agrees that:
The manuscript submitted is his/her/their own original work and has not been plagiarized from any prior work,
all authors participated in the work in a substantive way and are prepared to take public responsibility for the work,
all authors have seen and approved the manuscript as submitted,
the manuscript has not been published and is not being submitted or considered for publication elsewhere,
the text, illustrations, and any other materials included in the manuscript do not infringe upon any existing copyright or other rights of anyone.
ISTANBUL UNIVERSITY will publish the content under Creative Commons Attribution-NonCommercial 4.0 International (CC BY-NC 4.0) license that gives permission to copy and redistribute the material in any medium or format other than commercial purposes as well as remix, transform and build upon the material by providing appropriate credit to the original work.
The Contributor(s) or, if applicable the Contributor's Employer, retain(s) all proprietary rights in addition to copyright, patent rights.
I/We indemnify ISTANBUL UNIVERSITY and the Editors of the Journals, and hold them harmless from any loss, expense or damage occasioned by a claim or suit by a third party for copyright infringement, or any suit arising out of any breach of the foregoing warranties as a result of publication of my/our article. I/We also warrant that the article contains no libelous or unlawful statements and does not contain material or instructions that might cause harm or injury.
This Copyright Agreement Form must be signed/ratified by all authors. Separate copies of the form (completed in full) may be submitted by authors located at different institutions; however, all signatures must be original and authenticated.

Sorumlu Yazar; *Responsible/Corresponding Author;*	**İmza** / *Signature*	**Tarih** / *Date*
		……../……../……


T.C. İSTANBUL ÜNİVERSİTESİ
1453


T.C. İSTANBUL ÜNİVERSİTESİ SAĞLIK BİLİMLERİ ENSTİTÜSÜ
1982